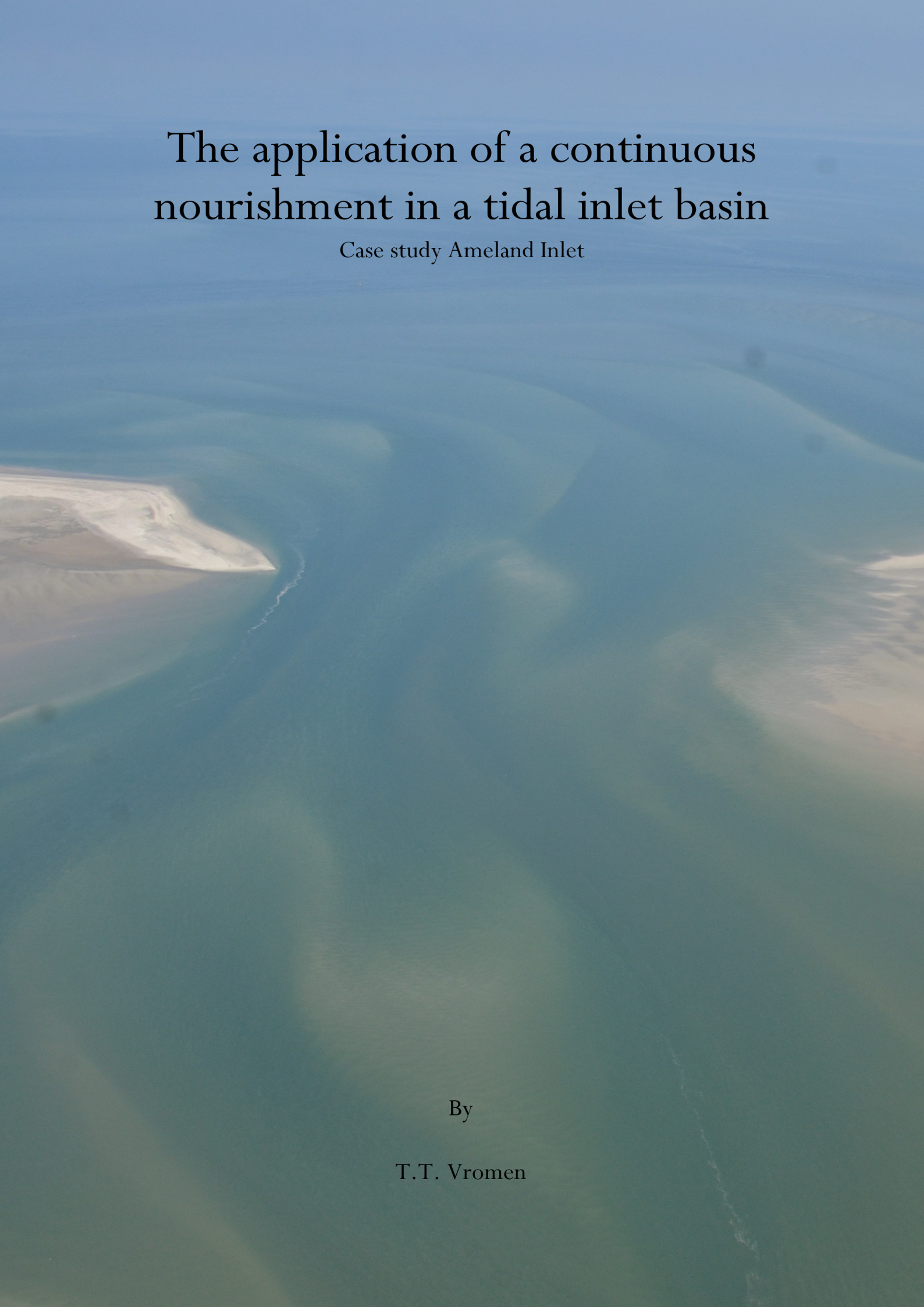

The application of a continuous nourishment in a tidal inlet basin

Case study Ameland Inlet

By

T.T. Vromen

THE APPLICATION OF A CONTINUOUS NOURISHMENT IN A TIDAL INLET BASIN

CASE STUDY AMELAND INLET

by

Tom Theodorus Vromen

To obtain the degree of Master of Science
at the Delft University of Technology
Track: Hydraulic Engineering
Speciality: Dredging

Student number: 4391535
Date: May 17, 2022

Thesis committee

Prof. Dr. Ir. S. Aarninkhof	TU Delft (Chair)
Dr. Ir. S.A. Miedema	TU Delft
Dr. B. Van Maren	TU Delft, Deltares
Ir. J. Kollen	Sweco

[1]Image on the frontcover is a made by Rijkswaterstaat during an inspection flight over the Northern part of the Netherlands

Acknowledgements

I would like to express my special thanks of gratitude to my daily supervisor from Sweco Jan Kollen, as well as the chairman of my thesis committee from the TU-Delft Stefan Aarninkhof, who gave me the golden opportunity to do this wonderful innovative project. Jan, you were always creative and looking for new opportunities on the found results. By means of simple visualisation and easy, but decisive preliminary calculations you ensured that this complex field of engineering remained understandable. Moreover, in this study complex software is applied which could easily be followed blindly. But, you always kept me informed about the underlying processes and the power of preliminary calculations, so once the results became clear they were easy to interpret. Jan, as founding father of the Zandwindmolen concept, I sincerely hope that this study contributes to the realisation of your project over which you have been working for the last decade.
Stefan, as head of my committee you helped orient me to a topic that matched my interests. In addition, you were very sharp on the big picture, which made it clearer during the analysis and writing phase where the focus should be. Moreover, you helped me connect to other vital members of my committee.
Bas van Maren, I would like to thank you very much for all the hours you spent with me on Delft-3D. The software still needs an additional user manual that consists of personal experience with the program. During all the times we met you were very patient with me and made sure I understood the content of what I was doing. I am extremely grateful for that, especially as further help has been difficult to come by due to the recent pandemic.
Sape Miedema, I would like to thank you for participating in the development of the nourishment technique needed to make the Zandwindmolen feasible. In addition to substantive conversations, we also had many personal conversations that I found very fun and dynamic. I want to thank you for the mutual interest in one another. Finally, I am one of your last, if not the very last, graduating student you supervise before you retire. I hope you have enjoyed your time at Delft University of Technology as a professor and that you are going into a great retirement.

Besides members of my thesis committee, many personal friends and family members supported me during the course of this project.
Gijs van Beek, you are a Matlab guru. It is truly insane what you can do with this program. Many times I found myself struggling between knowing what kind of image I wanted to create and also not really knowing how to create such an image. You always managed to program the code in such a manner that it suited to my preferences. Thank you so much for your contribution.
To my parents, Leo and Saskia, my sister and brother, Sanne and Timo, my girlfriend Floor and my roommates Daan and Alexander. Thank you for listening and supporting me, you really knew how to cheer me up when things weren't going my way. Or, you made sure I could focus on something else, which was really nice.
To Joost, this thesis marks the end of a great time at the TU-Delft. Much of this time has been spent with you on great (study) adventures to Nicaragua and Mexico. I will never forget all the amazing things we have experienced. I think it is something remarkable. Lets keep that up during our coming adventures!

Summary

Sea level has been rising since the end of the last ice age (10,000 years ago). Initially, the water rose rapidly, but in the last millennia it decreased to about 2 mm/year. Currently, anthropogenic climate change due to CO_2 emissions is expected to accelerate sea level rise again. The most recent report of the "KNMI Climate Signal '21" expects a sea level rise of 14 - 47 cm by 2050 and of 30 - 121 cm by 2100 (KNMI, 2021). To keep up with sea level rise and to keep the coastline in place, the Dutch sandy coast has been nourished with sand every year since 1990 (Van Koningsveld and Mulder, 2004). Between 1990-2000 this was about 6 million m^3 of sand, then the policy was scaled up to 12 million m^3 of sand to include the foreshore (Rijkswaterstaat, 2020a). This is now done with trailing suction hopper dredgers. These dredge the sand at a depth of 20m from the bottom of the North Sea and place it near the shore. Depending on the nourishment method, tides, waves and wind spread the sand further towards and along the coast. Trailing suction hopper dredgers use fossil fuels, which release large quantities of CO_2. In doing so, they themselves contribute to the problem of rising sea levels. There is therefore a demand for new CO_2-neutral methods of maintaining the coast.

One of these new methodologies could be the use of the Zandwindmolen. The Zandwindmolen is a fixed CO_2-neutral dredge, transport and nourishment concept that nourishes sediment continuously. The purpose of using a Zandwindmolen is to provide the entire surrounding area where the Zandwindmolen nourishes with sediment and allowing it to grow with the (accelerated) sea level rise. With the traditional nourishment method, it is often desired that the sand remain at the vulnerable site for as long as possible. Whereas, in a nourishment with the Zandwindmolen, it is often desirable for the sand to move to other nearby parts of the coast as quickly as possible.

An erosion hotspot on the Dutch coastline is the Ameland Inlet. The Ameland Inlet is a tidal inlet system, where all tidal inlet components jointly strive for an equilibrium state. The Ameland inlet is growing along with the current sea level rise and imports 1.2 Mm^3 / year of sediment from the surrounding coastline, the outer delta and the coastal foundation (Elias, 2020b). Between 2011 and 2020, 27.5 million m^3 of sand has been nourished in the Ameland Inlet (Rijkswaterstaat et al., 2020). Because of the fixed nourishment method of the Zandwindmolen and the continuous sand shortage at the Ameland Inlet, there is a match. However, the usefulness of a Zandwindmolen depends on the extent to which the nourished sand volume is dispersed by natural processes in the short and long term. Moreover, little is yet known about the dispersion behavior of continuous point nourishment in general, and near Ameland in particular. In addition, there is a demand for new methodologies to nourish sediment in the Wadden Sea. Based on the research by (Rutteman, 2021), it can be concluded that a continuous nourishment in a tidal inlet has potential to be effective already in the short term (order of magnitude months / years).

In this study, both the short and long term effect of a continuous point nourishment in a tidal channel is investigated for four sediment fractions (100,200,300 and 400 μm). The goal is that the sediment is dispersed by nature in order to allow the entire Ameland Inlet (adjacent coastlines, coastal foundation, outer delta and Wadden Sea basin) to grow along with sea level rise. In order to do this optimally, it has been investigated that the sediment should be nourished in a mixing plume as high

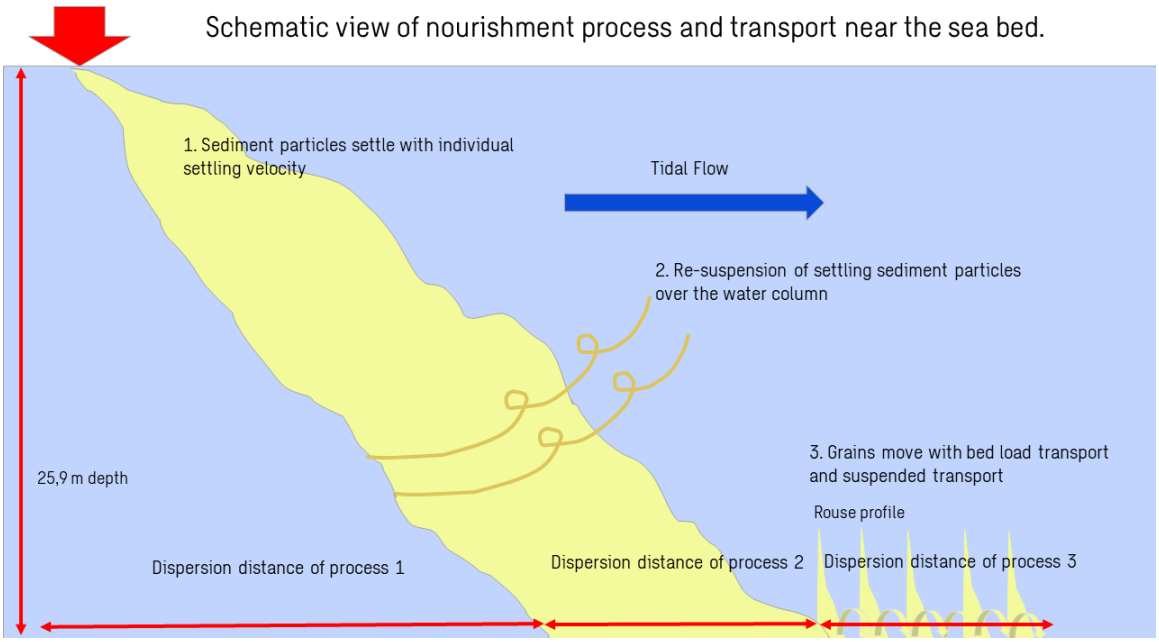

Figure 0.1: Schematic overview of the three dispersion processes. The mixing plume shape origins from (De Wit, 2015)

as possible in the water column. This can be done by means of a seaworthy spray pontoon and a sediment mixture concentration of 1-2%. Through the mixing plume, the nourished sediment mixture becomes prone to the tidal flow. Therefore, direction can be given to the mixing plume. Because of the ebb and flood flow of the sea channel, both the North Sea and the Wadden Sea can be nourished when placed properly. In order to allow the entire Ameland Inlet to grow, 1,128 Mm^3/year of sand is required (area x sea level rise). However, as sea level is expected to continue to rise, even more sediment will be required in the future. In addition, it was determined that the gross tidal sediment transport capacity of Borndiep (tidal channel Ameland Inlet) is 4.23 Mm^3/year. Therefore, in this study, a continuous nourishment at a rate of 2 Mm^3/year was chosen to nourish the tidal channel.

The following sediment transport processes can be distinguished when sediment is nourished on the top of the water column in a mixing plume (see Fig. 0.1):

1. Dispersion through the initial settling process of sediment
2. Dispersion through re-suspension of settling sediment particles
3. Dispersion after sediment is deposited on the sea bed (natural bed load transport and suspended transport)

In the short term (time scale: instantaneous to a few weeks), it appears that the dispersion of sediment is mainly determined by the initial sedimentation process of sediment and by re-suspension of settling sediment particles and that the dispersion by natural sediment processes is minimal. The distance that sediment displaces to the North Sea and Wadden Sea, depends on the sediment fraction (fine sediment fractions disperse further than coarse sediment fractions). The maximum bandwith distances from the nourishment location to the outer regions where the sediment is found between the sediment fractions is 6900m-9100m (coarse fraction - fine fraction) towards the North Sea and 7300m-10600m towards the Wadden Sea. So in the short term the sand disperses well.

In the longer term (timescale: half a year) the sediment spreads further after it has settled to the seabed. The extra maximum further dispersion that the sediment displaces through natural sediment transport processes towards the North Sea and Wadden Sea is between 100m-2100m (coarse fraction - fine fraction) towards the North Sea and between 100m-2300m towards the Wadden Sea. The total dispersion distance that sediment travels away from the nourishment location during half a year is between 7000m-11200m (coarse fraction - fine fraction) towards the North Sea and between 7400m-12600m towards the Wadden Sea. Concluding, in the long term the sand continues to disperse well. Based on half a year, the total dispersion is mainly determined by the short term dispersion. So due to both the good short term and long term dispersion, the Zandwindmolen is useful as a nourishment method in a tidal inlet.

Concluding, a point nourishment executed with a seaworthy spray pontoon in the Ameland tidal inlet with a sediment mixture concentration of 1-2 %, provides dispersion of sediment to both the North Sea and Wadden Sea in the short and long term. Towards the North Sea, it is found that the nourished fractions $\leq$350μm already cause accretion of the outer delta. Towards the Wadden Sea, it is found that the nourished fractions $\leq$150μm already reach the back-barrier of the basin after six months and accretion of intertidal areas is visible. In addition, accretion of the intertidal areas is visible for 150 to 350μm fractions. Fractions $\geq$350μm only disperse in the tidal channel. Because of this, it is not recommended to use this fraction for a continuous nourishment with the Zandwindmolen in a tidal channel. As sediment is well dispersed in the Wadden Sea basin due to the continuous nourishment, there is abundant availability of sediment in the Wadden Sea basin. Based on the historical past, the intertidal areas of the eastern part of the Wadden Sea have always been able to grow naturally with sea level rise. Therefore, a continuous nourishment with the Zandwindmolen is expected to ensure that the intertidal areas in the eastern Wadden Sea can continue to grow naturally with (accelerated) sea level rise. Moreover, the natural distribution of the nourished sand will, through sediment connectivity, compensate for the erosion (autonomous and due to sea level rise) of the inlet (especially the outer delta) and is also expected to contribute to keeping the North Sea coast of Terschelling and Ameland safe. The latter could not yet be demonstrated with this study.

Contents

1 Introduction

1.1. Background

Most of the Dutch coastal system consists of sand. The sandy coastal system forms the basis for numerous functions such as recreation, nature and water safety. The Dutch hinterland is very dependent on its sandy coastal system because the hinterland protects against flooding. This sandy coastal system is locally subject to erosion (Fig. 1.1) and in order to maintain the so-called Base Coast Line (BKL), nourishments are carried out.

Over longer time scales however, the coastal system comes under pressure from rising sea levels and (locally) land subsidence. Beach nourishments are carried out to compensate for the rise in sea level and subsidence. The total nourishment volume corresponds to the surface area of the coastal foundation x the sea level rise, and based on the current sea level rise of 2 mm per year, the sediment requirement for the Wadden Sea until 2035 is 9.1 million m^3 per year (Rijkswaterstaat, 2020a). However, the sediment requirements for both the North Sea and Wadden Sea will increase significantly with accelerated sea level rise (Table 1.1).

Table 1.1: Sea level rise scenarios according to KNMI (2021) for the Dutch coastline

Year	2050	2050	2050	2100	2100	2100
Emission scenario	SSP1-2.6	SSP2-4.5	SSP5-8.5	SSP1-2.6	SSP2-4.5	SSP5-8.5
Sea level rise [mm]	140-380	150-410	160-470	300-810	390-940	540-1210
Annual sea level rise rate [mm/year]	2.8-8.7	5.2-10.6	5.8-12.1	2.9-9.1	4.4-10.5	7.2-16.9

As a result of this projected increase in nourishment volumes, a change in nourishment policy is required. Coastal Genesis 2.0 sets two operational in coastal management objectives at two different time scales.

- Dynamic maintenance of the coastline by sand nourishment on a timescale of 0-20 years
- Remaining the equilibrium of the coastal fundament on a longer timescale (>20 years)

To respond to both operational goals, Kustgenese 2.0 proposes a hybrid strategy. The preferred strategy of Kustgenese 2.0 to meet both operational goals until 2032, is to nourish a total of 11.0 Mm^3 of sand per year on the three main regions along the Dutch coastline. The three main regions and their annual budgeted sediment volumes are; The Wadden area (5.7 Mm^3), Holland coast (3.1 Mm^3) and Zeeland Delta (2.2 Mm^3). These annual volumes are intended exclusively for dynamic maintenance of the coastline through sand nourishments on a time scale of 0-20 years. An additional 0.9 Mm^3 is budgeted to provide for the balance of the coastal foundation on a longer timescale (>20 years). The estimated cost is €46.2 million, which averages €4.2 per m^3. (Rijkswaterstaat, 2020a)

Over time, different types and methodologies of coastal maintenance and/or nourishments have been developed. The most classic form is beach maintenance, where sand is directly nourished and spread on the beach. Subsequently, foreshore nourishments and tidal channel wall nourishments were developed, where tides, waves, and wind further spread the nourished sediment along

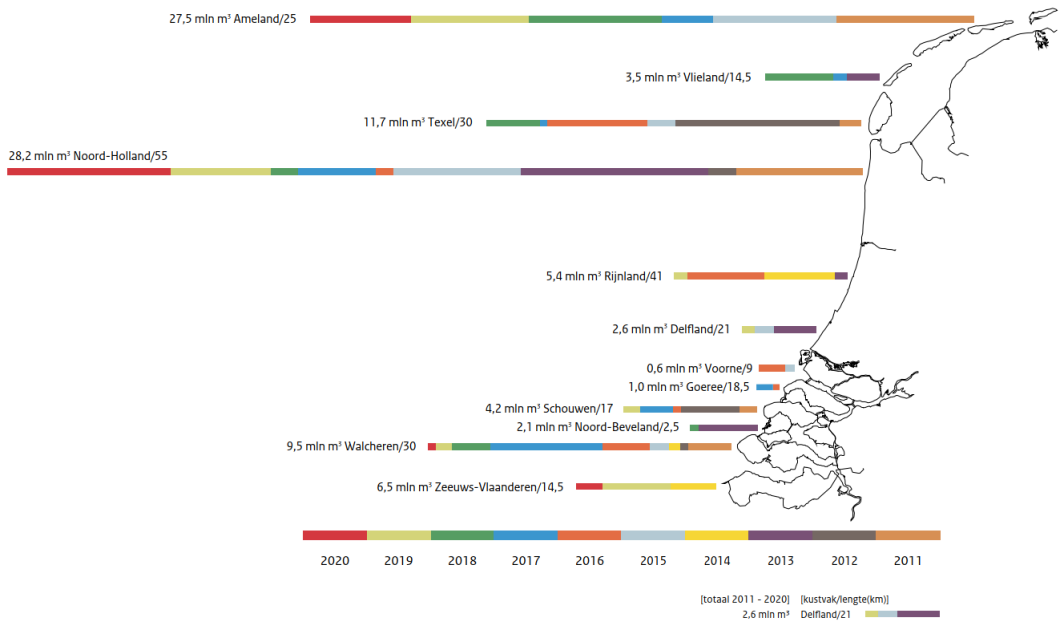

Figure 1.1: Coastline nourishment overview. Total amount of executed sand nourishments in Mm^3 in the period of 2011-2020. The image is obtained from (Rijkswaterstaat et al., 2020)

the coastline. Letting the sediment be spread by the forces of nature led to the development of the holistic Building with Nature (BwN) philosophy. One recognized project that stems from the Building with Nature philosophy is the Sand Engine. The Sand Engine is a mega-nourishment in which the forces of nature are central to spreading the sediment. Another new nourishment method that has not yet been recognized by RWS is the pilot nourishment on the outer delta near Ameland. The results and long term effects of this pilot nourishment are still being investigated by RWS.

The main equipment currently used to maintain the coastline are trailing suction hopper dredgers (TSHD). The estimated CO_2 emissions are 37.9 million kg CO_2 per year. (Rijkswaterstaat, 2020a). Therefore, they help to fight the effects of climate change while at the same time aggravating the problem. The ambition of the Dutch government is to achieve a net zero carbon footprint by 2050 (Rijkswaterstaat, 2021b). Therefore, it is crucial that the means to perform coastal maintenance achieve a net zero carbon footprint. Both Coastal Genesis 2.0 (Rijkswaterstaat, 2020a) and (Wang et al., 2018) argue that it is desirable to develop new innovative nourishment methods and techniques. In addition, there is a demand from the IKZ program to make the means by which the Dutch coast is maintained CO_2 neutral.

1.2. PROBLEM FORMULATION

The Zandwindmolen

One possible solution is the Zandwindmolen. The Zandwindmolen is a CO_2 neutral, win, transport and nourishment concept powered by wind energy. The sediment is transported from an offshore extraction area to the coast by means of pipelines. As long as the wind blows sufficiently, sediment can be moved. In Fig. 1.2 the sub-components are indicated in a system sketch. The Zandwindmolen is a site-specific system and nourishes the sand in a predefined area. The Zandwindmolen thus typifies itself as a fixed system which continuously nourishes sand to a predefined zone. Therefore, the Zandwindmolen has two major advantages over traditional nourishment methods. Firstly, it has the potential to constantly supply the erosion hotspots with sediment and thus maintain the

BKL (Fig. 1.1). Secondly, it offers a CO_2 neutral alternative for coastal maintenance instead of CO_2 emitting trailing suction hopper dredgers (TSHD).

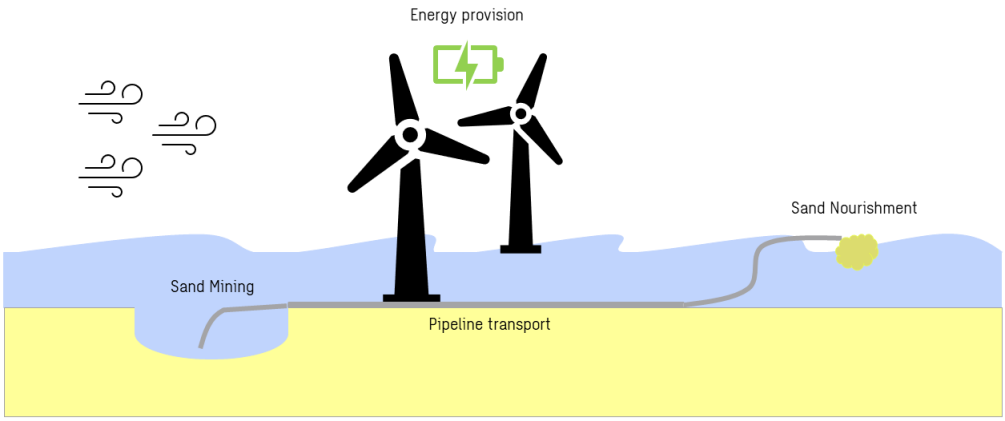

Figure 1.2: Overview of the Zandwindmolen concept. The sub-components are indicated

The purpose of using a Zandwindmolen is to provide the entire surrounding area where the Zandwindmolen nourishes with sediment and allowing it to grow with the (accelerated) sea level rise. It thus extends beyond the current BKL policy where only locations that exceed or tend to exceed the BKL limit at a specific time are maintained. The Zandwindmolen responds to both operational objectives in the proposed Coastal Genesis 2.0 policy. The long-term idea is to permanently nourish the Dutch coast with sand at erosive hotspots using a dozen of Zandwindmolens and to allow natural forces (tides, waves and wind) to spread the sand further along the coast, thus guaranteeing coastal safety in the long term. It is expected that the spreading of sediment over an entire area from the nourishment location takes an order of magnitude of 10 - 30 years. Near the nourishment locations there is of course an immediate effect.

In the traditional nourishment method, it is often desired that the sand remain at the vulnerable spot for as long as possible. With a nourishment with the Zandwindmolen, it is often desirable for the sand to move as quickly as possible to other nearby parts of the coast. After all, the vulnerable location is permanently resupplied with sand and is therefore no longer vulnerable.
Previous research conducted by (Rutteman, 2021) has shown that:

- A tidal channel wall nourishment at the tidal inlet of Marsdiep is well displaced by the tide (order months / years).
- A foreshore nourishment at the wave-dominated Callantsoog coast spreads slowly along the coast (expectation order decades).
- Grain size plays a crucial role in the rate of dispersion of the nourished sand.

Based on Rutteman (2021) his research, it can be concluded that a continuous nourishment has the potential to be effective in a tidal inlet already in the short term.
Appendix D provides a further consideration of the Zandwindmolen. The main considerations in this appendix are;

- The ecological impact of the Zandwindmolen

- Comparable dredge systems as the Zandwindmolen
- The win and transport sub-components
- The nourishment effects of the Zandwindmolen versus traditional equipment

Wadden Sea
The Wadden Sea can autonomously grow with sea level rise up to a sea level rise of 6-10 mm/year (Wang et al., 2018). This autonomously grow capacity will lead to sediment import from the outer delta, surrounding coastlines and coastal foundation. However, the amount of sand within a tidal inlet system is finite. Therefore, a continuity in sufficient sediment availability at the outer delta, along the barrier island coast and the coastal foundation is a prerequisite for growth of the tidal inlet system with (accelerated) sea level rise. Therefore, it is important to develop new sand nourishment methods that increase the import of sediment to the Wadden Sea (Wang et al., 2018). Because of the sediment connectivity of a tidal inlet system, it is possible to compensate for the sediment demand of the Wadden Sea by nourishing the adjacent coastlines or the outer delta (Wang et al., 2018). This method is currently under investigation through a pilot ebb-tidal delta nourishment at Ameland Inlet.

Ameland Inlet
From Fig. 1.1 it becomes apparent that Ameland Inlet is an erosion hotspot. An overview of the various coastal works of the past 10 years in the area of Ameland Inlet can be found in Appendix A.2. Amelander inlet is characterized as a tidal inlet system. Within a tidal inlet system the sediment from the adjacent coastlines, outer delta, coastal foundation and basin are connected. ((Wang et al., 2018): (Bosboom and Stive, 2021))

The Ameland inlet is growing along with the current sea level rise and imports 1.2 Mm^3 / year of sediment from the surrounding coastline, the outer delta and the coastal foundation (Elias, 2020b). However, the growth of the Ameland inlet with the current sea level rise does lead to erosion of the adjacent coastlines, outer delta and coastal foundation. This is one of the reasons why the Ameland inlet is characterized as an erosion hotspot in Fig. 1.1. In Appendix A.3 a more extensive and visualized explanation of the erosion of the adjacent coastlines, outer delta and coastal fundament due to sediment import to the Wadden Sea under the current sea level rise is provided.

In the future, the speed of sea level rise is expected to increase (KNMI, 2021). Due to the sediment connectivity of the tidal inlet system, the Wadden Sea will try to grow along with the (accelerated) sea level rise by means of sediment import from the outer delta, surrounding coastlines and coastal foundation. In addition, (accelerated) sea level rise will also increase the current import of 1.2 Mm^3 / year by the Ameland inlet. As a result, even more erosion will occur at these parts of the tidal inlet system due to (accelerated) sea level rise.

Match Ameland Inlet and Zandwindmolen
The Ameland inlet is an erosion hotspot which could be maintained from a fixed Zandwindmolen system. In addition, a characteristic of the inlet gorge of the Ameland inlet is that there are strong tidal velocities to both the North Sea and the Wadden Sea. A nourishment in the inlet gorge provides opportunities for the Zandwindmolen to disperse the nourished sediment from a fixed location by means of the forces of nature. As a result, the Zandwindmolen concept could be a potential solution to the erosion of the Ameland inlet. In previously conducted research by Rutteman (2021), a tidal channel wall nourishment was performed. In this nourishment type, the sediment is directly placed on the wall of the inlet. However, it is expected that if the sediment is placed at the top of the water column, the sediment will initially disperse much further as the sediment is carried along in the direction of the tidal current during the settling process. Therefore, this study investigates the most optimal manner to nourish sediment in a tidal channel. In addition, it is investigated by which

equipment a continuous nourishment can be carried out in practise.

Hypothesis
It is expected that the continuous nourishment of artificial sand in the tidal inlet will produce dispersion of the artificially nourished sand towards both the Wadden Sea and the North Sea. This is expected to eliminate the need for the sand to come from the outer delta, adjacent shorelines and coastal foundation. For the North Sea side of the tidal inlet system, this prevents erosion of the coastline and thus prevents risks to safety. For the intertidal areas located in the Wadden Sea, this will lead to natural growth of the intertidal areas (under the current sea level rise).

The usefulness of a Zandwindmolen depends on the extent to which the nourished sand volume is dispersed by natural processes in the short and long term. However, little is yet known about the dispersion behavior of continuous point nourishment in general, and near Ameland in particular. This leads to main questions of this research:

1. With what equipment can a continuous nourishment be practically carried out?
2. How and how far disperses the nourished sediment from the Zandwindmolen in the short and long term?
3. How much sand can be nourished without silting up the system? In other words, what sand transport capacity does the Ameland inlet have?

For this study, a distinction is made between near-field, mid-field and far-field. Near-field describes the behavior of the nourished sand immediately after deposition (time scale: instantaneous to several weeks). Mid-field describes the behavior of the sand once it is on the bottom and moves further with natural processes (months to years). Far-field describes the behavior into the distant future (years - decades). This study focuses on the near-field and mid-field transport processes. Subquestions have been formulated for this purpose. The far-field behavior is only examined contemplatively.

To explore these main questions in more detail, the following research questions (RQs) were prepared for each time scale:

Near-field research

1. What is the maximum dispersion of a settling sediment particle without re-suspension?
2. What is the spatial initial near-field dispersion?
3. What is the longitudinal distribution of the initial dispersion?

Mid-field research

1. What is the siltation of the channel after six months?
2. What is the mid-field dispersion after six months?
3. How much sediment can be processed by the tidal inlet?

Far-field consideration
Nourishing sediment continuously and allowing the environment of the Ameland inlet to grow with it, is a morphological issue that applies for the long term (years - decades). The long-term research is beyond the scope of this study. Here, the near-field and mid-field processes are addressed, since

that provides the basis for the far-field behavior. Moreover, the autonomous far-field behavior is already under research (Rijkswaterstaat, 2020a).

The main questions and sub-questions described above are investigated through a literature study and by applying a numerical model. Using the literature review, the following theoretical questions are investigated:

- How is sediment transported most efficiently by nature and how should the corresponding nourishment method be implemented?
- What is the relative importance of waves on sediment transport in a tidal inlet?
- What is the nourishment requirement of Ameland inlet?

Based on the literature review and quantitative data from the numerical model, the strategy of the nourishment is prepared. In it, the following questions are central:

- How does the dominant tidal flow relate across multiple locations in the tidal inlet?
- How much sediment can potentially be continuously nourished in the Ameland inlet?
- What is the optimal nourishment location in the Ameland inlet to nourish both the Wadden Sea and the North Sea?

1.3. DOCUMENT STRUCTURE

The document is structured as shown in Fig. 1.3. This figure also shows how the chapters are interrelated.

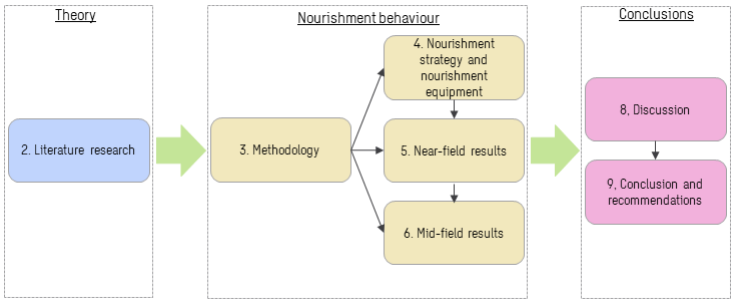

Figure 1.3: Overview of the document structure of this thesis. The red lines indicate the coherence between the different sections

Chapter 2: Literature research
Chapter 2 contains the theoretical foundation of this research. First a general description of the Ameland inlet is provided. In this general study, the focus is on hydrodynamics and morphodynamics. Thereafter, the posed theoretical research questions are answered based on associated theory.

Chapter 3: Methodology
Chapter 3 discusses how the Ameland inlet model was used to generate results on the research questions posed. The process of continuous nourishment was simulated in two successive steps. In the near-field model, the dispersion from the settling process of individual sediment particles is simulated over a spring tide neap tide cycle. In the mid-field model, the subsequent further dispersion of the sediment is simulated over a six-month period. In order to do this accurately, the near-field dispersion of the sediment found is continued to the mid-field behavior. The exact steps taken within

the model environment are explained in Appendix H. Reference to this appendix will be made in the introductions of chapters 5 and 6. This is done in such a way that the capabilities and limitations of the applied model are clear.

Chapter 4. Nourishment strategy
Chapter 4 discusses the nourishment strategy. The exact location and annual nourishment volume of the continuous nourishment are determined. The location is determined based on the literature study and general quantitative hydrodynamic data determined by a Delft-3D numerical analysis. Based on the found location and nourishment volume, a design of the nourishment is illustrated. Thereafter, the equipment needed to execute the continuous nourishment based on the nourishment strategy is determined.

Chapter 5. Near-field results
Chapter 5 analyzes the results regarding the near-field dispersion. By means of an extensive analysis, the near-field RQs are answered. While answering the RQs, the physical underlying processes are also discussed. Finally, a consideration regarding the near-field dispersion is given for the continuation of the study.

Chapter 6. Mid-field results
Chapter 6 analyzes the results regarding the mid-field dispersion. By means of an extensive analysis, the mid-field RQs are answered. While answering the RQs, the physical underlying processes are also discussed. Finally, a consideration regarding the mid-field dispersion is given for the continuation of the study.

Chapter 7. Discussion
The answers found in Chapters 5 and 6 are discussed in this chapter. In addition, the effect of waves on the results found is discussed. Finally, the expected far-field behavior of the continuous nourishment is determined.

Chapter 8. Conclusions and recommendations
In chapter 8, a conclusion is formed on the main questions based on the reflections in chapter 7 from the results in chapters 5 and 6. Finally, recommendations for possible follow-up research are given in this chapter.

2 | Literature study

Chapter 2 contains the theoretical foundation of this research. In addition to a description and hydrodynamic and morphodynamic behaviour of Ameland Inlet, the following knowledge gaps are answered within this theoretical framework:

- What is the relative importance of waves on sediment transport in a tidal inlet?
- How is sediment transported most efficiently by nature and how should the corresponding nourishment method be implemented?
- What is the nourishment requirement of the Ameland inlet?

2.1. Ameland Inlet general

Wadden Sea
Ameland Inlet is located in the Dutch Wadden Sea. The Wadden Sea is located in the Northern part of the Netherlands and stretches out towards Denmark. All together it contains the largest coherent tidal flat area in the world consisting of 1,434 km^2 (UNESCO World Heritage Centre, 2021). Moreover, the Wadden Sea is one of the last remaining large-scale, intertidal ecosystems where natural processes continue to function largely undisturbed. In Fig. 2.1, a general satellite image (Fig. 2.1a) and the conservation zone (Fig. 2.1b) of the entire Wadden Sea area is presented.

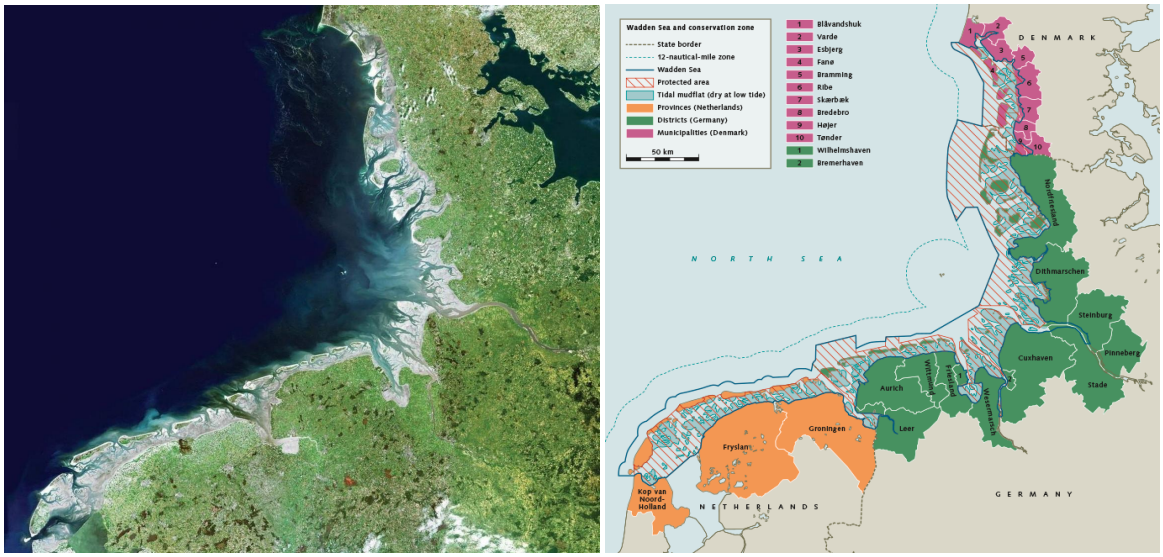

(a) Satellite image Wadden Sea, adopted from (UNESCO World Heritage Centre, 2021)

(b) Conservation zone Wadden Sea, adopted from (Heritage, 2021)

Figure 2.1: Satellite image and conservation zone of the Wadden Sea.

Ameland Inlet
In Fig. 2.2 the location of Ameland Inlet is depicted within the Wadden Sea region. The Ameland Inlet is located between Terschelling and Ameland. Most of the sediment found in the Ameland Inlet

originates from the North Sea. Sediment import through debouching rivers is of minor importance. Mud is mainly imported with North Sea water, while the sandy sediments are predominantly supplied by erosion of the ebb-tidal deltas, the barrier islands and the adjacent shore of the province North Holland (Van Straaten and Kuenen, 1957). The Wadden Sea is a sediment sharing tidal inlet system. This implies that the Ameland Inlet both receives as transports sediment from one basin to another (Wang et al., 2018). Within this thesis the focus is on sand, therefore the effect of mud is no longer taken into consideration.

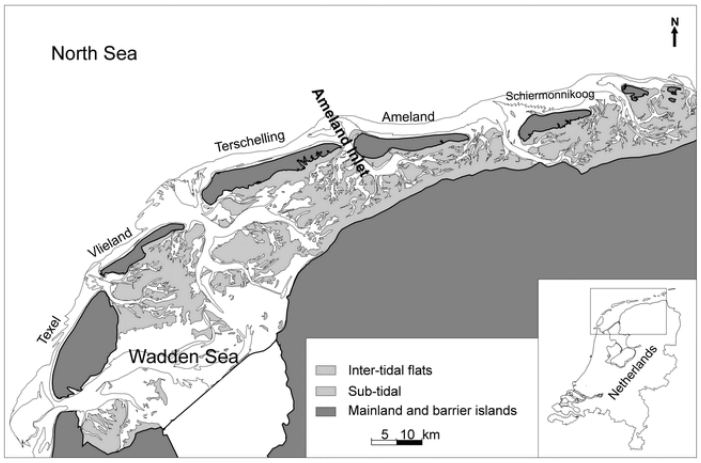

Figure 2.2: Location of Ameland Inlet in the Dutch Wadden Sea. Obtained from (Cheung et al., 2007)

In Appendix A, a global description of the Wadden Sea is provided. In this global description the following aspects can be found:

- The societal and environmental functions of the Wadden Sea
- The development of the Wadden Sea over time due to man made changes as the Afsluitdijk
- A topographical description of the shoals, ebb channels and intertidal areas of the Ameland Inlet
- A description of the consequences of sea level rise for the Wadden Sea in general
- Coastal maintenance activities between 2010-2022 at Ameland Inlet

2.2. HYDRODYNAMICS

Tides, waves and wind are the main physical forcing processes of water and sediment transport in the Ameland Inlet (Wang et al., 2018). According to Elias et al. (2012), the surface area of the basin of Ameland Inlet is 309 km^2 during MHW and during MLW 164km^2. Furthermore Elias et al. (2012) state that the average tidal prism is found to be in the order of 478 Mm^3.

At Ameland Inlet, the majority of the waves come in from the north-west, resulting in an eastward littoral drift. The significant wave height is 1.3 meters with a mean period of 5 seconds. During storms, wave heights over 6 meters and storm surges over 2 meters are measured. The North Sea mainly consists of locally generated wind waves with a significant wave height of 1.37m and a corresponding peak wave period of 7s. Waves in the Wadden Sea are mainly locally generated wind waves or are waves originating from the North Sea which penetrate through the Ameland Inlet. ((Elias et al., 2012) : (Wang et al., 2018) : (Bosboom and Stive, 2021))

A combination of a standing and progressive tidal tidal wave propagate from south to north in the North Sea. Due to this tidal wave alongshore velocities of 0.5 m/s to 1.0 m/s are found along the Dutch coast. Between Den Helder and the Eems-Dollard inlet the tidal range increases from respectively 1.4 to 2.5 meters. The increase of tidal range is because the Eems-Dollard inlet is located further away from the amphidromic point ((Elias et al., 2012): (Bosboom and Stive, 2021).

Hayes (1979) and Davis Jr and Hayes (1984) developed a hydrodynamic classification system based on the mean wave height and the mean tidal range. Based on this classification system, the Dutch Wadden Sea (and thus Ameland Inlet) can be typified as a mixed energy, wave dominant environment. However, the morphology shows tide-dominated features such as a large ebb-tidal delta and deep entrance channels (Elias et al., 2012). These features are caused by large tidal prisms and relatively low wave energy (Davis Jr and Hayes, 1984).

At Ameland Inlet, the tidal channels are small compared to the intertidal flats with ratios of intertidal flat over the total surface area of 0.7-0.8 (Elias et al., 2012).

2.3. MORPHODYNAMICS

In this section the morphological features regarding the Ameland Inlet are discussed. First the sediment transport mechanisms are discussed in Section 2.3.1. Thereafter, the mechanics of a tidal inlet are discussed in Section 2.3.2. Finally, the macro scale morphological sediment patterns are discussed Section 2.3.3.

2.3.1. SEDIMENT TRANSPORT MECHANISMS

Sediment can be transported both in suspension or as bed load. It is found by Bak (2017) and Pearson et al. (2020) that suspended sediment transport is the dominant transport mode for Ameland Inlet. When sediment is transported down-drift from Terschelling towards Ameland due to littoral drift, sediment is either imported or by-passed over the inlet. Sediment by-passing is either predominantly tide or wave driven. Bak (2017) found with the Bruun and Gerritsen (1960) parameter, which is determined by dividing the tidal prism by the total littoral drift, that sediment bypassing is predominantly tide induced.

The relevant mechanisms of residual sediment transport through the inlet are described by Wang et al. (2018). Net sediment import is defined as the difference between imported sediment through the tidal inlet during flood and the exported sediment trough the tidal inlet during ebb. The mechanism can be subdivided in barotropic and baroclinic processes. Barotropic processes are processes in which the the density is a function of pressure only. First the main barotropic mechanisms are introduced. The mechanisms are; residual flow, tidal asymmetry, jet flow asymmetry, spatial asymmetry in net sediment transport and deposition and finally dispersion.

Residual flow causes a residual sediment transport in the same direction the flow. Furthermore, it is strengthened by the tidal flow fluctuations (Van de Kreeke and Robaczewska, 1993). The types of of residual flow through a tidal inlet are; freshwater input, compensation flow caused by Stokes drift and meteorological effects as wind and set-up.

Tidal asymmetry occurs due to deformation of the tidal wave while propagating in shallow seas. If the system is flood dominant, the period of rising water levels become shorter and the period of falling water levels becomes longer. As a consequence, the flood velocities increase and the ebb velocities reduce causing a net import of sediment. If the system is ebb dominant, the complete opposite occurs and net export of sediment occurs. Tidal asymmetry compromises asymmetry in peak

flow velocities and asymmetry in duration of high water (HW) and low water (LW) slacks. (Wang et al., 2018):(Bosboom and Stive, 2021).

Jet flow asymmetry is caused by asymmetry in the velocity of the flow jet that develops in the inlet gorge. Jet flow is directed in the direction out of the constricted area, which in this case from the Ameland Inlet towards the North-Sea. Hence, sediments are exported out of the Ameland Inlet due to Jet flow asymmetry. Moreover, jet flow asymmetry contributes to the formation of the ebb-tidal delta (Wang et al., 2018).

Spatial asymmetry in net sediment transport and deposition is the result of spatial differences of the inlet. The ebb delta can for instance be ebb-dominant and the flood delta can be flood-dominant. Behaviour can be determined based on detailed analysis of three dimensional current patterns in Ameland Inlet.

Dispersion is a residual transport in the direction from high concentration towards low concentration. At Ameland Inlet this residual transport is caused by waves which stir up sediment at the ebb-tidal delta. The tidal flow functions as a mixing agent for dissolved and suspended matters. A residual transport in the direction opposite to the concentration gradient is generated, which in this case is basin inward. Hence, net sediment import is generated by dispersion (Bosboom and Stive, 2021): (Wang et al., 2018): (Elias and van der Spek, 2006).

The baroclinic processes are caused by the effects of density flows as a result of spatial gradients in salinity and water temperature (Wang et al., 2018). These processes are relevant if the back barrier of the inlet receives fresh water. In case of the vicinity of Ameland Inlet, almost no rivers debouch in the back barrier and are thus of minor importance.

There are ongoing discussions about which processes are more dominant. Current findings suggest that barotropic mechanisms are more dominant than baroclinic processes (Wang et al., 2018).

2.3.2. TIDAL INLET BEHAVIOUR

According to Wang et al. (2018) the barrier islands, inlet and its associated ebb-tidal delta and tidal basin that includes tidal flats and channels form a sediment-sharing system. In Fig. 2.3a a general overview of an ebb-tidal delta is illustrated and a generalized morphology of an ebb-tidal delta is depicted in figure Fig. 2.3b. These elements continuously strive to maintain a dynamic equilibrium between morphology and forcing conditions. Hence, when the system is disturbed from the "equilibrium state" by man-made changes, natural or both, an exchange of sediment between the sediment-sharing components is induced until the equilibrium state is restored (Wang et al., 2018).

In general the behaviour of the morphology of the ebb-tidal delta depends on the combined action of waves and tides. At the ebb-tidal delta waves break due to depth induced wave breaking and stir up sediment into suspension. The role of waves is to act as a bulldozer by pushing the sediment towards shore and thus removing sediment from the ebb-tidal delta. Furthermore, the area over which the ebb-tidal delta can spread out is limited due to wave action (Bosboom and Stive, 2021). A net offshore directed sediment flux is induced by the inlet currents driven by the tide. These offshore directed sediment fluxes built up the ebb-tidal delta. Hence, the overall morphology of the flood and ebb-tidal delta is generally determined by the dynamic balance between waves and tides (Bosboom and Stive, 2021). In general it can be stated that the ebb-tidal delta of the Ameland Inlet is highly dynamic (Oertel, 1972).

The empirical relations for tidal inlet basins which are used for this research are discussed in Ap-

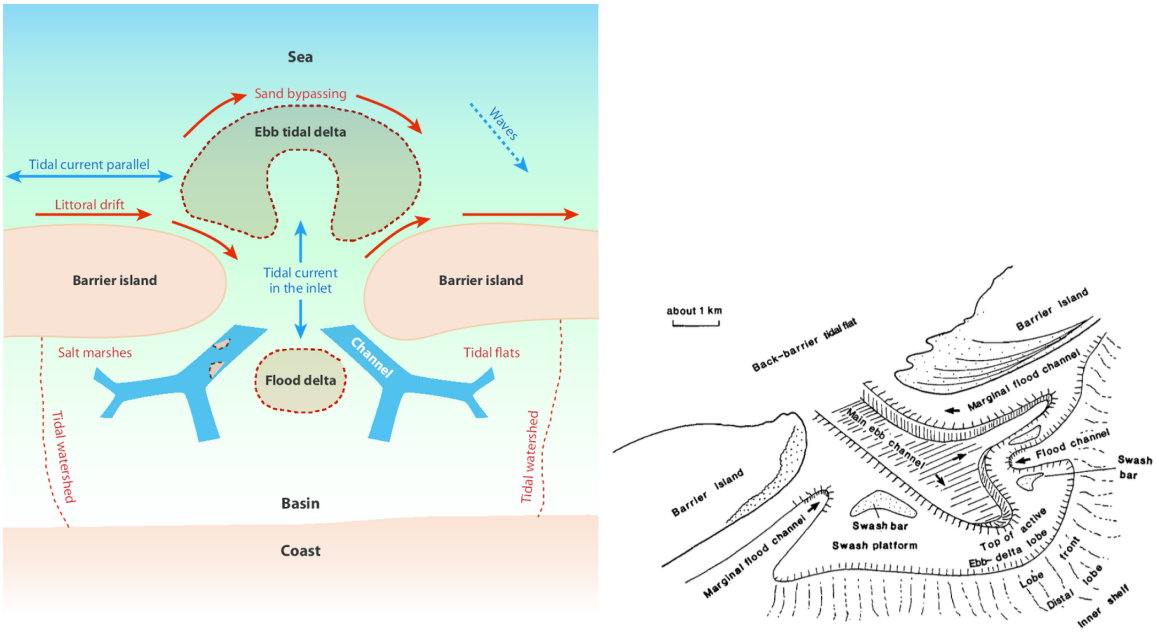

(a) Overview tidal inlet system, image obtained from (De Swart and Zimmerman, 2009)

(b) Generalized morphology of an ebb-tidal delta (Sha, 1990)

Figure 2.3: Overview of a tidal inlet and a closeup of an ebb-tidal delta

pendix B. The empirical relations discussed in this section are:

- The volume of sand stored in the outer delta and the tidal prism
- The development of the cross-sectional area versus the tidal prism
- Stability of cross-sectional area (Escoffier)

Cheung et al. (2007) performed a research about the morphodynamics and sand bypassing at Ameland Inlet. In this research, Cheung et al. (2007) state that the ebb-channels Borndiep and Boschgat show cyclic behaviour in eastward direction with a duration of about 40 years. The direction is mainly governed by the dominant littoral drift caused by the incoming waves from the north-west. Hence, Terschelling is the up-drift island and Ameland is the down-drift island. As an ebb-channel moves to the east in the Ameland Inlet it reduces in dominance until it vanishes. Simultaneously, a new channel emerges at the western up-drift side of the inlet, which takes over the function of the old ebb-channel (Elias et al., 2012). Within this process, the vanishing down-drift side ebb-channel of the inlet might cause severe erosion at Ameland. However, when a shoal reaches the coast of the down-drift barrier island Ameland, significant accretion can take place (Hayes, 1980).

In Fig. 2.4 an overview of the present mean grain size d_{50} is presented. It can be observed that further basin inwards, the d_{50} decreases. This is in line with observations from Elias et al. (2012) and Wang et al. (2012), in which it is stated that the grain size distributions is sorted according to the energy gradient in the vicinity of the tidal inlet system. From North Sea to Wadden Sea basin, the energy of tide and waves decreases and thus, so does the mean grain size (Wang et al., 2012). Hence, the largest fractions of around 300 µm are found where the flow velocities are the highest, which is in the ebb-channels and in the North Sea Region. Furthermore, the smallest fractions of <50 µm are found near the back barrier of the basin or at the watersheds, where water is almost stagnant. Although Fig. 2.4 is relatively old, it does represent the sediment distribution accurately.

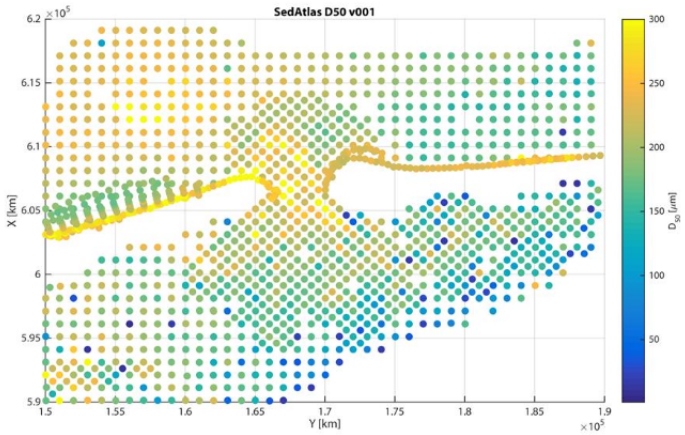

Figure 2.4: Overview of the median grain size (d_{50}) in Ameland inlet. Obtained from (Deltares, 1999)

2.3.3. MACRO SCALE MORPHODYNAMIC SEDIMENT PATTERNS

It was mentioned in Section 2.3.2, that the ebb tidal-delta together with spits, tidal inlets, barrier island and back-barrier basins are constantly striving towards an equilibrium state (Bosboom and Stive, 2021). In order to remain an equilibrium state, the different tidal components share sediment with one another. This sediment sharing behaviour of is studied by Pearson et al. (2020) and is referred to as the sediment connectivity of the tidal inlet components. Bak (2017) studied the behaviour of sediment transport for coarse and fine fractions. This allows to differentiate between different particle sizes. Both studies provide insight in the macro morphological behaviour of sediment.

Sediment transport is initiated by the suspension of sediment. The degree to which sediment can be brought into suspension depends on the forces exerted on the sediment (the amount of energy in the system) and the grain size. As the grain size increases, more energy is required to bring it into suspension and vice versa. Once the sediment is in suspension, it is carried along in the direction of the flow. Detailed information about the initiation of motion and Shields curve can be found in Appendix C.

In Fig. 2.5a the sediment connectivity of Ameland Inlet is depicted. Based on the morphological pathways, red numbers were added to provide detailed information on the direction sediment moves to when it is in a particular area in the vicinity of the Ameland Inlet.

Fig. 2.5a illustrates that transport patterns towards the Wadden Sea basin originate from the beach of Terschelling (1), the beach and foreshore regions east of Terschelling (2) and in the throat of the inlet or further basin inward (3).
Sediment transport patterns towards the ebb-tidal delta and Ameland-West coastline originate from the foreshore region of Terschelling or the ebb-tidal delta (2) and (4).
The Sediment by-passing between location (1) and (2) in Fig. 2.5a is predominantly tide dominant as discussed in Section 2.3.1 and thus contributes more to sediment import to the Wadden Sea basin than sediment by-passing in the form of migrating bars. However, the further offshore from the coastline of Terschelling, (more offshore directed than number 2 in Fig. 2.5a), the more likely it is that sediment by-passes the tidal inlet over the ebb-tidal delta due to the dominant littoral transport to the east (Section 2.2).

The findings of Pearson et al. (2020) are in agreement with Bak (2017). Besides sediment transport patterns, the main pathways of coarse and fine fractions can be distinguished in Bak (2017) his

research. The pathways of the different fractions are illustrated in Fig. 2.5b. It can be observed that smaller fractions travel further inward into the basin compared to coarser fractions. This is in agreement with researched performed by Wang et al. (2018) and the sediment atlas (Fig. 2.4) about the median grain size distribution in Ameland Inlet. Both illustrate that this has to do with the basin inward decreasing energy gradient.
In the North Sea region of the tidal inlet, it can be observed that fine fractions move further than coarse fractions parallel with the shoreline to Ameland. Moreover, fine fractions can by-pass the tidal inlet via deeper regions than the coarse fractions.

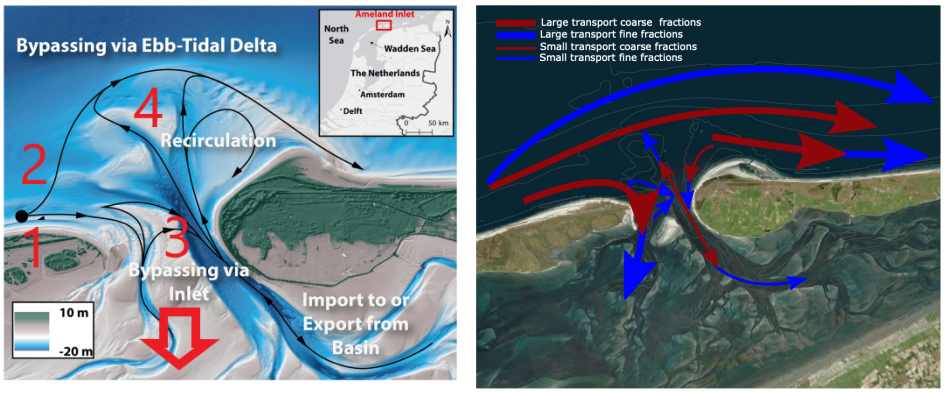

(a) Sediment connectivity with numerical indication Ameland Inlet Pearson et al. (2020)

(b) The main pathway of coarse and fine nourishment fractions (Bak, 2017)

Figure 2.5: The macro sediment pathways from previous researches (Pearson et al., 2020) and (Bak, 2017)

2.4. RELATIVE IMPORTANCE OF WAVES ON SEDIMENT TRANSPORT IN AMELAND INLET

Multiple researches have been performed to understand which regions are tide and wave dominant in the vicinity of Ameland Inlet. Two researches which are taken into consideration in this thesis are a report from Deltares about "Understanding the morphological processes at Ameland Inlet : Kustgenese 2.0 synthesis of the tidal inlet research " (Elias, 2020a) and "Exploring the relative importance of wind for exchange processes around a tidal inlet system" (Van Weerdenburg, 2019). The total sediment transport consists of sediment transport induced by waves, wind and tide. In the following section, the relative importance of the wind, wave, and tidal sediment transports are weighted against each other.

North Sea region of tidal inlet
From (Elias, 2020a) it can be concluded that on the ebb-tidal delta a very complex spatial distribution of tide and wave driven processes occur. Fig. 2.6a stresses this as an area in which tide and wave dominated areas blend into each other. Therefore, the sediment transport processes on the ebb-tidal delta are governed by both the waves and tide.
The North Sea coastlines of both Ameland and Terschelling are wave dominant. Therefore, the sediment transport processes are governed by waves at the adjacent North Sea coastlines of Terschelling and Ameland.

Wadden Sea region of tidal inlet
In the basin of Ameland Inlet a complex spatial distribution of tide and wave driven process occur. As mentioned in Section 2.2, waves in the North Sea and Wadden Sea area are mainly wind driven waves. Therefore, to differentiate between tide and wave dominant regions, the principles of the

relative influence of wind on shallow and deeper waters is applied. The shallow waters prevail at intertidal areas whereas relative deeper waters prevail at the channels. Wind driven waves have more influence on shallow waters than on deeper waters (Bosboom and Stive, 2021). The relative importance of wind in a tidal inlet system is further researched by (Van Weerdenburg, 2019). In this research the sediment transport of the 80% least windy tidal cycles in the basin are evaluated.

A result from (Van Weerdenburg, 2019) is used to indicate tide dominant regions of the basin. In Fig. 2.6b an overview is provided of Van Weerdenburg (2019) his findings.
Warm colours indicate locations where sediment transport is governed by (concentrated) tidal currents. Cool colours indicate locations where sediment transport is governed by meteorological forcing conditions as wind (Van Weerdenburg, 2019). The spatial pattern of wave and tide dominated areas highly corresponds with the bathymetry of Ameland Inlet.

The intertidal areas are more shallow and are thus susceptible for waves. Therefore, the total sediment transport is governed by wind, wave and tidal sediment processes at the intertidal areas.

The inlet gorge of Ameland Inlet is a deep channel which is thus less susceptible for waves. Therefore, the sediment transport by waves is likely to be minimal at this location. This implies that the relative importance of waves on sediment transport in a tidal inlet is minimal. Thus, the governing sediment transport process is the tidal sediment transport.

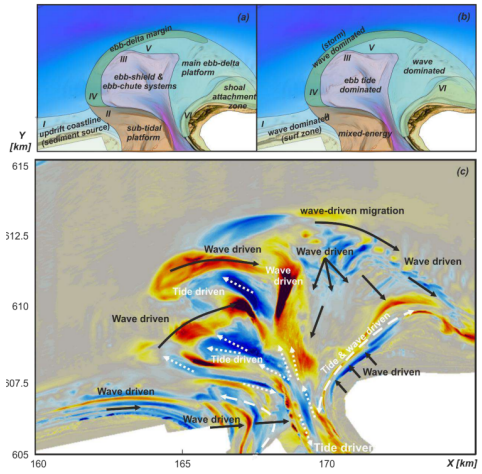

(a) Regions of the ebb-tidal delta in which wave and wind processes are dominant, adapted from (Elias, 2020a)

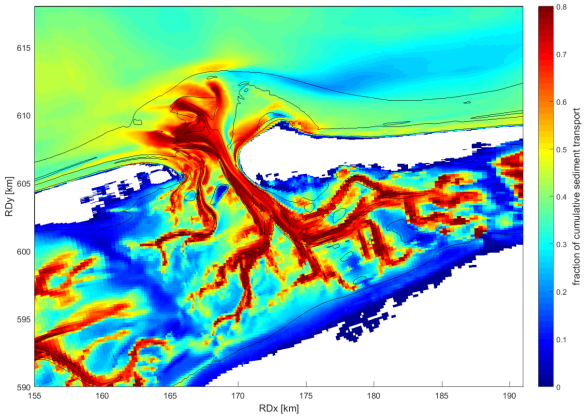

(b) Sediment transport in the 80% least windy tidal cycles (Van Weerdenburg, 2019)

Figure 2.6: Wave and tide dominated regions in for the tidal inlet components

2.5. NATURAL SEDIMENT TRANSPORT MECHANISM

In the traditional nourishment method, it is often desired that the sand remain at the vulnerable spot for as long as possible. With a nourishment with the Zandwindmolen, it is often desirable for the sand to move as quickly as possible to other nearby parts of the coast. After all, the vulnerable location is permanently resupplied with sand and is therefore no longer vulnerable.

The objective is to establish the quickest dispersion over the vicinity of Ameland Inlet from a continuous point nourishment by optimally using the forces of nature.

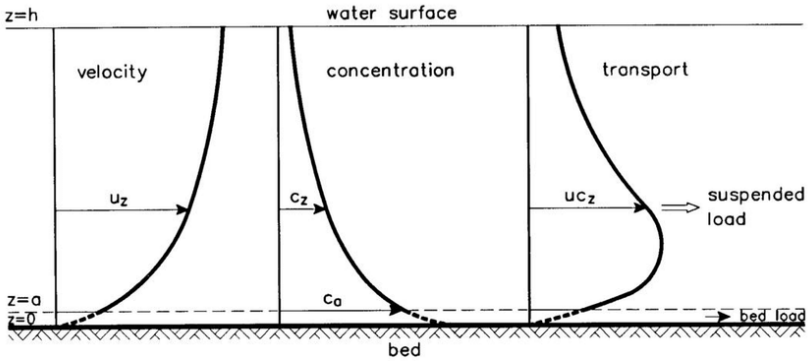

Figure 2.7: Regions of bed load transport and suspended transport (van Rijn, 1993)

The dominant sediment transport process in Ameland Inlet is suspended sediment transport (Section 2.3.1). The suspend sediment regime is from the top of the water column until a certain distance from the seabed. In order to fully utilize the dominant sediment transport and optimize the use of the forces of nature, the sediment must be placed as high as possible in the water column. Fig. 2.7 from (van Rijn, 1993) illustrates which part of the suspended load is transported by which transport regime. It can be concluded that on top of the water column, the velocity of the ambient water is the highest. Moreover, most of the sediment concentration is transported by means of the suspended sediment transport regime. Thus, optimal dispersion of sediment is obtained if sediment is nourished as high as possible in the water column.

Once the sediment is placed at the top of the water column, the sediment will begin to settle. In order to get as much horizontal displacement as possible, the sediment must be for as long as possible in the suspended sediment transport regime and the settling sediment must be maximally susceptible for ambient forcing.

In order to gain more knowledge about how the sediment can remain for as long as possible in the suspended load regime and how sediment mixtures can be influenced the most in the water column by ambient forcing, dredge plumes are studied in more detail. Dredge plumes typically represent the increase of turbidity caused by or during dredging operations (Winterwerp, 2002).

In general, near-field effects can be controlled while far-field effects have long time-lags and a strong impact on natural variability. Three types of dredging plumes may occur; a passive plume (mixing), dynamic plume (density current) or a transitional area in which both a passive and a dynamic plume occurs (Winterwerp, 2002). In Fig. 2.8 the conditions per type of plume are illustrated. From this figure it can be concluded that plumes depend on the Richardson number and velocity ratio.

Major distinctions between the passive and dynamic plume are described in the following section. A dynamic plume is a high-concentration mixture pumped into the water column and behaves as a density jet or as a cloud/plume (cloud settling) of particles. As a consequence, the sediments descend rapidly to the bed (dynamic plume moving due to internal forces) (van Rijn, 2020).

Basic processes for dynamic (density) plumes are according to van Rijn (2020):

- initial descent of plume to bottom (cloud or convective settling);
- settling from high-concentration near-bottom layers as density current;
- horizontal flow of density current along bed;

Passive plumes or mixing plumes are depicted by low-concentration mixtures whom are pumped into the water column and dispersed over the depth by turbulence and settling due to individual

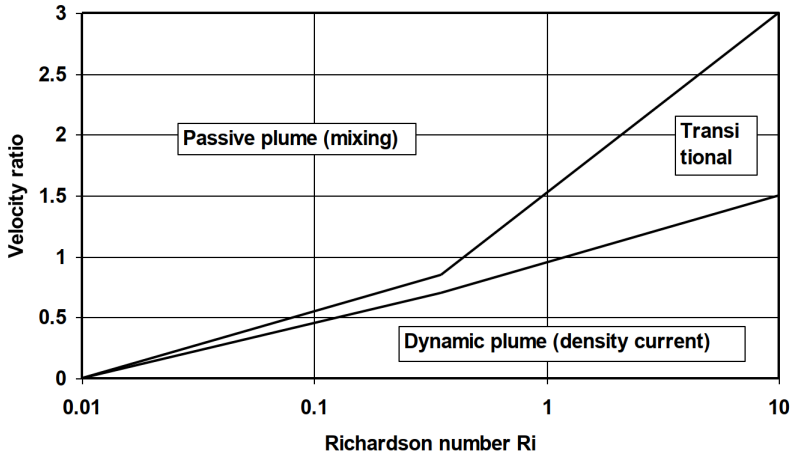

Figure 2.8: Dynamic and Passive plume (Winterwerp, 2002)

sediments (van Rijn, 2020). It can be considered as a passive plume since the plume moves due to to external forces.

Basic processes for passive plumes are according to van Rijn (2020):

- segregation of fractions (heterogeneous sediments); larger particles have larger settling velocities;
- horizontal advection by wind-driven, tide-driven and wave-driven currents;
- lateral diffusion due to turbulent forces generated by currents;

In a mixing plume the sediment settles according to the individual settling velocity of a particle. This is the slowest manner for a particle to reach the bed and thus optimizes the duration that a particle is in the suspended load regime. Moreover, in a mixing plume the sediment mixture is susceptible for the ambient tidal current. When nourished in the fast flowing tidal inlet, this is expected to lead to large initial dispersion during the initial settling process. Concluding, for nature to move the sediment as quickly as possible to other nearby parts of the coast, the nourished sediment must be nourished in the form of a mixing plume.

On the contrary, a density driven flow will accelerate towards seabed. Therefore, the ambient flow has minimal effect on the nourished sediments. As a result, nature has little influence on the initial dispersion and will yield a direct placement of sediment in the channel wall. This could be a manner to achieve a placed tidal wall nourishment as discussed in (Rutteman, 2021) his research. In this research, a density driven flow is not the desired plume effect.

In figure 2.9 the plume types are depicted in a cross-section of the water column. Although this representation is based on a hopper, it does give a clear overview of the behaviour per type of plume. In a dynamic plume, the mixture moves and accelerates towards the seabed by means of a density driven flow. Whereas by a passive plume, the mixture is mixed over the water column due to an ambient flow.
During traditional dredge operations the latter is an undesired effect as this might cause suspended sediment concentratations (SCC) to rise over the water column, which in turn could cause sublethal effects or even mortality to fauna and flora in the area (van Rijn, 2020). In Appendix F mitigating measures for such plumes are discussed for TSHDs.
However, the Zandwindmolen is a completely different dredge concept. The Zandwindmolen con-

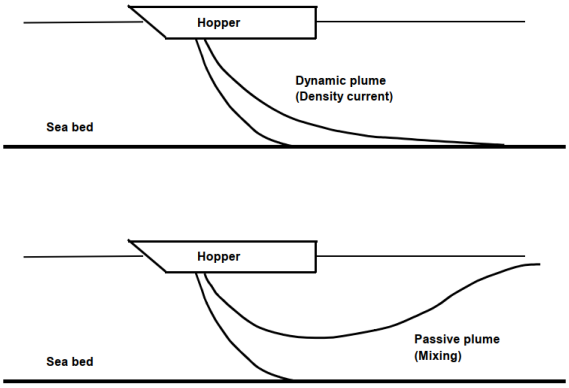

Figure 2.9: Behaviour of Dynamic and Passive plume (van Rijn, 2020)

tinuously nourishes a low volume and concentration sediment mixture. Therefore, the assumption is that the already existing background SCC of the system will not be exceeded in such a way that this might cause sub-lethal effects or even mortality of the surrounding natural system. Why this is expected is evaluated in the ecological impact of the Zandwindmolen (Appendix D.1). Hence, it is expected that a mixing plume is allowed for a continuous low volume nourishment.

2.5.1. REQUIREMENTS MIXING PLUME

A mixing plume is related to the degree of stratification. Stratification processes are described by the Richardson number (Kranenburg, 1998). Eq. (2.5.1) describes the Richardson number for a horizontal mixing process. According to Kranenburg (1998) the flow is stable if the Richardson number is larger than $\frac{1}{4}$ and unstable if the flow is « $\frac{1}{4}$. When the flow is stable it represents a dynamic (density) plume and when unstable a passive (mixing) plume.

$$Ri = \frac{-g\frac{\partial \rho}{\partial x}}{\rho_w \frac{\partial u}{\partial x}} \tag{2.5.1}$$

- g is the gravitational constant in $[\frac{m}{s^2}]$
- $\partial\rho$ is the difference between the mixture density ρ_{mixture} and the water density ρ_w in $[\frac{kg}{m^3}]$
- ∂x is the displacement in x direction in [m]; The x direction is considered to be along the tidal flow.
- ∂u is the difference between ambient flow (u_{ambient}) and mixture velocity (u_{mixture}) in $[\frac{m}{s}]$

Two parameters can be adjusted to ensure a mixing plume. The difference in density can be decreased by means of dilution or spreading and/or the difference between ambient flow and velocity by which the sediment mixture hits the water can be increased.

Mentioned in the elaboration of mixing plumes, was that sediment has to settle unhindered. When settling unhindered, the sediment settles according to their own settling velocity. Moreover, it was mentioned that mixing plumes are depicted by low-concentration mixtures. To satisfy both conditions the sediment concentration has to be lower than 1-2% (van Rijn, 1993). Within the Zandwindmolen project the pipes and pumps are developed by Royal IHC. According to their calculations the sediment volume concentration within the pipe is between 10-30 %. The actual sediment volume

concentration depends on the applied nourishment volume. Thus, the sediment has to be diluted by a factor 10-30 to ensure a mixture concentration lower than 1-2%.

2.5.2. CONCLUSION OPTIMAL DISPERSION BY NATURE

In conclusion, an optimal manner to transport sediment as efficient as possible by nature (and establish a high initial dispersion), depends on a combination of optimization of settling time and large ambient forcing. The settling time can be optimized by means of a large depth and the individual settling velocity of a particle. When sediment settles according to its individual settling velocity, the sediment is most prone to move with external forces. On a location where the external forces are the greatest, the sediment is carried the furthest in the direction of the ambient forcing. This can be accomplished by the implementation of a mixing plume.

2.6. NOURISHMENT REQUIREMENT AMELAND INLET

In this section an estimation of the nourishment requirement is determined based on solely sand. The relative nourishment requirement of the Dutch coastal system is determined by multiplying the SLR by the surface area of the coastal system.

$$\text{Nourishment requirement} = \text{SLR} \cdot \text{Surface Area} \tag{2.6.1}$$

For the determination of the relative nourishment requirement the following limitations should be taken into consideration. The nourishment requirement is relative, as the sand losses from the coastal system are not included. In addition, it is assumed that the nourished sand is distributed evenly in the coastal system and that it also rises proportionally with the rise in sea level. (Schuiling, 2019)

SLR
The SLR over the last decades was found to be 2 mm per year. However, there are also other scenarios in which the SLR is likely to be larger than the SLR over the last decades. According to KNMI (2021) the SLR is likely to accelerate. The different SLR scenarios for the dutch coastline are summarized in Table 1.1 (Chapter 1).

Surface area coastal system
The surface area of Ameland Inlet composes out of two components. On one hand there is the surface area of the basin and on the other hand there is the surface area of the ebb-tidal delta, adjacent coastline and coastal fundament. The basin is enclosed by the tidal sheds and the coastline of the main land. The surface area of the ebb-tidal delta, adjacent coastline and coastal fundament is enclosed by the seaward boundary and transects perpendicular to Terschelling and Ameland. The seaward boundary has been determined by RWS to be at -20m NAP. However, research shows that beyond the -15m NAP no more significant morphological changes occur. Nevertheless, in this study the set -20m NAP benchmark by RWS is used.

The surface area of Ameland basin with MHW is illustrated in Fig. A.1 in Appendix A.3 and is 309 km^2. The surface area of the ebb-tidal delta, adjacent coastline and coastal fundament of Ameland Inlet is found to be 255 km^2 (Walburg, 2002).

Nourishment requirement Ameland Inlet
The nourishment requirement is the amount of sand required to let the entire vicinity of Ameland grow along with the sea level rise (basin + outside regions). By applying Eq. (2.6.1) the nourishment

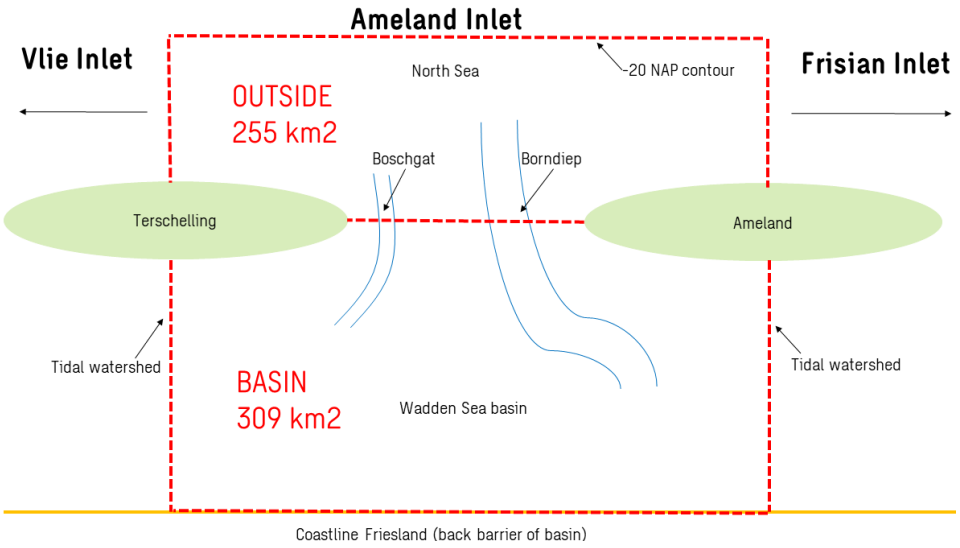

Figure 2.10: Sketch of outside and inside surface areas of the Ameland Inlet. The North Sea contour is closed by the -20NAP line. The tidal watersheds separate the Ameland Basin from the Vlie and Frisian Inlet. The nourishment requirements determined in Table 2.1 are based on the surfaces areas as depicted in this figure.

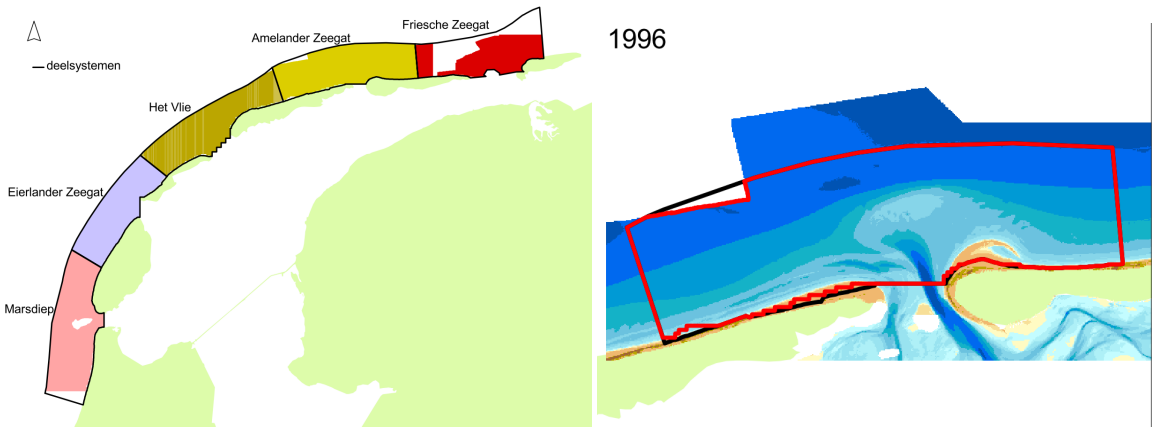

(a) Cubing of Dutch Wadden Sea Islands (from: (Walburg, 2002))

(b) Cubing of Ameland Inlet (from: (Walburg, 2002))

Figure 2.11: North Sea cubing of Dutch Wadden Sea Islands and Ameland Inlet in 1996 (from: (Walburg, 2002))

Table 2.1: Nourishment requirements for different SLR scenarios

SLR rate / year	**Historical**	**SSP1 bandwidth 2050**	
	2 mm	2.8 mm	8.7 mm
Basin (309 km^2)	0.618 Mm^3/year	0.865 Mm^3/year	2.688 Mm^3/year
Outside (255 km^2)	0.510 Mm^3/year	0.714 Mm^3/year	2.218 Mm^3/year
Nourishment requirement	**1.128 Mm^3/year**	**1.579 Mm^3/year**	**4.906 Mm^3/year**

requirement is determined based on the past decades and SSP1-2.6. The results are stated in Table 2.1. In this table the component outside is composed of the ebb-tidal delta, adjacent coastline and coastal fundament. According to this determination, the total nourishment requirement to let the vicinity of Ameland inlet grow as a whole with the sea level rise is 1.128 Mm^3 per year.
Concluding, based on Table 2.1 the current annual nourishment requirement composed of the sand demand and the outside region of Ameland inlet, is 1.128Mm^3/year. While anticipating on the future, it is expected that the sand requirement will only increase.

3 | Methodology

This study investigates the permanent nourishment of sand in the fast flowing Ameland inlet. Nourishing sediment continuously and allowing the environment of the Ameland inlet to grow with it, is a morphological issue that applies for the long term (years - decades). It was found in Section 2.4 that in the inlet the influence of waves on the sand transport process is limited. The effect of waves mainly affects the further redistribution of sediment at the coast. Therefore, the 2D Delft-3D Ameland Inlet model without waves was chosen for this study. In addition, more knowledge about how different particles sizes behave spatially in the vicinity of Ameland inlet is desired to know. Therefore, four sediment fractions of 100, 200 ,300 and 400 μm are examined in this research.

Delft-3D
Delft3D is a 3D/2D modelling suite for integral water solutions (Deltares, 2018) and is used as means to qualitatively and quantitatively analyse the Ameland Inlet. Within Delft3D multiple modules are available which are capable of simulating a variance of processes. As indicated, in the Ameland inlet the influence of waves on the sand transport process is limited, therefore the FLOW module is applied. The FLOW module is the main module within Delft3D and compromises a 2D or 3D simulation program that calculates the hydrodynamic conditions as a result of tidal forcing within a boundary fitted grid (Deltares, 2018). In Delft3D-FLOW, vertical density differences are taken into account in the horizontal pressure gradients and in the vertical turbulent exchange coefficients. So the application of Delft3D-FLOW is restricted to mid-field and far-field dispersion simulations of discharged constituents (Deltares, 2018).

3.1. Model background

In the following section the model background is discussed. The medium term model has been developed by (De Fockert, 2008). The model has been improved by (Jiao, 2014), and (Wang et al., 2016). Thereafter the Ameland Inlet model has been used for different scientific purposes. Bak (2017) has used the model to research different nourishment strategies within the vicinity of Ameland Inlet. Pearson et al. (2020) has used the model to research the sediment connectivity in the vicinity of Ameland inlet.
This model is set up based upon the latest version of Pearson et al. (2020). A more elaborated overview of the Delft3D modeling software can be obtained at (Deltares, 2018) and (Lesser et al., 2004).

The Flow module of Delft3D solves under the shallow water and Boussinesq assumptions the Navier stokes equations for an incompressible fluid. For this research a 2D and 3D model is used. For a 2D simulation, the vertical momentum equation is reduced to the hydrostatic pressure equation (Deltares, 2018).

3.1.1. Grid and Bathymetry

The original model is a 2D model and represents a 40 x 30 km domain. The west boundary crosses the midpoint of Terschelling whereas the east boundary crosses the midpoint of Ameland. Basin inward the model is delimited by the tidal watersheds of both islands and are considered to be closed

in this model. The flow grid has 174 by 162 cells, varying from 60m by 80m in the inlet to 600m by 700m in the offshore region. In north-south direction the model is delimited in the south by the main land of Friesland and in the north beyond the -20m NAP line.
The bathymetry in this model is constructed from the 2016 Vaklodingen survey (Rijkswaterstaat, 2016b).

3.1.2. FORCING MECHANISM

The forcing mechanisms in this model are solely based on a schematized morphological tide. It is stressed that waves and inter-basin wind-driven flows are not included in this model, although they are known to be important processes for Ameland Inlet (de Wit et al., 2019), (Van Weerdenburg, 2019). The schematized morphological tide (e.g. (Latteux, 1995)) propagates eastward along the offshore and seaward lateral boundaries.
This morphological tide is constructed by Lesser (2009) and represents the equivalent net transports observed in the main channel during a full spring-neap tidal cycle as two semi-diurnal tides using the M2,M4,M6 and artificial C1 diurnal component (Pearson et al., 2020).

3.1.3. BED COMPOSITION

Seabed sediment of Ameland inlet ranges between 100-400μm (Deltares, 1999) and is considered to be fine to medium sand. Therefore four sediment grain size classes were chosen (100, 200, 300, 400μm). A bed generation run (BCG) was carried out to redistribute the initial sediment distribution sampled by (Rijkswaterstaat, 1999) to a sediment distribution in equilibrium with the model bathymetry. In these BCG runs the bed level is static, but it does allow for the redistribution of sediments (van der Wegen et al., 2011). By doing so, a more realistic bed composition is generated compared to a minimal defined initial bed composition.
At the boundaries an equilibrium concentration is specified. The sediment load at the boundaries is equal to the sediment load in the interior of the model. This ensures that there is little erosion or accretion at the boundaries.
The sediment transport formula for both suspended as bed load transport is Van Rijn 2007. The morphological acceleration factor is set to 1.

3.2. MODEL METHODOLOGY

It was already introduced in Chapter 1 that for this study, a distinction is made between near-field, mid-field and far-field. Near-field describes the behavior of the nourished sand immediately after deposition (time scale: instantaneous to several weeks). Mid-field describes the behavior of the sand once it is on the bottom and moves further with natural processes (months to years). Far-field describes the behavior into the distant future (years - decades). This study focuses on the near-field and mid-field transport processes. The far-field behavior is only examined contemplatively and is therefore not within the model scopes.

This section provides a general description of how the model was used. Prior to the main study, which determines how the nourished sand volume is distributed by natural processes in the short and long term, a general hydrodynamic and morphodynamic model was simulated to acquire general data from the Vicinity of Ameland Inlet. Based on the results from this general hydrodynamic and morphodynamic model, in combination with the literature study (Chapter 2), a strategy of the continuous nourishment was determined. Fig. 3.1 provides an illustration of the methodology.

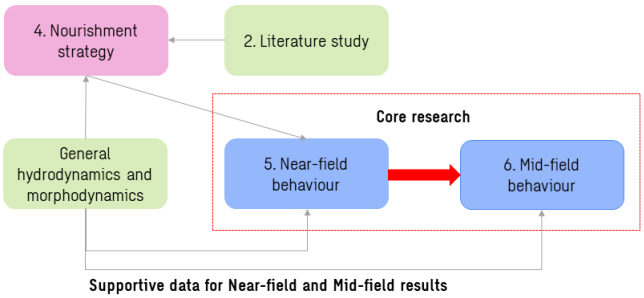

Figure 3.1: Overview of the methodology structure of this thesis.

Based on the strategy of the continuous nourishment, the core research on the usability of the Zandwindmolen is started. As indicated in Chapter 1, the usability of a Zandwindmolen depends on the extent to which the nourished sand volume is dispersed by natural processes in the short and long term. Therefore, first a short term model during a spring neap tide cycle was simulated. Afterwards, based on the near-field results found from the spring tide neap tide model, a mid-field model for six months was simulated.

Both the maximum and minimum dispersion were determined to determine a band width of the actual dispersion. Four natural background fractions are present in the applied Ameland Inlet model. The actual dispersion of nourished (artificial) sediment is determined by the mixing of artificial sediment with the background sediment. Delft3D works with a uniformly mixed bed (Deltares, 2018). In the case of deposition of artificial sediment in a grid cell with natural background fractions, the artificial sediment will be uniformly mixed through the natural background fraction sediment layer. The proportion of presence of artificial sediment to the natural background fraction determines how much artificial sediment is brought into suspension. In case of a low volume continuous nourishment, the proportion of artificial sediment to the natural background fractions is low and will eventually lead to an underestimation of the dispersion. This leads thus to a minimal dispersion. By deleting the natural background fractions, the bed forms a "concrete bed" and the artificial sediment does no longer mix with the natural background fraction. As a result, the sediment brought into suspension is always the artificial sediment. This leads to maximal dispersion. In conclusion, the minimal dispersion is obtained when the natural sediment background fractions remain in the model, while the maximum dispersion is obtained when the natural sediment background fractions are removed. Therefore, to determine both the maximum and minimum dispersion, the near-field and mid-field dispersion with and without natural background fractions are determined. The methodology is identical for both the maximum and minimum dispersion. An illustrative overview is depicted in Fig. 3.2.

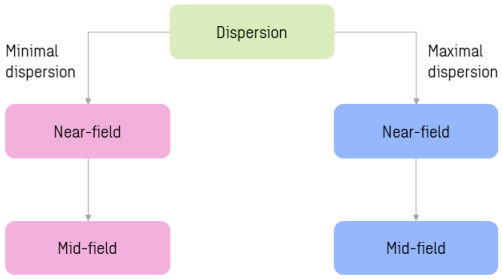

Figure 3.2: Overview determination of the minimal and maximal dispersion on different timescales

The following subsections provide a global methodology on the numerical model setup and how the results are analyzed. In chapters 5 and 6 a referral to Appendix H is made. In this appendix there is an exact description about how the successive models were modeled based on the results found earlier.

3.3. NUMERICAL MODEL SETUP AND DETERMINATION OF RESULTS

This section addresses how the numerical setup of the simulated models is performed globally, how the numerical analysis is performed and how results are formulated.

3.3.1. GENERAL HYDRODYNAMICS AND MORPHODYNAMICS

The objective of this model is to gain quantitative knowledge about the hydrodynamics and morphodynamics of the Ameland Inlet. In addition, these quantitative data are used, in conjunction with the literature review, to determine a nourishment strategy.

A spring neap tide cycle includes both maximum and minimum tidal flow regimes. To obtain an indication of the general hydrodynamics and morphodynamics, the model was simulated for a spring neap tide cycle. Measurements were taken per 10 minutes (600 seconds).

The exact model modifications to fit the Ameland model to this research are described in Appendix H.1.

The research questions which are answered based on the quantitative data are:

1. How does the dominant tidal flow relate across multiple locations in the tidal inlet?
2. How much sediment can potentially be continuously nourished in the Ameland inlet?
3. What is the expected initial dispersion of a settling sediment particle?

The following section describes for each research question how a numerical answer is determined based on the results found. The design of a nourishment is an iterative process in which "where should the sediment be nourished" and "how much sediment can potentially be nourished at a location" are interdependent.

1.) Dominant tidal flow

In reality, a water particle would make an elliptical motion across the inlet during an ebb and flow cycle. Because in a tidal inlet the water mainly flows in and out, this elliptical movement has been considered for convenience as a movement in and out of the tidal inlet. As a result, only the ebb and flow water velocities are considered.

The velocity signal contains an X and Y value and is either positive or negative depending on ebb or flood. With Eq. (3.3.1) the velocity signal is converted to a signal in either positive or negative direction.

$$v(t) = (\sqrt{X(t)^2 + Y(t)^2}) \cdot \frac{X(t)}{abs(X(t))} \tag{3.3.1}$$

In words, the velocities in X and Y components are squared and added to each other. Thereafter the square root of this value is taken to obtain the resulting velocity. By multiplying the resulting velocity with the value of the X component divided by the absolute value of the X component, the already obtained resulting velocity is translated in either a positive or negative value.

Then, how often a flow velocity occurs is measured. This is incorporated into a histogram with a bin-width of 0.5 m/s. This is done for multiple locations along the tidal inlet. Based on the desired nourishment effect, which is inducing artificial sediment towards the Wadden Sea and the intertidal components on the North Sea side, a choice can be made about where exactly in the inlet channel the nourishment can be carried out.

2.) Maximum potential nourishment
In order to understand the maximum potential nourishment, the maximum transport capacity has to be determined. It was found in Section 2.4 that in the tidal inlet the influence of waves is minimal. Therefore, the tidal transport is a good estimate for what the Ameland Inlet should be able to process as maximum potential nourishment.

Through the tidal inlet there is both an ebb and flood current. The ebb current is directed towards the North Sea and the flood current is directed towards the Wadden Sea. The potential tidal transport is determined by adding the cumulative sediment transport in the flood and ebb direction separately over a spring neap tide cycle. This is the tidal transport in either ebb or flood direction. Thereafter, the tidal transports in ebb and flood direction are added to one another. By doing so, the gross tidal transport is determined for a spring neap tide cycle. This is the potential tidal transport over a spring neap tide cycle. Finally, the found potential tidal transport is multiplied by (52 weeks annually / 2 (approximately a spring neap tide cycle) =) 26 to obtain the potential annual tidal transport.

3.) (RQ.1) Maximum initial dispersion without re-suspension

On the chosen nourishment location the expected initial dispersion by the settling process is determined. This is done for four (100, 200 ,300 and 400 μm) sediment fractions.

It was found in Section 2.5.2 that the distance over which the particles are transported depends on the depth, the individual settling velocity of the particles and the horizontal advection by the tide. The depth depends on at which moment it is measured during the ebb and flood cycle.

The individual settling velocity of the fractions of 100, 200, 300 and 400 μm is obtained from Stokes Eq. (3.3.2).

$$w_s = \frac{g(\frac{\rho_s}{\rho_w} - 1)d^2}{18\mu} \tag{3.3.2}$$

In which:

- g = gravitational constant = 9.81 $[\frac{m}{s^2}]$
- ρ_s = density solids = 2650 $[\frac{kg}{m^3}]$
- ρ_w = density water = 1030 $[\frac{kg}{m^3}]$
- μ = Viscosity = 4e^{-5} / (10 + T) Pa [· s] in which T in degrees Celsius
- d = d_{50} of particle diameter [m]

The settling velocities for the different fractions are respectively from the smallest to the largest fraction 0.0044, 0.0145, 0.0288 and 0.0435 $\frac{m}{s}$.

To determine the initial longitudinal distribution, it is assumed that the nourishment equipment is fixed (stationary nourishment). Furthermore, it is assumed that the nourished sediment directly

has the same horizontal flow velocity as the ambient flow. To obtain the settling time, the depth is divided by the settling time per fraction. The horizontal ambient flow acts as a horizontal advection transport mechanism for the individual settling particle. The horizontal distances are obtained by multiplying the settling times with the average horizontal flow velocity.

- Once a particle touches the water surface at x=0, it holds the initial horizontal ambient flow condition at that specific moment during the settling process
- The settling velocity of the different fractions is the individual settling velocity
- The settling velocity is constant and no turbulence occurs
- The seabed has an uniform depth

The determination of the preliminary longitudinal distribution is made by means of histogram analysis. A bin width of 500 meters is set to count the amount of times a particle settles in a predefined region. The different fractions are stacked to obtain the summed particles in a certain bin. In this study it was decided to have each fraction appear equally often in the nourishment. Therefore, the particle size distribution (PSD) is assumed to be an equal distribution of the four present particles.

3.3.2. NOURISHMENT STRATEGY METHOD

In this study, the determination of an optimal nourishment strategy that achieves the nourishment objective from a fixed location is an iterative trade-off process between:

1. Local flow conditions
2. Local sediment transport capacity
3. Regional flow conditions and tidal sediment transport capacity

The iterative process is illustrated in Fig. 3.3.

Firstly, the initial direction of dispersion during the settling process in a mixing plume is determined by the direction of local flow conditions in the tidal channel. Secondly, the nourishment location must locally be capable of processing a certain nourishment volume. Therefore, the local sediment transport capacity must be sufficient. Thirdly, flow conditions and sediment transport capacity must be regionally such that further spread of the nourished sediment occurs.

The results of this iterative process are described in Appendix I.

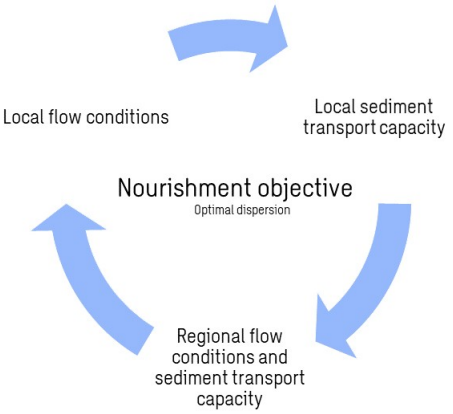

Figure 3.3: Iterative process to determine the exact location of the nourishment.

3.3.3. NEAR-FIELD DISPERSION

Near-field describes the behavior of the nourished sand immediately after deposition (time scale: instantaneous to several weeks).

The near-field numerical analysis is performed to assess on top of the maximum initial settling dispersion (Section 3.3.1) the effects of re-suspension and eventual dispersion after a spring neap tide cycle.

Numerical model setup
It follows from the literature study that the initial settling process is crucial for optimal initial dispersion. Therefore the 2D flow model was converted to a 10 layer 3D flow model. In this way the sediment can be modeled at the top of the water column using the discharge method of Delft-3D.

The particle size distribution (PSD) of the nourished sediment is an artificial curve in which each fraction (100, 200, 300, 400μm) occur equally. In this way, the behavior for each particle fraction can be determined and weighed against each other.

The simulation time of the model is a spring neap tide cycle period.

The further dispersion (mid-field dispersion) of the settled sediment during this spring neap tide cycle period is done by means of a 2D model because of time limitations. Therefore a 2D model is modeled in an identical manner to the 3D model. The difference lies in how the initial distribution of the nourished sediment is processed by the discharge method in Delft-3D. Again, if the depth is not layered, Delft-3D mixes the discharged sediment uniformly over the water column. The 2D model results serve as support to get the hot-start to the mid-field dispersion as accurate as possible. The results of the 2D model can be found in Appendix J.

In Fig. 3.4 an illustrative consideration is provided over how the sediment is modelled in both the 3D and 2D model.

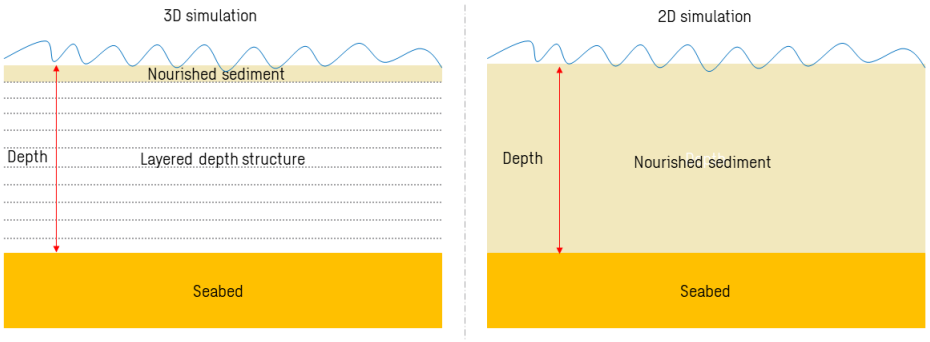

Figure 3.4: Illustration of how the sediment is discharged in the 3D and 2D model.

The model is simulated in duplicate to determine both the minimal and optimal dispersion during the initial settling process as illustrated in Fig. 3.2.

In the introduction of the near-field results a referral is made to Appendix H. In this Appendix the exact model steps are formulated. In Appendix G.1 the discharge parameters can be found.

Processing of Near-field dispersion RQs
How the RQs regarding the near-field dispersion are analyzed and answered is discussed in the following section.

RQ2: Spatial initial near-field dispersion
By means of the spatial dispersion, a qualitative analysis is performed in which it is determined to which components of the tidal inlet system the dispersion per fraction extends after a spring neap tide cycle of continuous nourishment. In addition, for each fraction the maximum displacement distance from the source (the nourishment location) to the outermost region where the corresponding fraction is observed is determined. This is done in both the North Sea and Wadden Sea directions. First the X and Y co-ordinates of the source and the outermost region where the respective fraction is observed are determined. Afterwards the absolute distance is determined by means of Pythagoras.

RQ3: Near-field longitudinal distribution of initial dispersion
A transect was made along the length and shape of the tidal channel to gain insight into the longitudinal distribution of each separate fraction after a spring neap tide cycle of continuous nourishment. Through this method, the degree of dispersion from the nourishment location is determined. It also shows where the most sediment per fraction settles over the length of the tidal channel. The transect is made with the Quickin tools from Delft-3D. The results lead to information regarding where the peak available mass of sediment can be found per fraction over the tidal channel. Besides that, the distance from the nourishment location to the peak available mass of sediment can be determined. By doing so, the regions in which the most accretion is likely to occur are determined.

3.3.4. MID-FIELD DISPERSION

The mid-field dispersion describes the behavior of the sand once it is on the bottom and moves further with natural processes (months to years).

Numerical model setup
The mid-field models are a 2D hot-start of the 3D near-field models. It is therefore emphasized, that at the start of these models artificial sediment is present in the models from the previous nourishment over a spring neap tide cycle. An illustration of the mid-field dispersion numerical setup is displayed in Fig. 3.5.

The available mass of sediment from the nourished fractions (100, 200, 300, 400μm) during the spring neap tide cycle were exported, processed with Quickin and loaded as bed at the start of the mid-field dispersion models. In this way, the initial dispersion found from the settling process is simulated most accurately.
The mid-field dispersion has a dichotomy in follow-up simulations. On the one hand, the mid-field dispersion over six months of only the nourished sediment from the near-field dispersion is determined. This mid-field dispersion is referred to as the simulation without continuous nourishment. On the other hand, the mid-field dispersion over half a year of the nourished sediment is determined from the near-field dispersion, while during the simulation time of half a year continuously sediment is nourished. This mid-field dispersion is referred to as the simulation with continuous nourishment.

The models **with** continuous nourishment over six months are modeled as follows. Based on the near-field dispersion longitudinal distribution, the distance at which the peak available mass of sediment lies relative to the original nourishment location was determined. This peak available mass of sediment, is considered the "new" nourishment location for the mid-field dispersion model with continuous nourishment. If a fraction shows a bi-modal spectrum, a new discharge location is modeled on both the North Sea and Wadden Sea side. For an illustrative and more exact methodology see Appendix H.2.

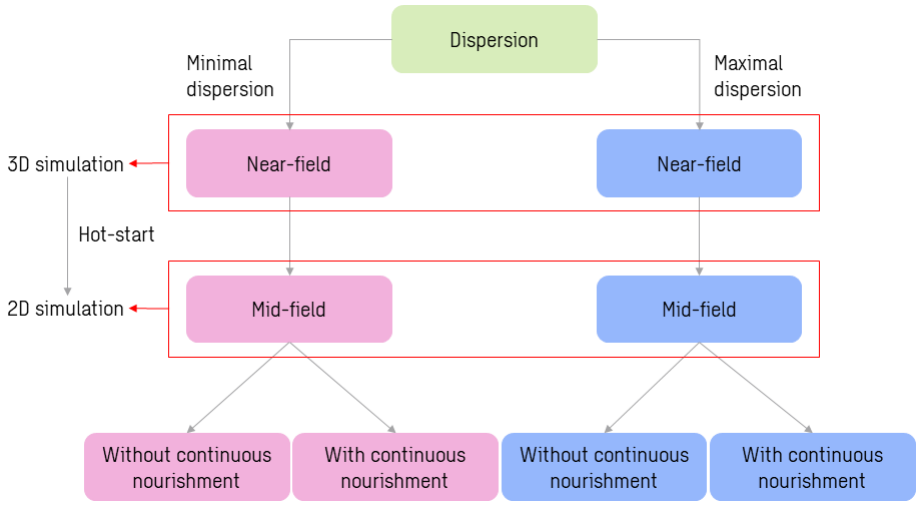

Figure 3.5: Illustration of the mid-field dispersion numerical model setup.

The models **without** continuous nourishment are solely a hot start of the near-field dispersion.

In the introduction of the mid-field results a referral is made to Appendix H. In this Appendix the exact model steps are formulated. In Appendix G.1 the discharge parameters can be found.

Processing of Mid-field dispersion RQs
The mid-field dispersion results are analyzed by means of the same tools and methodology as the near-field dispersion. An extra analysis is added regarding the siltation of the tidal channel. How the RQs regarding the mid-field dispersion are analyzed and answered is discussed in the following section.

RQ1: Mid-field siltation of tidal channel
The mid-field siltation of the tidal channel is determined by means of an evaluation over time of the cross-section at the nourishment location. The cross-section is made with the Quickin tools from Delft-3D. This evaluation is performed for both with and without continuous nourishment simulations.
The morphological update is turned on for the mid-field dispersion models. Therefore, under proper hydrodynamic forcing the sediment fractions can move on the sea bed. At the maximum dispersion model branch, the natural background fractions are removed. As a result, there is no natural background sediment in many areas in the model. Therefore, there are only morphological changes at locations where nourished sediment fractions are found. These are found due to the near-field dispersion, close to the nourishment location. Because sediment is being nourished above the deepest region of the tidal channel, the sediment most likely settles in the deepest part of the tidal channel.

As the tidal channel strives for an equilibrium cross-section, in reality the channel will be able to react through abrasion on the channel walls. Since these cannot abrase due to the absence of natural fractions (they are fixed), the behavior will be inaccurately described for the maximum dispersion. Therefore, the behavior of the wet cross section of the tidal channel can only be accurately described with the presence of the natural background fractions. As, this is where natural background fractions are present at the tidal channel walls. This belongs to the minimum mid-field dispersion model branch.

RQ2: Mid-field spatial dispersion
The mid-field spatial dispersion is determined the same as the near-field spatial dispersion. First a

qualitative analysis is performed in which it is determined to which components of the tidal inlet system the dispersion per fraction extends after a half year. Thereafter, the maximum dispersion distances are determined by means of Pythagoras. The spatial mid-field dispersion was determined for both with and without continuous nourishment simulations.

RQ3: Amount of sediment that can be processed by the tidal channel
The amount of sediment that can be processed by the tidal channel is determined by means of the mid-field siltation of the tidal channel and a mid-field longitudinal distribution. The mid-field longitudinal distribution is determined over the same longitudinal distribution as the near-field and with the same methodology. The mid-field longitudinal distribution is evaluated over time, to assess how the dispersion behaves over time. This evaluation is performed for both with and without continuous nourishment simulations.

4 | Nourishment strategy

This chapter discusses the nourishment strategy. First, the nourishment objective is determined. Based on the information from the literature study (Chapter 2) and quantitative hydrodynamic and morphodynamic results (Appendix I), an optimal nourishment location is chosen. In this chapter, only the conclusions from this iterative process are used to determine a nourishment strategy. Thereafter, the optimal nourishment design is illustrated. The nourishment is designed in such a manner to meet the nourishment objective.

4.1. NOURISHMENT OBJECTIVE

The objective of the nourishment is that the continuous nourishment must ensure growth with the sea level rise of the entire Ameland Inlet (Basin and outer delta, coastal foundation and surrounding coastlines).

Therefore, the fixed continuous nourishment strategy must be such that the dispersion of the sediment reaches the North Sea side (outer delta, coastal foundation and surrounding coastlines) and the Wadden Sea (intertidal areas).

Whether the objective of a continuous nourishment with a Zandwindmolen can be achieved, depends on the extent to which the nourished sand volume is dispersed by natural processes in the short and long term.

Short term dispersion objective
An objective of the short-term dispersion is to provide direction to the mix plume to the North Sea and Wadden Sea. Section 2.5 showed that direction during the initial settling process (short term) can be provided by horizontal external forces acting on the settling particle. Because the nourishment is continuous in the tidal inlet, this will cause the mix plume to be transported locally directly after placement with the tidal current towards the North Sea or Wadden Sea. Large dispersion is obtained if the horizontal forces are large.
Another objective is that the local sediment transport capacity must be sufficient to process large nourishment quantities.

Long term dispersion objective
The longer-term objective of the continuous nourishment is to keep the dispersion high towards the North Sea and Wadden Sea. To achieve this objective, sediment transport capacities and flow rates must remain regionally high towards the North and Wadden Sea.

4.2. OPTIMAL NOURISHMENT LOCATION AND NOURISHMENT VOLUME

An optimal nourishment location and nourishment volume positively influences both the set short- and long-term objectives. In the upcoming section, a nourishment location is first determined based on the tidal flow. Afterwards, a nourishment volume is determined based on the tidal sediment transport capacity at the chosen nourishment location.

How does the dominant tidal flow relate across multiple locations in the tidal inlet?
Fig. 4.1 illustrates a summary of the determined dominant flow regimes over the Borndiep channel

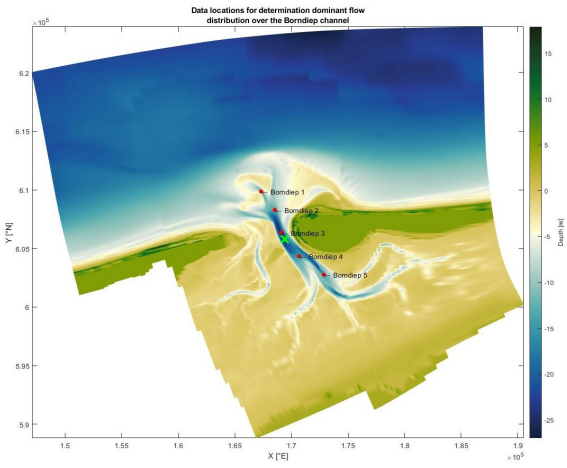

(a) Locations for further research regarding flow velocities. In red the locations over the Borndiep channel are indicated which are researched in the flow velocity is researched in more detail. In green the chosen nourishment location is depicted. The North Sea is depicted on the upper part of the image, whereas the Wadden Sea is depicted on the lower part of the image. In the Wadden Sea the channels are clearly visible. The island on the left is Terschelling and the Island on the right is Ameland.

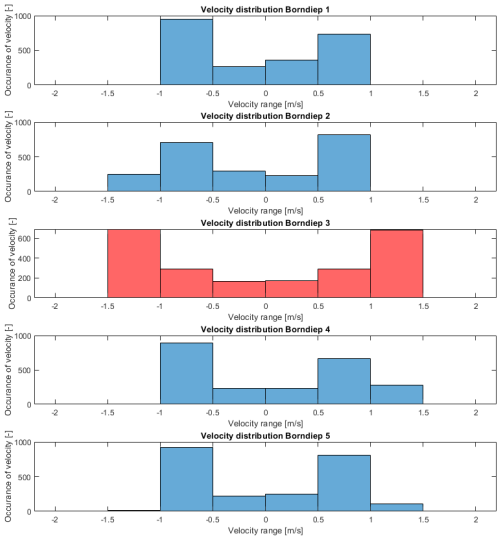

(b) Velocity distribution over the main channel. The negative flow velocities are directed to the North Sea and the positive flow velocities are directed to the Wadden Sea.

Figure 4.1: Dominant flow research over the length of the Borndiep channel.

(Appendix I.1). In Fig. 4.1a the locations where the flow is measured are illustrated and in Fig. 4.1b the histograms about the occurrence of a flow condition is illustrated.
From Fig. 4.1b it is concluded that over the length of the Borndiep the peak flow is dominantly dominant over milder flow conditions. So it flows mainly fast over the entire length of the Borndiep channel. At Borndiep 1 and 2, the peak flow velocities are dominant towards the North Sea. This is likely due to jet flow asymmetry (Section 2.3.1). At Borndiep 4 and 5 the peak flow velocities are dominant towards the Wadden Sea. This is likely due to tidal asymmetry (Section 2.3.1). At Borndiep 3, the highest peak flow velocities are measured to both directions and, these peak flow velocities occur most frequently compared to Borndiep 1,2,4 and 5.

What is the optimal nourishment location?
At Borndiep 3 the highest local flow velocities have been measured towards both the North Sea and Wadden Sea. The mixing plume here will be steered in such a way that it has the most chance of transporting sediment towards both the North Sea and the Wadden Sea. Whereas, the other locations are predominately directed towards the North Sea or Wadden Sea. Therefore, the location that suits the short term nourishment objective the best is the Borndiep 3 location. This location is located at the gorge of the inlet and is indicated in red in Fig. 4.1b.

How much sediment can potentially be continuously nourished in the Ameland inlet?
At the set nourishment location indicated with a green cross in Fig. 4.1a tidal sediment transport capacity is determined. The annual nourishment volume is determined based upon a trade-off between the tidal sediment transport capacity and the nourishment requirement of the Ameland Inlet. The nourishment requirement was found to be 1.128 Mm^3 under the current sea level rise (Section 2.6). E.g.: If another distribution of the sediment is required, another location can be chosen. If for instance more sand is needed along the North Sea side the locations of Borndiep 1 or Borndiep 2 are more logical. In this study however is location Borndiep 3 used, since this is expected to give the most distribution towards both North Sea and Wadden Sea.

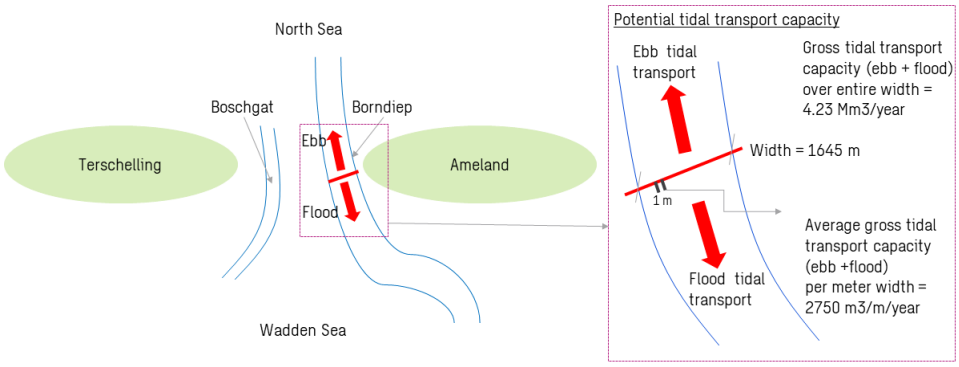

Figure 4.2: Overview of gross tidal sediment transport capacity of the Borndiep channel. This image also illustrates how the average gross tidal sediment transport capacity per meter is obtained.

It was found in Section 2.4 that in the Ameland tidal channel the tidal sediment transport is dominant over the wind and wave sediment transport. Thus to determine how much sediment transport potentially can be nourished continuously, the annual tidal sediment transport capacity is determined at the set nourishment location. In Appendix I.2 it is concluded that at this location, the Borndiep channel has the highest tidal transport capacity. It is determined that the Borndiep can process 4.23 Mm^3 per year over the entire cross-section of the Borndiep channel (sum of flood and ebb transport capacity). The width of the cross-section is 1645 meters. Thus, the average tidal sediment transport capacity per meter width is (4.23 Mm^3 / 1645 m =) 2750 m^3 per meter per year. In Fig. 4.2 a visualisation of the gross sediment transport capacity is provided.
The Zandwindmolen benefits from large nourishment volumes because of a reduction in marginal costs. Based on the tidal sediment transport capacity, the nourishment requirement and the expected growth of this nourishment requirement in the future, a system is studied with a nourishment rate of 2Mm^3 per year.
Because the Borndiep has an average annual tidal sediment transport capacity of 2750 m^3 per meter per year, the 2 Mm^3 nourishment can not be processed from a fixed location. To process a 2 Mm^3 nourishment, the nourishment must be spread over a total width of (2Mm^3 / 2750 m^3/m/year =) 700 perpendicular to the ebb / flood flow. As the annual tidal sediment transport capacity of 2750 m^3 per meter per year is a cross-sectional width averaged value, it is likely that when the sediment is continuously nourished in the deepest region of the Borndiep less meters of width are required perpendicular to the flow.
The average tidal prism of the Ameland Inlet is 478 Mm^3 (Elias et al., 2012). This is the water that flows in- and outwards per tidal cycle (12 hours and 25 minutes). An annual continuous nourishment of 2 Mm^3 is equal to a continuous nourishment per tidal cycle of 2778.3 m^3. The volume of sand that is added is therefore 0.13% of the tidal prism. This is considered to be very small and therefore does not affect the tidal prism.

4.3. NOURISHMENT DESIGN

Based on the aforementioned results a design of the continuous nourishment is made.
At the nourishment location, the depth averaged water velocity ranges between the -1.3 and +1.3 $\frac{m}{s}$. According to Fig. I.2b in Appendix I.1, the local depth fluctuations at the nourishment location range between 23.7 and 25.9m.

In Fig. 4.3 the nourishment design is depicted. Based on the aforementioned tidal transport capac-

ity, it is decided with Sweco to spread the continuous nourishment of 2Mm^3/year over a surface of (70m (length) x 540m (width)) = 37.800m^2. The nourishment is released at the top of the water column. On the depicted area in red (Fig. 4.3), continuously sediment is nourished. The fractions which are being nourished continuously are the 100, 200, 300 and 400 μm fractions. It was decided to nourish every fraction with the same amount. In this way, the behavior for each particle fraction can be determined and weighed against each other. The sand flux at which the sediment is nourished is 101.47$\frac{kg}{s}$ (Appendix G).

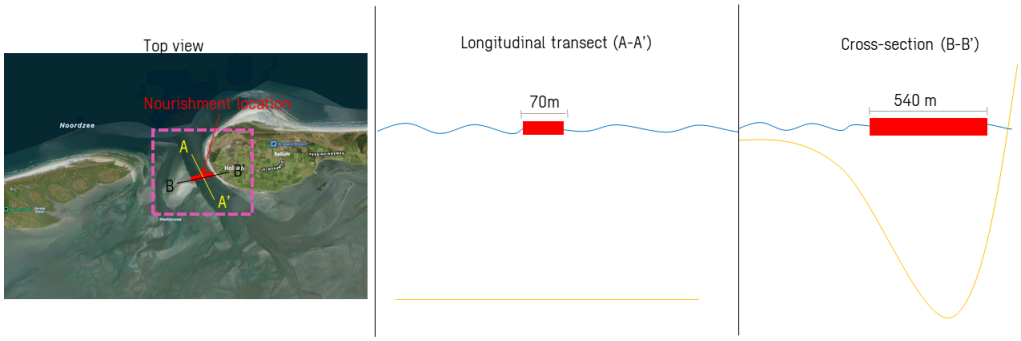

Figure 4.3: Nourishment strategy. Left figure is a top view of where the nourishment is executed. In red the nourishment area is depicted. In the center figure, the length over which the nourishment is spread out is depicted. In the right figure, the width over which the nourishment is spread is depicted.

4.4. NOURISHMENT EQUIPMENT

For the determination of the dredge equipment, an optimization issue is performed in Appendix L. From the foundation of the Zandwindmolen, the issue starts with a pipeline coming from an offshore area on the seabed. From Section 2.5, it appears that the sediment should be nourished as high as possible in the water column in order to maximize initial dispersion. In addition, the nourished sediment must exhibit mixing plume in order to achieve the greatest possible advection with the tidal current. A mixing plume cannot be realized with stationary open pipeline discharge. This is illustrated in Fig. 4.4. A nourishment carried out in this way generates a density plume. The by coming effects are not desired for a nourishment with the Zandwindmolen philosophy.
One method that does connect to forming a mixing plume is nourishment with a spray pontoon Fig. 4.5a. In the current practice a moving spreader pontoon may be used to place lifts of limited thickness. In general, a nourishment layer thickness up to 0.25 meters can be realised. As a result, the nourished layer has low densities (van't Hoff and van der Kolff, 2012). But, placing lifts is achieved by means of the segregation process and the corresponding individual settling of various particle sizes Fig. 4.5b. Therefore, the spreader pontoon uses a mixing plume to place sediment.
Another criterion is that the flow must be unstable (Richardson number « $\frac{1}{4}$) to form a mixing plume. Moreover, the sediment mixture has to be diluted to 1-2% (Section 2.5.1). This can be done on various manners and are described in Appendix L. However, a spray pontoon is normally used for inland waters. Therefore, for use in a tidal inlet, the spray pontoon must be made sea worthy. The foundation of the Zandwindmolen is that sediment is nourished continuously. Therefore, a 100%

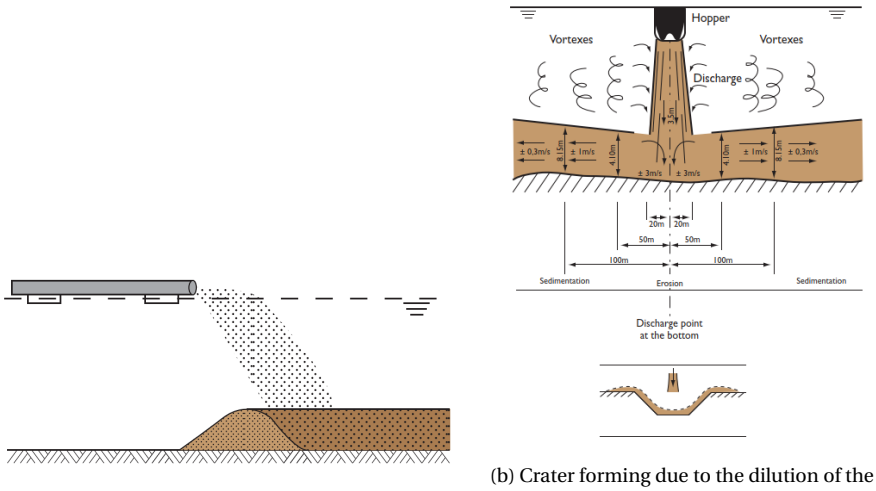

(a) Pipeline discharge on top of water column (van't Hoff and van der Kolff, 2012)

(b) Crater forming due to the dilution of the sand water mixture flow in the water column (van't Hoff and van der Kolff, 2012)

Figure 4.4: Illustration of open pipeline behaviour. This behaviour is undesired as it creates a density driven current to the seabed.

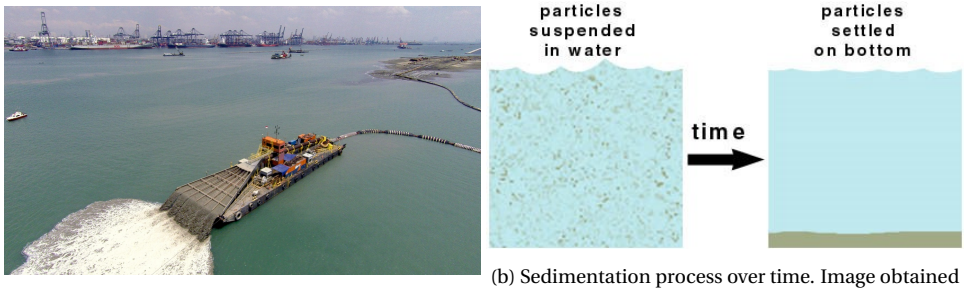

(a)

(b) Sedimentation process over time. Image obtained from (Casiday et al., 2008)

Figure 4.5: In the left image an example of the spreader pontoon is illustrated. In the right image the process over time which is desired to obtain by placing the sediment as a mixing plume is illustrated.

workability must be ensured. From Appendix I.4 it follows that the spreader pontoon must be designed such that it can operate while being exposed to a significant wave height (H_s) of 218 cm and significant wave period (T_s) between 3.8 - 10.7s.
The dimensions of the spreader pontoon are not such that it can cover the nourishment width of 540 meters at once (Section 4.3). Therefore, the spray pontoon must be movable. A pontoon can be hauled by winches between the 9-18 meters per minute (Dickhof, 2016). But, new winches allow to haul with a speed up to 120 meters per minute (2m/s) (Stema, 2022). Besides winch systems, propulsion systems are also optional. The propulsion speed of spreader pontoons can be up to 2-3 knots (1-1.5 m/s) (IADC, 2002). Therefore, it is assumed that the spreader pontoon must be able to move with a speed of 1 m/s. To cover the 540 meters of width, the spreader pontoon would need 540s (9min). Therefore, for the round trip the spreader pontoon would need approximately 18min. The bandwidth for hauling speeds between [9 m/min - 120 m/min] for a round trip are [60 - 4.5 min].
The total width of the Borndiep channel at the nourishment location is approximately 1600 meters. Therefore, the nourishment covers approximately a third of the total width of the tidal inlet. Clear signaling is required to ensure that (recreational) vessels do not collide with the spreader pontoon. But in general, the tidal inlet has plenty of space to allow vessels to pass while simultaneously nourish with a movable spreader pontoon.

5 | Near-field dispersion

In this chapter the near-field dispersion research questions are addressed. Near-field describes the behavior of the nourished sand immediately after deposition (time scale: instantaneous to several weeks).

The total near-field dispersion is composed of:

1. Dispersion through the initial settling process of sediment
2. Dispersion through re-suspension of settling sediment particles
3. Dispersion after sediment is deposited on the sea bed (natural bed load transport and suspended transport)

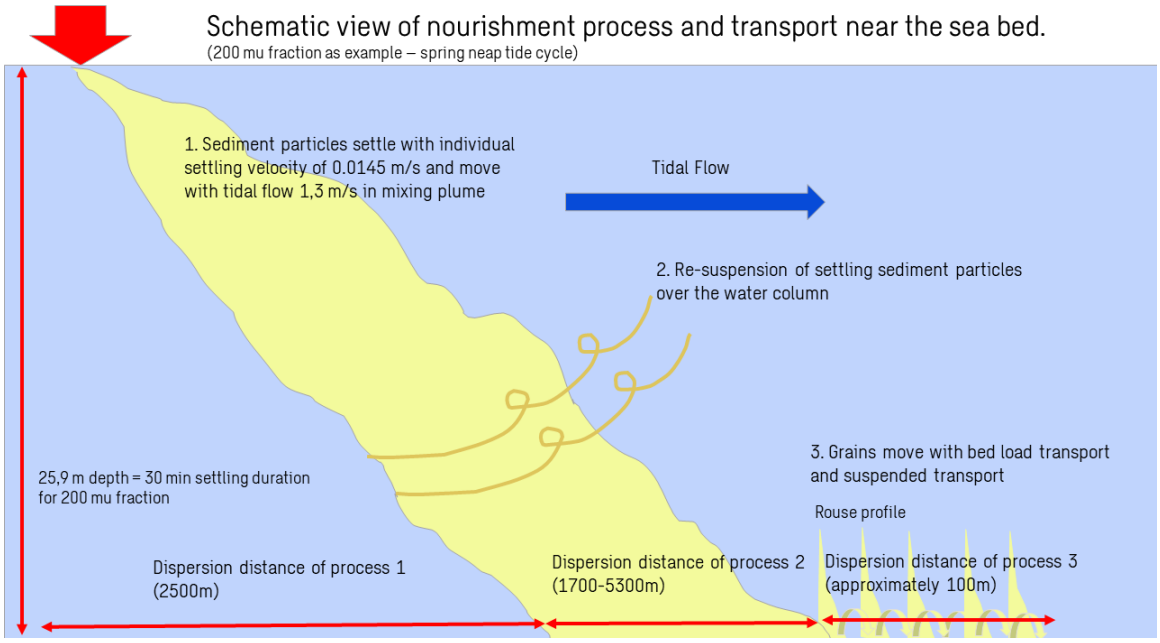

Figure 5.1: Schematic overview of the three dispersion processes. This image already has numerical values for the 200 μm fraction. This dispersion represents dispersion towards the North Sea. The results of dispersion process 1 and 2 are discussed in this chapter. The dispersion distance of process 3, is determined based on the mid-field dispersion results with continuous nourishment (Chapter 6). In these results it is found that the maximum dispersion distance of a half year minus the maximum dispersion distance of the near-field dispersion is approximately 1600 meters. This is on basis of a half year, thus per spring neap tide period corresponds to approximately (1600/13) 123 meters (approximately 100m). The mixing plume shape origins from (De Wit, 2015)

The dispersion through the initial settling process (1) and re-suspension during the settling process of sediment (2) have a larger effect on the total dispersion than than sediment which disperses by natural sediment transport processes (3) (bed load transport and suspended transport). This is due to the initiation of motion (Appendix C). Once a sediment particle is fully settled, it needs a certain flow rate to be brought back into suspension. This flow rate is only achieved after a certain time

between the ebb and flow (or vice versa) period. Therefore, the total time that a sediment particle can be carried along by the tidal current is smaller than the sediment particle that is already in suspension (by being released at the top of the water column).

Content chapter
In Section 5.1, the maximum dispersion of sediment during settling process is evaluated. This is without re-suspension and describes dispersion process 1. The numerical values are based on a preliminary calculation based on the general hydrodynamics and morphodynamics Appendix I.3. Thereafter, the Delft-3D results regarding a continuous nourishment over a spring neap tide cycle are used to determine the near-field dispersion of process 2 and 3. Based on the mid-field results, the two sediment transport processes can be distinguished. In Section 5.2, the spatial initial near-field dispersion is evaluated and considered. In Section 5.3, the near-field longitudinal distribution of initial dispersion is evaluated and considered. In Section 5.4, the overall near-field dispersion is considered.
During the spring neap tide cycle of 15 days, a part of the 2 Mm^3 is added. The part that is added can be determined by $\frac{15 days}{365 days} \cdot 2\ Mm^3$ and is 82191.8 m^3. Thus per fraction, a quarter of this volume is added as each fraction is added equally, which is 20547.9 m^3. In Appendix H.2 the exact numerical setup is explained.

5.1. DISPERSION OF SEDIMENT DURING SETTLING PROCESS

Based on the determined nourishment strategy, a preliminary calculation of the initial dispersion of sediment during the settling process is determined. This dispersion is the displacement of a particle without being re-suspended. So, this is just the distance a particle can disperse during continuous settling (dispersion process 1).
The distance of a tidal stroke is at an average current velocity of 1.0 m/s x 6 hours (ebb or flood period in 1 direction) = 21.6 km. The minimum and maximum individual settling duration during solely the settling settling process per fraction is determined at spring tide and the corresponding greatest and smallest depths (25.9m -23.7m) at the nourishment location. The results are illustrated in Table 5.1

Table 5.1: Individual settling duration from the greatest and smallest depths during spring tide.

Fraction	100μm	200μm	300μm	400μm
Maximum settling duration (min)	98	30	15	10
Minimum settling duration (min)	90	27	14	9

In Fig. 5.2 the distribution of particles per fraction is depicted. The y-axis represents the accumulation of sediment in mm and the x-axis represents the horizontal distance a particle travels. In Appendix I.3 an extensive consideration of the preliminary hand calculation can be found. This distance is determined in such a way that a particle keeps the initial horizontal flow velocity. Thus, when a particle is exhibited with a peak flow condition, it will yield the maximum dispersion. However, it is not likely that this peak flow velocity is present during the entire settling duration. Therefore, Table 5.2 illustrates the maximum found dispersion distances for a symmetrical tide (Borndiep 3 (Fig. 4.1b)).

Table 5.2: Maximum dispersion distances during settling process - preliminary calculation. In this example the maximum dispersion is determined under favorable circumstances. The found dispersion distances are an upper limit and are without re-suspension.

	Distance from Nourishment location [m]							
Direction	North Sea				Wadden Sea			
Fraction μm	100	200	300	400	100	200	300	400
Preliminary initial settling dispersion [m]	8000	2500	2180	1000	8000	2500	2180	1000

Based on the found longitudinal distribution, it can be concluded that the initial dispersion due to the settling process is large and depends on the particle size. Based on the initial settling dispersion, the nourishment strategy shows to be effective as sediment is transported towards both the North Sea and Wadden Sea. The distance of a tidal stroke is approximately 21.6 km and the maximum displacement of a particle (100μm) is 8000m. Thus, the 8km dispersion is not limited by the range of the tidal stroke distance. The sub conclusions based on the longitudinal distribution are:

- The dispersion per fraction is linked to the settling velocity of a fraction (i.e. large fractions settle more quickly than small fractions). Therefore large fractions have less dispersion compared to a small fraction
- It is uncertain whether the accumulated fractions close to the discharge location can be transported away by the system
- The depth (z-axis) is important due to the settling process of different sediment fractions.

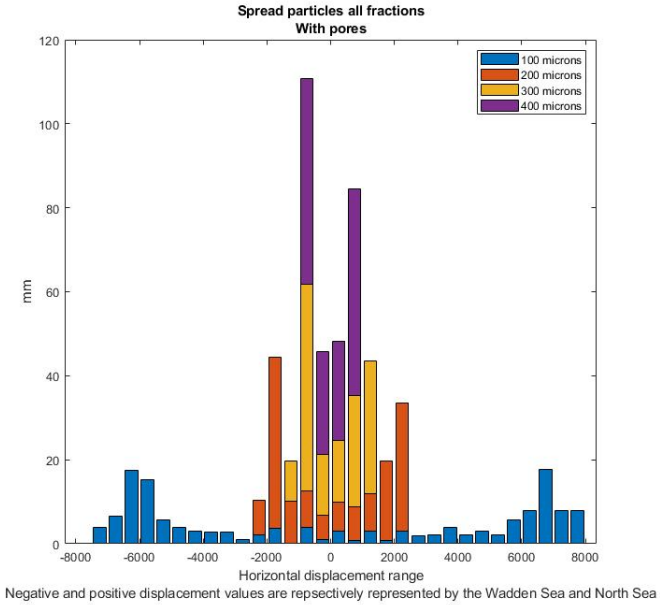

Figure 5.2: Increase in bed height determined with the density of sand with pores (1600 $\frac{kg}{m^3}$)

5.2. SPATIAL NEAR-FIELD DISPERSION

The scale on which the results are plotted is from 0-2 $\frac{kg}{m^2}$ or converted by the porous sand density of 1600 $\frac{kg}{m^3}$ 0-1,25mm sand accretion. Areas that are dark red are areas where 2 $\frac{kg}{m^2}$ or more has set-

tled. White areas are areas to which a nourished fraction has not yet been able to disperse to within the simulation duration. The contour line between the presence or absence is set at 0.5% sediment availability (transition blue to white areas in figures). The sediment of the seabed of the inlet of Ameland varies between 100-400μm and is considered fine to medium sand (Deltares, 1999). Nevertheless, the behavior of the four different sediment fractions is divided into three categories; fine (100μm), medium (200μm and 300μm) and coarse (400μm). The categories are chosen based on the found behaviour of the individual sediment particles.

In the Section 3.2 it was discussed that both the maximum and minimum dispersion were determined to determine a band-width of the actual dispersion. Both the maximum and minimum total near-field dispersion are composed of the three sediment transport processes illustrated in Fig. 5.1. The following general observation holds for both the minimum and maximum dispersion. The general trend is that the minimum and maximum dispersion spread to the same tidal inlet components, but that the maximum dispersion spreads further than the minimum dispersion.

Fine fraction
The fine fraction disperses the furthest compared to the medium and coarse fractions. The results show that the smaller fraction already covers the outer delta during a spring tide neap tide period (Fig. 5.3 and Fig. 5.5). The fine fraction disperses further Wadden Sea basin inward than towards the North Sea. The basin of the Wadden Sea is covered in the fine fraction to a large extent. The fine fractions also already cover a part of the intertidal areas.

Medium fraction
The medium fractions disperse less far than the fine fraction. The maximum dispersion for the medium fractions shows to reach the outer delta and shows significant dispersion into the Wadden Sea basin (Fig. 5.6). Whereas the minimum dispersion of the 300μm fraction remains in the tidal channel (Fig. 5.4). The medium fractions remain in general in the channel during the dispersion into the Wadden Sea area. Thus, the intertidal flats are not covered by the the medium fractions.

Coarse fraction
The coarse fraction disperses the least far compared to the medium and fine fractions. Although the coarse fraction reaches the outer delta and disperses relatively far into the Wadden Sea basin, it is found that most of the coarse fraction remains in the Borndiep channel (Fig. 5.6). Also, the coarse fraction shows to have a tendency to accumulate locally in the Borndiep channel (Fig. 5.4 and Fig. 5.6).

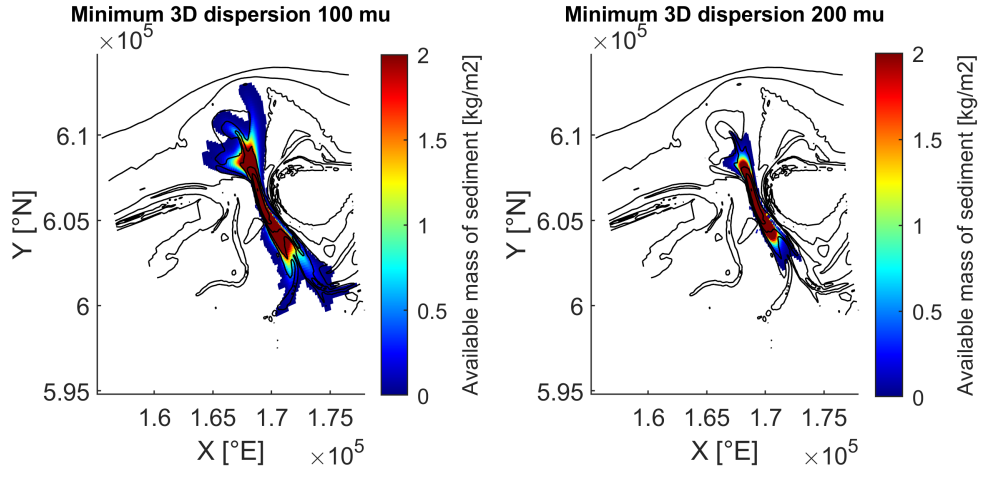

Figure 5.3: 100 and 200 μm minimum dispersion

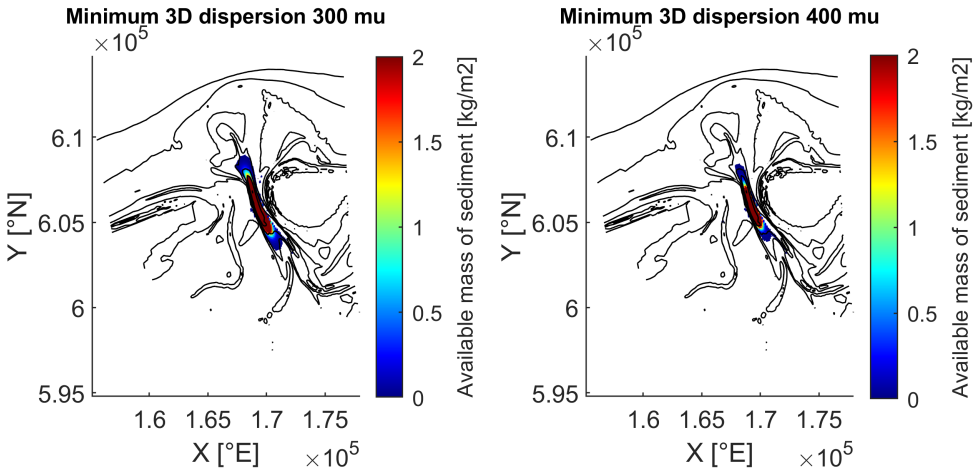

Figure 5.4: 300 and 400 μm minimum dispersion

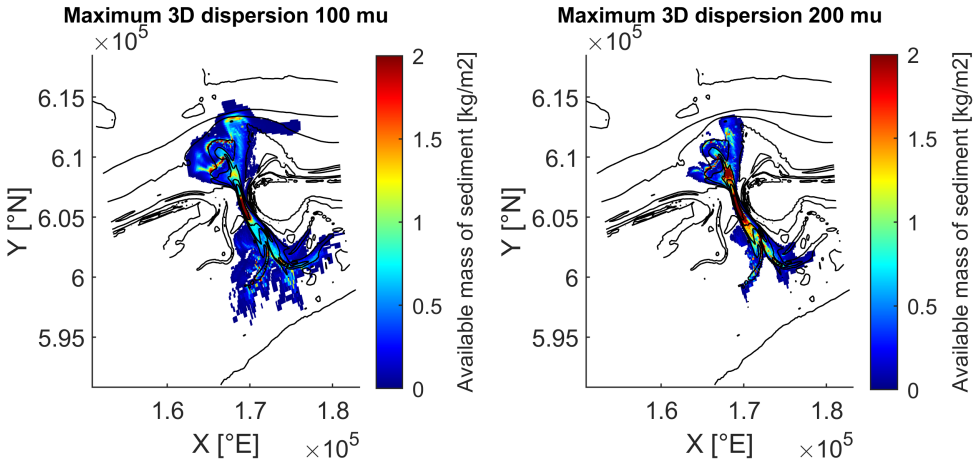

Figure 5.5: 100 and 200 μm maximum dispersion

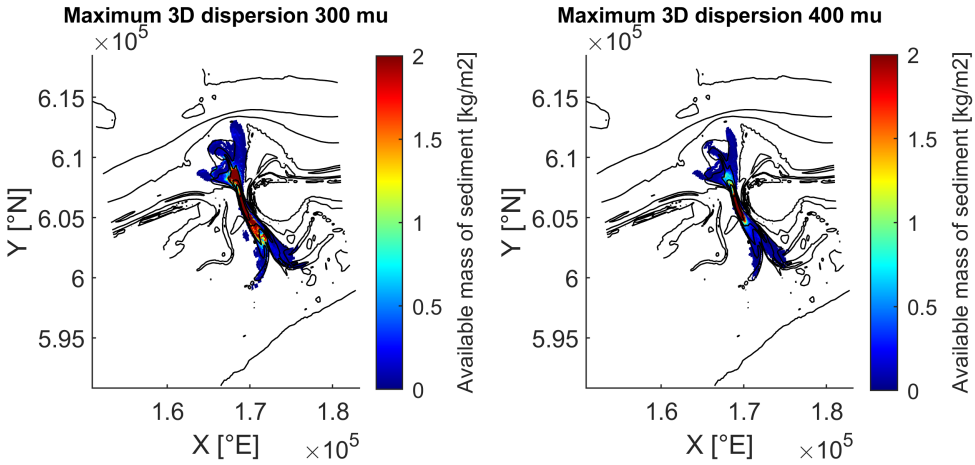

Figure 5.6: 300 and 400 μm maximum dispersion

In Table 5.3 the minimum and maximum near-field dispersion distances are depicted after a spring neap tide cycle. The maximum distances between the nourishment location and the outer region

Table 5.3: In this table the maximum distance from the nourishment location for both the minimum and maximum near-field dispersion are indicated. The near-field dispersion is composed of the indicated sediment transport processes (1,2 and 3). These are also shown in Fig. 5.1, using the 200mum fraction as an example. The dispersion from process 3 is determined based on the mid-field results (next chapter). The total mid-field dispersion over a half year (13 cycles) is divided by 13 spring neap tide cycles, to convert the dispersion of process 3 back to a single spring neap tide cycle.

	Maximum distance from Nourishment location [m]							
Direction	North Sea				Wadden Sea			
Fraction μm	100	200	300	400	100	200	300	400
1) Preliminary initial settling dispersion [m]	8000	2500	2200	1000	8000	2500	2200	1000
2) Dispersion distance due to re-suspension [m]	900	5300	4800	5900	2400	6200	6500	6300
3) Natural near-field sediment transport [m]	200	100	0	0	200	200	100	0
Maximum short term dispersion	9100	7900	7000	6900	10600	8900	8800	7300
Band-width								
Minimum NF dispersion [m]	6600	4200	3100	2300	7600	3700	2500	1800
Maximum NF dispersion [m]	9100	7900	7000	6900	10600	8900	8800	7300

where nourished sediment is found is determined by means of Pythagoras as explained in Section 3.3.3.
The sediment that is nourished on top of the water column settles in suspension while being carried by the tidal current. The maximum distances that can be covered during solely the initial settling process, are illustrated in the upper row of Table 5.3. The maximum NF (near-field) dispersion (Table 5.3) shows that each fraction reaches further than the preliminary initial settling dispersion. This is because the regional tidal flow velocities remain high (Fig. 4.1b) over the tidal channel. Therefore, the nourished sediment is re-suspended while fractions settle in the channel or, the fractions are re-suspended after the nourished sediment has reached the sea bed.
The results from Table 5.3 show that as particle sizes increase, the importance of the dispersion due to re-suspension (2) and dispersion due to natural sediment transport (3) increase for the maximum short term dispersion. The reason why the dispersion distance due to re-suspension is so significant is that suspended particles do not immediately settle to the sea floor, but are held in suspension by the turbulence of the fluid. It is assumed that suspended particles in a given vertical plane move horizontally across the plane with the water particles, and therefore at the same speed as the water particles (Bosboom and Stive, 2021). Since the tidal velocities in the tidal inlet are high, the re-suspension of sediment has a great effect on the near-field dispersion. This decreases the influence of the shorter settling time for larger sediment particles relative to smaller sediment particles. Nevertheless, the total dispersion distance depends on the particle size. Large particles disperse less far than fine particles.

Indicated in Fig. 4.1b is that when moving away from the nourishment location towards the North Sea or Wadden Sea, the appearance of the peak tidal velocities become skewed (tidal and jet flow asymmetry) to either the North or Wadden Sea compared to the evenly distributed peak tidal velocity signal at the nourishment location. As a consequence, the settled sediment at those locations is transported predominantly further by natural sediment transport processes towards either the

North Sea or Wadden Sea.
For sediments already dispersed out of the tidal channel (100,200 and 300 μm), the following applies. Regions outside of the tidal channel show an order of magnitude lower tidal transport capacity. This is illustrated in Appendix I.2 with Fig. I.4 and Table I.1. Because of the lower tidal transport capacity, and thus indirect flow velocities outside the tidal channel than inside the tidal channel, sediment dispersed outside the channel is exposed to flow velocities for a shorter period of time that may cause the particle to become re-mobilized. In other words, there is often too little energy in the system to initiate motion on a regular basis for certain particle sizes outside the tidal channel. Thus, natural sediment transport outside of the tidal channel is much slower than natural sediment transport inside the tidal channel.

5.3. NEAR-FIELD LONGITUDINAL DISTRIBUTION

In Fig. 5.7a is indicated by the black line where the transect of 15464m is located. The nourishment location is marked with the red dot. The depth profile over longitudinal transect illustrated in Fig. 5.7b shows the depth profile of this transect. At 0 m distance over longitudinal transect, the nourishment location is located and negative and positive distances are respectively away from the nourishment in the direction of the North Sea and Wadden Sea. First the results of the minimum and thereafter the results of the maximum longitudinal distributions are illustrated.

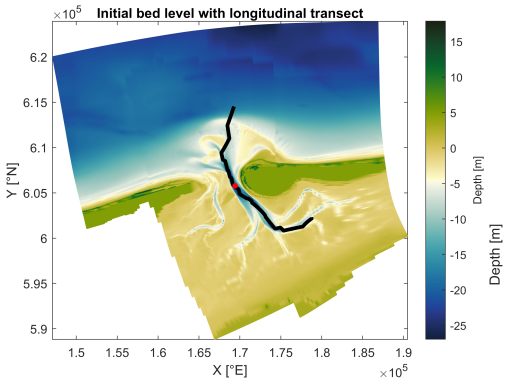

(a) Overview transect. The North Sea is depicted on the upper part of the image, whereas the Wadden Sea is depicted on the lower part of the image. In the Wadden Sea the channels are clearly visible. The island on the left is Terschelling and the Island on the right is Ameland.

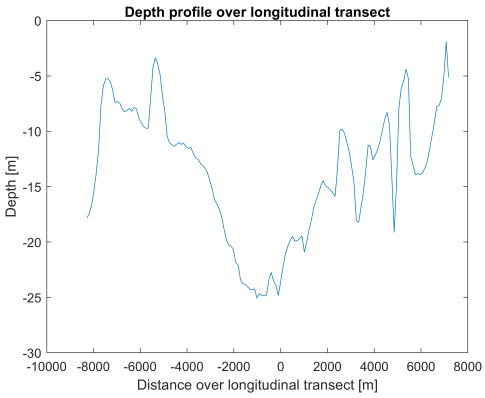

(b) Depth profile of transect. Negative distances are directed towards the North Sea and positive distances are directed towards the Wadden Sea.

Figure 5.7: Transect and depth profile for the determination of the longitudinal distribution.

Fig. 5.8 and Fig. 5.9 show that the degree of dispersion is determined by the size of the sediment fraction. The dispersion is greatest for the finer fractions and smallest for the coarser fractions. A bi-modal spectrum is observed for the minimum near-field dispersion. For the near-field maximal dispersion a multi-modal spectrum is observed for the 100 and 200 μm fractions. For the 300 and 400μm fractions, a bi-modal regime is observed. The longitudinal distributions indicate that sediment disperses to both the North Sea and the Wadden Sea. Table 5.4 and Table 5.6 provide an overview of what the peak available mass of sediments are per fraction, and at which distances away from the nourishment location they occur. For the maximum near-field dispersion, the peak available mass of sediment is lower than for the minimum near-field dispersion. This is because at the maximum near-field dispersion, the sediment is better dispersed and spread out over the area (as indicated by the spatial dispersion figures). Fig. 5.8a and Fig. 5.9a illustrate that most of the sedi-

Table 5.4: Minimum near-field dispersion distances to peak available mass of sediment [$\frac{kg}{m^2}$] peaks per fraction from the nourishment location

	North Sea				**Wadden Sea**			
Fraction μm	100	200	300	400	100	200	300	400
Peak [kg/m^2]	6.63	20.95	40.78	61.21	8.15	21.94	43.08	57.97
Distance from release point [m]	1010	606	404	303	1111	404	303	303

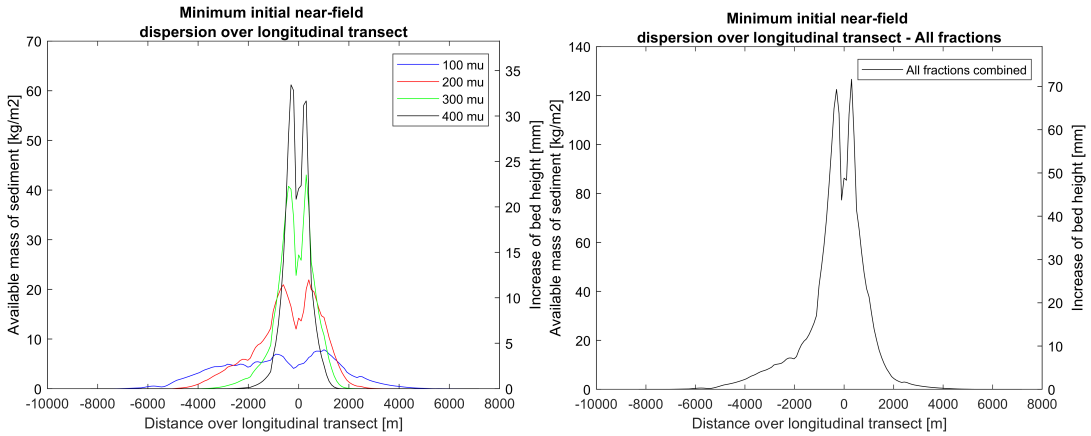

(a) Minimum longitudinal near-field distribution of individual sediment particles

(b) Minimum longitudinal near-field distribution of all sediment particles

Figure 5.8: Longitudinal transect of minimum near-field distribution. The longitudinal transect is taken through the tidal channel as depicted in Fig. 5.7a.

ment settles close to the nourishment location despite the high flow rates. Mainly the coarse and medium fraction accumulate close (within 1000 meters) to the nourishment. The fine fraction is more evenly distributed over the longitudinal transect.

Table 5.6: Maximum near-field dispersion distances to peak available mass of sediment [$\frac{kg}{m^2}$] peaks per fraction from the nourishment location

	Center		**North Sea**		**Wadden Sea**	
Fraction	100	200	300	400	300	400
Peak [kg/m^2]	3.9	13.41	29.38	58.4	28.57	54.54
Distance from release point [m]	0	303	303	202	303	303

The duration of the settling time for all fractions is shorter than the duration of a tidal stroke. Therefore, the settling time is the limiting factor in the dispersion distance. The optimal timeframe for maximum dispersion is therefore between tide turn from ebb to flood (or vice versa) and the the time of tide turn from flood to ebb minus (at least) the settling time of a sediment particle. The part of the continuous nourishment that is nourished within this timeframe can make use of a single tidal stroke to the Wadden Sea or the North Sea. Within this timeframe there are again optimal moments depending on when and for how long a peak flow condition occurs. This is again dependent on the moment within the spring neap tide cycle. During spring tide the largest water depth and flow velocities are observed (Fig. I.2a in Appendix I.1). Therefore, that specific moment within the aforementioned timeframe yields the highest dispersion. But, spring neap tide occurs only a fraction of the time in a spring neap tide cycle. The gross sediment settles between 4000 and 6000 meters from the nourishment location towards the North Sea and between 3000 and 4000 meters Wadden Sea basin inward. From the nourishment location to the back-barrier of the basin (West

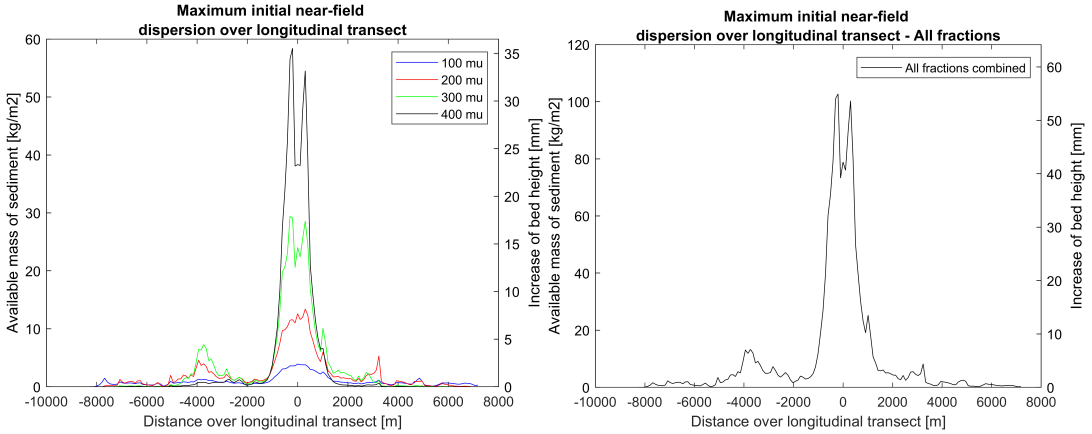

(a) Maximum longitudinal near-field dispersion of individual sediment particles

(b) Maximum longitudinal near-field dispersion of all sediment particles

Figure 5.9: Longitudinal transect of maximum near-field dispersion. The longitudinal transect is taken through the tidal channel as depicted in Fig. 5.7a.

Friesland coastline) is approximately 13km. Thus, during a spring neap tide cycle the nourished sediment disperses already between 23-30% basin inward.

Sand accretion per day
Despite being beyond the scope of this thesis, it is important from an ecological perspective to know how many mm of sand settles per day per location. The range of the sedimentation per day depends on the minimum and maximum dispersion. The minimum dispersion yields a higher sedimentation per day than the maximum dispersion. At the outer ends of the longitudinal distribution spectrum the sedimentation is between [0-10mm] per spring neap tide cycle. This corresponds to a sedimentation of [0-0.67mm/day]. Between [-2000 - 2000 m] from the nourishment location the sedimentation is significantly more. Between these locations the sedimentation is between [55-70mm] per spring neap tide cycle. This corresponds to a sedimentation of [3.67-4.67mm/day].

5.4. CONCLUSION NEAR-FIELD DISPERSION

Based on the initial sediment dispersion, the additional distance covered through re-suspension and natural sediment transport process as illustrated in Fig. 5.1, the conclusions about the near-field dispersion per fraction category are discussed below.

Maximum near-field dispersion during the settling process is obtained during the spring tide and within the optimal nourishment timeframe. The optimal timeframe for maximum dispersion is between tide turn from ebb to flood (or vice versa) and the the time of tide turn from flood to ebb minus (at least) the settling time of a sediment particle.

The near field dispersion is mainly determined by the initial settling process of sediment particles and the re-suspension of sediment particles while settling to the sea bed. The dispersion of sediment through natural sediment transport processes is minimal during a spring neap tide cycle.

Fine fraction
Fine fractions disperse mainly by the initial settling process. The settling duration is so large (Table 5.1), that the sediment can be transported over large distances by the tidal flow.

Medium fractions
Medium fractions disperse via initial settling of sediment particles and re-suspension of sediment

particles. During high tidal flow velocities, sediment can already disperse out of the tidal channel region due to the initial settling process and re-suspension of sediment particles while settling. Once out of the tidal channel region, the flow velocities severely reduce and sediment is more difficult re-mobilized. Therefore, natural sediment transport processes have little influence on the maximum dispersion during a spring neap tide cycle. On the other hand, the proportion that settles in the tidal channel due to initial mild flow conditions, can easily be transported out of the tidal channel by means of natural sediment transport processes due to the high peak flow velocities. As the tidal flow regimes become skewed (tidal and jet flow asymmetry), sediment is transported towards either the Wadden Sea or North Sea within the tidal channel.

Coarse fraction

Coarse fractions disperse mainly via re-suspension within the settling process. As a result, the coarse fraction remains mainly in the tidal channel. Therefore, this fraction does not lead to large dispersion. In the tidal channel high flow velocities occur. Therefore after the sediment is settled, it can be re-mobilized within the tidal channel. But, this fraction does not disperse out of the tidal channel during a spring neap tide cycle.

6 | Mid-field dispersion

The mid-field dispersion describes the behavior of the sand once it is on the bottom and moves further with natural sediment transport processes (months to years).

Fig. 6.1 shows the same longitudinal transect as the near-field dispersion to consider the mid-field dispersion longitudinal distribution. In addition, a cross-section was taken at the nourishment location to consider the tidal channel behaviour while prone under a continuous nourishment. During near-field dispersion, both minimum and maximum dispersion were considered. However, the mid-field minimum dispersion shows no further dispersion of the sediment nourished during the minimal near-field dispersion. So, the minimal near-field dispersion is equal to the minimum mid-field dispersion. Therefore, the minimum spatial dispersion results are added in Appendix K.2.

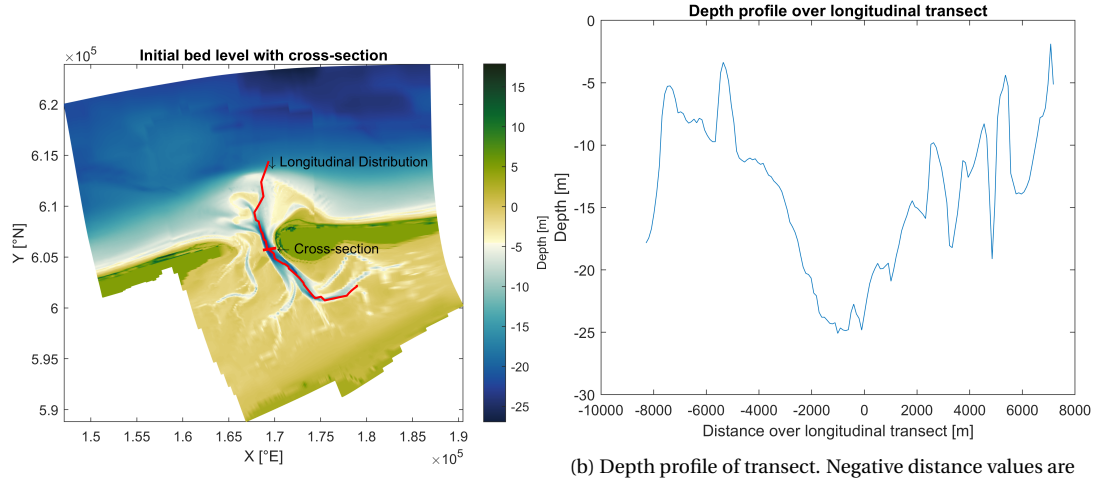

(a) Overview with the location of the Longitudinal transect and cross-section

(b) Depth profile of transect. Negative distance values are directed towards the North Sea and positive distance values are directed towards the Wadden Sea

Figure 6.1: Longitudinal transect, cross-section and depth profile

6.1. MID-FIELD SILTATION OF TIDAL CHANNEL

In Fig. 6.2 the behavior of the cross-section over time with and without continuous nourishment is depicted. Fig. 6.2a shows the behavior of the cross-sectional area when the continuous nourishment stops after a spring neap tide cycle. Fig. 6.2b shows what the behavior of the cross-sectional area is after a spring neap tide cycle after which the continuous nourishment persists. As the differences are small between the four time intervals, a more elaborate and close-up description of the cross-sectional area per 400 meters cross-sectional width is illustrated in Appendix K.1. Four measurements were taken with a constant time interval of 53 days. The t0 time interval cross-sectional area is equal to the last time measurement of the spring neap-tide cross-sectional area and the t1, t2 and t3 measurement are the thereon following measurements with a 53 days interval.
There is no surface of the cross section of the channel before the nourishment. But, it is assumed that before any sediment is nourished into the tidal channel, the area of the tidal channel is greater

than the found t0 (after a spring neap tide period of continuous nourishment) cross-sectional area. The changes in the tidal channel are not solely attributable to continuous nourishment. Nevertheless, an indicative response of the tidal channel to the continuous addition of sediment is described.

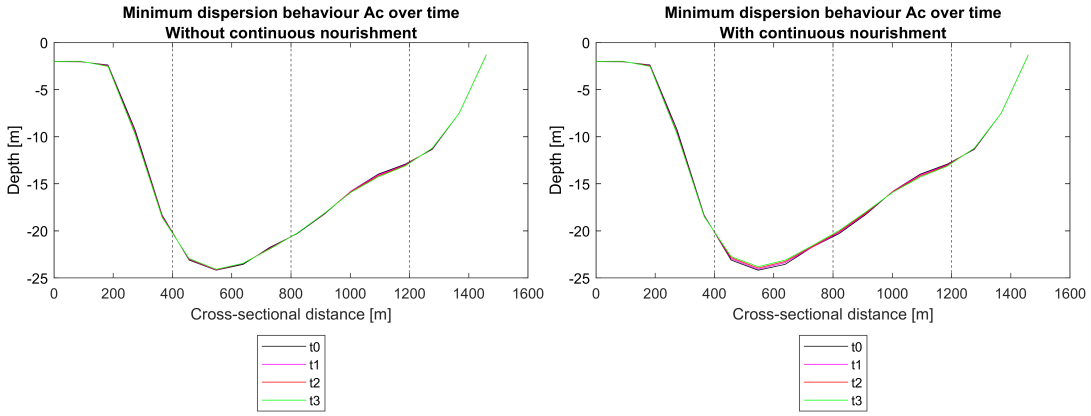

(a) Behaviour of the wet-cross section with minimal dispersion without continuous nourishment

(b) Behaviour of the wet-cross section with minimal dispersion with continuous nourishment

Figure 6.2: Behaviour of the wet cross-section with minimal dispersion. In the left image the behaviour of the wet cross-section is visible in which no nourishment is added over a half year time. In the right image the behaviour of the wet cross-section is visible in which a continuous nourishment is added over a half year time.

The near-field and mid-field responses of the cross-sectional area are schematically illustrated in Fig. 6.3. Below is an indicative description of the physical changes found over time.

Near-field response of cross-sectional area

Before the continuous nourishment, the Ameland Inlet was in a dynamic equilibrium. But, if sediment is nourished in the deepest part of the tidal channel during a spring neap tide cycle, it induces a change in the system. It was previously determined that the nourishment rate of 2 Mm^3/year covers only a fraction of the tidal prism (0,13% (Section 4.2)). Therefore, the tidal prism is hardly reduced by the continuous nourishment. However, the nourished sediment in the tidal channel will initially reduce the wet surface area of the tidal channel (Upper line in Fig. 6.3). A morphodynamic change induces a hydrodynamic change and vice versa. Based on Escoffier Eq. (B.0.3), this means that the flow velocity (u_e) must have been increased during the continuous nourishment as the cross-sectional area of the tidal channel became smaller.
Concluding, after a continuous nourishment over a spring neap tide cycle, the tidal prism remains approximately equal to the equilibrium situation ($P_{eq} = P_0$). The cross-sectional area is reduced compared to the equilibrium cross-sectional area ($A_{c,0} < A_{c,eq}$). As a response, the flow velocity after the continuous nourishment of a spring neap tide cycle is larger than the flow velocity before the continuous nourishment ($u_{e,0} > u_{e,eq}$).

Mid-field response of cross-sectional area without continuous nourishment

When the nourishment stops and the behaviour of the nourished sediment is assessed for a half year, the following results were found. Based on Table 6.1, the depth of the tidal channel remains approximately the same over time if no sediment is added for six months. In addition, at the same time, the cross-sectional area becomes larger (Table 6.2). Thus, after the nourishment stops, the cross-sectional area of the tidal channel recovers over time towards the original cross-sectional area ($A_{c,1,2,3} > A_{c,0}$ - (Table 6.2)). As a response of the recovery of the cross-sectional area, the flow velocity decreases and recovers to the equilibrium cross-sectional velocity ($u_{e,1,2,3} < u_{e,0}$). Thus, the nourished sediment is transported out of the channel by means of bed load transport and suspended

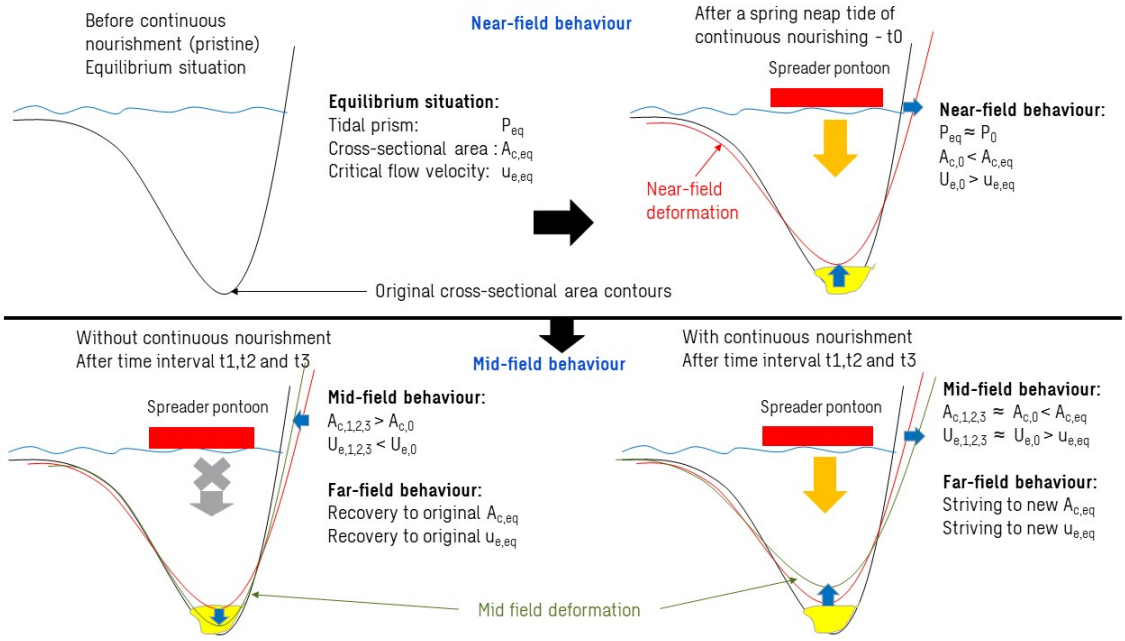

Figure 6.3: Illustrative behaviour of the cross-sectional area due to the continuous nourishment. In the upper row the pristine area is depicted and what happens to the continuous nourishment over a spring neap tide cycle. In the lower row, the response of the cross-sectional area due to the continuous nourishment is depicted for a situation in which the nourishment is stopped and a situation in which the nourishment persists over a half year.

transport when the continuous nourishment stops.
An additional effect is that during the period that the cross-sectional area is still smaller than the equilibrium cross-sectional area, the flow velocities will be higher. As the depth of the tidal channel remains approximately the same, this would suggest that the tidal channel erodes at the walls of the tidal channel (Fig. 6.2a) to compensate for the enlargement of the cross-sectional area. But the effect of the equal depth and tidal channel wall erosion is attributable to the autonomous behavior of the tidal channel and the numerical Delft-3D software imputing to its own equilibrium. Physically one would expect that the nourishment is cleared from the tidal channel once the nourishments stops and that tidal channel walls recover to the equilibrium state. This is illustrated in the lower left illustration in Fig. 6.3 and is considered to be more accurate.

Mid-field response of cross-sectional area with continuous nourishment
When the nourishment persists and the behaviour of the nourished sediment is assessed for a half year, the following results were found. Based on Table 6.1, the depth of the tidal channel decreases over time if sediment is continuously added for a period of six months. In addition, at the same time, the cross-sectional area remains approximately the same (Table 6.2) during the period that sediment is nourished in the tidal channel. But, as the initial cross-sectional area (before the continuous nourishment) is larger than the t0 measurement ($A_{c,1,2,3} = A_{c,0} < A_{c,eq}$ - (Table 6.2)), the cross-sectional area is reduced and remains reduced due to the continuous nourishment. Again, the tidal prism is hardly reduced by the nourishment rate of 2 Mm^3/year ($P_{eq} = P_0$). Therefore, the flow velocity is permanently increased in the situation where the continuous nourishment persists ($u_{e,1,2,3} = u_{e,0} > u_{e,eq}$). An additional effect is that the tidal channel erodes and widens at the walls of the tidal channel (Fig. 6.2a). The rate of channel wall erosion is equal to the rate of depth decrease as the cross-sectional area remains approximately equal ($A_{c,1,2,3} = A_{c,0}$). This is illustrated in the lower right corner in Fig. 6.3.

Table 6.1: Development trend of deepest trough part of Borndiep channel - Minimum dispersion

Model	**Without continuous nourishment**	Height difference	**With continuous nourishment**	Height difference
Depth t0	24.175 m	-	24.175 m	-
Depth t1	24.154 m	0.021 m	24.071 m	0.104 m
Depth t2	24.118 m	0.036 m	23.944 m	0.127 m
Depth t3	24.080 m	0.038 m	23.797 m	0.147 m

Table 6.2: Development cross-sectional area over time - Without and with continuous nourishment after a spring neap tide cycle. A consideration is that the t0 cross-sectional areas of both with and without continuous nourishment are equal. The pristine cross-sectional area is larger than the t3 area without continuous nourishment. The t0 area is thus smaller than the pristine cross-sectional area. So even though the percentages are > 100%, compared to the pristine cross-sectional area the percentages are less than 100%

	Without continuous nourishment		**With continuous nourishment**	
Timestep	Area [m^2]	% change to reference (t0)	Area [m^2]	% change to reference (t0)
CRS t0	17648	-	17648	-
CRS t1	17709	100.34 %	17669	100.12 %
CRS t2	17764	100.65 %	17674	100.15 %
CRS t3	17815	100.94 %	17664	100.09 %

6.2. MID-FIELD SPATIAL DISPERSION

First, the mid-field dispersion is observed by means of a spatial analysis. Thereafter, the physical processes are discussed and the dispersion distances by sediment transport processes (bed load and suspended sediment transport) are determined. In Fig. 6.4 an illustration is provided about the dispersion processes after a half year for the 200 μm fraction.

The scale on which the results are plotted is from 0-2 $\frac{kg}{m^2}$ or converted by the porous sand density of 1600 $\frac{kg}{m^3}$ 0-1,25mm sand accretion. Areas that are dark red are areas where 2 $\frac{kg}{m^2}$ or more has settled. White areas are areas to which a nourished fraction has not yet been able to disperse to within the simulation duration. The contour line between the presence or absence is set at 0.5% sediment availability (transition blue to white areas in figures).
In the Section 3.2 it was discussed that both the maximum and minimum dispersion were determined to determine a band width of the actual dispersion. However, the minimum dispersion shows no further increase in dispersion compared to the near-field dispersion. Therefore, the minimum spatial dispersion results are added in Appendix K.2. The same categorization for the sediment fractions is applied as the near-field dispersion.

Mid-field dispersion observation
Mid-field behaviour - fine fraction
It was found that during the spring neap tide cycle the fine fraction already covers the outer delta in the North Sea and that the intertidal flats of the Wadden Sea were already covered. The mid-field dispersion illustrates that the initial dispersion through settling and re-suspension is increased due to natural bed load and suspended transport. Thus, over time the fine fractions are dispersed further towards the North Sea and deeper into the Wadden Sea.

Mid-field behaviour - Medium fraction

It was found that during the spring neap tide cycle the medium fractions already reach the outer delta and show significant dispersion into the Wadden Sea basin. It was also found that the medium sized fractions do not cover the intertidal flats. However, after a half year, the results show that there is a clear onset of dispersion on to the intertidal areas for the 200μm fraction. The 300μm fraction mostly remains in the ebb channel. The mid-field dispersion illustrates that the initial dispersion through settling and re-suspension is increased due to natural bed load and suspended transport. Thus, over time the fine fractions are dispersed further towards the North Sea and deeper into the Wadden Sea.

Mid-field behaviour - Coarse fraction
It was found that during the spring neap tide cycle the coarse fraction reaches the outer delta and that it disperses relatively far into the Wadden Sea basin. Moreover, during a spring neap tide cycle the coarse fraction remains in the ebb channel. This holds during the half year simulation. Therefore, it can be concluded that the coarse fraction does not disperse onto the intertidal areas. Also, the dispersion during a half year does not increase between the the initial near-field and the mid-field dispersion results. Moreover, the coarse fraction keeps on accumulating in the deepest region of the Borndiep channel.

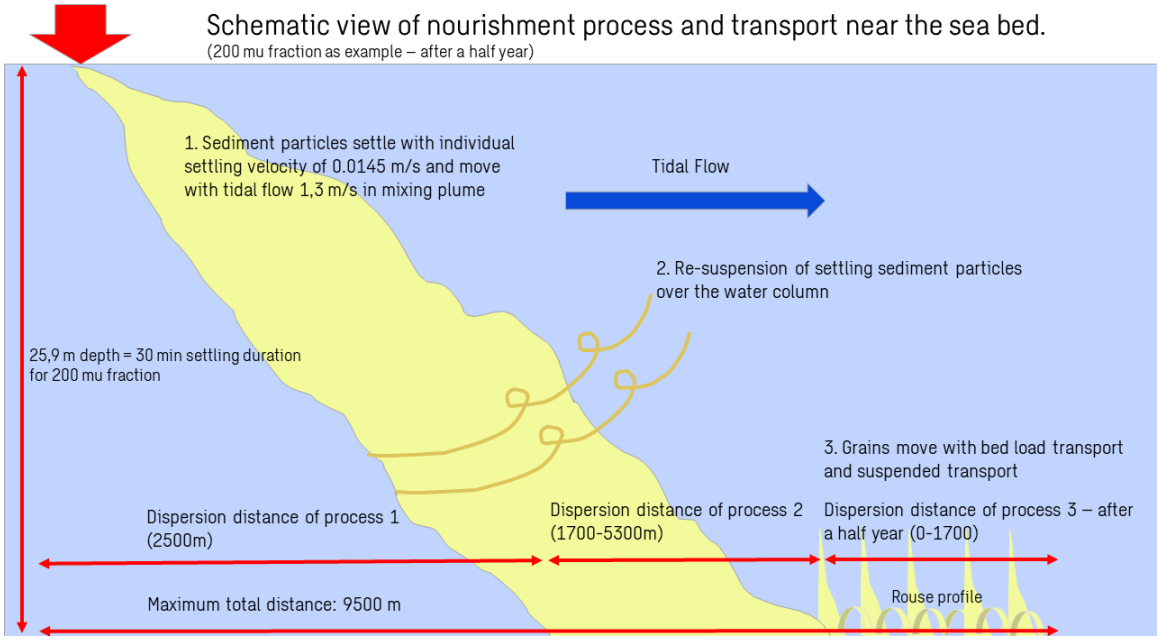

Figure 6.4: Three dispersion processes. This dispersion represents dispersion towards the North Sea. In the mid-field dispersion the focus lies on process 3. This image already has numerical values for the 200 μm fraction. The results of dispersion process 3 are discussed in this chapter. The dispersion distance of process 1, and 2, are discussed in Chapter 5. The mixing plume shape origins from (De Wit, 2015).

Mid-field dispersion physical processes
Table 6.3 shows the maximum distances measured from the nourishment location to the regions where they can still be observed for both the North Sea and the Wadden sea. From this table it can be deduced that the distances are larger when the nourishment persists than when the nourishment is stopped. This is because it was found in the analysis on the behavior of the wet cross section, that after continuous nourishment over a spring neap tide cycle the flow velocity in the tidal channel increased. It was also determined that if the nourishment stops, the flow velocity recovers toward the original equilibrium flow velocity. In addition, it is also determined that if the nourishment persists, the flow velocity exceeds the equilibrium flow velocity. The degree of bed load and suspended sedi-

ment transport depends on the flow velocity (Bosboom and Stive, 2021). In addition, a particle can be mobilized more easily and for a longer time due to a higher flow rate (Appendix C). Therefore, the observed mid-field dispersion distances of the sediment transport processes is larger when the nourishment persists than when the nourishment stops.

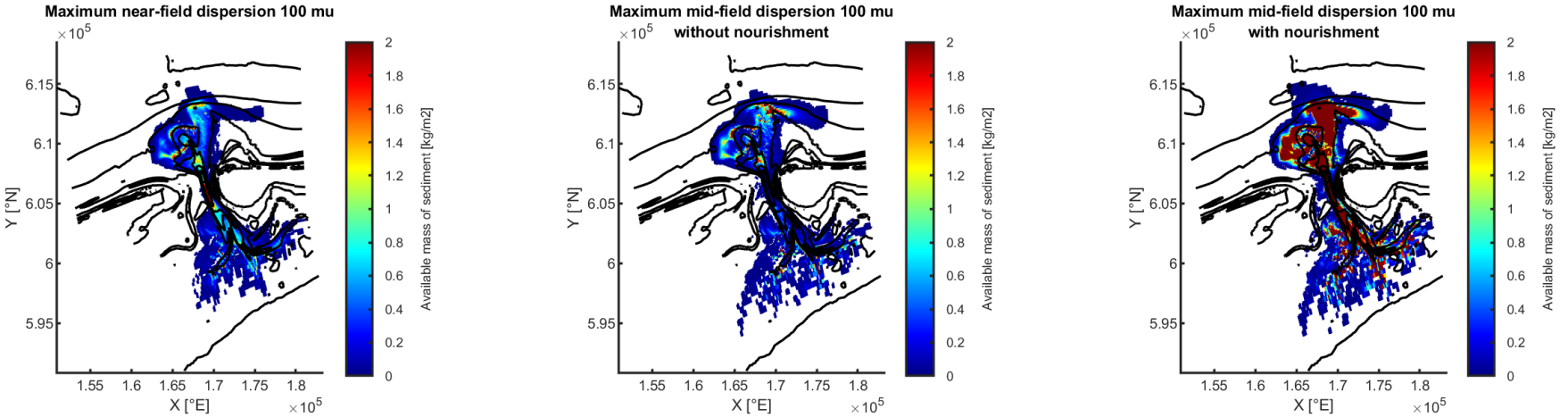

Figure 6.5: Combined figures of maximum dispersion. 3D spring neap tide cycle (left), 2D half year dispersion without continuous nourishment (center) and 2D half year dispersion with continuous nourishment (right) - 100μm

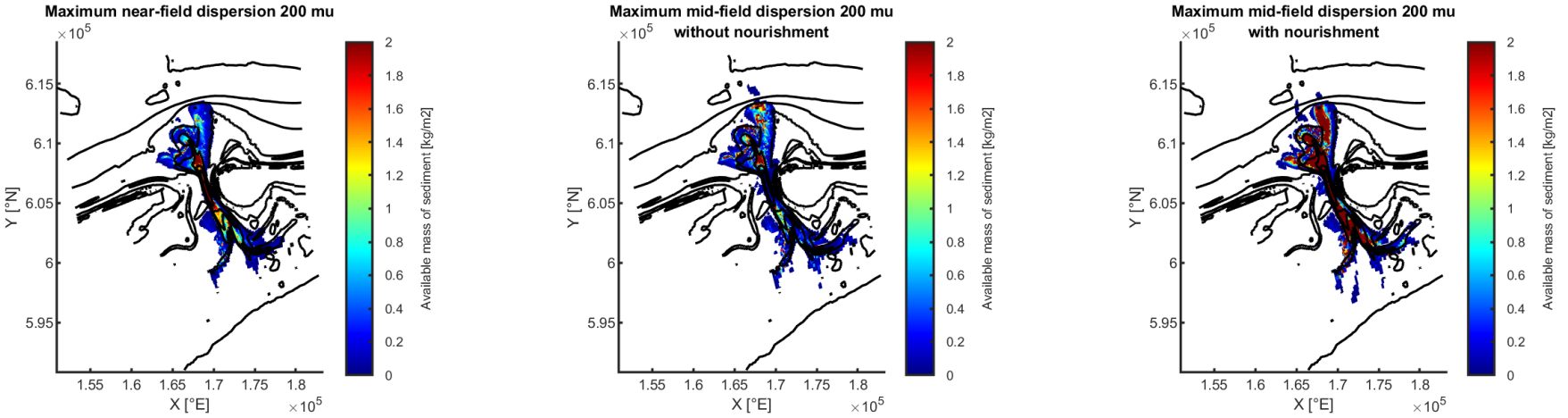

Figure 6.6: Combined figures of maximum dispersion. 3D spring neap tide cycle (left), 2D half year dispersion without continuous nourishment (center) and 2D half year dispersion with continuous nourishment (right) - 200μm

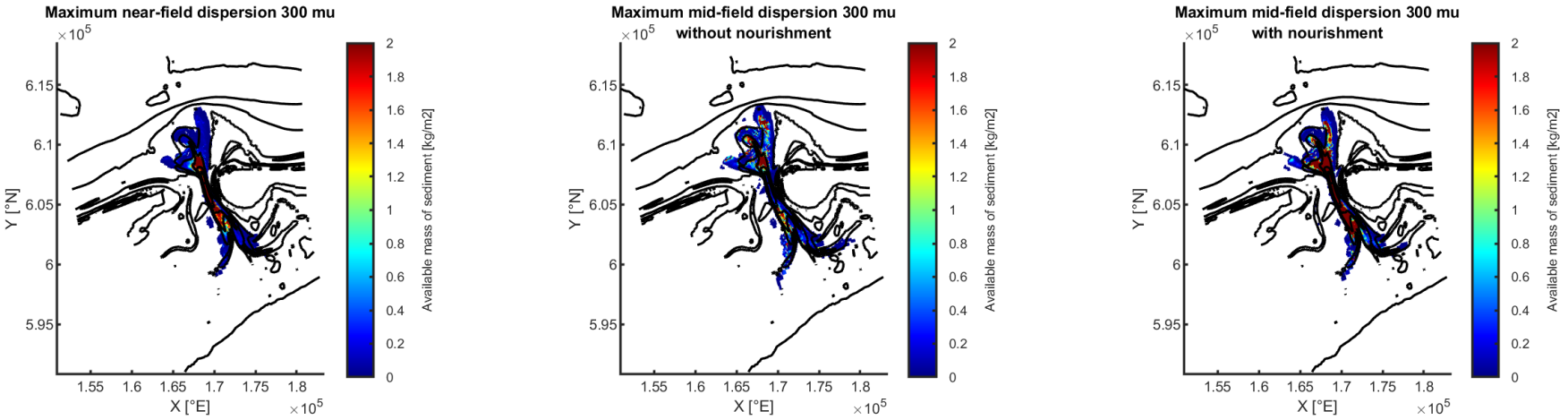

Figure 6.7: Combined figures of maximum dispersion. 3D spring neap tide cycle (left), 2D half year dispersion without continuous nourishment (center) and 2D half year dispersion with continuous nourishment (right) - 300μm

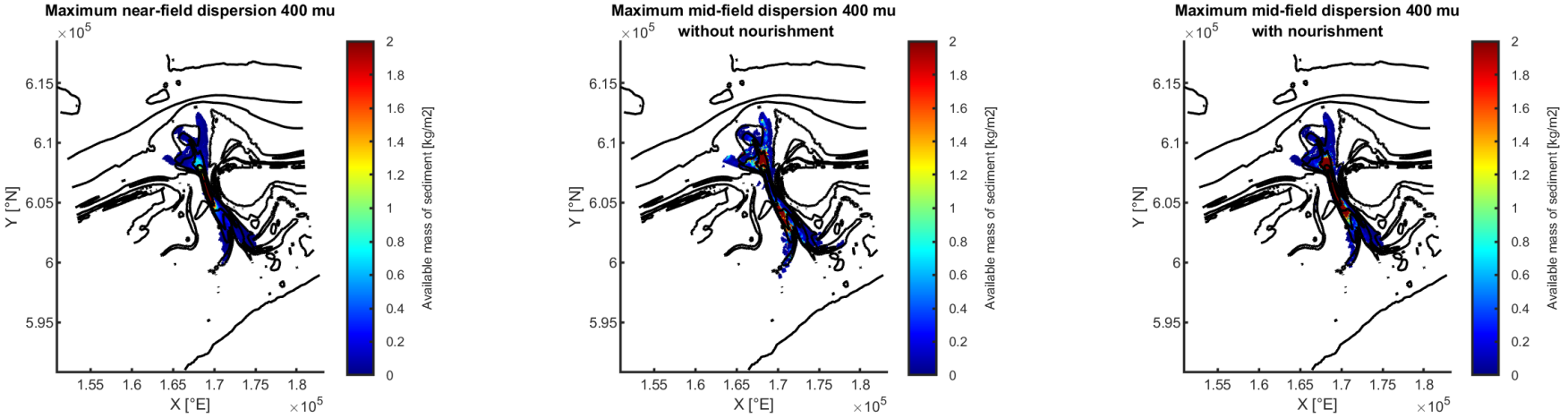

Figure 6.8: Combined figures of maximum dispersion. 3D spring neap tide cycle (left), 2D half year dispersion without continuous nourishment (center) and 2D half year dispersion with continuous nourishment (right) - 400μm

6.3. AMOUNT OF SEDIMENT THAT CAN BE PROCESSED BY THE TIDAL CHANNEL

The following figures show the longitudinal distribution over the transect indicated in Fig. 6.1. In these figures, all nourished fractions are shown combined at 4 different time intervals. The time intervals are identical as the time intervals used to determine the behavior of the wet surface of the tidal channel. Both maximum and minimum dispersion were determined. As indicated earlier, at the minimum dispersion, the sediment does not spread beyond the near-field dispersion found. This can also be observed from Fig. 6.9. The minimum longitudinal mid-field distribution corresponds to the spatial dispersion of Appendix K.2. In Fig. 6.10 the maximum longitudinal distribution is depicted. This figure corresponds to the maximum mid-field spatial dispersion illustrated in this chapter. Also, the two situations in which the continuous nourishment is stopped or still persists after a spring neap tide cycle are presented. The longitudinal distribution behaviours are illustrated by means of a distinction between the situation without or with a continuous nourishment.

Without continuous nourishment
The minimum and maximum longitudinal dispersion without continuous nourishment ((Fig. 6.9a) and (Fig. 6.9b)) show that over time presence of the available mass of sediment of the combined fractions reduce over the transect. Meaning, the nourished sediment during the spring neap tide cycle is transported out of the tidal channel. In particular, the maximum longitudinal distribution reflects this well. In this figure is can be well observed that the peak available mass of sediment at the nourishment location (x=0) reduces over time. The direction in which the sediment is distributed is dominantly towards the North Sea. Moreover, this sediment accumulates between the [-6000 - -2000] meters from the nourishment location. In this spatial interval the ebb tidal delta is located. Thus, growth of the outer delta is a result of a temporary (spring neap tide cycle) tidal channel nourishment. The nourished sediment is transported out of the tidal channel among others due to the temporary increase of the flow velocity. As the increase of the flow velocity reduces as the cross-sectional area of the wet surfaces increases (Section 6.1), the rate at which the sediment is transported out of the tidal channel also reduces over time. In conclusion, if sediment is temporarily nourished to the tidal channel at a rate of 2 Mm^3/year, then the system can process the nourished sediment by transporting it out of the tidal channel.

With continuous nourishment
The minimum and maximum longitudinal dispersion with continuous nourishment (Fig. 6.10a and Fig. 6.10b) show that over time the presence of the available mass of sediment of the combined fractions accumulate over the transect. In particular accumulation is found near the nourishment source. As a result the tidal channel reduces in depth over the longitudinal transect. The rate at which the tidal channel reduces is for e.g. t2 to t3 of the maximum longitudinal dispersion (depth reduction: 1600 - 1200 mm) = 400 mm/ 53 days (time interval) = 7,54 mm/day. Despite the tidal channel becoming shallower at a relatively high rate, it has previously been found that the surface area of the tidal channel remains relatively constant. This means that what the channel loses in depth is compensated for by erosion at the channel walls. As the nourishment continuous, a new equilibrium condition is expected to be found. However, on the basis of a half year this equilibrium is not yet been found. Based on the combination of the reduction of the depth of the channel over time and the approximately equal cross-sectional area over time of the tidal channel, it is concluded that the tidal channel is able to process a 2Mm^3/year nourishment over the time span of a half year. However, whether the tidal channel can process such nourishment quantities and with a rate of 2 Mm^3/year over larger timescales is after a half year not yet possible to conclude.

Table 6.3: In this table the maximum distance from the nourishment location for the mid-field dispersion with and without continuous nourishment are indicated. Also, the maximum distance from the nourishment location for both the minimum and maximum near-field dispersion are indicated. Besides the near-field and mid-field dispersion, the settling dispersion during the initial settling process from Section 5.1 is indicated. Based on both results, a distinction between the initial dispersion due to the settling process and the dispersion due to re-suspension can be determined. This is the dispersion distance due to re-suspension. Also, the dispersion distance through sediment transport processes (bed load and suspended sediment transport) is determined. This distance is obtained by subtracting the found maximum near-field dispersion distance of the mid-field dispersion with continuous nourishment distance.

	Maximum distance from Nourishment location [m]							
Direction	North Sea				Wadden Sea			
Fraction μm	100	200	300	400	100	200	300	400
1) Preliminary initial settling dispersion [m]	8000	2500	2200	1000	8000	2500	2200	1000
2) Dispersion distance due to re-suspension [m]	900	5300	4800	5900	2400	6200	6500	6300
3) Natural near-field sediment transport [m]	200	100	0	0	200	200	100	0
Maximum short term dispersion [m]	9100	7900	7000	6900	10600	8900	8800	7300
Band-width								
Minimum NF dispersion [m]	6600	4200	3100	2300	7600	3700	2500	1800
Maximum NF dispersion [m]	9100	7900	7000	6900	10600	8900	8800	7300
3) Natural mid-field sediment transport [m]	2100	1600	300	100	2000	2300	900	100
Maximum long term dispersion (half year) [m]	2100	1600	300	100	2000	2300	900	100
Sum NF + MF								
Maximum total dispersion with nourishment [m]	11200	9500	7300	7000	12600	11200	9700	7400
Band-width								
Maximum MF dispersion [m] - without nourishment	10900	8700	8100	7000	12400	10300	9600	7400
Maximum MF dispersion [m] -with nourishment	11200	9500	7300	7000	12600	11200	9700	7400

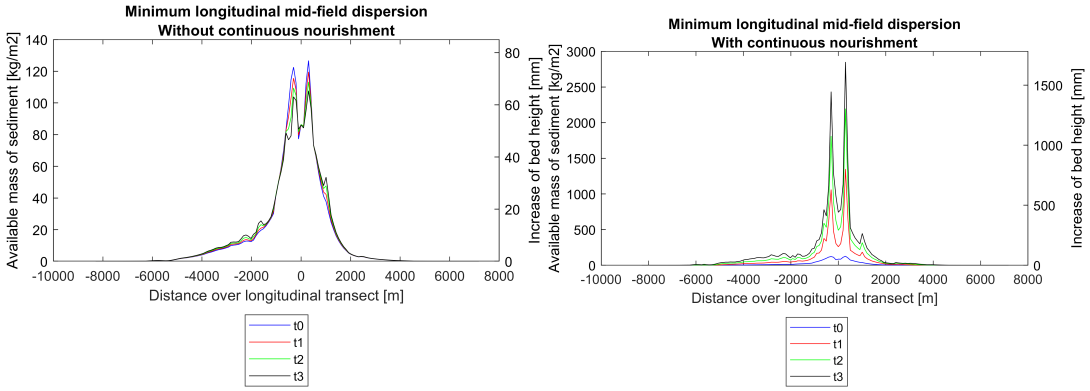

(a) The minimum dispersion over the longitudinal transect per fraction without the addition of a continuous nourishment over a half year.

(b) The minimum dispersion over the longitudinal transect per fraction with the addition of a continuous nourishment over a half year.

Figure 6.9: In these figures the minimum longitudinal distribution over a half year are determined. Over the half year period, four measurements were taken with the same time interval of 53 days.

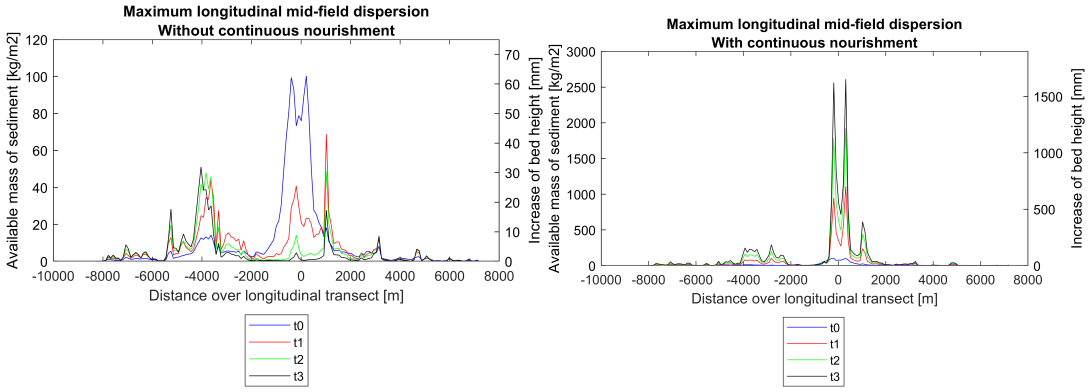

(a) The maximum dispersion over the longitudinal transect per fraction without the addition of a continuous nourishment over a half year.

(b) The maximum dispersion over the longitudinal transect per fraction with the addition of a continuous nourishment over a half year.

Figure 6.10: In these figures the maximum longitudinal distribution over a half year are determined. Over the half year period, four measurements were taken with the same time interval of 53 days.

6.4. CONCLUSION MID-FIELD DISPERSION

Mid-field siltation of tidal channel
Before the continuous nourishment, the tidal channel was in a dynamic equilibrium. The continuous nourishment during the spring neap tide cycle has reduced the wet area of the tidal channel. As a result, the flow velocity in the tidal channel has increased. When the nourishment stops, the cross-sectional area of the tidal channel restores to the equilibrium conditions. Thus, the cross-sectional area enlargers and the flow velocity reduces to the equilibrium conditions. When the nourishment persists, the cross-sectional area remains reduced and is thus smaller than the equilibrium condition. As a result, the flow velocity is increased and remains higher than the equilibrium condition.

Mid-field spatial dispersion
The degree of dispersion of sediment fractions is determined by the size of the sediment (i.e. small fractions are more easily mobilized than coarse fractions and are thus transported over larger distances). Due to the increase of flow velocity by a reduction of the cross-sectional area of the tidal channel the natural sediment transport processes are enhanced. The dispersion by the nourishment method (nourishing sediment on top of the water column in the tidal channel) yields the largest part of the total dispersion during a half year. Thus, the initial settling process and resuspension of sediment particles are more dominant for the determination of the total dispersion over a half year. The coarse fraction mainly accumulates in the tidal channel. The purpose of the Zandwindmolen is to disperse sediment as quickly as possible to areas where it is needed for coastal preservation. Because the coarse fraction does not disperse well, it is not recommended that this fraction is nourished. A combination of the fine and medium fraction provides good dispersion.

Amount of sediment that can be processed by the tidal channel
The sediment is being nourished at a rate of $2 Mm^3$/year. For a nourishment during a spring neap tide cycle, the amount of sediment added is easily processed by the tidal channel over a half year. From the longitudinal distribution without continuous nourishment it can be concluded that the available mass of sediment quickly reduces within the channel but accumulates outside of the channel. This leads to sediment import to the Wadden Sea and accretion of the ebb tidal delta. If a continuous nourishment is carried out for six months, then the depth of the channel continues to decrease. At the same time, the wet cross-section of the tidal channel remains approximately equal, causing erosion at the channel walls. It is found that based on a half year, the tidal channel is able to process sediment that is nourished at a rate of $2\ Mm^3$, because the wet cross-section remains approximately constant. Whether the tidal channel can continue to cope with this nourishment rate over longer periods of time cannot yet be concluded based on these measured results.

7 | Discussion

In this chapter the model restrictions, effect of waves on dispersion and far-field (timescale: years) consideration is given.

7.1. Model restrictions

The assessment of the nourishment dispersion in the Ameland Inlet with Delft-3D has given insightful information. The model has been set up in such a way that the essential processes are incorporated. Yet, there are some model limitations which have to be taken into consideration before an eventual conclusion can be determined. These are described below.

Absence of waves

A flow model was chosen in this study, in which only the tidal flow is simulated. As a result, waves are missing from the simulation. The dominant sediment transport process in the tidal channel is tidal flow. Therefore, the dispersion found in the tidal channel is accurately simulated. Outside the tidal channel, the sediment transport for both the North Sea and the Wadden Sea consists of a combination of tidal and wave transport. The general assumption is that an addition of waves in the simulation would increase the already found dispersion.

On the North Sea coast (Ameland and Terschelling) sediment spreads slowly along the coast (expectation order decades). In the Wadden Sea basin the influence of waves is especially important for the (shallow) intertidal areas. The accretion or erosion of the intertidal areas is an interplay between the curvature flow (accretion) and the waves (erosion). What is expected for the far-field dispersion behavior is discussed in Section 7.3.

Residual flow processes – intertidal areas

Curvature secondary flows are processes which are simulated by a 3D simulation but not by a 2D simulation. The near-field behavior is simulated by means of a 3D simulation while the mid-field behavior is simulated by means of a 2D simulation. Therefore, the near-field dispersion behavior does give an accurate consideration of the curvature secondary flows. Due to the absence of the curvature secondary flow in the (2D) half year simulation, an underestimation of the actual dispersion induced by the curvature secondary flow is given. This is important for the accretion of the intertidal areas. Therefore, the far-field consideration includes the expected effect of curvature secondary flow in combination with waves for intertidal areas.

Behaviour cross-sectional area Borndiep channel - Mixing of artificial nourished sediment with natural background fractions

Delft3D works with an uniformly mixed bed (Deltares, 2018). In the case of deposition of artificial sediment in a grid cell with natural background fractions, the artificial sediment will be uniformly mixed through the natural background fraction sediment layer. The proportion of presence of artificial sediment to the natural background fraction determines how much artificial sediment is brought into suspension. In case of a low volume continuous nourishment, the proportion of artificial sediment to the natural background fractions is low and will eventually lead to an underestimation of the dispersion. The behavior of the wet surface of the tidal channel was determined with the natural background fractions. This is because the combination of the the nourished sediment with the natural background fractions determine the full behavior of the tidal channel. The result

is that while sediment is continuously nourished, at the same time there was an underestimation (and therefore no good) of dispersion due to the natural background fractions. As a result, sediment accumulates at the nourishment location. Therefore, the increase in height found in the deepest part of the tidal channel and the erosion at the channel walls, is greater than it would be in reality. In reality, the nourished sediment in the channel will become the active sediment layer and this very layer will be suspended and transported out of the channel.

Near-field behaviour nourishment in Delft-3D
In Delft3D-FLOW, vertical density differences are taken into account in the horizontal pressure gradients and in the vertical turbulent exchange coefficients. So the application of Delft3D-FLOW is restricted to mid-field and far-field dispersion simulations of discharged constituents (Deltares, 2018). This study did use Delft-3D to simulate the near-field dispersion behavior of continuous nourishment. As a result, there are discrepancies in the actual near-field behavior. The continuous nourishment is simulated as a fixed nourishment over a predefined area, while the spray pontoon moves back and forth in reality. As a result, an overestimation of the near-field dispersion might have been obtained. To obtain a more accurate near-field behavior, computational fluid modeling (CFD) should be applied. In this, the point nourishment can be dynamically simulated and on a smaller spatial scale mixing processes of the sediment with the natural tidal flow are better simulated. Therefore, the Delft-3D simulation might have led to an underestimation of the near-field mixing processes. Because of the underestimation by not using CFD modeling and the overestimation by choosing the predefined area on which to apply the nourishment continuously, it is difficult to determine whether this yields an over or under estimation. This requires further research.

7.2. EFFECT OF WAVES ON DISPERSION

In the tidal channel, tidal flow is the dominant sediment transport process. Outside the channel on both the North Sea and Wadden Sea side, the influence of waves increases on the sediment transport. On the North Sea side, waves are dominant on the surrounding shorelines and on the outer delta. On the Wadden Sea side, waves play a role in the accretion or erosion of the intertidal areas. The chosen model accurately describes the sediment transport in the tidal channel, but will show deviations due to the absence of waves on the North Sea side and on the Wadden Sea side. Therefore, the near-field behaviour is found to be accurate as this describes the settling and re-suspension of sediment in the tidal channel. This section therefore discusses the expected effect of waves on the mid-field dispersion by natural sediment processes. First the effects of waves on the results on the North Sea side are discussed. Thereafter, the effect of waves on the Wadden Sea side (intertidal areas) are discussed.

North Sea
The North Sea mainly consists of locally generated wind waves with a significant wave height of 1.37m and a corresponding peak wave period of 7s (Wang et al., 2018). The significant wave height is 1.3 meters with a mean period of 5 seconds (Elias et al., 2012). During storms, wave heights over 6 meters and storm surges over 2 meters are measured. Moreover, the majority of the waves come in from the north-west, resulting in an eastward littoral drift. This littoral drift has the same direction as the tidal wave (Section 2.2).

Depth induced wave breaking occurs at the coastlines of Ameland en Terschelling. The waves approach the shore under an oblique angle and thus create alongshore and cross-shore directed sediment transport. Due to the dominant incoming waves from the North-West, it is therefore expected that the dominant alongshore sediment transport is from west to east. Moreover, it was illustrated that at the ebb-tidal delta waves break due to depth induced wave breaking and in the process stir up sediment into suspension. The role of waves is to act as a bulldozer by pushing the sediment

towards shore and thus removing sediment from the ebb-tidal delta. Furthermore, the area over which the ebb-tidal delta can spread out is limited due to wave action (Bosboom and Stive, 2021). A net offshore directed sediment flux is induced by the inlet currents driven by the tide. These offshore directed sediment fluxes built up the ebb-tidal delta. Hence, the overall morphology of the flood and ebb-tidal delta is generally determined by the dynamic balance between waves and tides (Bosboom and Stive, 2021). In general it can be stated that the ebb-tidal delta of the Ameland Inlet is highly dynamic (Oertel, 1972) and that very complex spatial distribution of tide and wave driven processes occur (Elias, 2020a).

The found results showed that the nourished fraction tend to travel over the outer delta and move towards deeper regions of the North Sea. However, when waves are incorporated in the found results it is expected that due to the bulldozer effect and the dominant eastward littoral drift the nourished sediment moves around the North western tip of Ameland and moves into down-drift direction. Thus, it is expected that less sediment settles at the outer delta due to the effect of waves and more sediment moves into down-drift direction. Based on the sediment atlas and the aforementioned expected effect of waves, the mid-field behaviour is once more assessed. Fine fractions (≤150μm) have potential to remain in suspension due to the energetic environment at the outer delta. Depending on the height of the waves and seasonality, these fractions can either settle or remain in suspension and move towards the down-drift island. Medium fractions 150-350μm are expected to reach, cover and ultimately grow the outer delta. Moreover, medium fractions can be mobilized. When mobilized, they are likely to be transported in down-drift direction. Coarse fractions (≥350μm) are expected to remain in the Borndiep channel. Based on the intended behaviour of the Zandwindmolen, in which sediment is required to disperse quickly over the vicinity of Ameland Inlet, coarse fractions of ≥350μm are undesired.

Wadden Sea - Intertidal areas

First the growth mechanisms of the tidal flats are mentioned. Thereafter, the expected effect of waves upon the growth mechanisms is discussed.

Growth of shoals

The curvature secondary flow results during flood and ebb in a flow near the bed towards the shoal. The upper part is always directed away from the center of curvature (or shoal). This means that near the bottom the secondary flow is towards the inner bend generating a transport of sediment from the outer bend. The outer bend erodes towards the inner bend, which accretes. Thus the curvature secondary flow causes growth of the intertidal areas (Bosboom and Stive, 2021). However, the applied 2D model does not solve secondary flow patterns (Deltares, 2018). Therefore, this form of accretion of the intertidal areas is missing in the applied simulations and will thus give an underestimation of the actual accretion of the shoals.

Also, due to inertia the tidal current tends to overshoot or take a wider bend than the actual pathway during both ebb and flood. Due to the overshooting of the currents ebb and flood chutes occur at the ending of the bends and are directed into the flat areas. The mean water level during flood is higher than during ebb. Therefore, the flood chutes are generally better developed than the ebb chutes. During flood the water spreads over the flats, while during ebb the ebb current flows through the main channels. The flats are especially fed with sand through the ebb and flood chutes. (Bosboom and Stive, 2021)

Effect waves on shoals

It was found that waves in the Wadden Sea are mainly locally generated wind waves or are waves originating from the North Sea which penetrate through the Ameland Inlet (Section 2.2). Wang et al. (2012) mentioned that from North Sea to the back-barrier of the Wadden Sea basin, the energy of

tide and waves decreases and thus, so does the mean grain size. The decrease of waves was also found in the wave analysis in Appendix I.4.

The influence and importance of waves increase in shallow areas. In shallow water, the contribution of wave motion to the magnitude of bed shear stress (and thus to sediment stirring) is frequently greater than the contribution of mean current. As a result, it is commonly stated that waves stir up sediment while currents transport it. The combination of wind, wave and tidal currents form a complex 3D interaction. Waves act as an eroding agent on the flats. The intensity of waves depends on seasonality and location in the basin (the wave height reduces basin inward). In the winter higher and more intense waves can be expected than during the summer months. Thus during winter more erosion and during summer less erosion of the tidal flats can be expected due to waves. (Bosboom and Stive, 2021)

In conclusion, the function of waves on shoals is that they tend to erode the tidal flats. The function of the flow is to increase the intertidal flats. Due to the absence of waves in the applied model, the found accretion of the tidal flats by mainly the fine fraction is likely an overestimation compared to what would happen in reality. Whether the intertidal flats increase or decrease is hard to predict as also mud has a role in the formation of intertidal areas. Based on historical past, the intertidal areas in the eastern Wadden Sea had no problem keeping up with sea level rise. Nor has it any problem keeping up with the current sea level rise (2mm/year). This implies that so far, the intertidal areas could grow along with sea level rise. Therefore it is likely to expect that if an abundance of sediment is nourished and that the nourished sediment is able to disperse over the entire back-barrier, the intertidal areas are able to grow along with sea level rise autonomously. The results show that the nourished sediment reach the entire back-barrier. Therefore, even though the accretion or erosion of intertidal areas depends on an interplay between waves and currents, it is likely to expect that the continuous nourishment contributes to natural growth of the intertidal areas. The intertidal areas in the western Wadden Sea however are transport limited. Therefore, it is uncertain whether this conclusion also holds for growth of the intertidal areas in the western Wadden Sea.

7.3. FAR-FIELD DISPERSION

In this section a far-field expert judgement of the expected effects of a continuous nourishment in the vicinity of Ameland Inlet is given. The developments of the continuous nourishment have been assessed on a half-year timescale, whereas the Zandwindmolen system will be built for a much longer-term application. It should therefore be evaluated to what extent the findings hold for the subsequent years.

The mid-field behaviour shows that the continuous nourishment of 2Mm^3 can be processed by the Borndiep ebb channel over the timescale of a half year. Moreover, the Borndiep channel strives to a smaller new equilibrium wet cross-sectional area than before. Therefore, the new equilibrium flow velocity is higher than the original equilibrium flow velocity. Whether the Borndiep channel remains able to process a continuous nourishment with a rate of 2 Mm^3/year depends on the sediment composition of the nourishment and the sediment transport capacities outside the Borndiep channel (vicinity Ameland Inlet). Fractions ≥350μm silt up the tidal channel and are therefore for the long term undesired from the perspective of the Zandwindmolen. The other fractions disperse well over the tidal channel, but it is unknown how well the sediment particles can keep on dispersing in areas where the sediment transport capacity is (at least) an order of magnitude lower (North sea coastline and back-barrier Wadden Sea basin).
However, when coarse fractions (≥350μm) are considered outside of the intended behaviour of the Zandwindmolen, then coarse fractions show some useful characteristics for the dispersion in general. As the coarse fractions mainly remain in the tidal channel, they significantly contribute to the

reduction of the wet cross-section of the tidal channel. As previously discussed, the reduction of the wet cross-section of the tidal channel generates a higher flow velocity, which in turn enhances the dispersion of fine and medium sized sediment. Therefore, the addition of coarse sediment enhances the dispersion of the fine and medium sediments, which is a positive effect.

It was found in the mid-field behaviour that the fine and medium sized sediment fractions reach and cover the outer delta. It is expected that this behaviour continues over time and therefore, enable the outer delta to grow. With the presence of waves, the finer fractions are expected to settle on the outer delta during mild energetic conditions and during energetic conditions to be transported by the eastward littoral drift to coastline of Ameland. The same behaviour is expected for the medium sized fractions, but the rate in which the medium sized fractions are mobilized compared to the fine sediment fraction is lower. Thus, over time it is expected that the continuous nourishment contributes to the BKL enforcement of the Ameland coastline with fractions ≤350μm. Based on sediment connectivity, a secondary effect of the continuous nourishment could be that due to the reduction of the sand hunger of the Wadden Sea basin by artificial sediment, the coastline of Terschelling is also less prone to erosion.

Whether the tidal flats accrete or erode depend and on a complex interaction between waves and currents. Waves cause erosion and the currents cause accretion. Which process is dominant depends on seasonality and the absence or presence of storm events. Based on historical behaviour, the intertidal areas in the eastern Wadden Sea were able to grow along sea level rise. Therefore, if there is an abundance of dispersed artificial sediment available, it is likely that this causes the intertidal areas of the eastern Wadden Sea to grow along sea level rise autonomously.

In conclusion, this study has shown for a period of six months that the sediment can disperse well through the tidal current towards the North and Wadden Sea. The natural distribution of the nourished sand will, through sediment connectivity between the separate parts of a tidal inlet system, compensate for the erosion (autonomous and due to sea level rise) of the inlet (especially the outer delta). Also, the dispersion of sediment towards the Wadden Sea (partly) eliminates the need for the sand to come from the outer delta, adjacent shorelines and coastal foundation. For the North Sea side of the tidal inlet system, this prevents erosion of the coastline (Terschelling and Ameland) and thus prevents risks to safety. The latter could not yet be demonstrated with this model in which there are no waves and which is only six months in advance. For the intertidal areas located in the eastern Wadden Sea, the abundance of dispersed sediment will lead to natural growth of the intertidal areas (under the current sea level rise).

8 | Conclusions and Recommendations

In this chapter a conclusion is formed and recommendations are given for future research.

8.1. Conclusion

In this study the usefulness of a Zandwindmolen is determined by assessing to which extent the nourished sand volume is dispersed by natural processes in the short and long term. The usefulness is determined based on three main questions:

1. With what equipment can a continuous nourishment be practically carried out?
2. How and how far disperses the nourished sediment from the Zandwindmolen in the short and long term?
3. How much sand can be nourished without silting up the system? In other words, what sand transport capacity does the Ameland inlet have?

These research questions were answered through a near-field, mid-field and far-field dispersion study.

With what equipment can a continuous nourishment be practically carried out?
To execute a continuous nourishment while simultaneously ensuring that the nourished sediment does not accumulate and disperses over a large distance, a mixing plume has to be formed and the sediment has to be placed as high as possible in the water column. A characteristic of a mixing plume is that sediments settle according to their individual settling velocity and become prone to ambient currents (sediment concentration ≤1-2%). Therefore, direction during the initial settling process (short term) can be provided by horizontal external forces acting on the settling particle. Because the nourishment is continuous in the tidal inlet, this will cause the mix plume to be transported locally directly after placement with the tidal current towards the North Sea or Wadden Sea. In the tidal inlet the tidal flow velocities are large (> 1 m/s) and peak flow velocities are the dominant flow velocities. Therefore, nourished sediment can be transported over large distances due to the settling and re-suspension processes.
A spreader pontoon is able to nourish sediment in a mixing plume and is therefore suitable as dredging equipment for a continuous nourishment.

How and how far disperses the nourished sediment from the Zandwindmolen in the short and long term?
Sediment placed as high as possible in the water column is dispersed based on three sediment transport processes.

1. Dispersion through the initial settling process of sediment
2. Dispersion through re-suspension of settling sediment particles
3. Dispersion after sediment is deposited on the sea bed (bed load transport and suspended transport)

Table 8.1: In this table the short term and long term sediment transport processes are quantified. Sediment processes 1 and 2 lead to the maximum short term dispersion. Sediment process 3 leads to the maximum long term dispersion (half year). The maximum total dispersion is a summation of the three individual sediment transport processes.

	Maximum distance from Nourishment location [m]							
Direction	North Sea				Wadden Sea			
Fraction μm	100	200	300	400	100	200	300	400
1) Preliminary initial settling dispersion [m]	8000	2500	2200	1000	8000	2500	2200	1000
2) Dispersion distance due to re-suspension [m]	900	5300	4800	5900	2400	6200	6500	6300
3) Natural near-field sediment transport [m]	200	100	0	0	200	200	100	0
Maximum short term dispersion	9100	7900	7000	6900	10600	8900	8800	7300
3) Natural mid-field sediment transport [m]	2100	1600	300	100	2000	2300	900	100
Maximum long term dispersion (half year) - with continuous nourishment	2100	1600	300	100	2000	2300	900	100
Maximum total dispersion	11200	9500	7300	7000	12600	11200	9700	7400

Dispersion through processes 1 and 2 are short term dispersion processes (time scale: instantaneous to several weeks) and dispersion through process 3 is a long term dispersion process (months to years). In Table 8.1 the dispersion distances for the short and long term are depicted and quantified per sediment fraction. The total dispersion based on a continuous nourishment which is carried out by nourishing the sediment by a spreader pontoon in a tidal inlet over the duration of a half year, is mainly governed by the short term sediment transport processes. Besides that the greatest dispersion distance origins from the short term dispersion processes, the direction of the dispersion is also determined by the short term dispersion.

How much sand can be nourished without silting up the system? In other words, what sand transport capacity does the Ameland inlet have?
It was found that the Borndiep channel has a tidal transport capacity of 4.23 Mm^3 per year (sum of flood and ebb transport capacity). Moreover, it was determined that the vicinity of Ameland Inlet (Wadden Sea basin, adjacent coastlines, outer delta and coastal fundament) requires 1.128 Mm^3 to grow along with the current sea level rise (2 mm/year). Therefore, it is decided to nourish sediment continuously with a rate of 2 Mm^3/year.

First, the cross-sectional area of the tidal channel reduces compared to the pristine cross-sectional area due to the continuous nourishment. It is found that the depth of the channel continues to decrease as sediment settles on the seabed of the tidal channel. Simultaneously, if the continuous nourishment persist over a half year, the new wet cross-section of the tidal channel remains approximately constant. In order to sustain a constant wet surface cross-sectional area, erosion at the channel walls occurs as a compensating effect for the depth reduction. Based on the approximately constant cross-sectional area of the Borndiep channel, it is found that the tidal inlet is able to process a continuous nourishment of 2 Mm^3/year over the timescale of a half year.
Whether the Borndiep channel can keep on processing a nourishment with a rate of 2 Mm^3/year

depends on the actual composition of the nourishment. In this study a nourishment composition is applied in which each fraction occurs with the same proportion. It is found that fractions ≥350μm fraction do not disperse out of the Borndiep tidal channel. Therefore, it is not recommended that this fraction is nourished. Fractions ≤350μm disperse out of the tidal channel and are therefore recommended as nourishment sediment.

General conclusion
Due to the supply of sand and silt from the North Sea, the bed of the Wadden Sea rises autonomously with the sea level. However, this causes erosion on the outer delta, adjacent coastlines and coastal foundation the Ameland Inlet system. If the sea level rise accelerates, the autonomous sediment import will be able to follow the sea level rise up to 6-10 mm/year (Wang et al., 2018). Thereafter, the autonomous sediment import is insufficient to allow the Wadden Sea to grow along with the sea level rise and might cause the intertidal areas of the Wadden Sea to drown. In addition, an acceleration of sea level rise will have an even greater negative impact on the stability of the coastline of Terschelling and Ameland, the outer delta and the coastal foundation. Without nourishments these will deteriorate. Therefore, this study focused on the possibility of whether sand nourished in a tidal inlet can disperse sufficiently well to ensure growth of the vicinity of Ameland Inlet as a whole. Based on sediment connectivity between the separate parts of a tidal inlet system, this study has shown for a period of six months that the sediment can disperse well through the tidal current. Waves are expected to amplify this process. The natural distribution of the nourished sand will, through sediment connectivity, compensate for the erosion (autonomous and due to sea level rise) of the inlet (especially the outer delta). Moreover, sediment is imported to the Wadden Sea and accretion of intertidal areas is already observed in a time-span of six months. Therefore, a continuous nourishment in a tidal inlet could serve as a new nourishment method to enhance sediment import to the Wadden Sea. Finally, it is also expected that the continuous nourishment in the tidal inlet contributes to keeping the North Sea coast of Terschelling and Ameland safe. The latter could not yet be demonstrated with this model in which there are no waves and which is only six months in advance.

This study focused on only sand, while a lot of silt is also present in the Wadden Sea. Also, the question of how much extra sand and silt is needed at a certain sea level rise to allow the reservoir area of the Ameland inlet to rise along with the sea level rise has not been studied in this study. This research mainly focused on the dispersion of sand due to a nourishment in the Ameland tidal inlet.

8.2. RECOMMENDATIONS

In this section the recommendations for successive research are listed.

Based on this study, an indicative image has been drawn up of the effects of continuous nourishment in a tidal inlet. The results are only based on currents and a simulation duration of a half year. Therefore, the results cannot yet provide insight into what the effects of the continuous nourishment are on the North Sea coastline. It is therefore recommended to add waves to the Ameland Inlet model and to increase the simulation duration to 5-10 years.

Adding waves also gives multiple options for deciding on an optimal nourishment location. In this research all possible locations on the North Sea side were eliminated due to the lack of waves in the model. In addition to the promising results of this research through continuous nourishment in the Borndiep, it is also important for the entire Zandwindmolen concept to be able to investigate possible nourishment locations closer to the coast. This decreases the transportation distance from the extraction site to the nourishment location and thus reduces the costs of the pipeline. An example

of this could be continuous nourishment on the outer delta. Again, based on sediment connectivity, this could also lead to growth of the Wadden Sea basin with sea level rise.

For in-depth research into the consequences of continuous nourishment for growth of the intertidal areas in the Wadden Sea basin, it is recommended to perform a 3D model simulation with the addition of waves. Accretion of the intertidal areas, is mainly determined by the curvature secondary flow, which can only be simulated with a 3D model. In addition, erosion of the intertidal flats is mainly determined by the waves. A combination of both will provide more insight into whether the intertidal areas in the Wadden Sea will grow and with what rate they might grow due to the continuous nourishment. This can then be used to determine the SLR scenario to which the intertidal areas can grow through continuous nourishment.

In this study, a random nourishment with a sediment concentration of 1-2 % consisting of different sediment fractions was composed. It is recommended to investigate the extraction locations as close as possible to the Ameland inlet and to carry out more realistic nourishment. In this study it was found that mainly the 400 μm fraction does not disperses significantly further than the Borndiep. For optimal dispersion it is therefore recommended to find the finest possible composition of nourishment sediment at the extraction site. However from a dredge contractor point of view, the 1-2% sediment concentration might be hard or expensive to achieve. Therefore, it is also recommended to study the effects of a continuous nourishment with a higher sediment concentration in the tidal inlet. Such a nourishment is expected to initially behave like the $\geq$350μm fraction and thus accumulate in the tidal channel, because the sediment cannot spread optimally due to the favorable properties of the mixing plume. Nevertheless, fractions $\leq$350μm are expected to slowly move out of the channel and over longer time scales (order months/years) also contribute to BKL maintenance, growth of intertidal areas and accretion of the outer delta. Also, because sediment initially accumulates in the tidal channel it will cause a reduction in wet surface area and thus induce an increase in flow velocity. The latter is beneficial to the further dispersal of sediment.

The behaviour of the wet cross-section should be researched in more detail based on the addition of a continuous nourishment. The Borndiep channel is the primary channel of the entire cross-sectional inlet of the Ameland basin. But, the secondary Boschgat channel is likely to react on the continuous nourishment in the primary channel. As the systems strives towards an equilibrium, a found reduction of the Borndiep channel might cause an enlargement of the Boschgat channel. This could be researched by means of this model as in the Borndiep and Boschgat the tidal flow is the dominating process. An addition of waves, increasing the simulation duration and transforming the 2D to a 3D model will yield more accurate results.

The initial settling process of sediment particles is described by Delft-3D in this study, whereas there is much more accurate software available to simulate a mixing plume and to find the eventual dispersion. An example is CFD (computational fluid dynamics) modelling. Also, this study assumed a continuous nourishment over a predefined area. In reality, the spreader pontoon is not able to cover and nourish this entire area at once. CFD modelling is required to simulate an accurate nourishment strategy in which the spreader pontoon moves perpendicular over the ebb/flood direction while nourishing sediment.

A more accurate simulation of the dispersion can be achieved by integrating layers in the bed of the Delft-3D model. Due to the creation of extra levels in the bed, the active sediment layer can be depicted more accurately. By doing so, the eventual dispersion with the presence of the natural background fraction can be simulated more accurately.

An ecological study is also recommended. The sedimentation is found to be approximately 1 mm/-day in regions far away from the source (order $\geq$2 km). Closer to the nourishment source (order

≤2 km) in the tidal channel the sedimentation is between 5-7 mm/day. This is due to the large dispersion. Another nuisance can be the increase in turbidity. The nourishment concept is based on a mix plume. In the regular dredging industry, this plume type is avoided because it can lead to the smothering of vulnerable ecosystems and/or a reduction of light to the seabed. Therefore, it might cause any harm to vulnerable ecosystems. It is expected that no effects will be visible due to the small continuous supplementation and the very low sediment mixture concentration. But this should be validated by an ecologist.

References

Arends, A. (2016). Kustlijnzorg rijkswaterstaat. Technical report, Rijkswaterstaat.

Baart, F., Van Gelder, P. H., De Ronde, J., Van Koningsveld, M., and Wouters, B. (2012). The effect of the 18.6-year lunar nodal cycle on regional sea-level rise estimates. *Journal of Coastal Research*, 28(2):511–516.

Bahlke, C. (2019). Harbours and shipping. Technical report, Wadden Sea Secretariat.

Bak, J. (2017). Nourishment strategies for the ameland inlet.

Bosboom, J. and Stive, M. (2021). Coastal dynamic i: Lecture notes cie4305. *Delft, The Netherlands: Delft University of Technology, 573p.*

Boswood, P. and Murray, R. (2001). World-wide sand bypassing systems: data report. Technical report, Queensland Government Environmental Protection Agency.

Bruun, P. and Gerritsen, F. (1960). Stability of coastal inlets. *Coastal Engineering Proceedings*, (7):23–23.

Casiday, R., Noelken, G., and Frey, R. (2008). Treating the public water supply: What is in your water, and how is it made safe to drink. *Department of Chemistry, Washington University*.

Cheung, K. F., Gerritsen, F., and Cleveringa, J. (2007). Morphodynamics and sand bypassing at ameland inlet, the netherlands. *Journal of Coastal Research*, 23(1 (231)):106–118.

Dankers, N. and Zuidema, D. R. (1995). The role of the mussel (mytilus edulis l.) and mussel culture in the dutch wadden sea. *Estuaries*, 18(1):71–80.

Davis Jr, R. A. and Hayes, M. O. (1984). What is a wave-dominated coast? In *Developments in Sedimentology*, volume 39, pages 313–329. Elsevier.

De Fockert, A. (2008). Impact of relative sea level rise on the amelander inlet morphology.

De Swart, H. and Zimmerman, J. (2009). Morphodynamics of tidal inlet systems. *Annual review of fluid mechanics*, 41:203–229.

de Wit, F., Tissier, M., and Reniers, A. (2019). Characterizing wave shape evolution on an ebb-tidal shoal. *Journal of Marine Science and Engineering*, 7(10):367.

De Wit, L. (2015). 3d cfd modelling of overflow dredging plumes.

Deltares (1999). Dataset documentation. `https://publicwiki.deltares.nl/display/OET/Dataset+documentation`.

Deltares, D. (2018). Delft3d-flow user manual. *Delft, the Netherlands*.

Dickhof, H. (2016). Design and construction of a spray pontoon and maintenance of ham 310.

Elias, Pearson, A. V. d. S. (2020a). Understanding the morphological processes at ameland inlet : Kustgenese 2.0 synthesis of the tidal inlet research. Technical report, Deltares.

Elias, E. (2017). Understanding the present day morphodynamics of ameland inlet. Technical report, Deltares.

Elias, E. (2019-2020b). Een actuele sedimentbalans van de waddenzee. Technical report, Deltares.

Elias, E. P. and van der Spek, A. J. (2006). Long-term morphodynamic evolution of texel inlet and its ebb-tidal delta (the netherlands). *Marine Geology*, 225(1-4):5–21.

Elias, E. P., Van der Spek, A. J., Wang, Z. B., and De Ronde, J. (2012). Morphodynamic development and sediment budget of the dutch wadden sea over the last century. *Netherlands Journal of Geosciences*, 91(3):293–310.

Flemming, B. and Delafontaine, M. (1994). Biodeposition in a juvenile mussel bed of the east frisian wadden sea (southern north sea). *Netherland Journal of Aquatic Ecology*, 28(3):289–297.

Flemming, B. W. and Davis Jr, R. (1994). Holocene evolution, morphodynamics and sedimentology of the spiekeroog barrier island system(southern north sea). *Senckenbergiana maritima. Frankfurt/Main*, 24(1):117–155.

Hayes, M. (1979). Barrier island morphology as a function of wave and tide regime. in 'barrier islands from the gulf of st. lawrence to the gulf of mexico'.(ed. sp leatherman.) pp. 1–29.

Hayes, M. O. (1980). General morphology and sediment patterns in tidal inlets. *Sedimentary geology*, 26(1-3):139–156.

Heritage, W. N. (2021). The long road to the wadden sea world natural heritage site. https://https://worldoceanreview.com/en/wor-5/improving-coastal-protection/the-art-of-coastal-management/the-long-road-to-the-wadden-sea-world-natural-heritage-site/.

Hoeksema, H., Mulder, H., Rommel, M., De Ronde, J., and De Vlas, J. (2004). Bodemdalingstudie waddenzee 2004: Vragen en onzekerheden opnieuw beschouwd. *Rapportnr.: 2004.025*.

Holthuijsen, L. H. (2010). *Waves in oceanic and coastal waters*. Cambridge university press.

IADC (2002). Terra et aqua. Technical report, IADC.

IADC (2014). Facts about trailing suction hopper dredgers. Technical report, IADC.

IHC, R. (2015a). Floating dredge assortment. https://www.royalihc.com/-/media/royalihc/products/dredging/hopper-dredging/tshd-dredge-line-components/floating-discharge-line-assortment-2.jpg.

IHC, R. (2015b). Floating dredging hoses. https://www.royalihc.com/-/media/royalihc/products/dredging/hopper-dredging/tshd-dredge-line-components/d3-floating-discharge-lines-2015.pdf.

Jiao, J. (2014). Morphodynamics of ameland inlet: medium-term delft3d modelling.

King, S. E. and Lester, J. N. (1995). The value of salt marsh as a sea defence. *Marine pollution bulletin*, 30(3):180–189.

KNMI (2021). Knmi klimaatsignaal'21. https://www.knmi.nl/kennis-en-datacentrum/achtergrond/knmi-klimaatsignaal-21.

Kranenburg, C. (1998). Dichtheidsstromen. *Collegedictaat CT5302*.

Laboyrie, P., Van Koningsveld, M., Aarninkhof, S., Van Parys, M., Lee, M., Jensen, A., Csiti, A., and Kolman, R. (2018). *Dredging for sustainable infrastructure*. CEDA/IADC.

Latteux, B. (1995). Techniques for long-term morphological simulation under tidal action. *Marine geology*, 126(1-4):129–141.

Lesser, G. R. (2009). An approach to medium-term coastal morphological modelling.

Lesser, G. R., Roelvink, J. v., van Kester, J. T. M., and Stelling, G. (2004). Development and validation of a three-dimensional morphological model. *Coastal engineering*, 51(8-9):883–915.

Lotze, H. K. (2005). Radical changes in the wadden sea fauna and flora over the last 2,000 years. *Helgoland Marine Research*, 59(1):71–83.

Loza, P. R. G. et al. (2008). Sand bypassing systems: masters in environmental engineering.

Meehl, G., Meehl, G., Stocker, T., Collins, W., Friedlingstein, P., Gaye, T., Gregory, J., Kitoh, A., Knutti, R., Murphy, J., et al. (2007). Global climate projections. in 'climate change 2007: the physical science basis'.(eds s solomon, d qin, m manning, z chen, m marquis, kb averyt, m tignor, hl miller) pp. 747–845.

Meltofte, H. (1994). *Numbers and distribution of waterbirds in the Wadden Sea: results and evaluation of 36 simultaneous counts in the Dutch-German-Danish Wadden Sea 1980-1991*. CWSS.

Oertel, G. F. (1972). Sediment transport of estuary entrance shoals and the formation of swash platforms. *Journal of Sedimentary Research*, 42(4):858–863.

Pearson, S. G., van Prooijen, B. C., Elias, E. P., Vitousek, S., and Wang, Z. B. (2020). Sediment connectivity: A framework for analyzing coastal sediment transport pathways. *Journal of Geophysical Research: Earth Surface*, 125(10):e2020JF005595.

Reise, K., Baptist, M., Burbridge, P., Dankers, N., Fischer, L., Flemming, B., Oost, A., and Smit, C. (2010). The wadden sea-a universally outstanding tidal wetland. In *The Wadden Sea 2010. Common Wadden Sea Secretariat (CWSS); Trilateral Monitoring and Assessment Group: Wilhelmshaven.(Wadden Sea Ecosystem; 29/editors, Harald Marencic and Jaap de Vlas)*, volume 7.

Rijkswaterstaat (1999). Sedimentatlas waddenzee. Technical report, Rijkswaterstaat.

Rijkswaterstaat (2012). Suppletieprogramma 2012-2015.

Rijkswaterstaat (2016a). Suppletieprogramma 2016-2019.

Rijkswaterstaat (2016b). Vaklodingen 2016. Technical report, Rijkswaterstaat, Haren.

Rijkswaterstaat (2020a). Kustgenese 2.0: kennis voor een veilige kust. Technical report, Rijksoverheid.

Rijkswaterstaat (2020b). Suppletieprogramma 2020-2023.

Rijkswaterstaat (2021a). Diepe delfstoffen. `https://www.waddenzee.nl/themas/diepe-delfstoffen`.

Rijkswaterstaat (2021b). Duurzame energie. `https://www.rijksoverheid.nl/onderwerpen/duurzame-energie/meer-duurzame-energie-in-de-toekomst`.

Rijkswaterstaat (2021c). Kustlijn kaart. `https://maps.rijkswaterstaat.nl/geoweb55/index.html?viewer=Kustlijnkaart`.

Rijkswaterstaat (2021d). Planning van het kustonderhoud. https://www.rijkswaterstaat.nl/water/waterbeheer/bescherming-tegen-het-water/maatregelen-om-overstroming en-te-voorkomen/kustonderhoud/planning-en-aanpak.

Rijkswaterstaat (2021e). Waterbeheer. https://waterinfo.rws.nl/#!/nav/themakaarten/.

Rijkswaterstaat, R., Noordzee, R., Noord-Nederland, R., Noord-Holland, R., Zuid-Holland, R., and Zeeland, R. (2020). Kustlijnkaarten 2020.

Rutteman, H. (2021). The application of a continuous nourishment on wave and tide-dominated systems.

Schuiling, T. (2019). Suppletiebehoefte van de nederlandse kust: een onderzoek naar zandverliezen op dieper water en een vergelijking tussen de suppletiehoefte van de nederlandse kust en de gerealiseerde suppletievolumes. B.S. thesis, University of Twente.

Sha, L. P. (1990). Sedimentological studies of the ebb-tidal deltas along the west frisian islands, the netherlands. *PhD Thesis, Utrecht University*.

Stema (2022). New developed high speed power tow winch 11 kw. https://stema-systems.nl/equipment/high-speed-power-hydrographic-tow-winch/.

STOWA (2021). Effect van zandsuppleties op de kust en het wad. https://www.stowa.nl/deltafacts/waterveiligheid/innovatieve-dijkconcepten/effect-van-zandsuppleties-op-de-kust-en-het.

Swinkels, C. M. and Bijlsma, A. C. (2012). Understanding the hydrodynamics of a north sea tidal inlet by numerical simulation and radar current measurements. In *Proceedings of 3rd International Symposium on Shallow Flows, Iowa City, USA*.

UNESCO World Heritage Centre (2021). Wadden sea. https://whc.unesco.org/en/list/1314/.

van de Kreeke, J. and Brouwer, R. L. (2017). *Tidal inlets: hydrodynamics and morphodynamics*. Cambridge University Press.

Van de Kreeke, J. and Robaczewska, K. (1993). Tide-induced residual transport of coarse sediment; application to the ems estuary. *Netherlands Journal of Sea Research*, 31(3):209–220.

Van der Spek, A. J. F. (1994). *Large-scale evolution of Holocene tidal basins in the Netherlands*. Universiteit Utrecht, Faculteit Aardwetenschappen.

van der Wegen, M., Dastgheib, A., Jaffe, B. E., and Roelvink, D. (2011). Bed composition generation for morphodynamic modeling: case study of san pablo bay in california, usa. *Ocean Dynamics*, 61(2):173–186.

Van Koningsveld, M. and Mulder, J. M. (2004). Sustainable coastal policy developments in the netherlands. a systematic approach revealed. *Journal of Coastal Research*, 20(2 (202)):375–385.

van Rijn, L. (1993). Principles of sediment transport in rivers, estuaries and coastal seas. Technical report, University of Utrecht, Delft Hydraulics.

van Rijn, L. (2020). Turbidity due to dredging and dumping of sediments. Technical report, Leo van Rijn.

Van Straaten, L. and Kuenen, P. H. (1957). *Accumulation of fine grained sediments in the Dutch Waddensea*.

Van Weerdenburg, R. (2019). *Exploring the relative importance of wind for exchange processes around a tidal inlet system: the case of Ameland Inlet*. PhD thesis, Msc. Thesis, Delft University of Technology, Delft, The Netherlands.

van't Hoff, J. and van der Kolff, A. N. (2012). *Hydraulic fill manual: for dredging and reclamation works*, volume 244. CRC press.

Walburg, L. (2002). Zandvolumes in het kustsysteem van de wadden. Technical report, Rijksinstituut voor Kust en Zee/RIKZ.

Wang, Y., Yu, Q., Jiao, J., Tonnon, P. K., Wang, Z. B., and Gao, S. (2016). Coupling bedform roughness and sediment grain-size sorting in modelling of tidal inlet incision. *Marine Geology*, 381:128–141.

Wang, Z., Hoekstra, P., Burchard, H., Ridderinkhof, H., De Swart, H., and Stive, M. (2012). Morphodynamics of the wadden sea and its barrier island system. *Ocean & coastal management*, 68:39–57.

Wang, Z. B., Elias, E. P., van der Spek, A. J., and Lodder, Q. J. (2018). Sediment budget and morphological development of the dutch wadden sea: impact of accelerated sea-level rise and subsidence until 2100. *Netherlands Journal of Geosciences*, 97(3):183–214.

Williams, G. L., Clausner, J. E., and Neilans, P. J. (1994). *Improved eductors for sand bypassing*. US Army Engineer Waterways Experiment Station.

Winterwerp, J. (2002). Near-field behavior of dredging spill in shallow water. *Journal of waterway, port, coastal, and ocean engineering*, 128(2):96–98.

List of Figures

List of Tables

A | General information Wadden Sea

In this appendix additional information regarding the Wadden Sea is described.

A.0.1. Dutch Wadden Sea Islands

Fig. A.1 provides an overview of the different elements in the Wadden Sea area. The Dutch Wadden Sea has five different barrier islands with a total surface of 4000 km^2. From respectively left to right; Texel (a), Vlieland (b), Terschelling (c), Ameland (d) and Schiermonnikoog (e). In between these islands inlets are located. The watersheds are not fixed and can move due to human interference (Bosboom and Stive, 2021). The Western and Eastern Wadden Sea respectively compromises the Inlets; Texel Inlet (A), Eierlandse Gat Inlet (B), Vlie Inlet (C) and Ameland Inlet (D), Frisian Inlet (E) and the Groninger Wad and Ems Estuary (F). In the eastern part, the basins are relatively shallow and narrow. The tidal channels are small compared to the intertidal flats with ratios of intertidal flat over the total surface area of 0.7-0.8 (Elias et al., 2012). Whereas in the western part, the basins are relatively wider resulting in ratios of intertidal flat over total surface area is 0.3 to 0.4 (Elias et al., 2012).

Fig. A.1 also illustrates the Wadden Sea area before and after major human activities and provides the current morphology of the Wadden Sea area. Both human interventions and relative sea level rise have caused morphological changes in the Wadden Sea system. Although human constructions are ongoing since the Middle Ages, the most significant human intervention in the Wadden Sea area is the creation of Afsluitdijk. The eventual reason to construct the Afsluitdijk was due to a storm surge in 1916. In 1932 the 32 kilometres long Afsluitdijk closed of the late Zuiderzee permanently and created the Ijselmeer. Another major flooding in 1952 initiated the closure of the Lauren-szee, which was completed in 1969. Both closures reduced the basin dimensions significantly and changed the morphology of the Wadden Sea system. The large scale human interventions together with the dykes protecting the remainder of the mainland form the Wadden Sea as we know it today (Elias et al., 2012) ; (Wang et al., 2018) ; (Flemming and Davis Jr, 1994).

The volume of water (excluding any fresh water) that flows in and out through an Inlet during one tidal cycle is the tidal prism. In Fig. A.1 the tidal prism and surface areas for respectively mean high water (MHW) and mean low water (MLW) are provided for each the tidal basin individually. Furthermore, the depth in m to NAP is illustrated for the Wadden Sea area in Fig. A.1.

Most of the sediment found in the Wadden Sea originates from the North Sea. Sediment import through debouching rivers is of minor importance. Mud is mainly imported with North Sea water, while the sandy sediments are predominantly supplied by erosion of the ebb-tidal deltas, the barrier islands and the ajdacent shore of the province North Holland(Van Straaten and Kuenen, 1957). The Wadden Sea is a sediment sharing tidal inlet system. This implies that the previously mentioned inlets transport sediment from one basin to another (Wang et al., 2018). Within this thesis the focus is on sand, therefore the effect of mud is no longer taken into consideration.

Gas is won in the sea area of Zuidwal, west of Harlingen. Furthermore, gas is won ashore on Ameland, Blija, Moddergat en Ruidhorn. Furthermore, rock salt is extracted near Harlingen. (Rijkswaterstaat, 2021a).

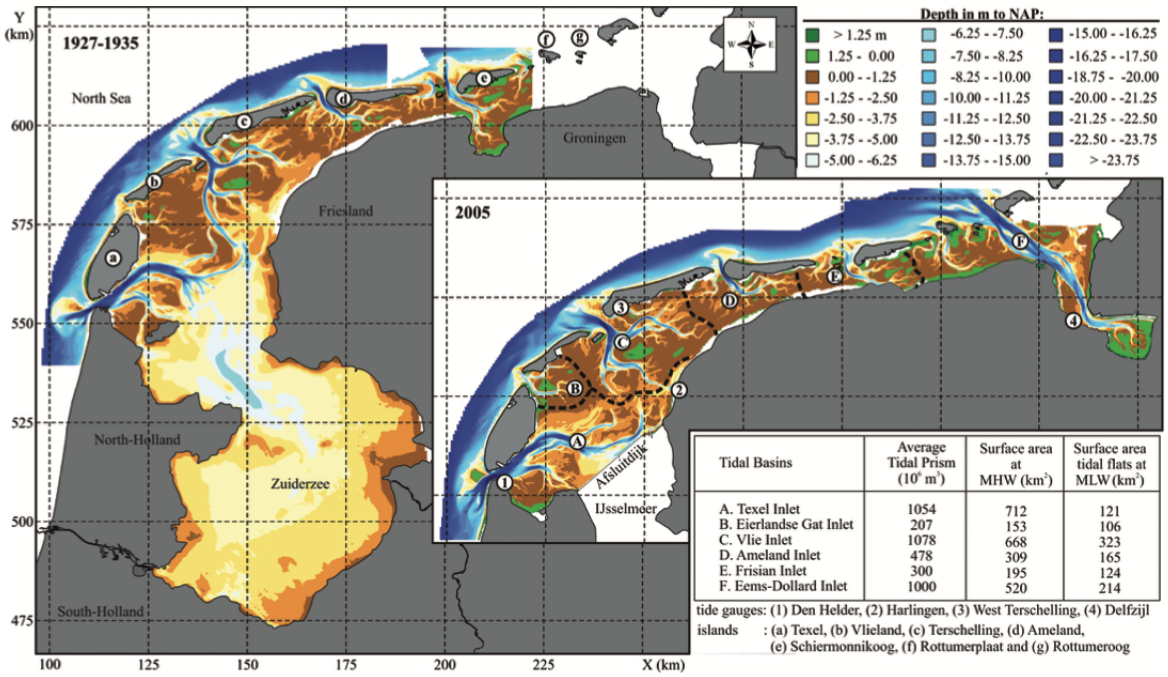

Tidal Basins	Average Tidal Prism (10^6 m^3)	Surface area at MHW (km^2)	Surface area tidal flats at MLW (km^2)
A. Texel Inlet	1054	712	121
B. Eierlandse Gat Inlet	207	153	106
C. Vlie Inlet	1078	668	323
D. Ameland Inlet	478	309	165
E. Frisian Inlet	300	195	124
F. Eems-Dollard Inlet	1000	520	214

tide gauges: (1) Den Helder, (2) Harlingen, (3) West Terschelling, (4) Delfzijl
islands : (a) Texel, (b) Vlieland, (c) Terschelling, (d) Ameland, (e) Schiermonnikoog, (f) Rottumerplaat and (g) Rottumeroog

Figure A.1: Wadden Sea before and after large scale human interventions. This image is adapted from (Elias et al., 2012)

The tidal inlet between Terschelling and Ameland is known to the local population as the "Amelander Zeegat". Internationally, it is better known as Ameland Inlet.

The Ameland Inlet is located in between Terschelling and Ameland Fig. A.1. The lengths of Terschelling and Ameland are respectively 28 and 23km. In between the two islands, two ebb-channels are located named Borndiep (1) and Boschgat (20). The depths of the Borndiep and Boschgat channel are respectively approximately 25 and 10m (Swinkels and Bijlsma, 2012). Furthermore an ebb-tidal delta is located at the north side in between Terschelling and Ameland. These regions are mostly referred to as the Kofmansplaat (28) and Bornrif (30) Fig. A.2. The main ebb-channel Borndiep (1) splits up in de Kromme Balg (9), Westgat (3) and Molengat (7). The secondary ebb-channel Boschgat (20) splits up in Blauwe Balg (23) and Nieuwe Oosterom (24).

A.1. FUNCTION WADDEN SEA

The Wadden Sea has many functions for both human and nature. The main functions are; ecological, cultural, economical and industrial, sea defence and recreational.

The Wadden Sea is of ecological importance as 10,000 animal, fungi and plant species live in the Wadden Sea (Reise et al., 2010). For approximately 10 million migrating birds it is a very important staging, wintering and breeding area (Meltofte, 1994). On the intertidal flats and in the subtidal zone large amounts of mussels find their home. Mussels are an important factor of the ecosystem since they filter the seawater, making it possible for lots of other species to live in the Wadden Sea (Dankers and Zuidema, 1995). Also fish species generously use the tidal channels and the basin area as nursery and feeding area (Lotze, 2005). Finally, the Wadden Sea is inhabited for over 5000 years making it of great cultural importance. Due to these characteristics it is listed on the UNESCO World Heritage list.(UNESCO World Heritage Centre, 2021).

The Wadden Sea also functions as an important Sea Defence for the main land. The barrier islands, ebb-tidal deltas, intertidal flats and the salt marches severely reduce the wave height at the back

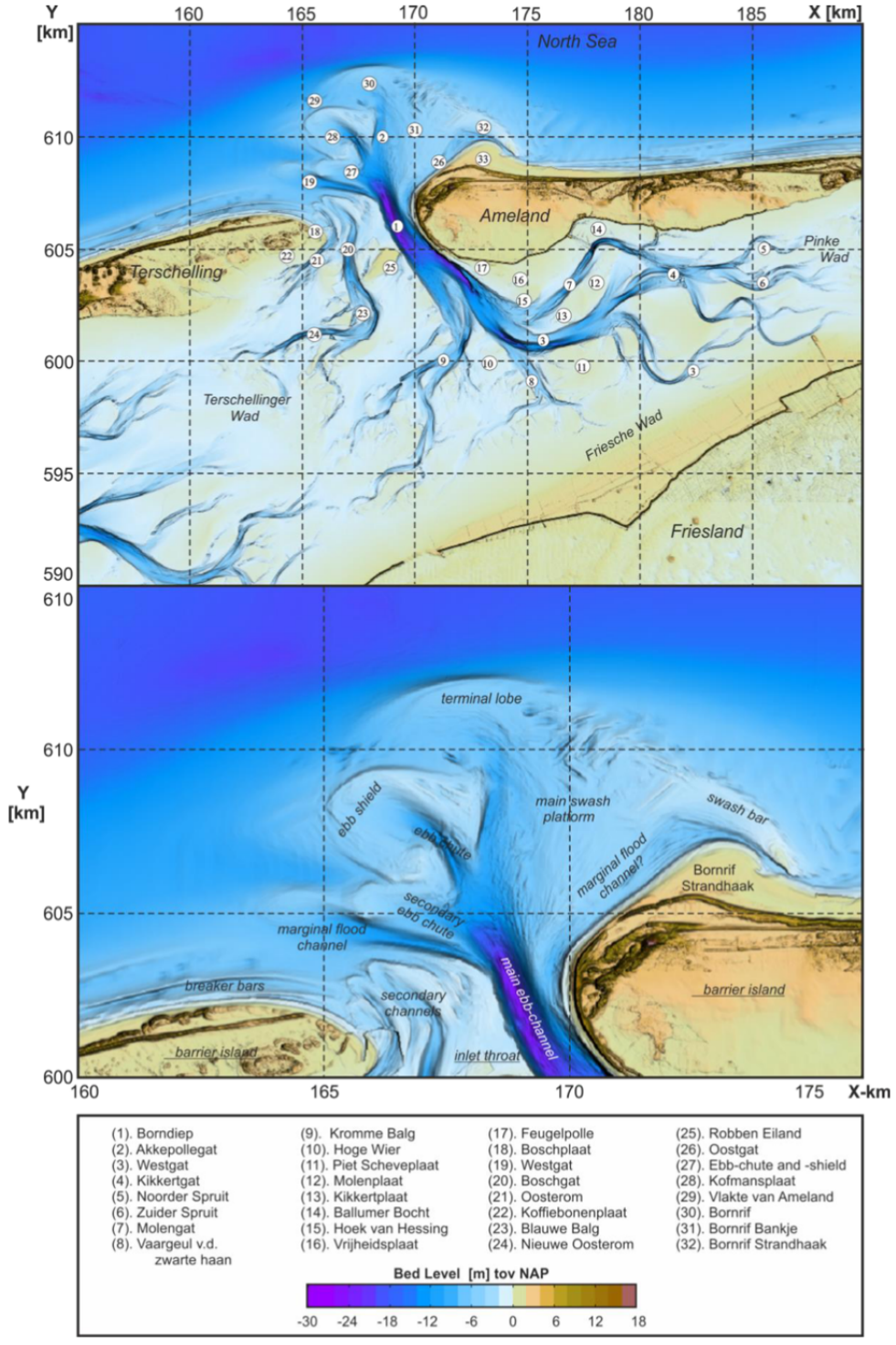

Figure A.2: Upper image: Amelander zeegat with a grid and numerical values to indicate locations. Lower image Components of a tidal Inlet system. The image is obtained from (Elias, 2017)

barrier of the basin. The intertidal flats are at some locations covered by mussels, which cause a higher roughness of the bed. A higher roughness cause more friction and thus wave dissipation (Flemming and Delafontaine, 1994). However, intertidal flats do not contribute as much as salt marshes to wave dissipation. Salt marshes dissipate almost all wave energy before waves reaches the landward shoreline. The dissipative effect of the salt marsh depend on are the width, water depth, vegetation and bottom friction of the salt marsh (King and Lester, 1995).

In the back barrier of the Wadden Sea many ports are located. The sheltered location behind the barrier islands is favorable for the reduced hydrodynamic conditions, but does also induces sedimentation in the harbor basins.
The major ports in the area of the Wadden Sea are the German ports of Hamburg and Bremen/Bremerhaven, the oil refinery and port of Wilhelmshaven, as well as the ports of Esbjerg in Denmark and Delfzijl and Harlingen in the Netherlands (Bahlke, 2019). The presence of these ports emphasize the economical importance of the Wadden Sea.

The abundant functions of the Wadden Sea require proper management in order to maintain their function. Hence, knowledge of future development of the Wadden Sea system is of utmost importance for the management of the system (Wang et al., 2018).

A.2. COASTAL MAINTENANCE IN THE VICINITY OF AMELAND INLET

Coastal maintenance is required due to the dynamic preservation policy which is established in 1990 in the Netherlands. This Dynamic Preservation policy prescribes that the North-Sea coastlines may not retreat landward of a reference line that is based on their 1990 position (Van Koningsveld and Mulder, 2004). This line is also referred to as the Basiskustlijn (BKL). The current strategy of I&W is to make use of "soft" sand nourishment to maintain the BKL. This in combination with hard solutions at e.g. the island tips or series of groins ensures that the Dutch geographical position remains fixed. In order to maintain the BKL in the Netherlands, per four year a total volume of approximately 48 million m^3 is nourished. Of all the nourishments in the Netherlands, roughly 70% is placed by means of underwater nourishments and 30% is placed by means of beach nourishments. In 2016 the costs were approximately €55 million including €1.4 million for research (Arends, 2016).

The instantaneous coastline (In Dutch Momentane kustlijn (MKL)) is the actual position of the coastline measured every year. From here the "to test coastline" (In Dutch de te toetsen kustlijn (TKL)) is determined. If the TKL is landward of the BKL, the Dutch ministry of I&W is obliged to nourish the coastline at that specific section. Once in every four years, RWS releases a document in which the upcoming coastal maintenance works are substantiated. Nourishments of three time intervals (2012-2015 (Rijkswaterstaat, 2012); 2016-2019 (Rijkswaterstaat, 2016a) ; 2020-2023 (Rijkswaterstaat, 2020b)) are summarized in the vicinity of the Amelander Zeegat and provide an overview of the coastal maintenance works in the past 10 years.

Between 2012-2015 two nourishments took place on Ameland Midden and Ameland Noordwest and none at Terschelling. The Nourishment at Ameland Midden contained a shore face nourishment of 2 Mm^3 and a beach nourishment of 1 Mm^3. The Nourishment at Ameland Noordwest contained a beach nourishment of 1 Mm^3.

Between 2016-2019 three nourishments took place on Ameland Midden, Ameland West and Amelander Zeegat. The Nourishment at Ameland Midden contained a shore face nourishment of 4 Mm^3. The Nourishment at Ameland West contained a beach nourishment of 2.4 Mm^3. The Nourishment at the Amelander Zeegat contained a pilot nourishment of 5 Mm^3. The focus of the pilot nourishment was to acquire insights in the behaviour of sand, water replacement and the ecological condition of the area around the inlet. Regarding the behaviour of sand, it is researched how much

sediment is imported by the Wadden Sea and adjacent coastline of the down drift positioned island Ameland from the ebb-tidal delta. Moreover, the consequences of the export of sediment from the ebb-tidal delta is researched (Rijkswaterstaat, 2020a). The area will be monitored in the upcoming years.

Between 2020-2023 no nourishments are planned for the vicinity of the Ameland Inlet. The judgement of Rijkswaterstaat (2020b) is that there has already been a nourishment or, growth of the coastline is expected. For Terschelling in specific, flexible governance of the BKL is applied and the BKL has been exceeded for a longer period without extra erosion (Rijkswaterstaat, 2020b). In Fig. A.3 the BKL trend of Terschelling and Ameland as a whole (Fig. A.3a) and a close-up of the island tips of Terschelling and Ameland (Fig. A.3b) are provided in their most recent status. Green is a seaward trend with a seaward position of the MKL to the BKL. Checkered green and white is a landward trend with a seaward position of the MKL to the BKL. Red is a landward trend with a landward position of the MKL to the BKL. Checkered red and white is a seaward trend with a landward position of the MKL to BKL.

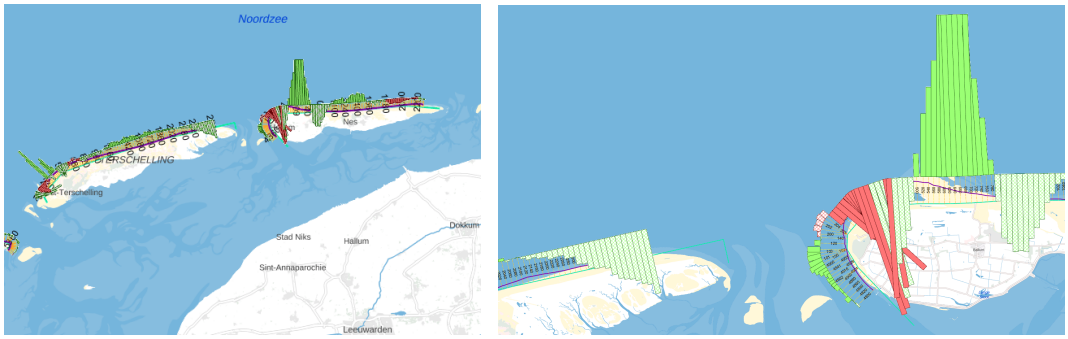

(a) Overview of Terschelling (left) and Ameland (right). Obtained from (Rijkswaterstaat, 2021c)

(b) Close up of the island tips of Terschelling (left) and Ameland (right). Obtained from (Rijkswaterstaat, 2021c)

Figure A.3: Coastline with trends (Rijkswaterstaat, 2021c)

A.3. EFFECT SEA LEVEL RISE WADDEN SEA

SLR is likely to accelerate in the future due to global warming (Meehl et al., 2007) (KNMI, 2021). Relative sea level rise consists of the relative difference between sea level rise (SLR) and subsidence of the seabed. Measurements of the mean sea level over the last 150 years reveal a fairly constant increase of 0.20 m per century along the Dutch coast (Baart et al., 2012). In addition, sea-floor subsidence due to glacial isostacy and compaction adds 0.10 m till 2100. Locally, in the eastern part of the Dutch Wadden Sea, an extra subsidence of 0.32 m by 2050 due to gas extraction is expected (Hoeksema et al., 2004).

A consequence of relative SLR is more sediment accommodation space in the Wadden Sea area which in turn generates a net landward sediment transport (Elias et al., 2012). Due to the previously mentioned sediment-sharing system of a tidal inlet, SLR disturbs the equilibrium of the tidal inlet. Previous research showed that during the Holocene the geological evolution of the Wadden Sea could keep up with relative SLR (Wang et al., 2018). To date, the Wadden Sea basin compensated this accommodation effect by importing sediment from the ebb-tidal deltas and the North Sea Coast of the barrier islands. The compensation effect by the Wadden Sea resulted in severe erosion of the adjacent shorelines and ultimately led to a landward retreat of the entire barrier-Inlet basin system (Wang et al., 2018). As a result, the intertidal flats in all basins increased in height to compensate for relative SLR (Wang et al., 2018). The above mentioned consequences of SLR is summarized in Fig. A.4.

This observation is also confirmed by (Elias et al., 2012). In Fig. A.4a, Elias et al. (2012) illustrates that the basins import sediment while the adjacent coasts and ebb-tidal deltas erode. Also Van der Spek (1994) states that extra accommodation space leads to ingression by the sea. As a consequence, the Wadden Sea can be seen as a sediment sink in the Dutch coastal system.

Research of both Wang et al. (2018) and Elias et al. (2012) explain the erosion of the adjacent barrier islands and ebb-tidal delta and coastal fundament and illustrate why the large amounts of coastal maintenance are required in the Vicinity of Ameland Inlet (Appendix A.2).

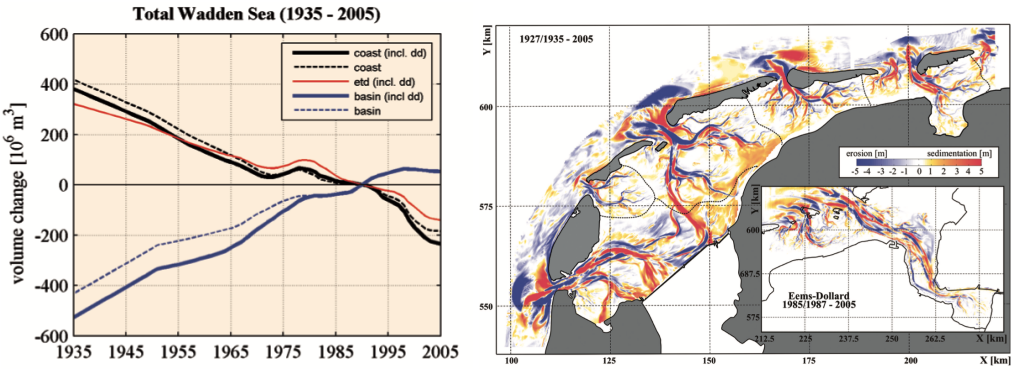

(a) Volume change of the Wadden Sea Area Elias et al. (2012)

(b) Sedimentation-erosion map over the period 1935-2005 of the Wadden Sea Elias et al. (2012)

Figure A.4: Volume change and erosion and sedimentation maps

The difference between the basin volume at a certain stage and its equilibrium basin volume is the sediment demand (Wang et al., 2018). To provide more insight in how much sediment is imported from the adjacent coast and ebb-tidal delta, Elias (2020b) determined the actual sediment balance of the Wadden Sea Inlets. According to Elias (2020b), the net import through all tidal Inlets is 4.5 Mm^3 per year. Furthermore, a large amount of sediment is still needed to regain morphological equilibrium in most tidal basins in the Dutch Wadden Sea (Elias et al., 2012). The actual sediment import volumes per year are provided in table Table A.1.

Table A.1: Sediment import or export volume per year for the Dutch tidal Inlets(Elias, 2020b)

Inlet	Import (+) or export (-)
Texel	+ 2.0 Mm^3/year
Eierlandse Gat	- 0.3 Mm^3/year
Vlie	+ 1.2 Mm^3/year
Ameland	+ 1.2 Mm^3/year
Frisian	+ 0.5 Mm^3/year

A.3.1. CONSEQUENCES ACCELERATED SLR AMELAND INLET

There are three types of limitations that can restrict sediment import into a tidal basin; transport-limited, accommodation-limited and supply-limited (Wang et al., 2018). In figure Fig. A.5 the state of the sediment budget is indicated. Supply-limited occurs when there is not enough sediment at the adjacent coastline or ebb-tidal delta to satisfy the sediment demand by the basin. But this limitation type is not prevailing in the Dutch Wadden Sea area. According to Wang et al. (2018), the western Wadden Sea is transport-limited, which means that there is enough sediment volume available, but the sediment transport capacity to deliver the sediment to the basin is too small. For

the Western area this implies that the annual import volume does not depend on the dimension of the accommodation space in the basins (Wang et al., 2018). The Eastern Wadden Sea is classified as accommodation-limited. This limitation type occurs when there is enough sediment supply, but there is a lack of accommodation space. For the Eastern area this implies that there is little accommodation space and consequently there is little net sediment import (Wang et al., 2018). Ameland Inlet lies in the eastern part of the Wadden Sea area and has thus a accommodation space limitation.

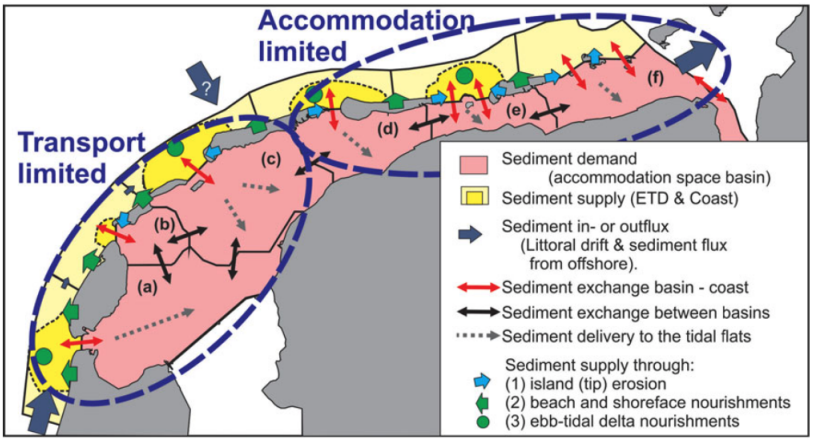

Figure A.5: In the legend; ETD stands for ebb-tidal delta. Schematic overview of the elements, sources, sinks and their linkages that form the sediment-sharing system of the Dutch Wadden Sea.(Wang et al., 2018)

With a likely increase of relative SLR in the future (Meehl et al., 2007) the sediment demand in most tidal basins is predicted by Elias et al. (2012) to increase depending on different accelerating SLR scenarios. For Ameland Inlet in specific, the accommodation space will increase in case of increasing relative SLR. As a result, more sediment can be accommodated in the Ameland Inlet basin. Since ebb tidal deltas together with spits, tidal inlets, barrier island and back-barrier basins are constantly striving towards an equilibrium state, the sediment import volume illustrated in Table A.1 is likely to increase for Ameland Inlet. As depicted in figure Fig. A.4 and substantiated by Elias et al. (2012) , Van der Spek (1994) and Wang et al. (2018) the sedimentation of the basins is accompanied by the erosion of the adjacent coastlines and ebb-tidal delta.

In conclusion, to date Ameland Inlet was able to grow with SLR, but at the cost of a finite sand source from the adjacent coastlines and ebb-tidal delta. Hence, the large erosion and coastal maintenance as illustrated in Appendix A.2.

Wang et al. (2018) states that the future development of the Wadden Sea system will have implications for various management issues of the functions of the Wadden Sea area described in Appendix A.1. Coastal maintenance is expected to increase in the future (Wang et al., 2018). Furthermore, Wang et al. (2018) states that a continuity in sufficient sediment availability at the ebb-tidal deltas and along the coast of the barrier islands is a prerequisite. A method to compensate the sediment demand is by nourishing the islands coast or ebb-tidal delta (Wang et al., 2018). This method is currently under investigation by means of the aforementioned pilot ebb-tidal delta nourishment at Ameland Inlet. However, while anticipating on accelerated SLR, new development of nourishment strategies that will increase sediment import to the Wadden Sea are recommended.

B | Empirical relations tidal inlet systems

The volume of sand stored in an ebb-tidal delta is often much larger than the volume of sand stored on the adjacent beaches. Although, there is still unclarity about the physical processes (Waves and currents and sediment transport patterns at the outer delta) due to their complexity (Section 2.2; Section 2.3 and Section 2.3.1). However, it is found that sediment exchange takes place between the adjacent barrier beaches and the ebb-tidal delta due to the sediment sharing system. There is an empirical relation (Eq. (B.0.1)) between the volume of sand stored in the ebb-tidal delta to the tidal prism of the back-barrier system. (Bosboom and Stive, 2021)

$$V_{od} = C_{od} P^{1.23} \tag{B.0.1}$$

In which:

- V_{od} = sand volume stored in the ebb-tidal delta [m^3]
- C_{od} = empirical coefficient $m^{-0.69}$
- P = tidal prism [m^3]

The empirical coefficient C_{od} is dependent on the wave climate. For instance, more energetic waves for the same tidal prism result in a smaller ebb-tidal delta (Bosboom and Stive, 2021). The empirical relation Eq. (B.0.1) is represented in Fig. B.1. The ebb-tidal delta together with spits, tidal inlets, barrier island and back-barrier basins with the accompanied intertidal flats are constantly striving towards an equilibrium state (Bosboom and Stive, 2021). For example; following Fig. B.1 and Eq. (B.0.1), an enlargement of the tidal prism causes an enlargement of the volume of sand in the ebb-tidal delta and vice versa. As for this example, the sand has to origin from somewhere from the tidal inlet sharing system. Thus, for an enlargement of sand volume in the ebb-tidal delta, the sand most probably originates from the other components (e.g. the adjacent beaches) of the tidal inlet system.

Based on the aforementioned empirical relation between the volume of sand stored in the ebb-tidal delta to the tidal prism, the following consequences are possible for disturbances of the equilibrium condition of the intertidal flats. As previously mentioned, disturbances can either be man made or natural. For the intertidal flats two scenarios are possible depending on their capability to grow with (accelerated) SLR. There is either a scenario in which the intertidal flats are unable to adapt to SLR and a scenario in which the intertidal flats are able to adapt to SLR. Due to the sediment-sharing system of a tidal inlet, completely different consequences follow due to each scenario (Bosboom and Stive, 2021).

If the increase of SLR is faster than the height adaptation of the tidal flats, the tidal prism will increase and the area of intertidal zones will decrease. Although the consequences are difficult to predict, a possible outcome may be that the channels in the basin will widen and induce transport of sand to the outer delta. However, SLR has relatively more impact on the water depth on the tidal flats than on the channels. Thus, the sediment transport in the channels is likely to be less affected by SLR than sediment transport on the intertidal flats. Therefore it seems realistic to assume that the natural response has more impact on the tidal flats (Bosboom and Stive, 2021).

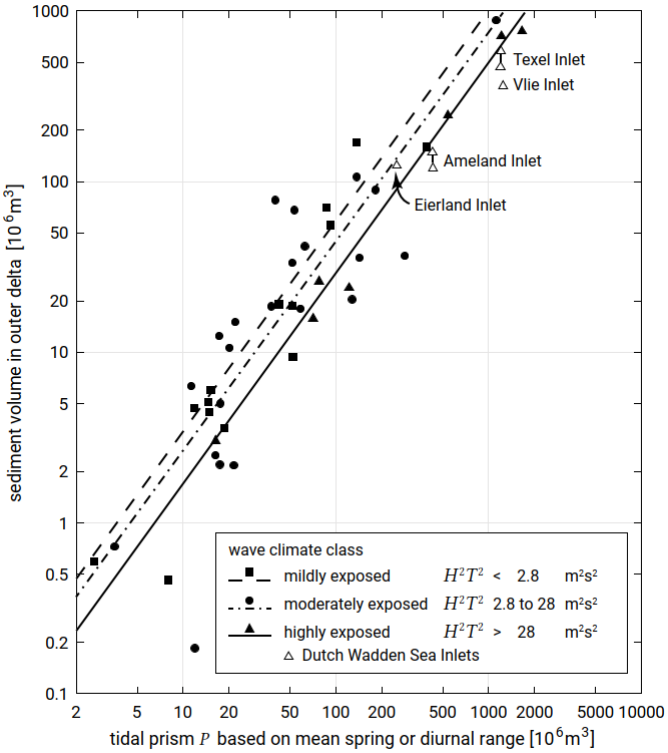

Figure B.1: Empirical relationship between volume of sand in the outer delta and the tidal prism (Bosboom and Stive, 2021)

If the height adaptation of the tidal flats is equally paced as the SLR, the tidal prism will not increase or decrease, whereas the volume of the channels increase. This will ultimately lead to a sand demand from the ebb-tidal delta, adjacent coastlines and coastal foundation (Bosboom and Stive, 2021).

Besides that the sediment volume stored in the outer delta is related to the tidal prism of an inlet, van de Kreeke and Brouwer (2017) also relate the cross-sectional area (A_c) to the tidal prism as illustrated in Eq. (B.0.2). For the Dutch Wadden islands, the cross-sectional area plotted versus the tidal prism yields a similar linear result as figure Fig. B.1.

$$A_c = C_l P \tag{B.0.2}$$

In which:

- A_c = Cross-sectional area of the tidal inlet [m^2]
- C_l = empirical coefficient ($6.5 \cdot 10^{-5}$ m^{-1})
- P = tidal prism [m^3]

With Eq. (B.0.2) disturbances of the cross-sectional area (A_c) to the tidal prism (P) or vice versa can be determined. Although, it has to be taken into account that the stability of a tidal inlet is not fixed but a dynamic entity, which can either be disturbed on a stable or unstable manner (Bosboom and Stive, 2021). The stability of the cross-sectional area (A_c) is described by Escoffier's model in Eq. (B.0.3). In his research he connected the maximum cross-sectional averaged entrance channel velocity u_e (the subscript e denotes the entrance) to the hydraulic radius of the channel (R), its cross-

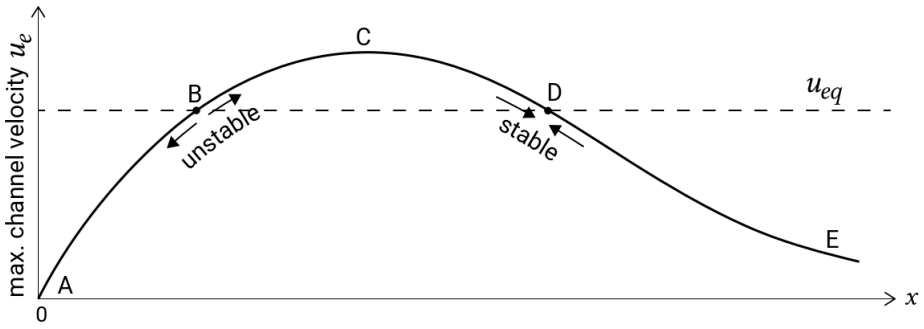

Figure B.2: Escoffier's maximum cross-sectional averaged entrance channel velocity u_e versus stable and unstable perturbations (Bosboom and Stive, 2021)

sectional area (A_c) and the tidal range in the estuary (Δh). Stable and unstable perturbations on the maximum cross-sectional averaged entrance channel velocity u_e are illustrated in figure Fig. B.2. If a stable perturbation is applied to the tidal inlet system, the system will restore to its equilibrium conditions, whereas when an unstable perturbation causes permanent changes of the tidal inlet system.

$$u_e = \frac{\pi P}{A_c T} \tag{B.0.3}$$

C | Initiation of motion

In this section the initiation of motion of a particle is discussed.

The initiation of motion
Sediment can only be transported if the movement of water causes a sufficiently large shear stress (τ_b) of the particles. The critical bed shear stress ($\tau_{b,c}$) describes the starting point of motion. If this condition is exceeded, the particles will move, roll or be suspended. The forces acting on an individual particle can be divided into forces which tend to move the grain – the drag force F_D and the lift force F_Lnd a force which tries to keep the grain in its place; the gravity force F_G.

$$\tau_{b,c} = \rho \cdot (u_{*cr})^2 \tag{C.0.1}$$

Since the bed shear stress is proportional to the velocity squared times the water density, one could also write the bed shear stress expressed as the critical Shields parameter. Shields parameter, along with grain Reynolds number (Re_*) (depicted on the x-axis in figure Fig. C.1), determine the initiation of motion velocity (shear stress velocity (u_*)) of a particle with a certain diameter.

$$\Theta_{cr} = \frac{\tau_{b,cr}}{(\rho_s - \rho)gD} \tag{C.0.2}$$

In relation to this study, in which four different particles sizes are used, it can be determined that coarser fractions require higher flow velocities to be set in motion.

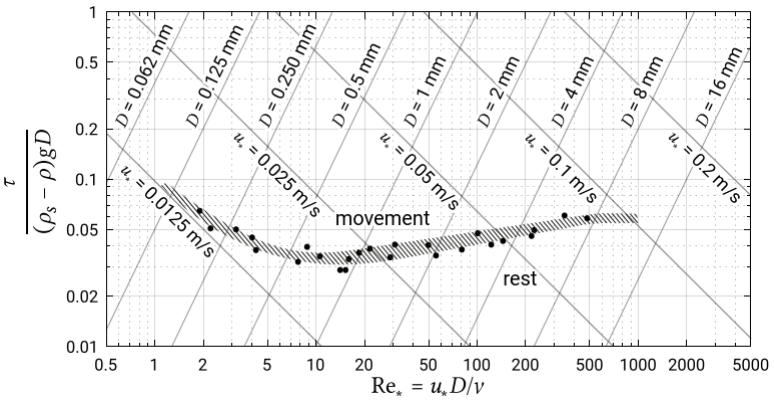

Figure C.1: Shields curve of initiation of motion (Bosboom and Stive, 2021)

The shaded band is found to be approximately 0.05, but the following aspects should be taken into consideration:

The Shields curve is valid for uniform flow on a flat bed. The effect of bed ripples and the effect of the combination of unidirectional and oscillatory flow on initiation of motion are largely unknown;

Gradation of the bed material may be important, particularly for poorly sorted sediment ($D_{90}/D_{10} > 3$). The smaller particles will be hidden in the voids between the larger particles in these cases, while the larger particles will be more exposed. After the exposed smaller particles are washed away, a top layer of coarser particles (with higher critical flow velocities) remains and prevents the underlying smaller particles from moving. This is known as bed armouring; (Bosboom and Stive, 2021)

It can be argued that for a sloping bed in the flow direction, the critical flow velocity will be slightly lower for downward sloping beds and slightly higher for upward sloping beds;(Bosboom and Stive, 2021)

Cohesive forces between grains, caused by the presence of cohesive sediment in the bed, may significantly increase erosion resistance. Biological activity and consolidation may also be important in this regard.(Bosboom and Stive, 2021)

The equation of the bed shear stress in combination of waves is the summation of the bed shear stress induced by currents and the bed shear stress induced by waves. τ_{cw} is time-averaged shear stress magnitude for the combined wave-current motion. The total equation yields:

$$\tau_{cw} = \tau_c \left[1 + \frac{1}{2} \left\{ \zeta \frac{u_0}{U} \right\}^2 \right] \tag{C.0.3}$$

In which:

- u_0 is the maximum orbital velocity at top of wave boundary layer
- U is the depth-averaged velocity
- ζ is combination of various parameters

D | The Zandwindmolen general

A potential new nourishment strategy that might increase sediment import to the Wadden Sea while simultaneously let the rest of the vicinity of Ameland inlet grow along sea level rise is by means a continuous nourishment in a tidal inlet. It is believed that a continuous nourishment can be executed by a fixated Zandwindmolen concept.

As indicated in the introduction, the Zandwindmolen consists of a fixed nourishment system powered by wind energy, making it a CO_2 neutral alternative for current applied coastal maintenance equipment. The separate sub-components of the Zandwindmolen consist of a win, transport, and nourishment component. Previous research by (Rutteman, 2021) yielded knowledge about the financial competitiveness of the Zandwindmolen versus traditional equipment and the morphological response of a continuous shoreface and tidal channel wall nourishment.

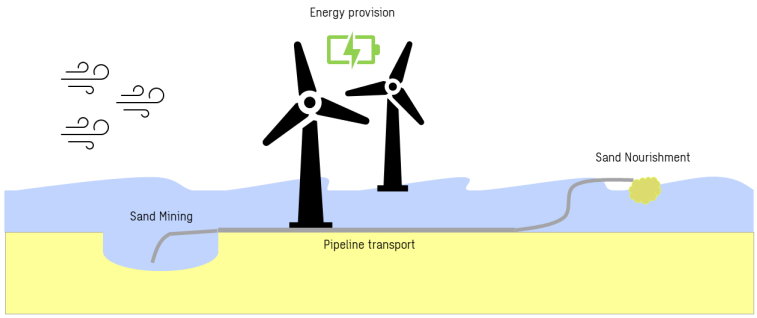

Figure D.1: Overview of different components of the Zandwindmolen concept

The financial competitiveness of the Zandwindmolen versus traditional dredge equipment is a substantial challenge. Therefore, the sub-systems of the Zandwindmolen were assessed separately. From the assessment it was found that the inter-dependency of the sub-systems complicates the cost optimization. Thus, a competitive system design requires an accurate harmonization of these sub-systems. (Rutteman, 2021)

The other results regarding the financial competitiveness are:

- The costs per m^3 decrease with an increasing nourishment volume. Therefore, determination of marginal costs per nourishment quantity is essential for the determination of the feasibility of the system.
- Based on a certain annual nourishment volume, the pump capacity and windmill size should be attuned. Batteries can support the system to ensure operation in case of insufficient wind. This is mainly the case if the system has wave-induced limited operational times. The cost-optimum is found to a set-up in combination with batteries and leads to a yearly operational time of approximately 70%.

The Zandwindmolen is a sustainable nourishment method. The ecological effects are discussed in Appendix D.1. The general issues of the Zandwindmolen at the time of producing this thesis along with how the dredge, transport and nourishment concept of the Zandwindmolen relate to traditional dredge equipment are described in Appendix D.2. Moreover, possible optimizations are mentioned in Appendix D.2. For other information regarding the sub-components of the Zandwindmolen Rutteman (2021) his thesis is recommended.

D.1. ECOLOGICAL IMPACT ZANDWINDMOLEN

Sediments are mobilized during the dredging process and cause turbidity levels over the water column to increase. A common impact indicator for turbidity and sedimentation is the Suspended Sediment Concentration (SCC) (Laboyrie et al., 2018). The actual amount of sediment released and the footprint of possible effects depend on a number of factors.

- Sediment type (including size and distribution)
- Sediment cohesiveness
- Volume of material dredged
- Dredging methodology (type of dredger, production rate, placement method)
- Presence, type and level of contaminants
- Best practice or management measures utilised
- Hydrodynamic conditions during and after dredging

During traditional dredging operations the environmental impact has to be considered, since turbidity can cause loss of light and burial/ smothering of sensitive ecosystems (Laboyrie et al., 2018). Impact of both stresses on ecology depends on their magnitude and the duration and is species-dependent. These effects are typically implicated by a Species Response Curve (SRC) Fig. D.2. An SRC describes the response of individual species (such as a specific type of sea grass, mussel, etc.) to various combinations of intensity and duration of stresses caused by an increase of SCC (Laboyrie et al., 2018).

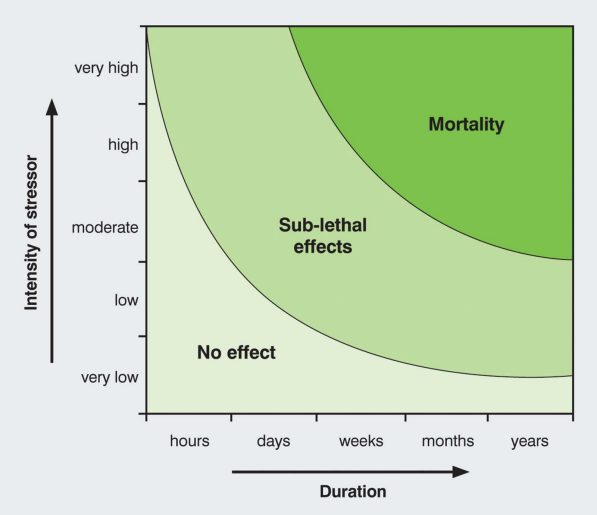

Figure D.2: Species Response Curve (SRC). Image is obtained from (Laboyrie et al., 2018).

For the Zandwindmolen it is estimated that the intensity of stressor, which is illustrated on the y-axis of the SRC curve (Fig. D.2), remains very low due to the continuous low volume nourishment method. Moreover, the duration, which is illustrated on the x-axis of the SRC curve (Fig. D.2) is years. Thus, it is assumed that the Zandwindmolen is in the lower right corner of Fig. D.2. Thus, the assumption is that the already existing background SCC of the system will not be exceeded in such a way that this might cause sub-lethal effects or even mortality of the surrounding natural system. However, it has to be studied whether this assumptions is actually true for the Zandwindmolen. But, ecological effects are not within the scope of this thesis.

D.2. ZANDWINDMOLEN SET-UP

The Zandwindmolen is still under development causing uncertainties about different sub-components of the Zandwindmolen.

The difference of the system set-up between traditional coastal maintenance equipment and the Zandwindmolen mainly has to do with the fixation of the system. In general traditional coastal maintenance equipment as a TSHD or CSD are spatially very dynamic due to the ability to sail to wherever the vessel is required. Whereas, the Zandwindmolen is a fixed construction and tailored to the requirements of a specific part of the coastal system. Therefore, the system set-up of the Zandwindmolen is similar to a sand bypass system. In a sand bypass system, sand is won by (mainly) autonomous dredgers, sand is transported by means of pipeline transport and sand is discharged by means of pipeline discharge.

Sand winning techniques and pipeline transport of the Zandwindmolen are placed in perspective to the already existing sand bypass systems. This assessment is performed to point out knowledge gaps and challenges of the winning technique and pipeline transport. The following information is used to assess sand bypass systems. (Boswood and Murray, 2001) is used for case studies; (Loza et al., 2008) is used for win, transport and nourishment systems; (Williams et al., 1994) is used for HDPE en polyurethane pipeline information.

Sand winning
At the sand winning side ongoing research is performed to find a suitable dredger which fits to the static transportation pipeline and fits the scope of the Zandwindmolen. Similar to the nourishment strategy, in which nature brings sediment to regions where it is required, an optimal situation for the sand winning side would be that sediments move actively towards a dredger. Unfortunately, Dutch legislation state that sand has to be won beyond the offshore -20 NAP line in the North Sea. Beyond the -20 NAP line different morphological processes play a role in the morphology of sediments. In offshore regions beyond the -20 NAP line, there is no long-shore transport induced by waves (Bosboom and Stive, 2021). Traditional sand bypass systems operate in nearshore regions before the -20 NAP line where sand is mobile due to the presence of waves and the thereon following alongshore sediment transport processes. Based on these sediment transport processes, a sediment trap can be created to ensure that the sediment moves actively towards the dredging equipment. Sand bypass systems use the following sand winning techniques:

Mechanical dredgers:

- Bucket ladder dredgers
- Backhoe
- Clamshell

- Grab dredgers

Hydraulic dredgers:

- Cutter suction dredgers
- Trailing suction hopper dredgers
- Stationary suction dredgers

Other types:

- Water injection dredger
- Punaise
- Jet pumps
- Submersible pumps (alternatieve jet pump met meer flexibiliteit)
- Fluidizer system (d50 tot max 0.5 mm)

However, due to the missing sediment transport processes in offshore regions, sand does not move active towards a dredger and thus, sand winning techniques used for traditional sand bypass systems are not applicable.

Hence, due to the missing sediment transport processes the dredge equipment has to be dynamic and be able to move towards the sediment for dredging operations. An option could be the use of a crawler, but this has to be researched in more detail.

Transportation
The distance from offshore regions towards onshore locations where the sediment is nourished is approximately between 8 and 12 km. The costs to maintain the pipes are a significant cost item on the estimated budget. Therefore, it is desired that the pipes have an optimal lifespan. Challenges for the optimal lifespan relate to the high pressures which are required to pump a sediment mixture over such a distance. Moreover, the pipeline has to be resistant against fatigue, abrasion or other kind of damage. The sediment mixture in a pipeline can be compared to sand paper on wood; over time the mixture will sand out the pipe. Thus, robust and resilient materials are required for the pipeline to cope with the sand paper effect.

Traditional pipelines are built of steel. However, other possible types of pipelines that can be used include; Polyethylene (PE) and Polyurethane (PU). These two forms are already used in the dredging industry. In addition to these two variants, there are countless other types of concepts that can be chosen depending on the application (e.g. options such as metal ceramic liner with composite or cement mortar linings (CML)).

Polyethylene is used in the form of Ultra High Molecular Weight Polyethylene (UHMWPE) high density polyethylene (HDPE) and medium density polyethylene (MDPE).

The benefits of the use of UHMWPE HDPE or MDPE in contrast to steel are;

- 3-5x more resistant to wear
- Due to its flexibility, it is more flexible, which means fewer corners. A side effect is better hydraulic conductivity which yields in less required power to pump

- Less pressure loss along the length of the pipe

The cons of the use of UHMWPE, HDPE or MDPE in contrast to steel are;

- Structural stiffness of the material is less than steel, making the pipe less resistant to external forces, bending and torque.
- HDPE and MDPE are lighter than water and thus float. An anchoring system is needed for HDPE and MDPE pipes.

Polyurethane is a liner in a steel pipe. It combines the best properties of plastic and rubber. This material is mainly for high service life, low wear and low friction between fluid and pipe. An example of a sand bypass system where Polyurethane is applied is in Nerang river entrance bypass system – Australia.

D.3. NOURISHMENT EFFECTS

The effects of a nourishment with the Zandwindmolen is put into contrast by comparing the desired effects of the Zandwindmolen with already existing dredge and nourishment methods of RWS. Exact working methods of traditional equipment can be found in Appendix E. In this section the procedure of beach maintenance, seabed maintenance and sea channel maintenance is explained in more detail. As reference frame, Table D.1 from STOWA (2021) is applied in which the volume per meter coastline, effect on coast, effect on load embankment, repetition time, effect on beach, coastal profile, visibility and costs per m^3 per type of nourishment is discussed. Based on these regular applied nourishment types by RWS, the desired effects of a nourishment with the Zandwindmolen is placed in more perspective.

For regular applied nourishment types the rule of thumb is; the further away from the coastline the nourishment takes place, the longer it takes to obtain the desired effect (STOWA, 2021).

The nourishment type of the Zandwindmolen is new compared to already existing nourishment strategies of RWS. Though, the Zandwindmolen can be compared to the pilot nourishment of Ameland Inlet.

The application of a nourishment with the Zandwindmolen can either be on a beach or under water/ foreshore. In the foreshore nourishment, sediments are distributed by means of natural transport processes, whereas manual labour is required for a beach nourishment. In this thesis the application of a tidal channel nourishment is further researched.

The volume per meter coastline by the Zandwindmolen deviates from the common nourishment types depicted in Table D.1. The objective of a Zandwindmolen is to distribute the continuous nourished sediments over a hinterland as large as possible by means of the natural transportation capacity of the vicinity. By doing so, sediments are dispersed to the places where it is most needed for the conservation of the Dutch coastline. Therefore, the exact volume per meter coastline is irrelevant for the Zandwindmolen. The nourished volume depends on site specific requirements and is thus unique. This brings opportunities over the common applied beach and foreshore nourishments, as during these nourishments typically more sand than a system requires is nourished.
Technical challenges arise due to the fixed construction of a Zandwindmolen and the continuously applied nourishment. To ensure a continuous nourishment over time from a fixed construction, the pipe exit has the be prevented from end of pipe clogging. A result of end of pipe clogging might cause island forming at the end of the discharge pipeline. Besides risks of a water-hammer through the pipe due to closure unexpected closure of the pipe end, it also deviates from the scope of the

Zandwindmolen in which nature brings the sand to the places where it is most needed for the conservation of the Dutch coastline.

In order to achieve the nourishment scope of the Zandwindmolen, the applied equipment has to be harmonized with the hydrodynamic and morphodynamic processes in the vicinity of the nourishment. Therefore, the required equipment for a continuous nourishment is site specific.

In this thesis, the harmonization of hydrodynamic and morphodynamic processes with the applied dredge equipment is researched.

The effect on the coast is still unclear for the Zandwindmolen. However, the desired effect on the coast by using a Zandwindmolen with a foreshore nourishment is growth with SLR. The frame of reference for a Zandwindmolen is the enhancement of natural sediment import/export processes due to the low volume extra nourished sediment by means of a Zandwindmolen. Another frame of reference is the ebb-tidal delta nourishment. The effects of an ebb-tidal delta nourishment are still under investigation by RWS.

The effect on the embankment is also still unclear when a Zandwindmolen is applied. The effects on the embankment are outside of the scope of this thesis.

The repetition time of the Zandwindmolen is irrelevant as the nourishment type is continuously. This is in contrast with common applied nourishment strategies.

The effect on the beach as coastal profile is unclear due to the new continuous nourishment strategy. As mentioned previously the desired effect is growth with relative SLR. Moreover, the **visibility** is unknown as the nor the equipment as the effect on the beach and coastal profile are unknown.

The costs are related to the IKZ program. Within the IKZ program a reference cost price of 1 m3 of sand is set to be below €4/m3. This cost price is based on life cycle cost analysis (LCC) and an environmental impact indicator (mileukosten indicator) (MKI).

Table D.1: General overview of nourishment types obtained from STOWA (2021)

Type of nourishment	Dune	Beach	Under water	Mega
Volume per meter coastline	~ 200m^3/m'	~200m^3/m'	200-500m^3/m'	2000m^3/m'
Effect on coast	Strong momentarily effect	Short term increase	Increase on long-term, beach or dune grow with SLR	Increase on short and long term
Effect on load embankment	None	Momentarily decrease	Limited momentarily decrease	Momentarily decrease
Repetition time	Dependent on coastline maintenance and storms	1: 4-5 year	1:5-10 year	25 years
Effect on beach	Small	Unnatural	Natural	Natural
Coastal profile	Steeper profile	Somewhat steeper profile	Stability of slope is maintained	Stability of slope is maintained
Visibility	High	High	Low	High
Costs	~ > € 16/ m^3	~ € 5/ m^3	~ € 2,75/ m^3	> € 2,75/ m^3

E | Coastal maintenance

E.1. Beach maintenance

The goal of beach maintenance is to make the beach wider and higher. Two types of beach maintenance can be performed depending on e.g. the foreshore depth. The nourishment techniques is either rainbowing or it may be pumped ashore through pipelines, which may be submerged or floating (IADC, 2014).

When a foreshore is very shallow, a TSHD is unable to get to the deposition location within rainbowing reach. In this situation, the beach maintenance is carried out by connecting the TSHD to a zinc piece on the seabed (submerged) or on a floating pipe. For the submerged technique, in between the TSHD and the zinc piece a flexible pipe is connected. The zinc piece lies perpendicular to the shoreline and is attached to a seamless pipe piece that ends on the beach. The floating pipe ends onshore and is then connected to a pipe.

For both submerged or floating the direction of the pipeline system has to be changed from a perpendicular (cross-shore) orientation towards an alongshore orientation. In order to make the pipeline parallel to shore, a corner piece is installed. From here on a caterpillar crane and personnel are present to attach more pipes to increase the reach of the pipeline system. When connected the TSHD can discharge the dredged sand-water mixture through a pipeline towards shore. Onshore, the mixture is spread out by bulldozers.

E.2. Seabed maintenance

Seabed maintenance is also referred to as shore-face nourishments. During seabed maintenance sand is nourished on the seabed closely to the shoreline at a depth of 5-8 meters (Rijkswaterstaat, 2021d). By opening the hatches in the bottom of the ship, sand is deposited at the placement site (IADC, 2014). The goal of seabed maintenance is to form a sand bank on which waves break. When waves break, sediment is mobilized and is picked up by the currents and transported towards shore to enable growth of the coastline (Rijkswaterstaat, 2021d).

E.3. Sea channel maintenance

Sea channel maintenance is required because currents cause deep channels in the seabed. Furthermore, these deep channels might have a tendency to travel towards the coastline. Hence deep channels can cause instability of the coastal fundament (Rijkswaterstaat, 2021d). The same technique is applied as for seabed maintenance. Thus, by opening the hatches in the bottom of the vessel.

F | Near-field processes TSHD

Processes governing dispersion of sediments from a Trailer Suction Hopper Dredger (TSHD) are different for near, mid and far-field (Laboyrie et al., 2018).

- Near-field: Initial conditions of overflow (momentum, density differences) and vessel movements
- Mid-field: Transition from dominant initial conditions to role of ambient conditions – both are important
- Far-field: Ambient conditions (bed properties, large-scale current and wave climate)

In general, near-field effects can be controlled while far-field effects have long time-lags and a strong impact on natural variability.

Turbidity occurs when fine sediments tend to mix over the water column. The type of dredging plume depends on the Richardson number (Ri) and the velocity number (ζ) (van Rijn, 2020).
The Richardson number is a measure of stratification and the velocity number is the relative importance of the ratio of horizontal and vertical flow velocity. The relevant variables are the downward outflow velocity (W), outflow diameter (D), overflow density(ρ_{of}) and the relative horizontal velocity (U). With these parameters the Richardson number and the velocity number can be determined. In case of fine sediments, which are a driver of turbulence, the downward settling velocity (W) and the overflow density (ρ_{of}) are small.

$$Ri = \frac{\frac{\rho_{of}-\rho_w}{\rho_w} gD}{W^2} \tag{F.0.1}$$

$$\xi = \frac{U}{W} \tag{F.0.2}$$

Hindrance by placement can be formed by:

- Confinement by the water depth
- Influence of propeller
- Flow around the ship
- Air bubbles
- Non-steady release (cloud formation)

The top three mitigating near-field solutions for these issues are the use of a green valve, a green pipe and/ or sailing with the flow. Besides, siltation curtains can be installed. These silt screens should have a connect and disconnection system in order to disconnect when typhoons or storms with large significant wave heights reach the region.

G | Discharge parameters

G.1. Discharge parameters M2: Near-field behaviour

Delft-3D requires two parameters for the discharge operation; The Flow [m^3/s] and the Conservative Spill [$\frac{kg}{m^3}$]. These two parameters are further referred to as the fluxes of the discharge. The fluxes of a $2Mm^3$ for Model 2 are elaborated in the following section.

- ρ_w = density water = 1030 [$\frac{kg}{m^3}$]
- ρ_s = density solids (in situ) = 2650 [$\frac{kg}{m^3}$]
- $\rho_{s,p}$ = density solids (with pores) = 1600 [$\frac{kg}{m^3}$]
- C_{vol} = Volume concentration = 0.105% (Royal IHC)
- V = Nourishment volume = $2Mm^3$

The Conservative Spill (CS) [$\frac{kg}{m^3}$] is determined with equation Eq. (G.1.1)

$$\begin{aligned} CS &= \rho_{s,p} \cdot C_{vol} \\ CS &= 1600 \cdot 0.105 \\ CS &= 168 \frac{kg}{m^3} \end{aligned} \tag{G.1.1}$$

In Eq. (G.1.2) the sand concentration C_{sand} [$\frac{kg}{m^3}$] is determined:

$$\begin{aligned} C_{sand} &= \rho_s \cdot C_{volume} \\ C_{sand} &= 2650 \cdot 0.105 \\ C_{sand} &= 278.25 \frac{kg}{m^3} \end{aligned} \tag{G.1.2}$$

In Eq. (G.1.3) the total Mass [$\frac{kg}{year}$] is determined:

$$\begin{aligned} Mass &= V \cdot \rho_{s,p} \\ Mass &= 2650 \cdot 0.105 \\ Mass &= 3.2 \cdot 10^9 \frac{kg}{year} \end{aligned} \tag{G.1.3}$$

In Eq. (G.1.4) the total flux of sand F_{tot} [$\frac{kg}{s}$] is determined:

$$\begin{aligned} F_{tot} &= \frac{Mass}{356 \cdot 24 \cdot 3600} \\ F_{tot} &= \frac{3.2 \cdot 10^9}{356 \cdot 24 \cdot 3600} \\ F_{tot} &= 101.47 \frac{kg}{s} \end{aligned} \tag{G.1.4}$$

It was determined that for a 2Mm^3 nourishment a width of approximately 540 meters is required to ensure transportation of the added nourishment volume. As a single cell has a width of approximately 70 meters at the nourishment location, a total of six grid cells in the model are required as Discharge location. Moreover, all four fractions are nourished at the same location and at the same time. The sand flux per discharge cell and fraction ($F_{d,f}$ $[\frac{kg}{s}]$) is determined in equation Eq. (G.1.5).

$$\begin{aligned} F_{d,f} &= \frac{F_{tot}}{6 \cdot 4} \\ F_{d,f} &= \frac{101.47}{6 \cdot 4} \\ F_{d,f} &= 4.228 \frac{kg}{s} \end{aligned} \tag{G.1.5}$$

The Flow (Flow) $[\frac{m^3}{s}]$ parameter of the Discharge operation is found in Eq. (G.1.6)

$$\begin{aligned} Flow &= \frac{F_{d,f}}{CS} \\ Flow &= \frac{4.228}{168} \\ Flow &= 0.0252 \frac{m^3}{s} \end{aligned} \tag{G.1.6}$$

G.2. DISCHARGE PARAMETERS M3: MID-FIELD BEHAVIOUR

In the third model stage the discharge operation is carried out per fraction per available mass of sediment peak found in the 3D longitudinal distribution. There is a twofold study between the models which determine the maximum and minimum dispersion. The difference is based on the presence or absence of natural background sediment. Per model branch the longitudinal distribution is unique, therefore, the discharge parameters have to be determined separately.

Minimum dispersion
All parameters remain the same, except that instead of the previous determined six discharge locations and four sediment fractions, the sediment is now nourished per fraction per peak location from the 3D longitudinal spectrum. Hence, the sand flux per discharge cell and fraction ($F_{d,f}$ $[\frac{kg}{s}]$) is now twelve by four (instead of six by four). The new $F_{d,f}$ can be found in Eq. (G.2.1).

$$\begin{aligned} F_{d,f} &= \frac{F_{tot}}{12 \cdot 4} \\ F_{d,f} &= \frac{101.47}{12 \cdot 4} \\ F_{d,f} &= 2.114 \frac{kg}{s} \end{aligned} \tag{G.2.1}$$

Hence, the Flow (Flow) $[\frac{m^3}{s}]$ for the 2D dispersion model of a half year is determined in Eq. (G.2.2).

$$\begin{aligned} Flow &= \frac{F_{d,f}}{CS} \\ Flow &= \frac{2.114}{168} \\ Flow &= 0.0126 \frac{m^3}{s} \end{aligned} \tag{G.2.2}$$

The Conservative Spill CS remains the same and is $168 \frac{kg}{m^3}$ per fraction.

Maximum dispersion

In the longitudinal distribution without natural background sediments the 100 and 200μm fractions have a somewhat trinomial distribution, in which most of the fractions settle near the nourishment location. Thus, these fractions are all nourished on a single string and have thus a flow of 0.0252 $\frac{m^3}{s}$ and a conservative spill of 168 $\frac{kg}{m^3}$.

The 300 and 400μm fractions have a bi-modal distribution, which is equal to the longitudinal distribution found for the 3D with natural background sediments. Therefore, these fractions are modelled on two strings of which one lies north and one lies south of the original nourishment locations of the spring neap tide cycle model. The northward and southward distances are again determined by means of the peak available mass of sediment from the original nourishment location. Thus the flow is set to 0.0126 $\frac{m^3}{s}$ and the conservative spill to 168 $\frac{kg}{m^3}$. Which is equal to the with natural background sediment fractions.

H | Numerical model setup

This section explains how the numerical models were modeled. The basis of the numerical methodology comes from the results of the near-field behavior (Chapter 5) and the technical comparison between the results of the 2D and 3D near-field dispersion models (Appendix J).

H.1. Set-up general hydrodynamics and morphodynamics model

This model is a follow-up of the model applied in Pearson et al. (2020). The modifications to fit this research on Pearson et al. (2020) his model are described below.

First, the bed layers in the model are removed and a single bed layer is created. By means of Quickin, a module in Delft3D, the sediment tracers generated by Pearson et al. (2020) were added upon the bed composition generated by the aforementioned BCG run.

Initially, a cold start with a simulation duration of one day was performed to ensure that the water level has a semi-diurnal form. Within this cold start the morphological spin up interval was set to a day to ensure that only water was able to move through the spatial domain. Thereafter a hot start of one spring neap cycle was performed to obtain the results for phase 1. Within this simulation period the morphological spin up interval was set to 0, as sediment was able to move through the spatial domain as well.

H.2. Set-up near-field dispersion model

It was determined in Chapter 4 that a continuous nourishment is simulated as high as possible in the water column. The width was 70 meters and the length perpendicular to the flow is 540 meters.

This nourishment is modelled according to the nourishment strategy and is depicted in purple in Fig. H.1. The nourishment is modelled over six grid cells. The discharge fluxes are described in Appendix G.1.

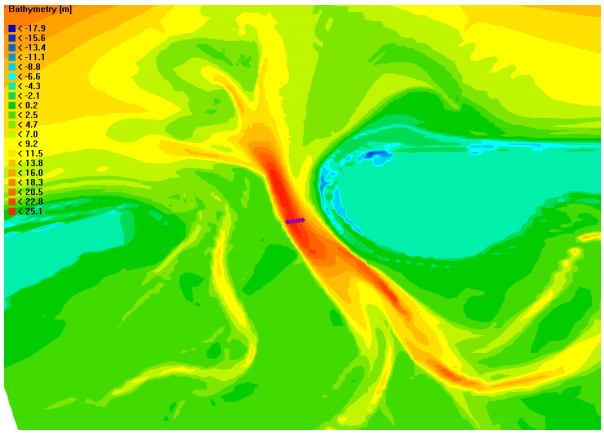

Figure H.1: Overview of discharge locations in Delft-3D for 2D and 3D simulation

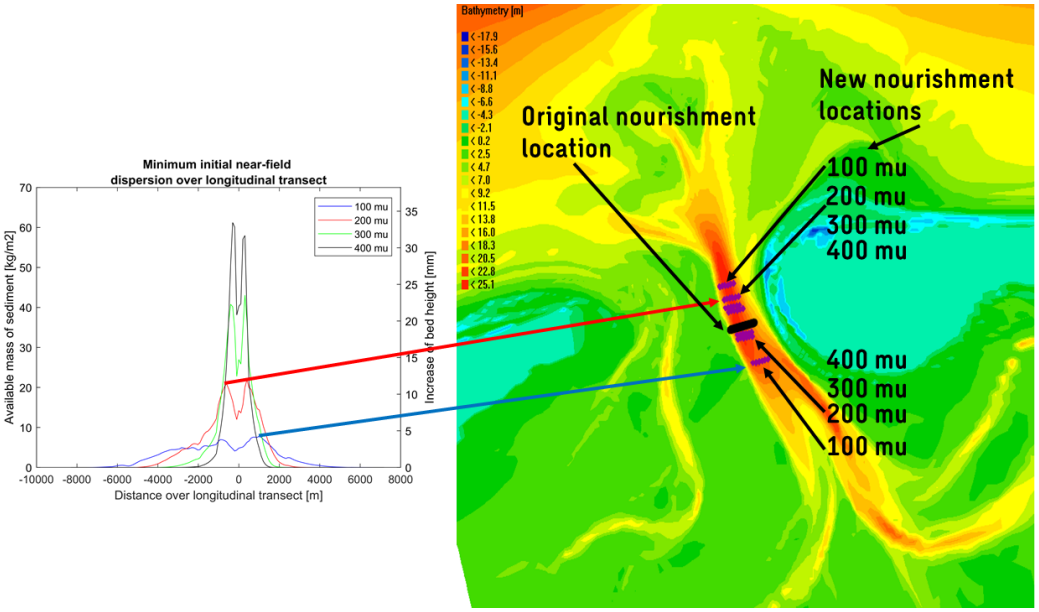

Figure H.2: Overview of how the longitudinal distribution is used to determine the new nourishment locations.

H.3. SET-UP MID-FIELD DISPERSION MODEL

The third model scope describes the mid-field behaviour of the nourishment. The simulation period is 158 days, which is 22.57 weeks or 5.19 months. But, this simulation is a morphological hot start from the 3D spring neap tide cycle model. Thus, the simulation period becomes 173 days, which is 5 months and three weeks. The simulation time is close to a half year and is therefore referred to as the half year dispersion model.

In Appendix J.3 an analysis for the transition from the near-field to the mid-field model stage is performed. It appears that the 3D model reflects the initial dispersion due to the settling process the most accurately. This is done by a spatial 2D image in which the degree of dispersion is visible per fraction and by means of a longitudinal cross-section over the length of the Borndiep channel. Moreover, the speed of dispersion is analysed.

Based on the conclusion of the Appendix J.3, the available sediment masses of all fractions are exported from the 3D spring neap tide simulation and added as a starting condition to the 2D half year simulation.

The maximum and minimum dispersion is determined for two scenarios. The first scenario describes a model where the continuous nourishment is not further implemented. Here, therefore, the previously found near-field dispersion is further investigated. This model does not need any modulation steps regarding the export of the available masses of sediment from the near-field research.

The second scenario describes a model in which the continuous nourishment is carried out further. In this case, the previously found near-field dispersion and the sediment that is continuously nourished are investigated. For this simulation, the longitudinal distribution of the near-field dispersion is used to set new discharge locations as nourishment input. The locations are determined based on the location of the peak available mass of sediment.

The discharge parameters are setup for the maximum and minimum dispersion in Appendix G.2.

I General hydrodynamics and morphodynamics

This appendix contains results from the general hydrodynamic and morphodynamic simulation. As mentioned in Chapter 4. The process to determine the nourishment location is an iterative process. The reasoning in this appendix is from the already chosen nourishment location.

In Appendix I.1 a study regarding the local and regional flow velocities is discussed. In Appendix I.2 the tidal sediment transport capacity is determined at the chosen nourishment location. Moreover, a spatial consideration is provided over the tidal sediment transport capacity. In Appendix I.4, a wave analysis is performed over the length of the Borndiep channel. Moreover, at the chosen nourishment location the cumulative distribution functions are determined. In Appendix I.3 a preliminary calculation is performed to gain an expectation for the initial dispersion of the settling sediment particles.

I.1. TIDAL FLOW

The horizontal advection generated by the flow is examined on two different scales. First, the dominant flow velocities are determined locally. A location with high flow velocities is preferred over a location with less high flow velocities. Also, the direction of the high flow velocities is important as these determine the initial direction of the mixing plume. Thereafter, the dominant flow velocities are determined regionally along the length of the Borndiep. Together they provide an indication of the expected initial dispersion during the settling process of particles (Appendix I.3).

In Fig. 4.1a an overview is depicted about which locations are studied in more detail to acquire insight in the flow velocities in the Borndiep tidal channel.

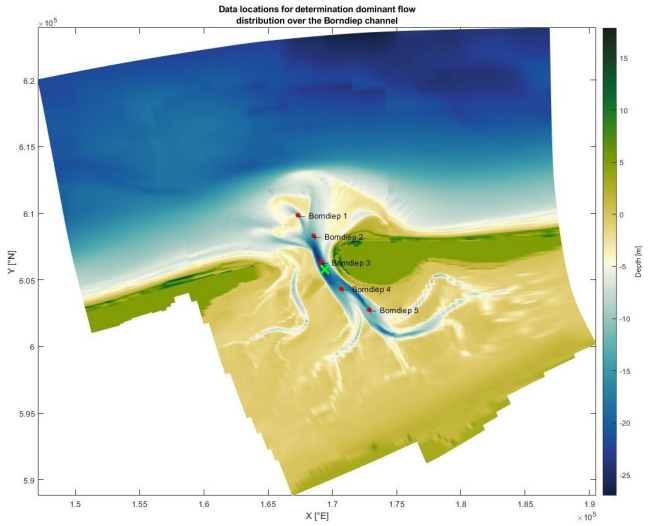

Figure I.1: Locations for further research regarding flow velocities. In red the locations over the Borndiep channel are indicated which are researched in the flow velocity is researched in more detail. In green the chosen nourishment location is depicted.

Local water velocity and depth fluctuations at the nourishment location
It was found that the velocity signal at Borndiep 3 shows the highest flow velocities compared to the other measurement locations. The depth averaged water velocity ranges between the -1.3 and +1.3 $\frac{m}{s}$. According to Fig. I.2b the local depth fluctuations at the nourishment location range between 23.7 and 25.9m.

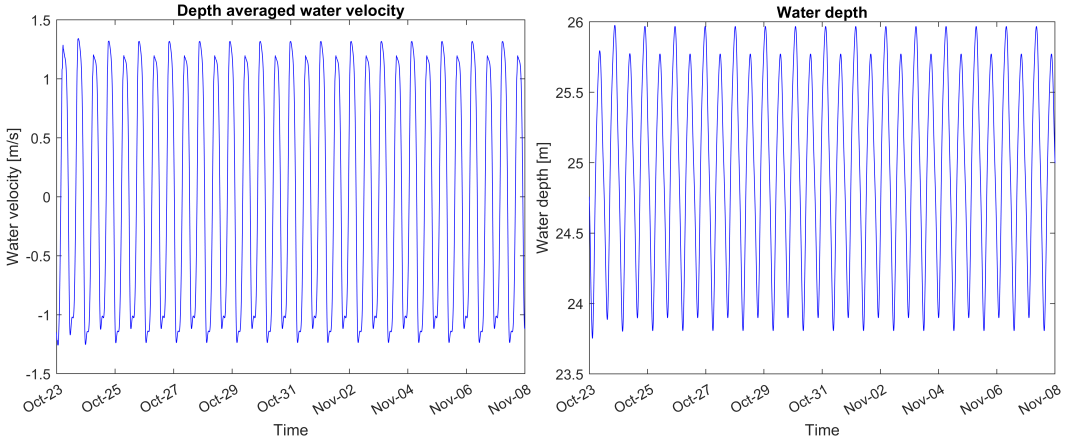

(a) Depth average velocity fluctuations at nourishment location in Ameland Inlet

(b) Depth fluctuations at nourishment location in Ameland Inlet

Figure I.2: Water depth and water velocity fluctuations at nourishment location

Regional water velocity and depth fluctuations near the nourishment location
The dominant flow distributions are studied in more detail over the length of the Borndiep channel by means of histograms. The measured data locations for the determination of the dominant flow distribution over the Borndiep channel are illustrated in Fig. 4.1a. By means of the green cross near Borndiep 3, the chosen nourishment locations is depicted.

In Fig. 4.1b, the dominant ambient tidal flow at Borndiep 3 is depicted in red. On the x-axis, the positive values are flow velocities directed to the Wadden Sea, whereas the negative values are flow velocities directed to the North Sea. From this histogram it can be concluded that at the nourishment location in general, high depth averaged velocities occur. The dominant velocities are located in the bins of [-1.5, -1] and [1, 1.5] $\frac{m}{s}$. This is in line with the previously found depth averaged velocity maximum and minimum. Due to the occurrence of mainly high flow velocities, it is expected that a nourishment at this location would yield locally high dispersion.

Whether the dispersion is likely to continue over the Borndiep channel, is determined by assessing the locations Borndiep 1, 2, 4 and 5 and are indicated by blue histograms in Fig. 4.1b.

At locations that are towards the North Sea relative to the nourishment location as well as locations that are towards the Wadden Sea relative to the nourishment location, the dominant flow velocity is between [-1, -0.5] and [0.5 ,1] $\frac{m}{s}$. According to Fig. 4.1b, dominant peak flow velocities in the bins between [-1.5, -1] and [1, 1.5] $\frac{m}{s}$ hardly occur at locations surrounding the nourishment location. Despite that, it is concluded that over the length of the Borndiep the peak flow is dominantly dominant over milder flow conditions. It confirms that the Borndiep channel is a tidal channel where high flow velocities are dominant.

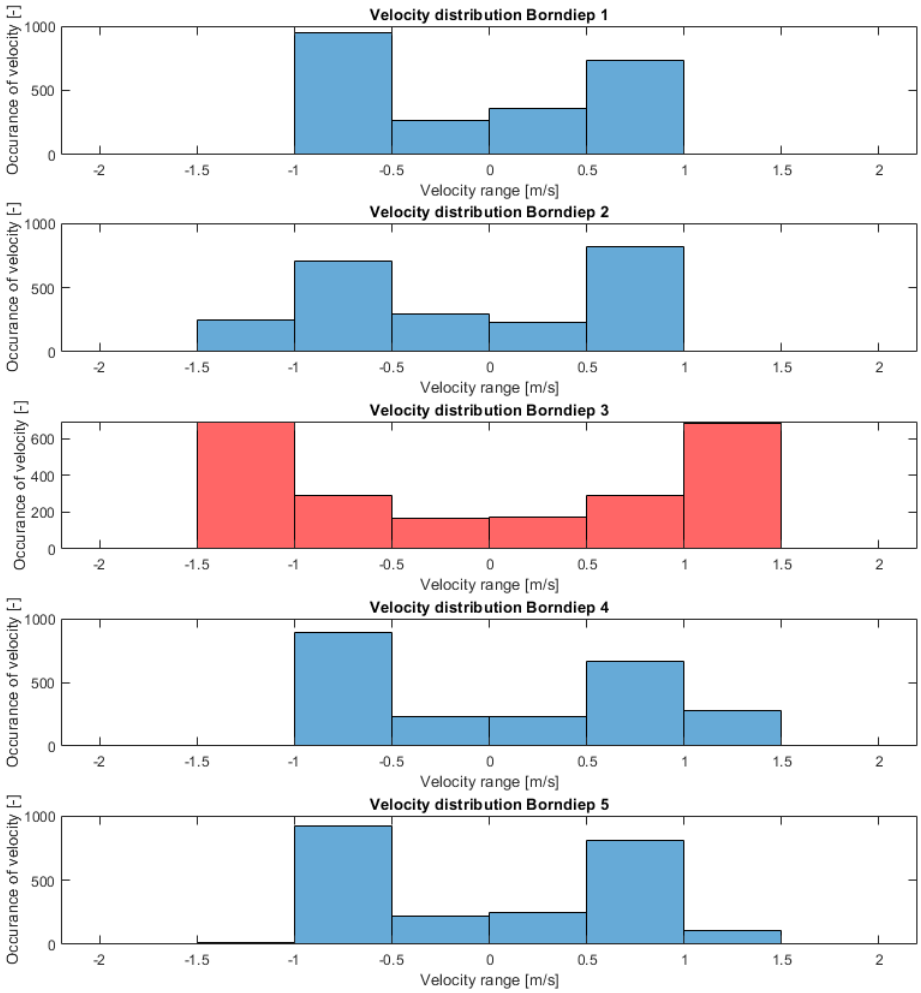

Figure I.3: Velocity distribution over the main channel

I.2. TIDAL SEDIMENT TRANSPORT

Through the tidal inlet there is both an ebb and flood current. Hence, the transport of sediment is also directed in two directions. In this model, negative transport corresponds with transport towards the North Sea, whereas positive transport corresponds with transport towards the Wadden Sea. The net transport is the difference between the positive and negative oriented transport.
To determine how much sediment can be added through a nourishment in the tidal channel, the spring-neap tide cycle tidal sediment transport capacity is determined. In order to determine the gross tidal sediment transport, the positive and negative directed transports are added to one another. The gross tidal sediment transport capacity is a potential upper bound of what the system can process.
The annual tidal sediment transport is determined by a multiplication of 26 (amount of spring neap tide cycles in a year) of the spring neap tide tidal sediment transport capacity.

A spatial overview of where the tidal sediment transport is measured is illustrated in Fig. I.4.

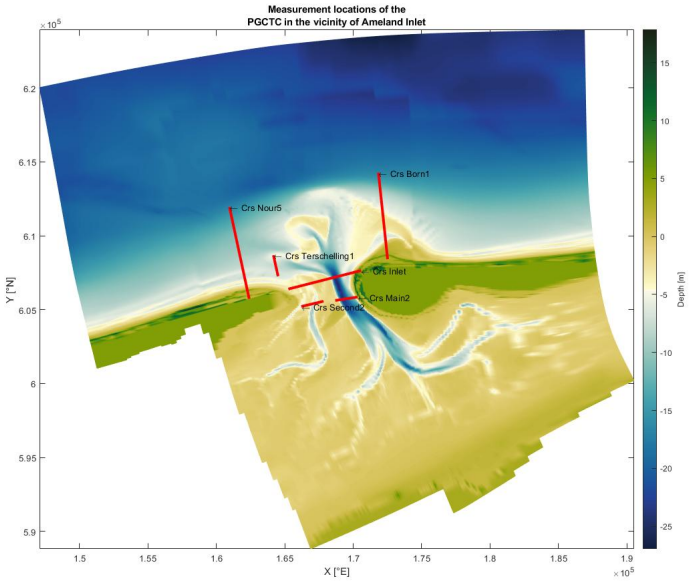

Figure I.4: Locations in the vicinity of Ameland Inlet where the tidal sediment transport is determined.

The methodology of how the annual tidal sediment transport capacity is determined, is illustrated by an example of the tidal sediment transport capacity over the entire tidal inlet. Fig. I.5 shows the tidal sediment transport during a spring neap tide cycle per sediment fraction and for all fractions combined. In red the tidal transport to the Wadden Sea is depicted. In black the tidal transport to the North Sea is depicted and in blue the net tidal transport is depicted. The cumulative tidal sediment transport capacities are illustrated in Table I.1.

Based on Table I.1, the annual tidal transport capacity can be derived by multiplying the gross transport of 23.54x10^4 m^3 by 26 = 6.12 Mm^3 per year.

Cross-section Inlet

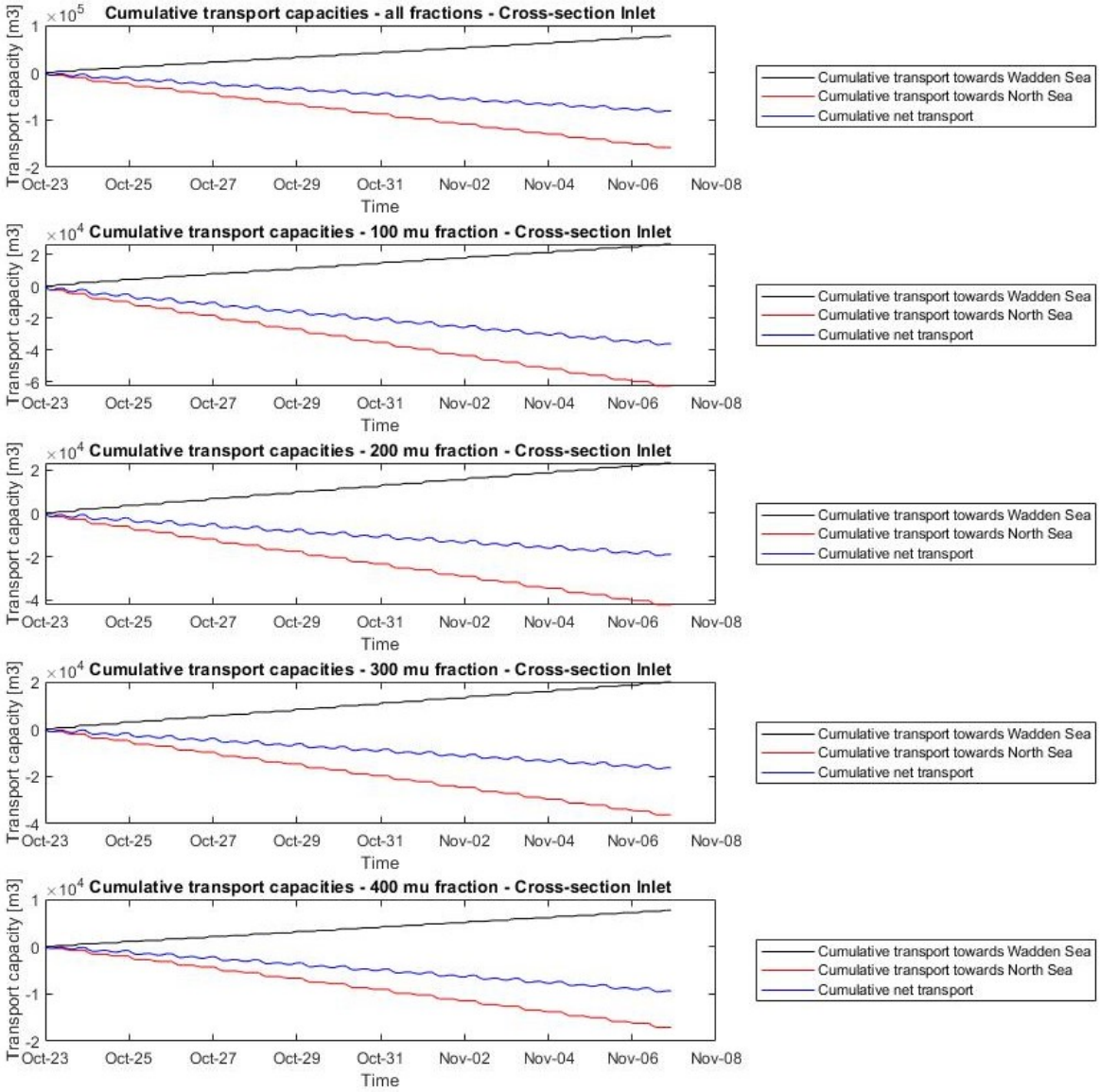

Figure I.5: Tidal transport for all fractions combined and per fraction over a spring neap tide cycle over the Inlet

Table I.1: Cumulative tidal sediment transport capacity over entire cross-section. These tidal sediment transport capacities are the values over a spring neap tide cycle

Tidal sediment transport x 10 ^{4} [m^3]	**Fraction** All	100 μm	200 μm	300 μm	400 μm
Transport towards North Sea	- 15.83	- 6.26	- 4.23	- 3.63	- 1.71
Transport towards Wadden Sea	7.71	2.63	2.32	1.99	0.77
Net transport	- 8.09	- 3.61	- 1.90	- 1.64	- 0.94
Gross transport	23.54	8.89	6.55	5.62	2.48

The nourishment will be carried out in only one tidal channel. Table I.2 shows that the annual tidal

sediment transport capacity of the Borndiep (cross-section main2) is the largest.

The tidal sediment transport capacity is measured over the entire width. To acquire the tidal sediment transport capacity per meter width, the annual tidal sediment transport capacity is divided by the width. These values show how much sediment annually can be transported per meter width.

Table I.2: This table illustrates the annual tidal sediment transport capacity. Moreover, the widths of the cross-sections over which the sediment transport capacity is measured is provided. Finally, the annual sediment transport capacity per meter width is illustrated

Cross-section Parameter	Inlet	Main2	Second2	Born1	Terschelling1	Nour5
Annual tidal sediment transport capacity [Mm^3/year]	6.12	4.23	1.8	0.82	0.17	0.04
Width cross-section [m]	5465	1645	1668	5890	1460	6371
Annual tidal sediment transport capacity per meter [Mm^3/m/year]	1200	2750	1079	139.4	117.4	6.9

The following figures illustrate the tidal sediment transport capacity of the other measured locations in Fig. I.4. The analyses to obtain the values from Table I.2 is equal to the example showed above.

Cross-section main2

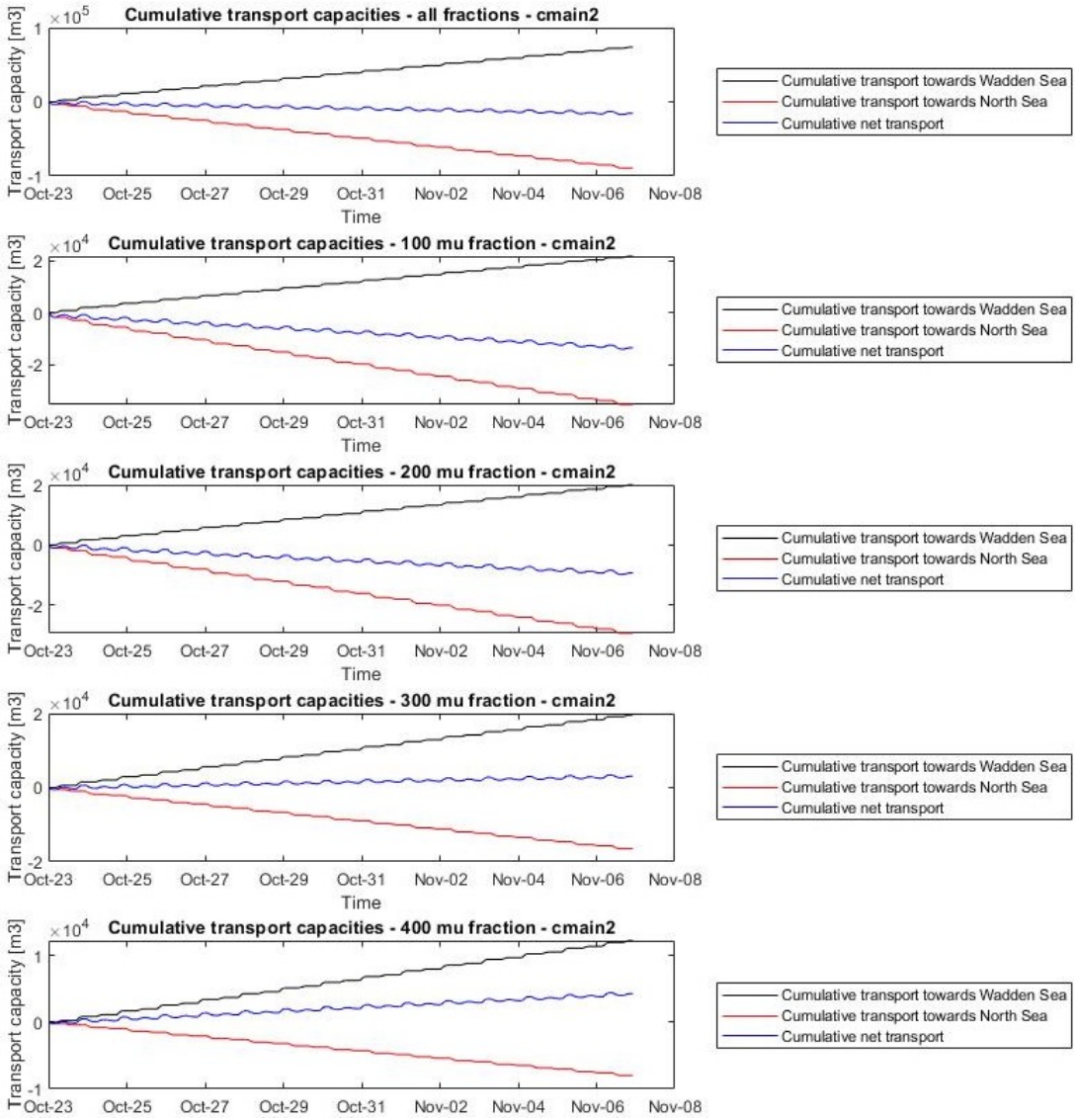

Figure I.6: Tidal transport for all fractions combined and per fraction over a spring neap tide cycle at location cmain2.

Cross-section born1

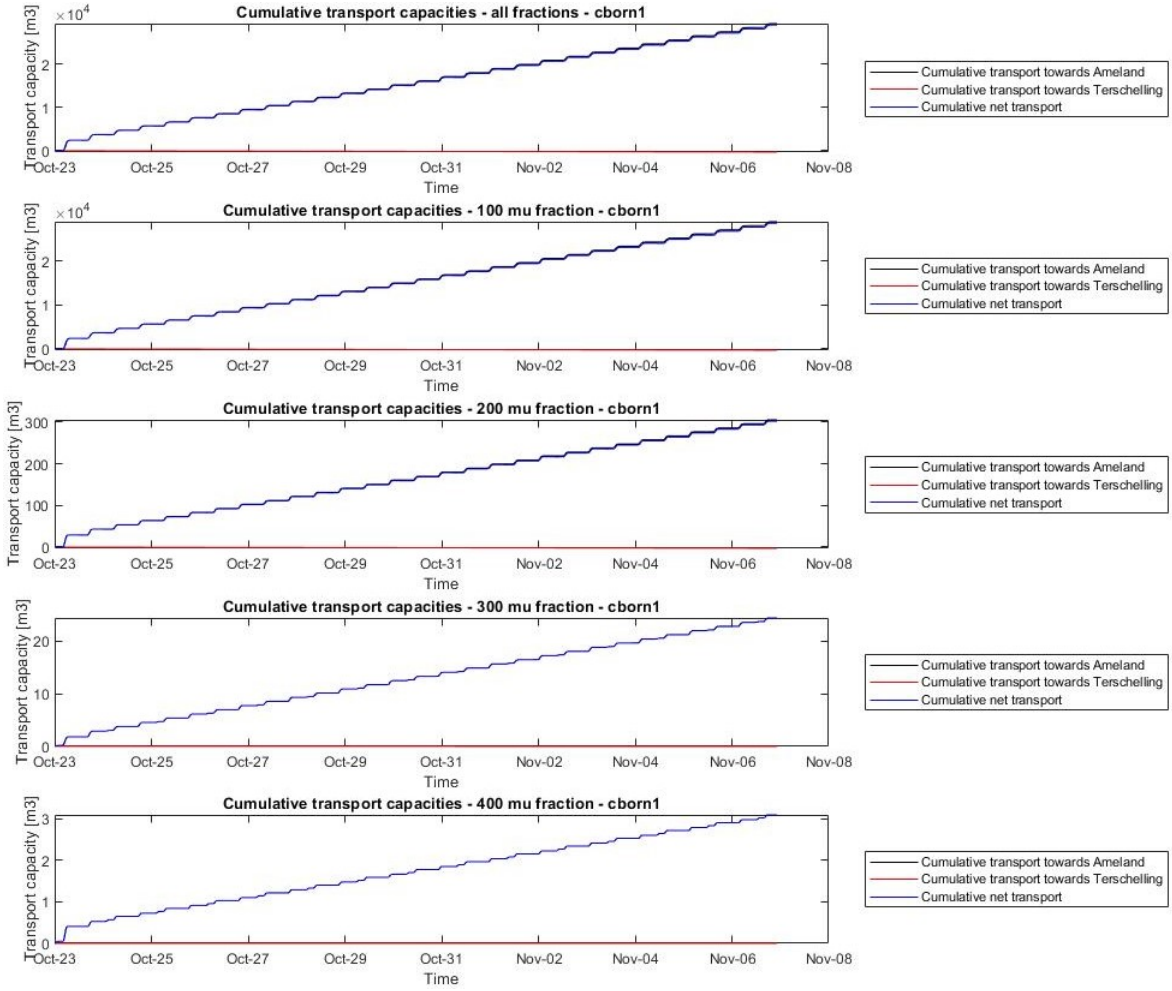

Figure I.7: Tidal transport for all fractions combined and per fraction over a spring neap tide cycle at location cborn1.

Cross-section Terschelling1

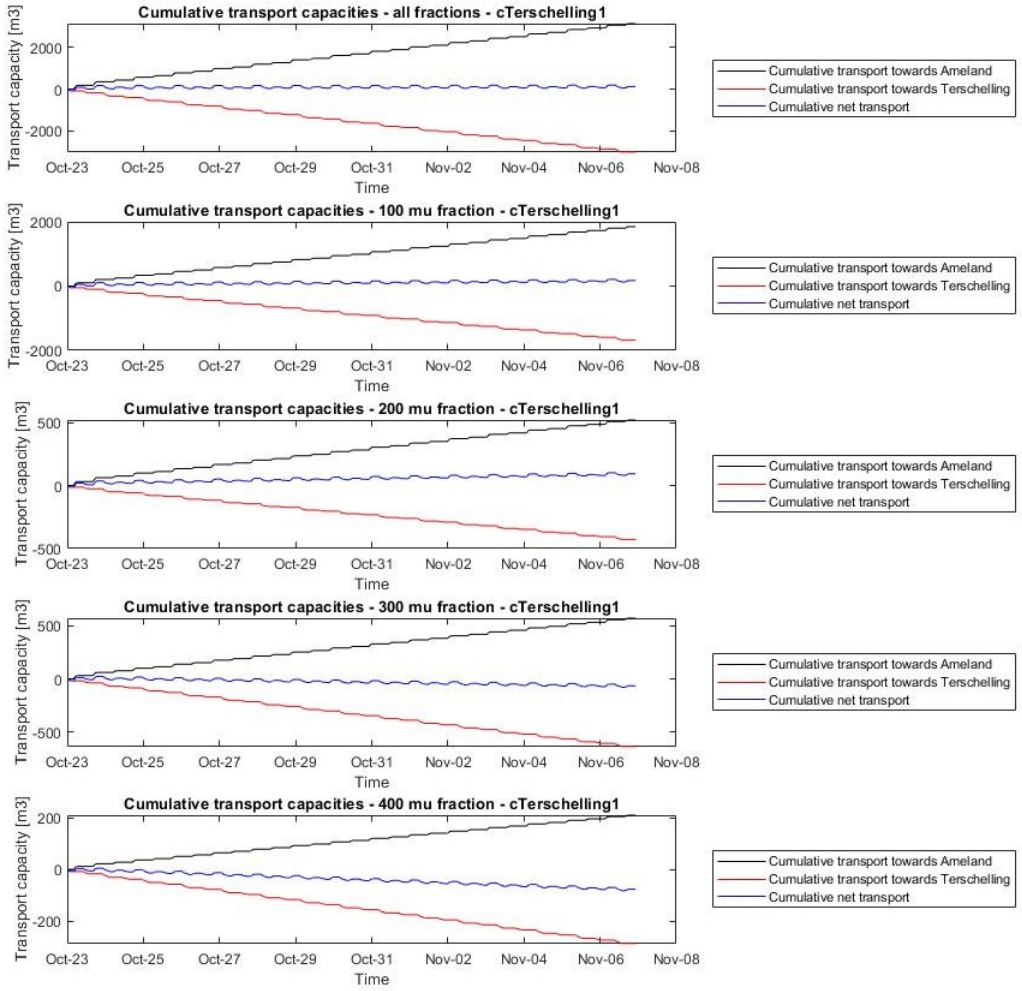

Figure I.8: Tidal transport for all fractions combined and per fraction over a spring neap tide cycle at location cterschelling1.

Cross-section second2

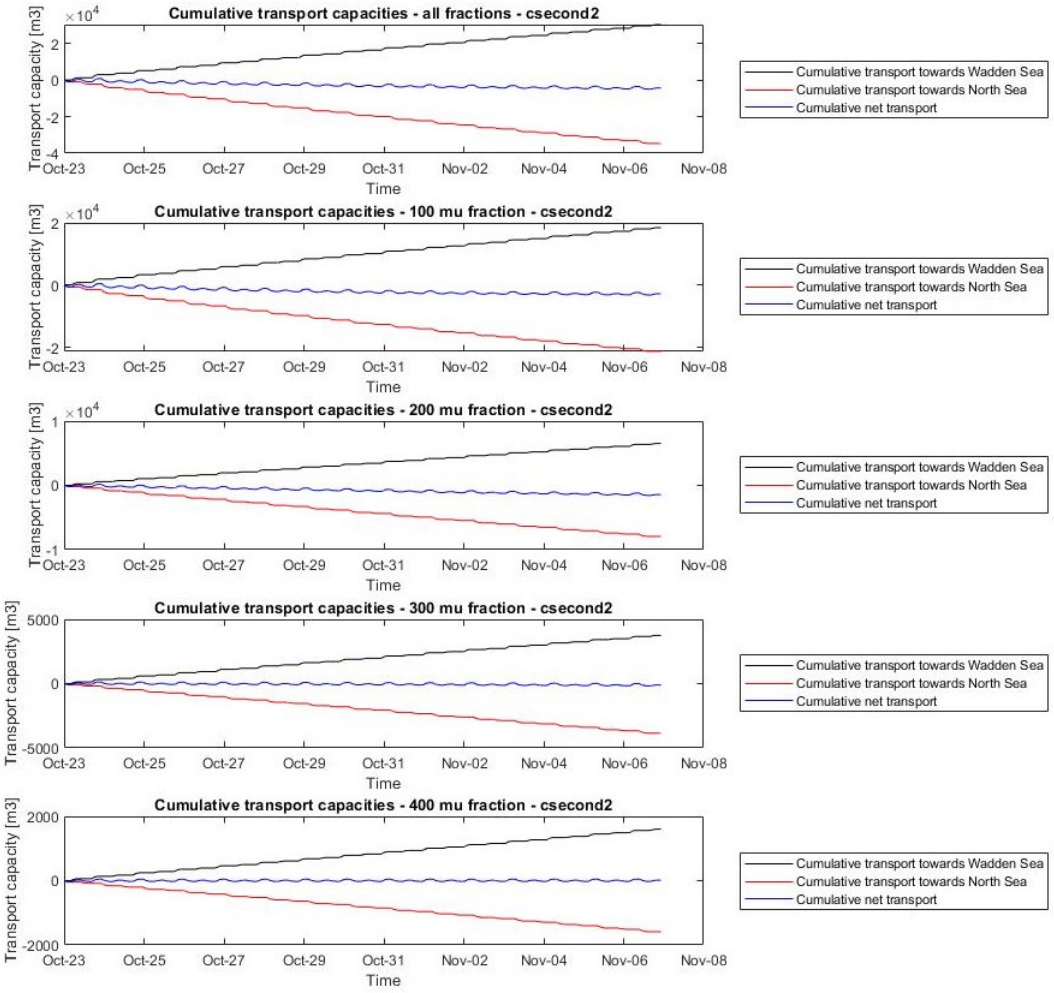

Figure I.9: Tidal transport for all fractions combined and per fraction over a spring neap tide cycle at location csecond2.

Cross-section nour5

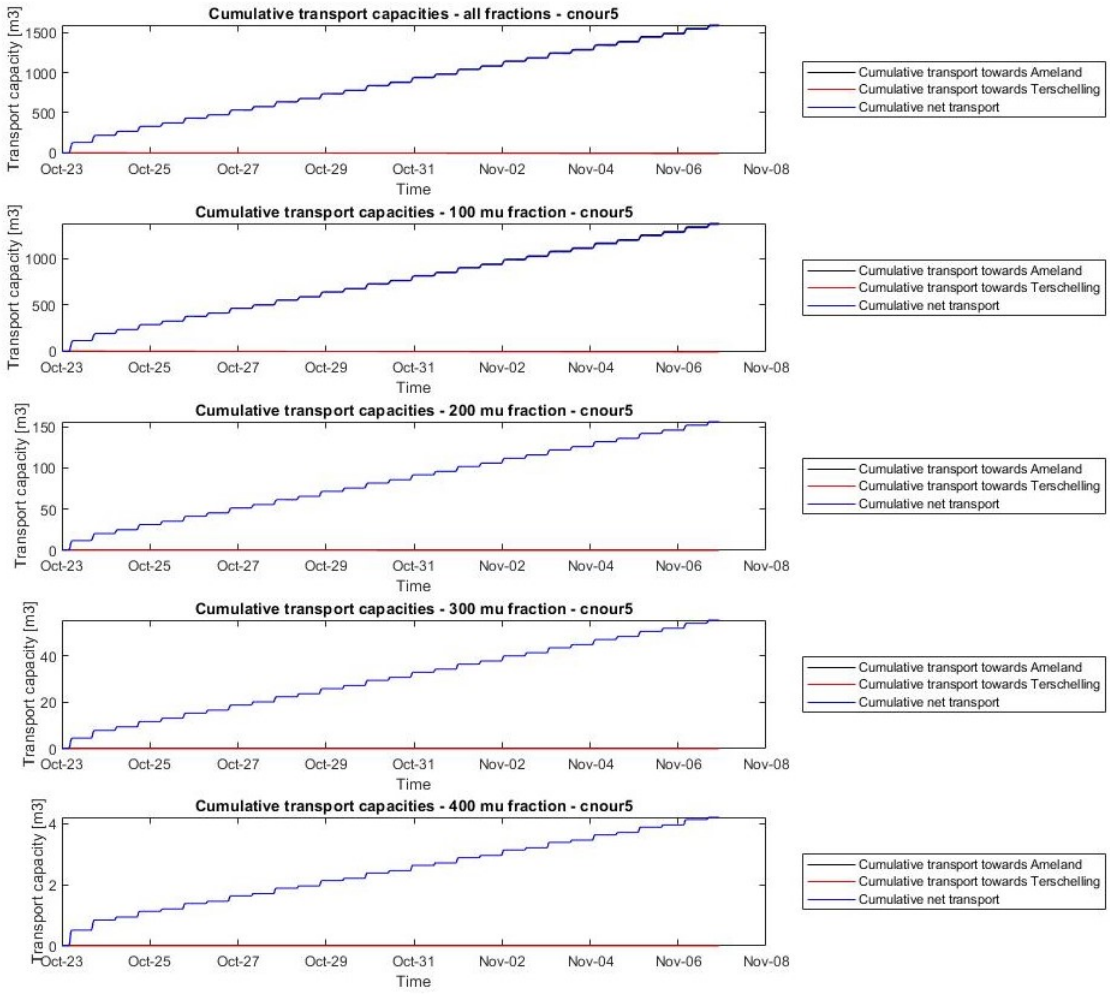

Figure I.10: Tidal transport for all fractions combined and per fraction over a spring neap tide cycle at location cnour5

I.3. DISPERSION OF SETTLING SEDIMENT PARTICLES

In this section a preliminary hand calculation is made about how the longitudinal distribution of settling sediment particles looks like.

To calculate this, it is assumed that the nourishment equipment is fixed (stationary nourishment). Furthermore, it is assumed that the nourished sediment directly has the same horizontal flow velocity as the ambient flow.

To obtain the settling time, the depth is divided by the settling time per fraction. The horizontal ambient flow acts as a horizontal advection transport mechanism for the individual settling particle. The horizontal distances are obtained by multiplying the settling times with the average horizontal flow velocity. The data from the Borndiep 3 Fig. 4.1a measuring point is used as data input. Other initial assumptions are:

- Once a particle touches the water surface at x=0, it holds the initial horizontal ambient flow condition at that specific moment during the settling process
- The settling velocity of the different fractions is the individual settling velocity

- The settling velocity is constant and no turbulence occurs
- The seabed has an uniform depth

The determination of the longitudinal distribution is made by means of histogram analysis. A bin width of 500 meters is set to count the amount of times a particle settles in a predefined region. The different fractions are stacked to obtain the summed particles in a certain bin.

In this study it was decided to have each fraction appear equally often in the nourishment., Therefore, the particle size distribution (PSD) is assumed to be have an equal distribution of the four present particles.

In Model 1: General hydrodynamics and morphodynamics, the measurements were taken per 10 minutes (600 seconds). In Appendix G.1 the total sand flux per second is determined. It is found to be 101,47 $\frac{kg}{s}$.

In Fig. I.11 the distribution of particles per fraction is depicted. The y-axis represents the amount of kg and the x-axis represents the horizontal distance a particle travels. From the location where the particles are released (x = 0) the following dispersion per particle size is found. The 100 μm fraction has a range of 8000 meters towards the North Sea and 7500 meters towards the Wadden Sea. The 200 μm has a range of 2500 meters towards both the North Sea and Wadden Sea. The 300 μm has a range of 2180 meters towards both the North Sea and Wadden Sea. The 400 μm has a range of 1000 meters towards both the North Sea and Wadden Sea.

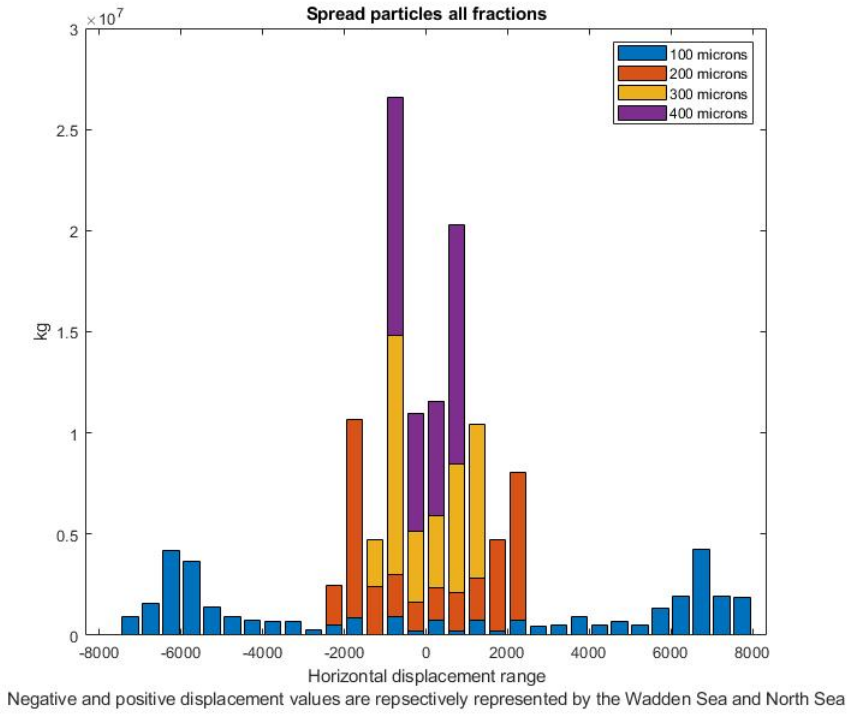

Figure I.11: Mass [kg] distribution of settling particles

The amount of mass [kg] is converted to an increase in bed height. As an assumption, it is estimated that in the settling process, particles settle over a width perpendicular to the dominant ebb flood direction of 300 meters. Also, the amount of kg per bin is divided by the bin width of 500 meters. The assumed direction of 300 meters perpendicular to the flow and the bin width of 500 meters are the surface area on which the particles settle. By dividing the found kilograms by the surface area,

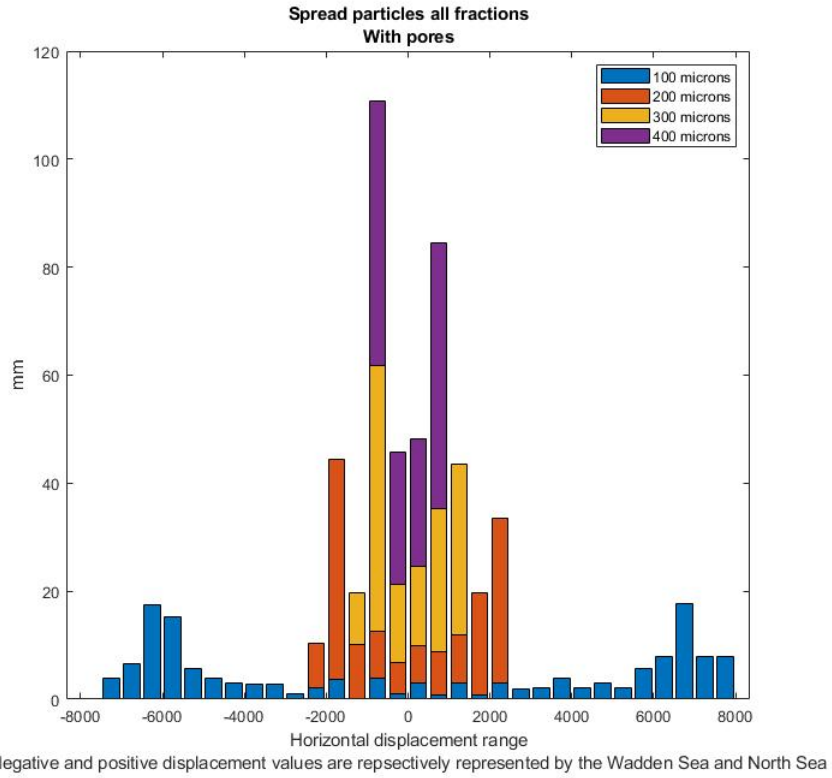

Figure I.12: Increase in bed height determined with the density of sand with pores (1600 $\frac{kg}{m^3}$)

the y-axis of figure Fig. I.11 is translated to an axis with unit kg/m^2. Finally, the obtained kg/m^2 is divided by the density of sand with pores (1600 $\frac{kg}{m^3}$) in order to obtain an increase in bed level height [mm].

According to Fig. 5.2, sand particles of 100 μm form 20 mm of bed height over a spring neap tide cycle at 6000 meters away from the initial release position. This is approximately between the 1 and 2 mm per day. It is expected that the ecological system does not find any hindrance from this amount. However, on a distance of 1000 meters from the initial release position a total of 110 mm over a spring neap tide cycle settles of all fractions summed. This is approximately 10 mm per day. It has to be validated whether the system can transport such a daily amount without silting up. Whether an accumulation of 10mm per day could be harmful for the ecological system is beyond the scope of this thesis.

Based on the found longitudinal distribution, it can be concluded that the initial dispersion due to the settling process is large.

The sub conclusions based on the longitudinal distribution are:

- The dispersion per fraction is linked to the settling velocity of a fraction (i.e. large fractions settle more quickly than small fractions). Therefore large fractions have less dispersion compared to a small fraction
- It is uncertain whether the accumulated fractions close to the discharge location can be transported away by the system
- The depth (z-axis) is important due to the settling process of different sediment fractions.

I.4. WAVE ANALYSIS

Wave heights and wave periods are a limiting factor during dredging operations as they influence workability (Laboyrie et al., 2018). The yearly operational time of the Zandwindmolen may not interfere with the harmonization of the sub-systems. Therefore, the nourishment process must have an operational time of 100%. The significant wave height in the Ameland Inlet area is being further investigated to determine the design criteria for the nourishment equipment. The significant wave height over 2016 is acquired at Rijkswaterstaat as they offer an open-source database for water management (Rijkswaterstaat, 2021e). Unfortunately, the data-set lacks wave data during the summer months. However, during winter more severe storms and thus waves are expected, therefore the data set is applicable to gain knowledge about exceeding wave heights during winter months.

In Fig. I.13 the buoys and their corresponding number and locations are indicated in red and the green cross is the nourishment location in the Borndiep channel.

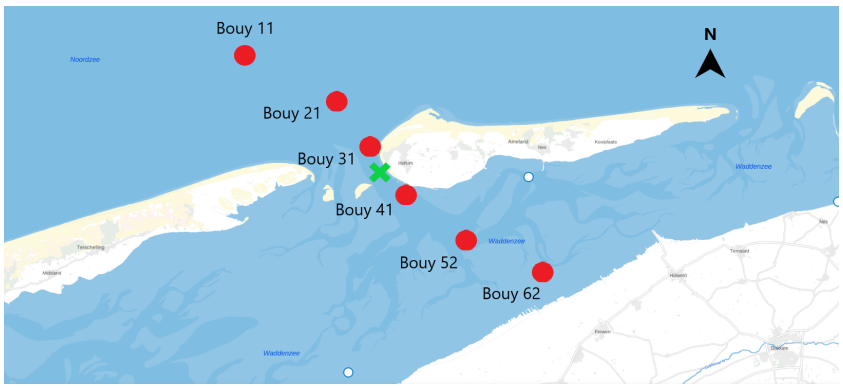

Figure I.13: Buoy locations over which significant wave height (H_s) data is acquired in the year 2016

The significant wave height H_s is plotted over a year in fig Fig. I.14. According to this figure, at buoy 11 and 21 the largest wave heights are present. Buoy 11 is located in a more offshore region, where no depth induced breaking occurs. Buoy 21 however, is located near the ebb tidal delta where it is likely that wave breaking and shoaling processes occur. This might explain the occurrence of sometimes larger waves at buoy 21 than at buoy 11. Buoy 31 till buoy 62 are located over the entrance of the Borndiep channel until the back barrier of the inlet. From Fig. I.14, it can be assessed that inlet inwards the H_s decreases. The decrease of H_s implies wave breaking which in turn yields a decreasing energy gradient from the inlet to the back barrier of the basin. This is in line with the aforementioned decreasing energy gradient and median grain size distribution in the inlet (Section 2.3.2 and Fig. 2.4).

The nourishment location is set at the interface of the Wadden Sea and North sea in the Borndiep channel. This is also known as the inlet gorge. The nourishment location is located in between buoy 31 and 41. To determine the actual wave heights at these locations, buoys 31 and 41 are studied in more detail by means of probability density and cumulative probability functions.

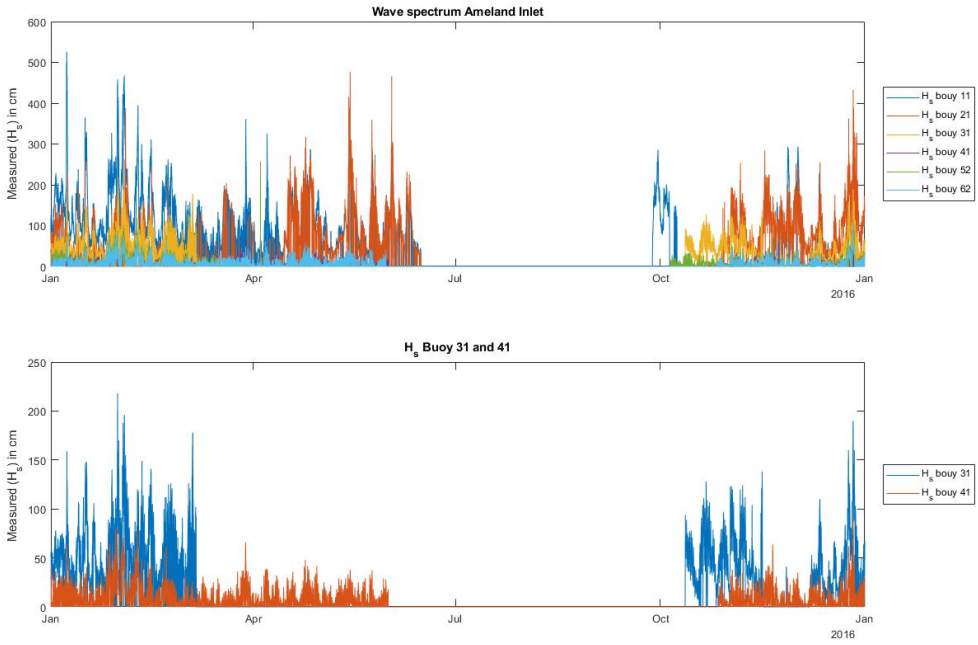

Figure I.14: Significant wave height (H_s) of all buoys

To assess the workability of floating dredging equipment the exceedance probability of the wave spectrum in buoy 31 and 41 is determined. From the exceedance probability, the corresponding wave height for a non interfering operational time can be determined. First, the wave spectrum is fitted along a Weibull distribution to create a probability density function (pdf). The Weibull distribution is chosen as this is a common distribution for wave heights (Holthuijsen, 2010). Thereafter, the cumulative distribution functions (cdf) are determined. The missing data in the data-set is deleted. Therefore, both the pdf and cdf only provide information over the spring, autumn and winter period. In Fig. I.15 the Weibull probability density functions and the corresponding the cumulative distribution functions are illustrated.

Besides the pdf and cdf, the minimum, maximum and mean significant wave height (H_s) are determined. Also, the corresponding minimum, maximum and mean significant wave period (T_s) are determined. All values are illustrated in Table I.3. The maximum observed wave period for buoy 41 is expected to be too large. The rest of the data is in line with data found in previous researches (Section 2.2).

Table I.3: Significant wave height and period characteristics buoy 31 and 41

Parameter	Mean Hs [cm]	Max Hs [cm]	Min Hs [cm]	Mean Ts [s]	Max Ts [s]	Min Ts [s]
Buoy 31	55.11	218	3	6.24	10.7	3.8
Buoy 41	13.88	89	2	5.65	27.7	3.1

As previously mentioned, the technical requirement is that the nourishment equipment may not be a limiting factor on the operational time of the Zandwindmolen. Therefore, the nourishment equipment must be able to persevere during all conditions in Ameland Inlet. In comparison be-

tween buoy 31 and 41, more extreme wave heights occur at buoy 31 and is therefore normative for the design of the nourishment equipment.

In conclusion, the wave height at which the nourishment equipment must be developed is 218 cm Fig. I.15a. In addition, the equipment must be able to withstand wave periods between 3.8 and 10.7 seconds.

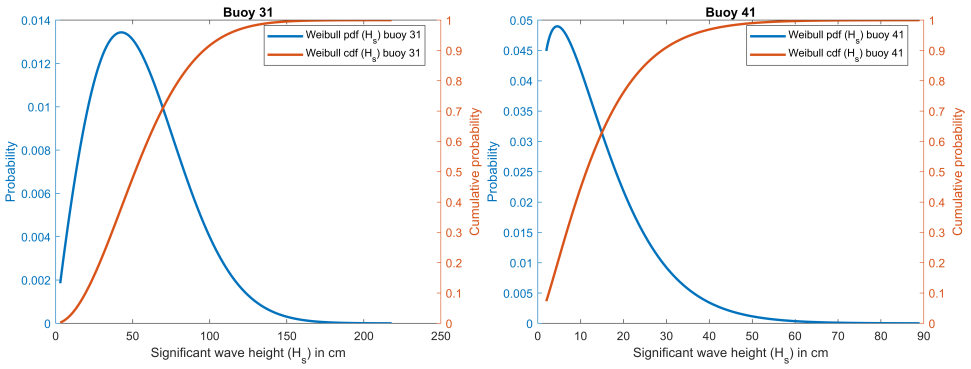

(a) Weibull pdf and cdf buoy 31

(b) Weibull pdf and cdf buoy 41

Figure I.15: Probability denisty function (pdf) and cumulative distribution function (cdf) of buoys 31 and 41

J | Near-field 2D results

J.1. NEAR-FIELD DISPERSION 2D MODEL

For the near-field dispersion a 2D model is simulated besides a 3D model. The duration of the simulation period is a spring neap cycle. The 2D simulation is identical to the 3D simulation. The mid-field dispersion is determined based on a 2D numerical model. Therefore, numerical errors or deviations between the 2D and 3D model are already identified by means of this model approach.

There are two 2D models, one with minimum dispersion and one with maximum dispersion. The minimum or maximum dispersion depends on the absence or presence of background sediment fractions. The results of the 2D simulation are illustrated below. First the spatial dispersion is illustrated. Thereafter, the longitudinal distribution is illustrated. Finally, tables are introduced in which the rate of correspondence with the dispersion of the 3D simulations is studied.

This chapter does not address where sediment ends up in the tidal inlet system. It is purely a technical analysis. Therefore, this chapter only looks at the differences and similarities between the 2D near-field simulation and the near-field 3D simulation. From this chapter follows a methodology on how the 2D mid-field dispersion model should be simulated based on the 3D near-field dispersion results.

Spatial dispersion

The scale on which the results are plotted is from 0-2 $\frac{kg}{m^2}$ or converted by the porous sand density of 1600 $\frac{kg}{m^3}$ 0-0.06 mm sand accretion. Areas that are dark red are areas where 2 $\frac{kg}{m^2}$ or more has settled. White areas are areas to which a nourished fraction has not yet been able to disperse to within the simulation duration. The contour line between the presence or absence is set at 0.5% sediment availability.

The distances of the minimum and maximum dispersion is provided in Table J.1.

Table J.1: Minimum and maximum dispersion distances for the 2D near-field dispersion simulation

	Distance from Nourishment location [m]							
Direction	North Sea				Wadden Sea			
Fraction [μm]	100	200	300	400	100	200	300	400
Minimum 2D dispersion	5330	3331	1806	523	5743	2798	1394	573
Maximum 2D dispersion	7996	7745	6321	3600	9740	9599	7017	2880

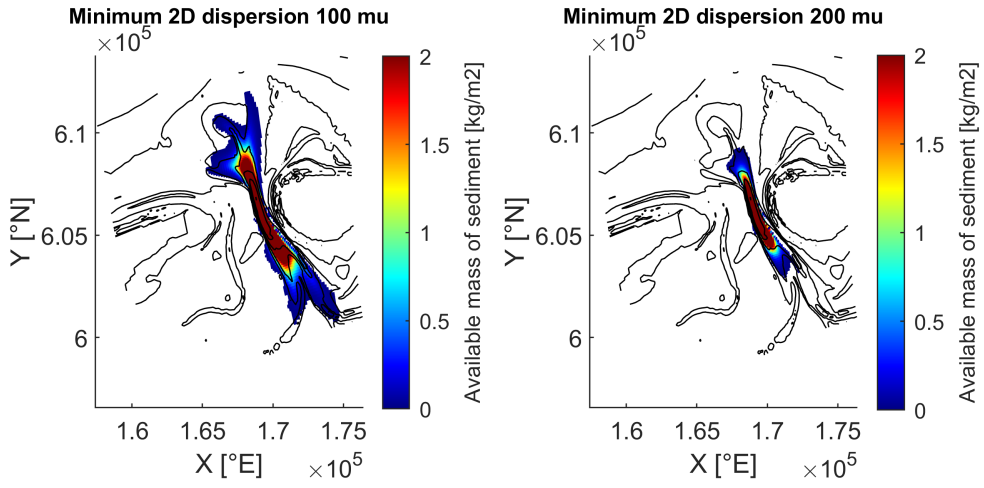

Figure J.1: 100 and 200 μm minimum dispersion 2D

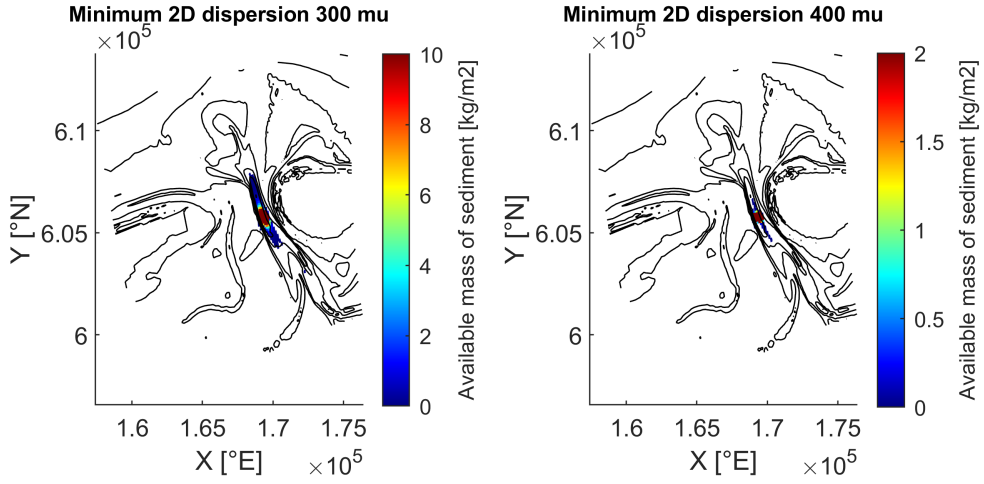

Figure J.2: 300 and 400 μm minimum dispersion 2D

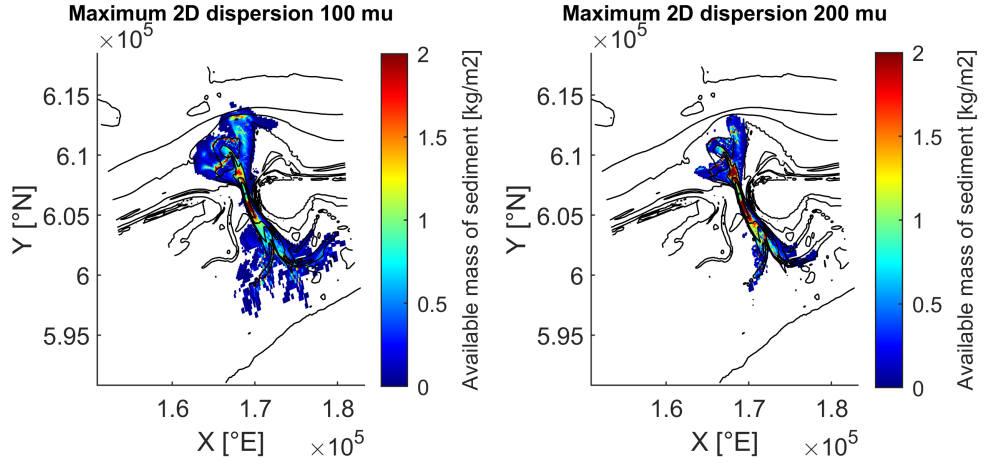

Figure J.3: 100 and 200 μm maximum dispersion 2D

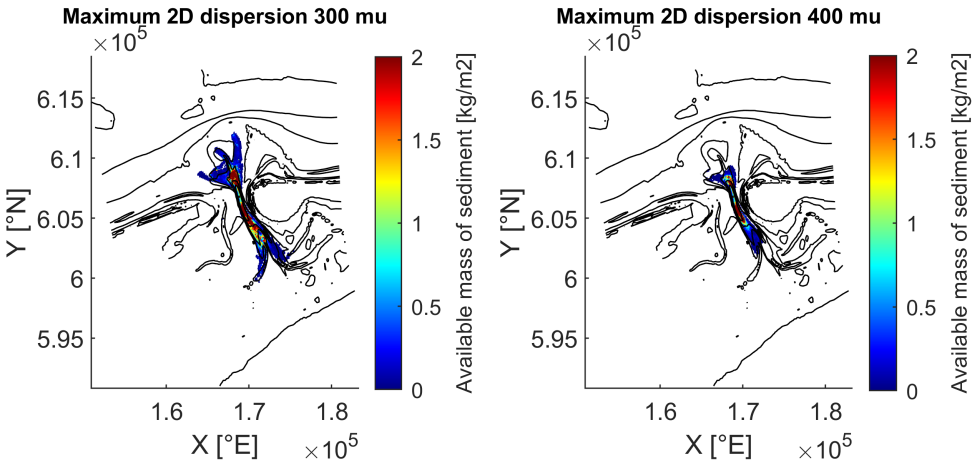

Figure J.4: 300 and 400 μm maximum dispersion 2D

Longitudinal distribution

In Fig. 5.7a is indicated by the black line where the transect of 15464m is located. The nourishment location is marked with the red dot. The depth profile over longitudinal transect illustrated in Fig. 5.7b shows the depth profile of this transect. These figures are repeated below. At 0 m distance over longitudinal transect, the nourishment location is located and negative and positive distances are respectively away from the nourishment in the direction of the North Sea and Wadden Sea. First the results of the minimum and thereafter the results of the maximum longitudinal distributions are illustrated.

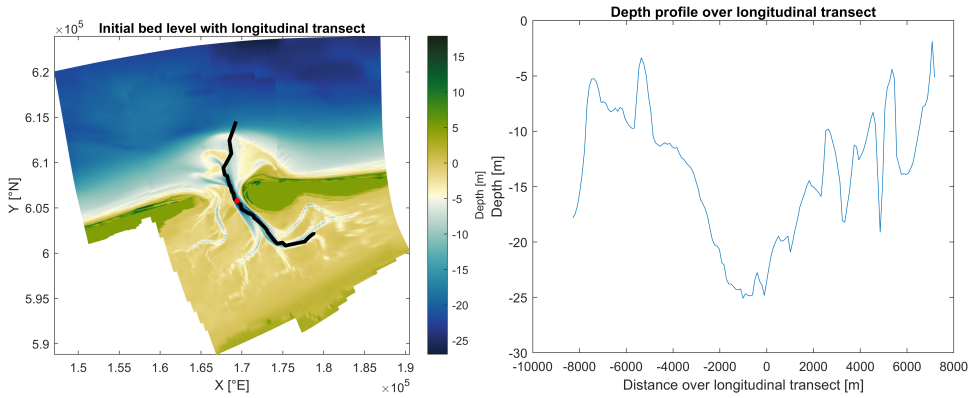

(a) Overview transect left branch

(b) Depth profile of transect

Figure J.5: Transect and depth profile for the determination of the longitudinal distribution

Fig. J.6a shows that the degree of dispersion is determined by the size of the sediment fraction. The dispersion is greatest for the finer fractions and smallest for the coarser fractions. In addition, a peak is visible at the nourishment location (x=0). Thus most sediment settles directly below the nourishment location. In Table J.2 the peak available mass of sediment are illustrated per fraction. From Table J.2 and Fig. J.6a it follows that coarser fractions have higher available masses of sediment under the nourishment locations compared to finer fractions. Fig. J.6b shows the initial dispersion over the transect for all fractions summed. The maximum mass of sediment that settles directly under the nourishment location is 1000 $\frac{kg}{m^2}$ (or a 600 mm increase of bed height).

Table J.3: Available mass of sediment [$\frac{kg}{m^2}$] per fraction for maximum longitudinal distribution

	Accumulated available mass of sediment [$\frac{kg}{m^2}$]			
Fraction [μm]	100	200	300	400
Peak [$\frac{kg}{m^2}$]	39.9	117.0	233.3	391.7

Table J.2: Available mass of sediment [$\frac{kg}{m^2}$] per fraction for minimum longitudinal distribution

	Accumulated available mass of sediment [$\frac{kg}{m^2}$]			
Fraction [μm]	100	200	300	400
Peak [$\frac{kg}{m^2}$]	50.7	150.9	314.1	478.0

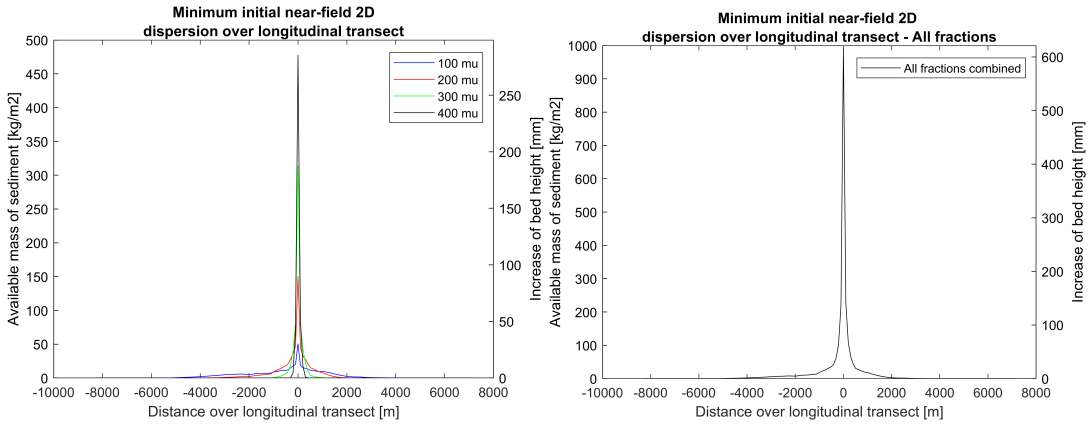

(a) Minimum longitudinal near-field distribution of individual sediment particles

(b) Minimum longitudinal near-field distribution of all sediment particles

Figure J.6: Longitudinal transect of minimum near-field distribution. The longitudinal transect is taken through the tidal channel as depicted in Fig. 5.7.

Fig. J.7a shows that the degree of dispersion is determined by the size of the sediment fraction. The dispersion is greatest for the finer fractions and smallest for the coarser fractions. In addition, a peak is visible at the nourishment location (x=0). Thus most sediment settles directly below the nourishment location. However, in the spectrum of Fig. J.7a also small accumulations of available mass of sediment along the longitudinal transect can be observed.

In Table J.3 the peak available mass of sediment are illustrated per fraction. From Table J.3 and Fig. J.7b it follows that coarser fractions have higher available masses of sediment under the nourishment locations compared to finer fractions.

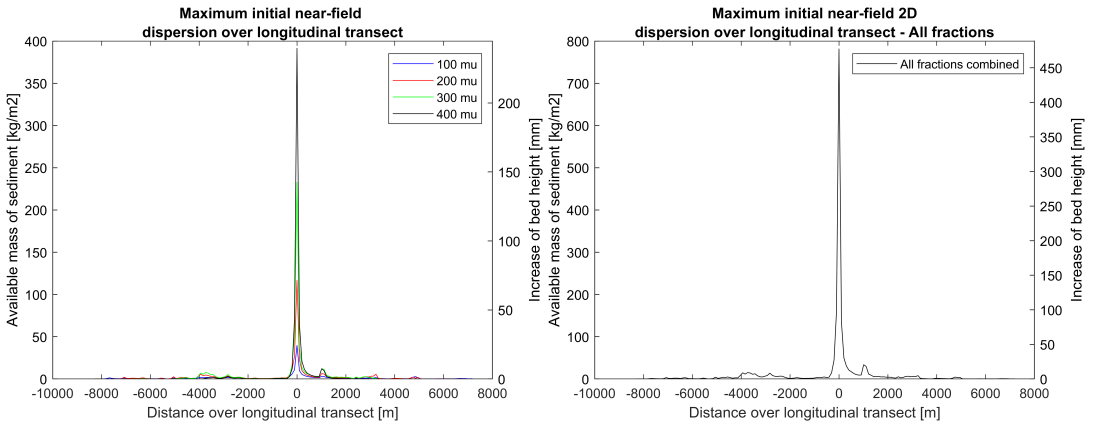

(a) Maximum longitudinal 2D near-field distribution of individual sediment particles

(b) Maximum longitudinal near-field distribution of all sediment particles

Figure J.7: Longitudinal transect of maximum near-field distribution. The longitudinal transect is taken through the tidal channel as depicted in Fig. 5.7.

J.2. 2D VERSUS 3D NEAR-FIELD SIMULATIONS

In this section, a consideration is given between all the different near-field models. First, the 2D models of the minimum and maximum dispersion are compared. Then, the 3D models of the minimum and maximum dispersion are compared.

In the tables in the upcoming section the term "the correspondence in percentage" is mentioned. This terms is used to compare the two models. The benchmark is the minimum dispersion simulation. When the difference in percentage is 100%, this implies that the two models show high correspondence (are equal). When below 100%, the minimum dispersion simulation has lower values than the maximum dispersion simulation and vice versa.

Minimum dispersion versus maximum dispersion - 2D
The 2D models yield approximately the same trend for both minimum and maximum dispersion. The main difference lies in the rate of dispersion. In Table J.4 the maximum dispersion distances from the discharge locations for both 2D models is illustrated. From this table it can be observed that the maximum 2D dispersion simulation disperses the sediment more than the minimum 2D dispersion simulation for each fraction. There are especially large differences in dispersion for the coarse fractions (300 and 400μm). But in general it can be stated that most of the fractions disperse more than 200% further.

Table J.4: Maximum dispersion distances from discharge location per fraction and per transported direction for the 2D models.

	Distance from Nourishment location [m] - 2D comparison							
Direction	North Sea				Wadden Sea			
Fraction [μm]	100	200	300	400	100	200	300	400
Minimum 2D dispersion [m]	5330	3331	1806	523	5743	2798	1394	573
Maximum 2D dispersion [m]	7996	7745	6321	3600	9740	9599	7017	2880
Correspondence in percentage [%]	150	233	350	688	170	343	503	503

Also, the maximum dispersion per fraction is higher for the maximum dispersion than the minimum dispersion for the longitudinal distribution. This also yields smaller peak available mass of sediment per fraction for the maximum dispersion as in this simulation the sediment is better

spread out over the area of Ameland Inlet. This is illustrated in Table J.5. According to this table the difference of available mass of sediment is relatively constant (between 74 and 82 %) between both simulations.

Table J.5: Comparison peak available mass of sediment between minimum and maximum dispersion

	Accumulated available mass of sediment [$\frac{kg}{m^2}$]			
Fraction [μm]	100	200	300	400
Minimum dispersion peak [$\frac{kg}{m^2}$]	50.7	150.9	314.1	478
Maximum dispersion peak [$\frac{kg}{m^2}$]	39.9	117.0	233.3	391.7
Correspondence in percentage [%]	78.6	77.5	74.2	81.9

Minimum dispersion versus maximum dispersion - 3D

The 3D models yield approximately the same trend for both branches. The main difference lies in the rate of dispersion. The results of the 3D models are depicted in Chapter 5. In Table J.6 the maximum dispersion distances from the discharge locations for both the minimum and maximum dispersion 3D models is illustrated. The maximum dispersion is for each fraction further than the minimum dispersion. There are especially large differences in dispersion for the coarse fractions towards the Wadden Sea (300 and 400μm). But in general it can be stated that most of the fractions disperse more than 200% further.

Table J.6: Maximum dispersion distances from discharge location per fraction and per transported direction for the minimum and maximum 3D simulations.

	Distance from Nourishment location [m] - 3D comparison							
Direction	North Sea				Wadden Sea			
Fraction [μm]	100	200	300	400	100	200	300	400
Minimum 3D dispersion [m]	6650	4222	3094	2349	7594	3727	2485	1809
Maximum 3D dispersion [m]	9079	7940	6990	7014	10609	8956	8821	7327
Correspondence in percentage [%]	137	188	226	299	140	240	355	405

Also for the longitudinal dispersion transects of the minimum and maximum model simulations, the the maximum dispersion simulation shows a larger distribution than the minimum dispersion simulation. Which results in smaller peak available mass of sediment per fraction. The 100 and 200 μm fractions show a Gaussian curve of the maximum dispersion simulation near the nourishment location. While, the minimum dispersion simulation shows for all fractions a bi-modal spectrum. But, when the extremes are also taken into consideration of the maximum dispersion simulation, the 100,200 and 300μm fractions show a multi-modal spectrum.

In Table J.7 the 3D simulations are compared. For the 100 and 200 μm fraction no comparison can be made since they depict different behaviour. But, the 300 en 400μm fraction can be compared. The peaks of available mass of sediment are lower for the minimum dispersion simulation for the 300 μm fraction. Whereas the 400 μm show great correspondence. Regarding the distance from the release location, again the 100 and 200μm fraction can not be compared. However, the 300 and 400μm fraction show correspondence. Especially the 400μm fraction.

Table J.7: Distances to peak available mass of sediment [$\frac{kg}{m^2}$] per fraction - comparison 3D minimum and maximum dispersion simulations

	Center		**North Sea**				**Wadden Sea**			
Fraction [μm]	100	200	100	200	300	400	100	200	300	400
Minimum dispersion Peak [$\frac{kg}{m^2}$]	-	-	6.63	20.95	40.78	61.21	8.15	21.94	43.08	54.97
Maximum dispersion Peak [$\frac{kg}{m^2}$]	3.9	13.41	-	-	29.38	58.4	-	-	28.57	54.54
Correspondence in percentage [%]	-	-	-	-	72	95	-	-	66	99
Distance from release location minimum dispersion [m]	-	-	1010	606	404	303	1111	404	303	303
Distance from release location maximum dispersion [m]	0	303	-	-	303	202	-	-	303	303
Correspondence in percentage [%]	-	-	-	-	75	67	-	-	1	1

J.3. NEAR-FIELD 3D SIMULATION TO MID-FIELD 2D SIMULATION

The transition from the spring neap cycle 3D models in Chapter 5 to the half year 2D dispersion models is done based on the speed of dispersion after sediment has settled and the initial dispersion differences due to the settling process between the models.

The following analysis holds for both mid-field simulation branches.

Speed of dispersion after sediment has settled
The speed of dispersion involves the process after the sediment has settled and starts to disperse over the area. No large masses per square meter are visible in the extreme regions of the distribution area after a spring tide cycle, the scale has been set between 0-2 $\frac{kg}{m^2}$. (See Fig. J.1, Fig. J.2, Fig. J.3, Fig. J.4).

For the speed of dispersion, the difference between the dark red and the dark blue / light blue areas in the area is analysed. These are the areas with respectively much artificial sediment or little artificial sediment. The dispersion of sediment after it has settled is from the dark red regions towards the dark blue/ light blue areas.
The speed of sediment movement from the dark red regions is more or less equal between the 2D and 3D models per fraction. An exception is the 400 μm fraction, which gives very large differences for the 2D and 3D model. This has to do with the found initial spread through the settling process of the sediment fraction. Thus, the differences do not lie in the speed of dispersion but in the initial settlement of the sediment.

The dispersion of the sediment fractions is determined to have the same speed for the 2D and 3D model. Hence, it is not expected that major deviations will occur for the speed of dispersion in the half year models. Therefore, no modulation measures (e.g. morphological acceleration) are taken for the speed of dispersion.

Another note is that for the minimum dispersion simulations, the dispersion processes further away from the source become less accurate as the distance increases. This is due to the ratio of natural fractions versus the nourished sediment fractions in a gridcell as explained in Section 3.2.

Dispersion due to settling process
The initial dispersion due the settling process is the dispersion which has a dark red color. The scale has been set between 0-2 $\frac{kg}{m^2}$ in Chapter 5. Also, the longitudinal distributions are used for this analysis. The difference between the 2D and 3D dispersion per fraction is again considerable. The initial dispersion due to the settling process is correctly displayed in the 3D model. Thus, the bed composition of the spring neap 3D model should be applied in the 2D mid-field dispersion models.

Conclusion transition from 3D near-field dispersion models to 2D mid-field dispersion models
Based upon the speed of dispersion, it is not necessary to undertake any action for the modulation of the mid-field dispersion models. Based upon the initial dispersion due to the settling process, a conclusion is formed for the restart of the 2D mid-field dispersion model. Based upon the findings of the longitudinal distribution in both Appendix I.3 and Chapter 5 the dispersion of the 3D near-field dispersion model has to be used as start condition for the 2D mid-field dispersion. This is because the differences between the 2D and 3D near-field dispersion is too large and will yield an inaccurate result in the restart. Therefore, the bed composition of the 3D model with initial distribution of the added fractions is used as a starting condition for the 2D mid-field dispersion model.

K | Supporting mid-field dispersion results

In this section supporting analyses are performed for the mid-field dispersion results in Chapter 6. First, an extensive analysis is performed regarding the behaviour of the wet-cross section. Thereafter, the minimum mid-field dispersion results are depicted. Finally, the mid-field dispersion longitudinal distribution is discussed.

K.1. BEHAVIOR WET CROSS-SECTION

Minimum dispersion behaviour A_c
Part 1
Fig. K.1 illustrates part 1 of the mid-field behaviour of the wet cross-section. The development of the wet profile over time is virtually the for both situations. A small increase of sediment can be seen between 0-100 meters. Between 100 and 180 meters a converging process is visible from t1, t2 and t3 with respect to the reference line. At 120 meters the times t1,2 and t3 intersect the reference line. From this location, the wet profile is subject to abrasion. This process continues until the end of this sub-section at 400 meters cross-sectional distance, where t0,t1,t2 and t3 seem to converge to one another.

Despite the fact that the behavior is the same, there is a slight difference between the wet profile without and with continuous nourishment. The degree of abrasion is greater **without** continuous nourishment than **with** continuous nourishment around 350 meters cross-sectional distance.

Part 2
Fig. K.2 illustrates part 2 of the mid-field behaviour of the wet cross-section. The wet surface development without continuous nourishment differs significantly from the development with continuous nourishment. Between 400 and 450 meters a diverging process is visible for both results, where t1, t2 and t3 are above the reference line. This results in sanding of the wet surface. The extent to which sedimentation takes place is significantly greater for the model with continuous nourishment than the model without continuous nourishment.

The results **without** continuous nourishment, a converging process of t1, t2 and t3 with respect to t,0 takes place between 650m and 700m. At 680 meters these lines again intersect the reference line and thus abrasion of the wet surface takes place. Until the end of this sub-section, t0, t1, t2, t2, and t3 converge again. At 800 meters, the wet profile over time is equal to the reference frame.

The results with continuous nourishment, at 700 meters cross-sectional distance t0 is equal to t1. Sanding of the Borndiep channel will also continue up to the 800 meter cross-sectional distance.

In Table 6.1 the development of the deepest trough of the Borndiep channel is evaluated. Based on the height difference trend, the same conclusion can be drawn. Which is, the depth of the Borndiep channel decreases.

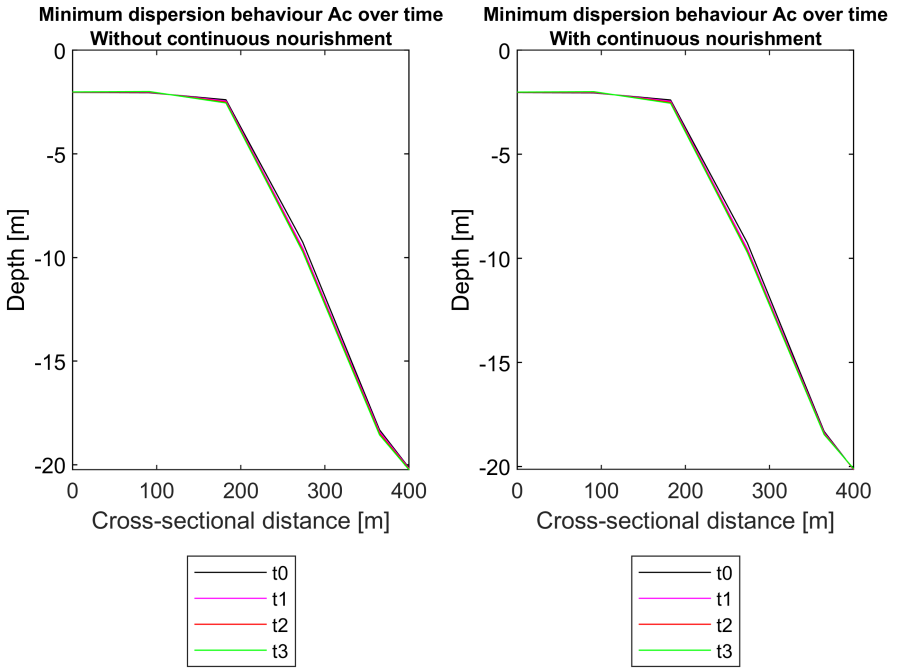

Figure K.1: Behaviour of cross-section over time with a continuous nourishment - Part 1

Table K.1: Development trend of deepest trough part of Borndiep channel - Minimum dispersion

Model	**Without continuous nourishment**	Height difference	**With continuous nourishment**	Height difference
Depth t0	24.175 m	-	24.175 m	-
Depth t1	24.154 m	0.021 m	24.071 m	0.104 m
Depth t2	24.118 m	0.036 m	23.944 m	0.127 m
Depth t3	24.080 m	0.038 m	23.797 m	0.147 m

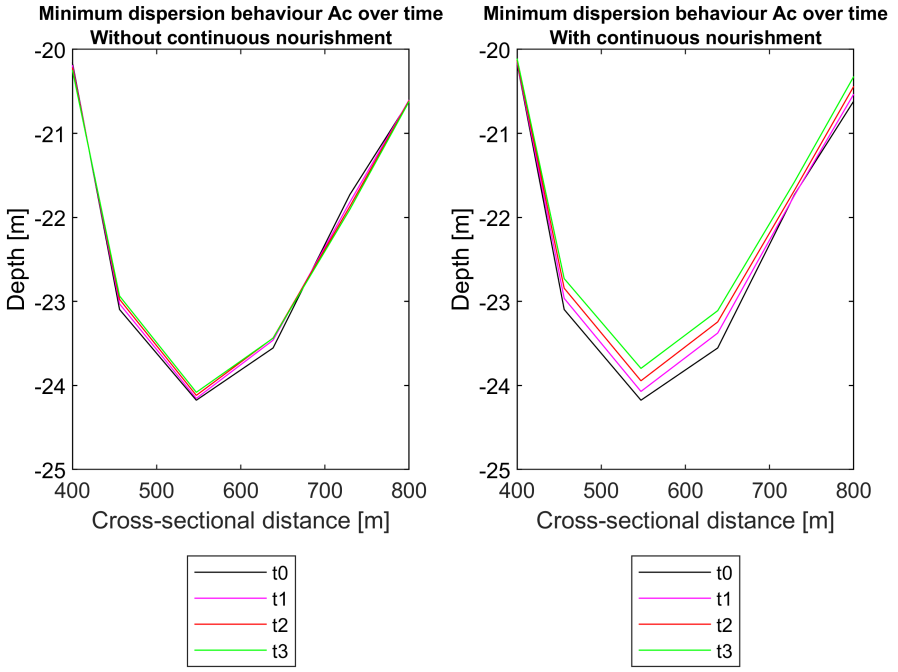

Figure K.2: Behaviour of cross-section over time with a continuous nourishment - Part 2

Part 3
Fig. K.3 illustrates part 2 of the mid-field behaviour of the wet cross-section. In this subsection, the wet surface development without continuous nourishment does not differ with the development of with continuous nourishment. The difference between **without** and **with** continuous nourishment is the starting condition from part 2. In **with** continuous nourishment there was more siltation in the channel than **without** continuous nourishment. From 970 meters, the t1, t2 and t3 lines intersect the reference line. Thus, from this point on, abrasion of the wet surface takes place. This trend continues until the end of this sub-section at 1200 meters cross-section.

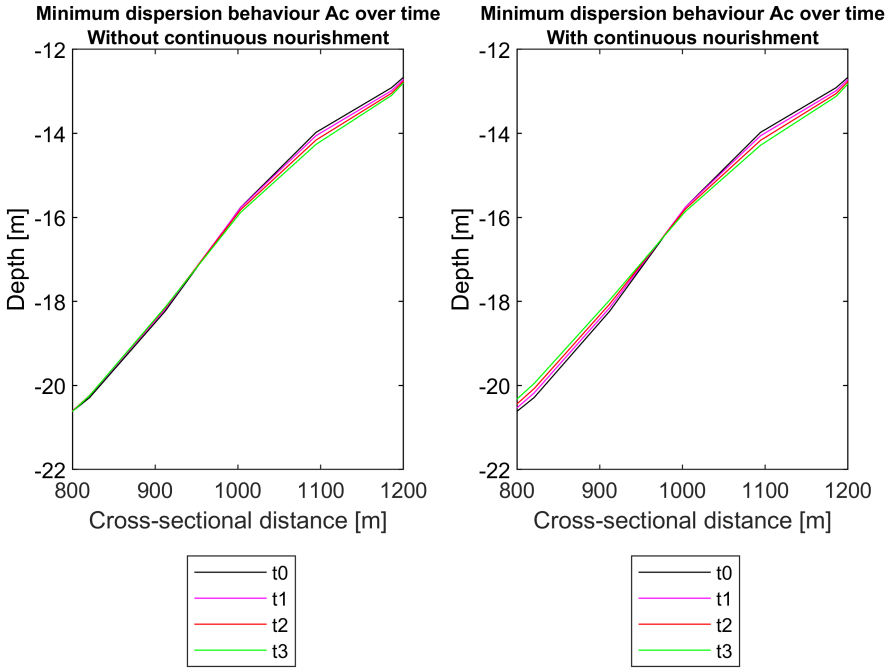

Figure K.3: Behaviour of cross-section over time with a continuous nourishment - Part 3

Part 4
Fig. K.4 illustrates part 2 of the mid-field behaviour of the wet cross-section. In this sub-section, the development of the wet profile is the same between **without** and **with** continuous nourishment. Between 1200 and 1270 meters the t1, t2 and t3 lines intersect the reference line, ending the abrasion behavior of part 3 and then again leading to light accretion of the tidal channel. The accretion continues until the end of the cross-sectional distance.

Maximal dispersion behaviour A_c
Fig. K.5a illustrates the development of the wet surface **without** continuous nourishment and Fig. K.5b illustrates the development of the wet surface **with** continuous nourishment. First, the development of the wet surface without continuous nourishment is analysed. Then the development of the wet surface with continuous nourishment is analysed. For both cross-sections, a close-up of the part of the cross-section most subject to change was taken to identify the trend of the behavior. These are depicted in Fig. K.6a and Fig. K.6b.

Based on the figures **without** continuous nourishment, t1, t2, and t3 are observed to be below the reference line t0. Based on this observation the ebb channel subject to abrasion. The extent to which the ebb channel is subject to abrasion can also be deduced on the basis of the underlying distances between the various time measurements. Based on this, it is observed that the distances between successive time measurements reduce over time.

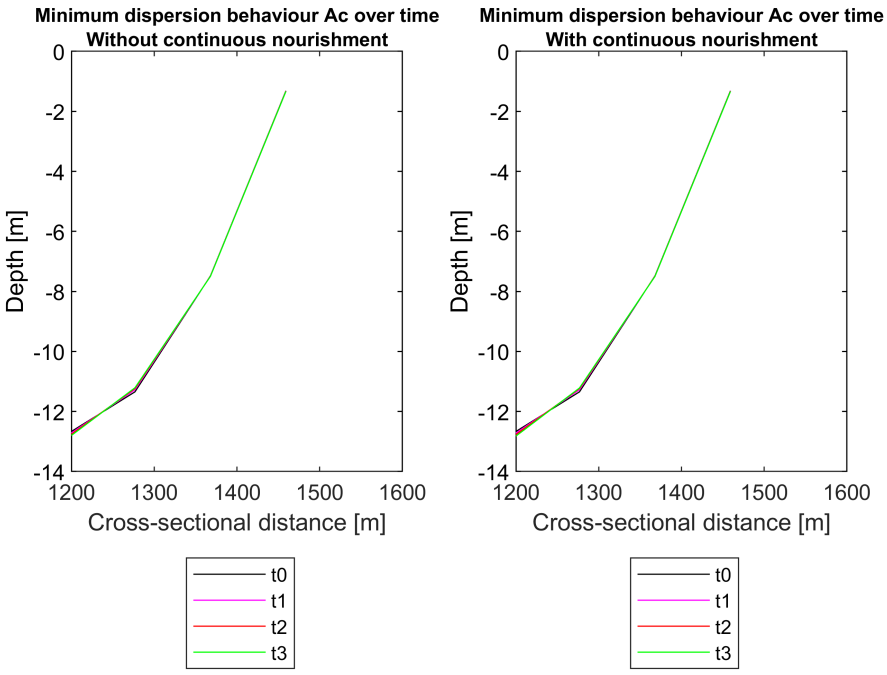

Figure K.4: Behaviour of cross-section over time with a continuous nourishment- Part 4

Table K.2: Development trend of deepest trough part of Borndiep channel - Maximum dispersion

Model	With continuous nourishment	Height difference
Depth t0	24.1754 m	-
Depth t1	24.0226 m	0.1528 m
Depth t2	23.8541 m	0.1685 m
Depth t3	23.6899 m	0.1642 m

Based on the figures **with** continuous nourishment, t1, t2, and t3 are observed to be above the reference line t0. Based on this observation the ebb channel subject to silting up. The extent to which the channel is silting up is difficult to deduce on the basis of the underlying distances between the various time measurements. To clarify this, the underlying distances of the time measurements were measured in the deepest point of the ebb channel. These are shown in table Table K.2. Based on these observations, the underlying distance increases first. After that, the underlying distance decreases.

Moreover, the development over time of the wet surface area which represents the cross-section of the ebb-channel (A_c) is determined in Table K.3. According to this table, the surface area increases over time **without** continuous nourishment and decreases **with** continuous nourishment. Fig. K.6a and Fig. K.6b also confirm this behaviour over time.

Table K.3: Development cross-sectional area over time - Maximum dispersion

	Without continuous nourishment		**With continuous nourishment**	
Timestep	Area [m2]	% change to reference (t0)	Area [m2]	% change to reference (t0)
CRS t0	21691	-	21691	-
CRS t1	21712	100.10 %	21605	99.60 %
CRS t2	21720	100.13 %	21519	99.21 %
CRS t3	21723	100.15 %	21438	98.83 %

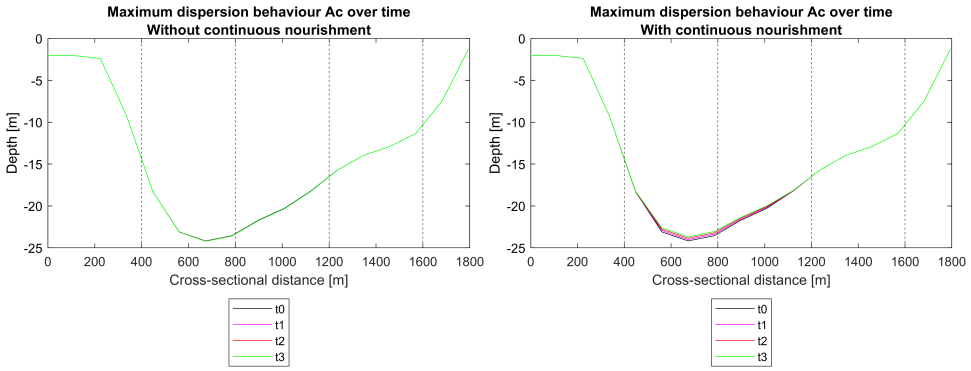

(a) Behaviour of the wet-cross section with maximal dispersion without continuous nourishment

(b) Behaviour of the wet-cross section with maximal dispersion with continuous nourishment

Figure K.5: Behaviour of the wet cross-section with maximal dispersion. In the left image the behaviour of the wet cross-section is visible in which no nourishment is added over a half year time. In the right image the behaviour of the wet cross-section is visible in which a continuous nourishment is added over a half year time.

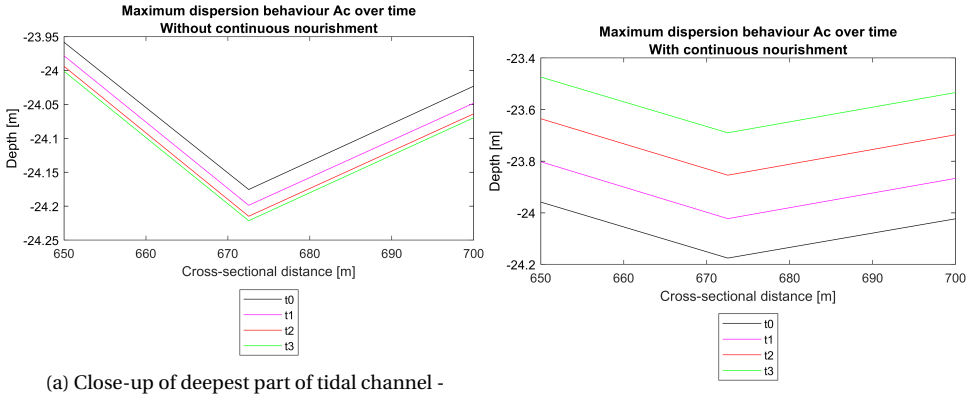

(a) Close-up of deepest part of tidal channel - Maximum dispersion without continuous nourishment

(b) Close-up of deepest part of tidal channel - Maximum dispersion with continuous nourishment

Figure K.6: Close-ups of the maximum dispersion behaviour of the wet cross-section

K.2. MID-FIELD DISPERSION

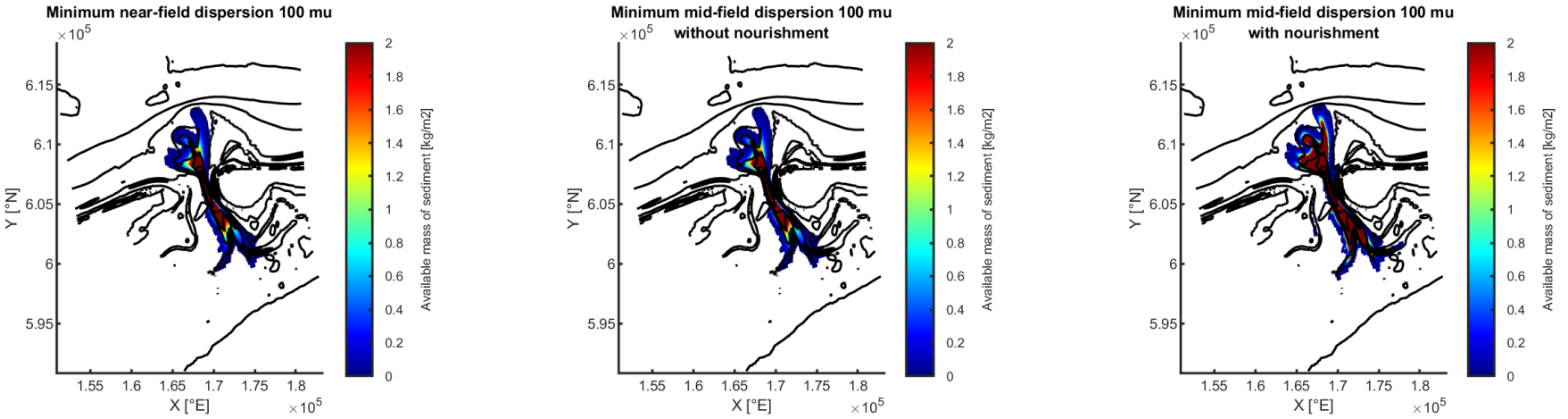

Figure K.7: Combined figures of minimum dispersion. 3D spring neap tide cycle (left), 2D half year dispersion without continuous nourishment (center) and 2D half year dispersion with continuous nourishment (right) - 100μm

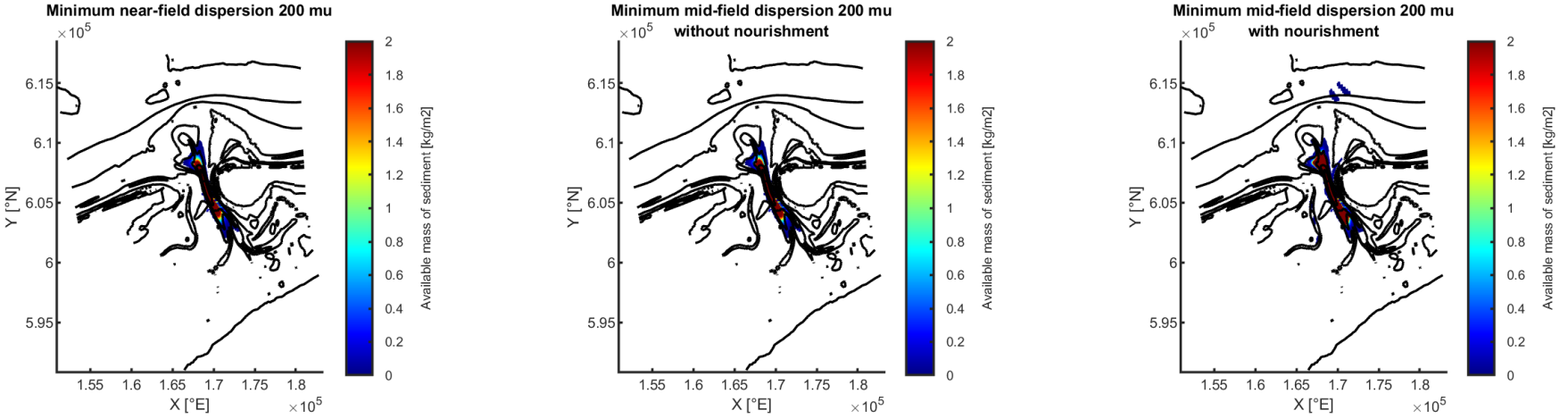

Figure K.8: Combined figures of minimum dispersion. 3D spring neap tide cycle (left), 2D half year dispersion without continuous nourishment (center) and 2D half year dispersion with continuous nourishment (right) - 200μm

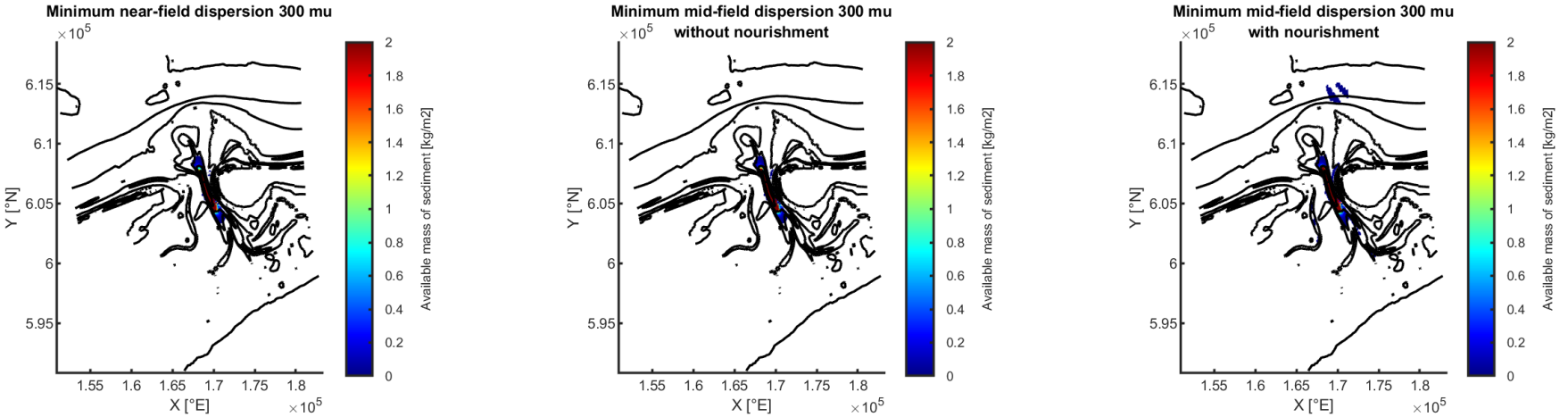

Figure K.9: Combined figures of minimum dispersion. 3D spring neap tide cycle (left), 2D half year dispersion without continuous nourishment (center) and 2D half year dispersion with continuous nourishment (right) - 300μm

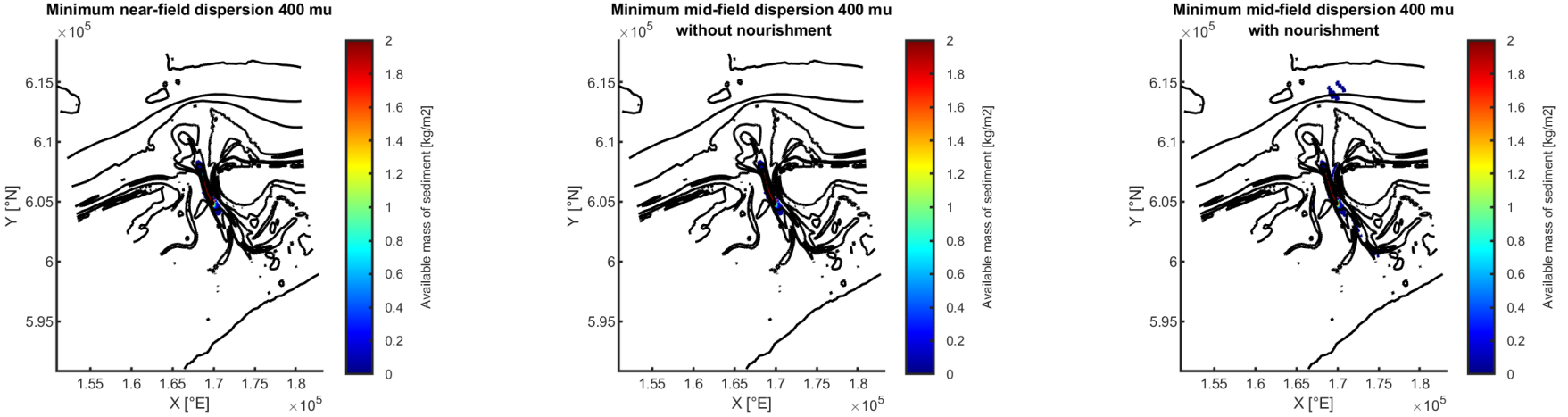

Figure K.10: Combined figures of minimum dispersion. 3D spring neap tide cycle (left), 2D half year dispersion without continuous nourishment (center) and 2D half year dispersion with continuous nourishment (right) - 400μm

L | Dredge equipment

In this appendix dredge equipment is described. Mainly information from Royal IHC is provided as they are part of the consortium of the Zandwindmolen.

L.1. Design nourishment equipment

The required nourishment equipment is determined on the basis of an optimization issue. The optimization issue starts with an approaching pipeline on the seabed from offshore regions. From hereon forward, a fitted set-up is determined for the Zandwindmolen based on the two main fundamentals of the nourishment strategy of the Zandwindmolen.

- The nourishment of sand should cause as little ecological damage as possible.
- Nature brings the sand to the places where it is most needed for the conservation of the Dutch (coastal/dune area and raising the Wadden Sea).

The conclusions from the in-depth literature study on dredge plumes Section 2.5 are used as a basis. From this in-depth literature study it followed that the optimal plume is a mixed plume. The following processes depict a mixing plume;

- Segregation of fractions occurs (settling due to individual sediments)
- Horizontal advection by wind-driven, tide-driven and wave-driven currents
- Lateral diffusion due to turbulent forces generated by currents

Moreover, it was determined that placement of sediment has to be as high as possible in the water column to make full use of the suspended load regime. Moving up in the water column can be achieved through a buoyant pipe, also called a hiser hose Appendix L.2. In Appendix L an overview is provided of existing dredge equipment. Fig. L.5 illustrate how different pipes and/or discharge hoses can be combined. Fig. L.6 illustrates a more general overview of possible set-ups and an assortment of different pipelines by Royal IHC.

Once at the top of the water column, the sediment can be nourished. Easiest would be to do this directly with open single point pipeline discharge. Unfortunately, single point discharge from a pipeline usually results in a density driven flow to the seabed. A consequence of this plume type is that the flow of the discharge entrains the individual particles of the fill, until the coarse fraction lies stable on the fill location. The fine fraction of the nourishment either become trapped within the coarse fraction or remain in suspension until calm or stagnant water is reached. When calm or stagnant water is reached, the fine fraction also settles on the seabed. As a result, this type of nourishment results in a fill with spatial variability. Within the center coarse fractions are found and depending on the local depositional environment, finer fractions can be found on the outer edges. (van't Hoff and van der Kolff, 2012)

In Fig. 4.4a an image is provided of the density flow which occurs for open pipeline discharge above the water level.

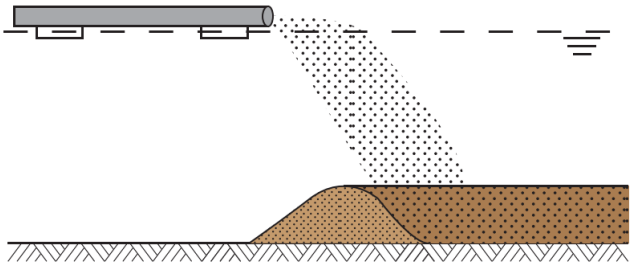

Figure L.1: Pipeline discharge on top of water column (van't Hoff and van der Kolff, 2012)

Due to the density driven flow, craters are formed near the outlet of the pipeline and erosion channels can occur due to the flow of the sand - water mixture (van't Hoff and van der Kolff, 2012). An overview of crater forming is depicted in Fig. 4.4b

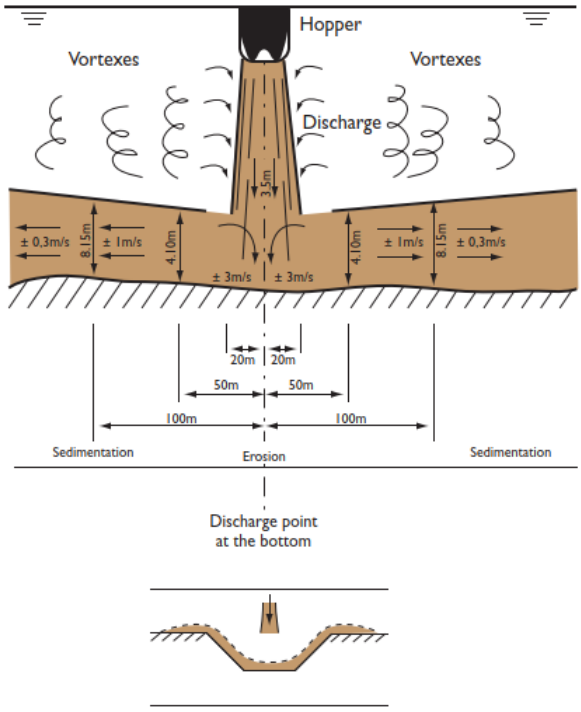

Figure L.2: Crater forming due to the dilution of the sand water mixture flow in the water column (van't Hoff and van der Kolff, 2012)

Open pipeline discharge is thus not in line with the nourishment fundamentals as it does not full fill both nourishment foundations of the Zandwindmolen. Another method is to attach a spray pontoon to the floating pipeline.

A spreader pontoon is illustrated in Fig. 4.5a.

Figure L.3: Example spray pontoon

In the following section a general description of a spreader pontoon is provided. A spray pontoon is composed out of winches, pipes and a spray head. The winches position the pontoon. Normally a pontoon is connected to either a cutter suction dredge or trailing hopper suction dredge by means of a floating pipeline. The sediment water mixture is nourished by means of a spray head. The spray head regulates the flow of the material and reduces or increases the speed. There are different kinds of spray heads, but combinations of systems are also possible:

- Chute
- Cooking pot
- Spreader bar

A chute is depicted in Fig. 4.5a. A spray head approximately has the width of the pontoon.

A moving spreader pontoon is able to place lifts of limited thickness. In general, a nourishment layer thickness up to 0.25 meters can be realised. As a result, the nourished layer has low densities.
Due to the segregation process, which is caused by the difference in settling velocity of the various particle sizes, the nourished layer ranges from coarse sediments on top of the initial sea bed to fine sediments on top of the new layer. Due to the segregation process a relatively uniform, but stratified fill is created. Characteristics of the fill are low shear strength and a compressibility that may be higher than that of clean sand (van't Hoff and van der Kolff, 2012).

If the thickness of the layer has to fulfill certain characteristics, it is possible to place the fill in lifts by using a maneuverable pontoon. The pontoon can be maneuvered by means of winches and anchors. The maneuverability is limited by the attached floating pipeline, which needs to have sufficient flexibility and slack to allow for the movements of the pontoon. Moreover, the use of a floating pipeline which connects to a pontoon is restricted by the draught of the pontoon or pipeline and the auxiliary equipment for handing of the pipeline (van't Hoff and van der Kolff, 2012).

Also, waves can cause workability limitations on the spray pontoon.

5) It follows from the general description that a spray pontoon is able to place lifts from coarse sediments on top of the initial sea bed to fine sediments on top of the new layer. This is achieved by means of the segregation process and the corresponding individual settling of various particle sizes. Segregation of fractions is a requirement of the formation of a mixing plume and thus falls within the nourishment fundamentals of the Zandwindmolen.

However, in order for a spray pontoon to match the requirements of the Zandwindmolen project and its nourishment foundations, some additional adjustments have to be taken into consideration.

For the formation of a mixing plume, the flow has to be unstable. This is achieved when the Richardson number is much smaller than $\frac{1}{4}$ (Ri « $\frac{1}{4}$). According to Richardson's formula depicted below and previously illustrated in Section 2.5, two main parameters can be adjusted to create an unstable flow. These two parameters are the density and the velocity of the sediment mixture.

$$Ri = \frac{-g\frac{\partial \rho}{\partial x}}{\rho_w \frac{\partial u}{\partial x}} \tag{L.1.1}$$

The two parameters must be adjusted in the following manner to create a mixing plume. The density must decrease and the velocity of the sediment mixture must increase. The process is comparable to a traffic jam on the highway. To solve a traffic jam, there must first be more space for the cars to drive on. However, these cars also have to accelerate, otherwise the created space will not affect the cars in the back off the traffic jam.

In the following section it is described how the mixing plume can be generated by adjusting the density and the velocity of the sediment mixture.

It is found in Section 2.5 that unhindered settling or settling of individual sediments occurs when the mixture concentration is lower than 1-2%. The sediment volume concentration within the Zandwindmolen project is between 10-30 % and depends on the nourished sediment volume. Thus, the sediment has to be diluted by a factor 10-30 to ensure a mixture concentration lower than 1-2%.

Several options are possible to achieve a diluted sediment mixture lower than 1-2%. Two of them are illustrated below. The sediment mixture can be mixed with clean ambient water before the sediment mixture reaches the spray head of the pontoon. Or a chute can be applied as spreader head to spread the sediment mixture over a larger surface.

When a chute is applied as spreader head for the spray pontoon, the sediment mixture is spread out over a larger surface when it touches the water surface compared to when it is in the pipe diameter (see illustration Fig. 4.5a). Based on the continuity equation, it can be determined what the surface area of the spread should be in order to obtain the 1-2% sediment mixture concentration. Though, when the discharge remains constant and the consecutive surfaces change, the flow velocity of the mixture must decrease according to the continuity equation. This is in contradiction with the previous statement in which the flow must be accelerated to get a mixing plume. To solve this, the chute has to be placed under an angle to stimulate the sediment mixture flow velocity.

For the application of a spray pontoon for the Zandwindmolen, a combination of dilution by adding clean ambient water and using a chute as a spreader head is required. This is determined in consultation with Royal IHC. The combination of both applications positively stimulates each other. The spreader of the chute and the dilution of the sediment mixture by adding clean ambient water promote the reduction of the density. Moreover, while diluting the sediment mixture by clean ambient water, extra discharge is added to the sediment mixture. As a consequence, the flow velocity of the sediment mixture will automatically be accelerated and therefore promote the increase of flow velocity.

By combining both applications, an unstable flow with (Ri « $\frac{1}{4}$) can be achieved. Therefore, a spreader

pontoon fits to the needs and the nourishment foundations of the Zandwindmolen project.

However, the application of a spreader pontoon in an ebb channel also brings new challenges. Normally a spreader pontoon is used on inland waterways or other areas where waves are absent. Within the Zandwindmolen project, the spray pontoon must be deployed at sea. It was already mentioned that a competitive system design of the Zandwindmolen as a whole, requires an accurate harmonization of the sub-systems. Therefore, a technical requirement of 100% workability is set by the consortium. In Appendix I.4 a wave analysis of the vicinity of Ameland Inlet was performed. It was found that the spreader pontoon has to be able to resists waves of 1.5 meters with a wave period between 3.8 and 10.7 seconds. In conclusion, the spreader pontoon has to be made sea worthy. However, the development of a seaworthy spreader pontoon is beyond the scope of this thesis.

The main intention of the Zandwindmolen is to ensure that the nourishment disperses as much as possible by the forces of nature. It is therefore important to know whether sediment accumulates during stationary nourishment, or whether nature is able to disperse the nourished sediment. Whether a stationary nourishment can be performed depends on a trade-off between how much the system can process per meter width and how much is nourished during the nourishment operation. Within the Zandwindmolen mainly large nourishment volumes (0.5 - 1 or 2 Mm^3 per year) have to be nourished to make the Zandwindmolen cost competitive. In this case study it determined that the system can process approximately 2750.00 $m^3/m/year$ at the center of the Borndiep channel (Appendix I.2). Therefore, a stationary nourishment of 0.5 - 1 or 2 Mm^3 per year by means of a spreader pontoon will result in silting up of the channel. Thus, the spreader pontoon has to be able to manoeuvre perpendicular to the ebb flood flow velocity. The distance over which it has to travel perpendicular to the ebb flood flow velocity is based on the nourishment volume.

Moving a spreader pontoon can be done in different ways. The spray pontoon can be motorized with a propulsion or jet system. In addition, it is also possible to move the spray pontoon with winches. At least three winches are required (Dickhof, 2016) to move the spreader pontoon. The wires from the winches are guided of the pontoon by means of fairleads. Due to the positioning process of the pontoon with the wires and the winches, lots of hauling takes place on the fairleads. They should therefore be wear resistant. Traditional spreader pontoons can be hauled by winches with a speed of 9-18m/min (Dickhof, 2016). But, new winches allow to haul with a speed up to 120m/min (2m/s) (Stema, 2022).

In line with the sustainable aspect of the Zandwindmolen project, it is interesting to electrify the drive of the spreader pontoon. an electric drive system can be powered by sustainable forms of energy. In addition to being able to move the spray pontoon independently, the amount of force that has to be installed depends on the floating pipe that is attached to the pontoon for the supply of the sediment mixture. Moreover, the electric drive must be able to power the pump for the dilution of the sediment mixture. However, this is beyond the scope of this thesis.

In Fig. L.4 an overview is provided of where the different components of a spray pontoon are located. In this image a spreader bar is attached (bar on right side).

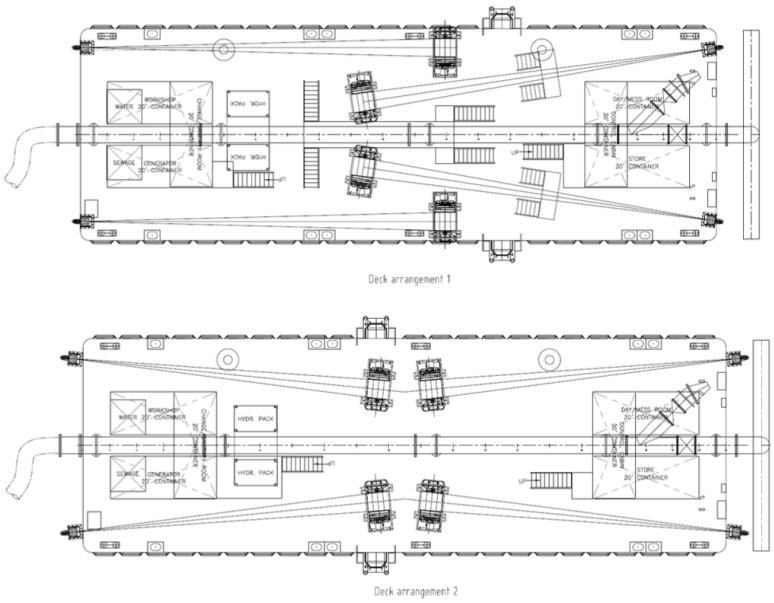

Figure L.4: Deck arrangements spray pontoon (Dickhof, 2016)

L.2. FLOATING PIPELINES

Floating pipeline information is obtained from (IHC, 2015b)

Floating hose configurations can contain:

- pressure hoses
- riser hoses
- sinker hoses
- floating discharge hoses
- tapered hose
- connection hose
- bow floater

Figure L.5: Royal IHC floating discharge lines (IHC, 2015b)

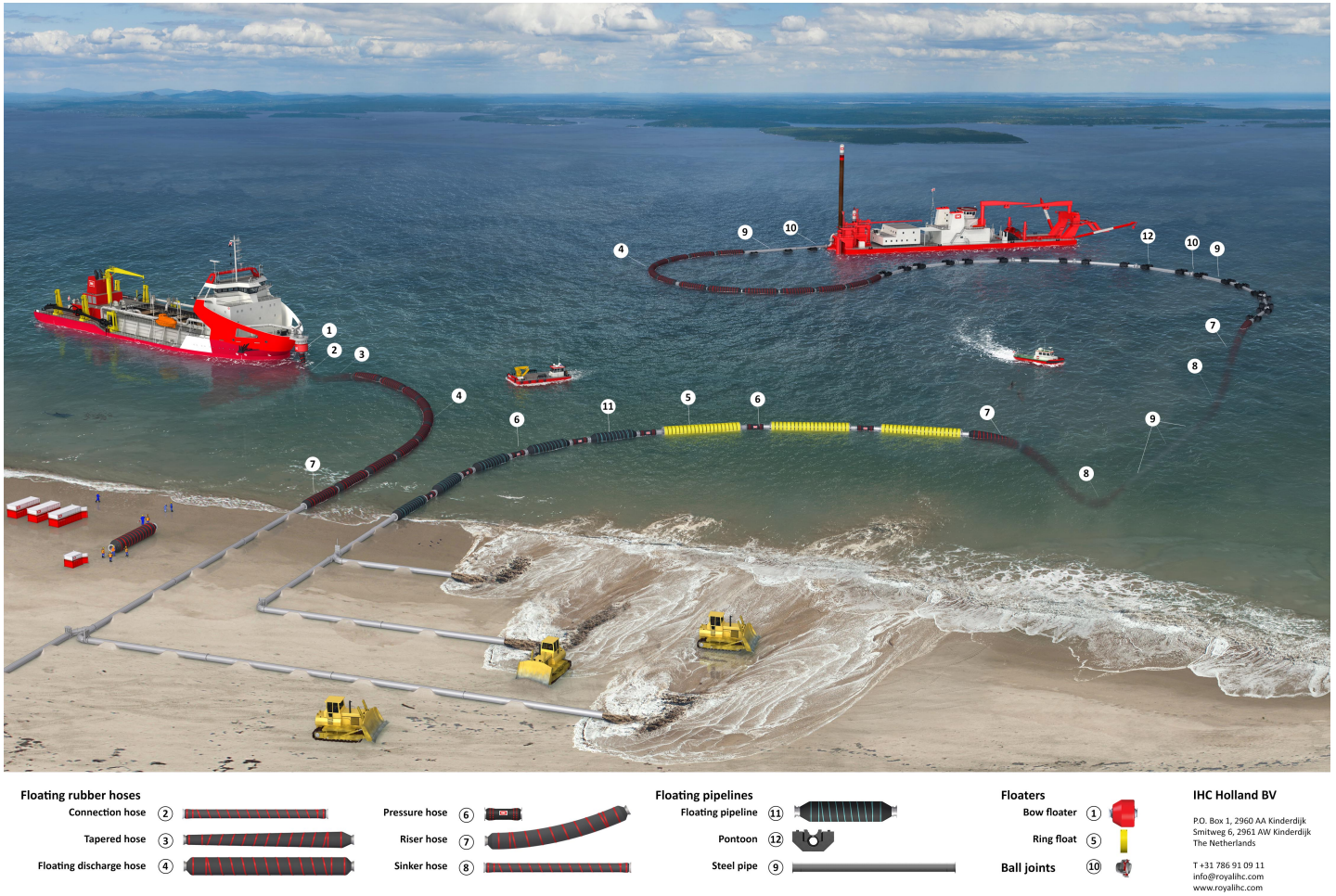

Figure L.6: Royal IHC floating dredge assortment (IHC, 2015a)